Martin CR 65-93 (Vol II)

Copy No. 2

SOLID PROPELLANT ROCKET EXHAUST EFFECTS (SPREE) AND METHODS OF ATTENUATION

VOLUME II PART II, PHASE II FINAL REPORT

JANUARY 1966

prepared by

MARTIN MARIETTA

N66 30607
(ACCESSION NUMBER)
192
(PAGES)
CR-76235
(NASA CR OR TMX OR AD NUMBER)
(THRU)
1
(CODE)
33
(CATEGORY)
FACILITY FORM 602

prepared for

KENNEDY SPACE CENTER
NATIONAL AERONAUTICS AND SPACE ADMINISTRATION
JOHN F. KENNEDY SPACE CENTER, FLORIDA

Reproduced by
NATIONAL TECHNICAL INFORMATION SERVICE
Springfield, Va. 22151

N O T I C E

THIS DOCUMENT HAS BEEN REPRODUCED FROM THE BEST COPY FURNISHED US BY THE SPONSORING AGENCY. ALTHOUGH IT IS RECOGNIZED THAT CERTAIN PORTIONS ARE ILLEGIBLE, IT IS BEING RELEASED IN THE INTEREST OF MAKING AVAILABLE AS MUCH INFORMATION AS POSSIBLE.

Martin-CR-65-93 (Vol II)

Contract NAS 10-2300

SOLID PROPELLANT ROCKET EXHAUST EFFECTS (SPREE) AND METHODS OF ATTENUATION

VOLUME II: PART II, PHASE II FINAL REPORT

January 1966

Authors

E. Lays, BSAE, PE
E. A. Darrow, BSMS, MSEE, PE

Approved

E. A. Darrow, Program Manager, SPREE

MARTIN-MARIETTA CORPORATION
MARTIN COMPANY
Denver Division
Denver, Colorado

Martin-CR-65-93 (Vol II)

Contract NAS 10-2300

SOLID PROPELLANT ROCKET EXHAUST EFFECTS (SPREE) AND METHODS OF ATTENUATION

VOLUME II: PART II, PHASE II FINAL REPORT

January 1966

Authors

E. Lays, BSAE, PE
E. A. Darrow, BSMS, MSEE, PE

Approved

E. A. Darrow, Program Manager, SPREE

MARTIN-MARIETTA CORPORATION
MARTIN COMPANY
Denver Division
Denver, Colorado

2

FOREWORD

This report provides the data developed during Part II, Phase II of the Solid-Propellant Rocket Exhaust Effects (SPREE) Program under Contract NAS10-2300. Volume I also includes data previously provided from the Phase I and Part I, Phase II SPREE investigations performed under Contracts NAS10-389 and NAS10-1107. The three contracts have been administered by NASA at the Kennedy Space Center, John F. Kennedy Space Center, Florida. Technical direction of the program has been provided by the Future Studies Branch of the Launch Support Equipment Engineering Division, Kennedy Space Center. The report is submitted in two volumes that are described below.

Martin-CR-65-93 (Vol I) SPREE Project Summary - This volume is submitted as a project summary of all work performed, results obtained, and recommendations evolved during the entire SPREE program.

Martin-CR-65-93 (Vol II), Part II, Phase II Final Report - This volume documents the results of the test program performed during the Part II, Phase II portion of the program. Where applicable, this volume also updates portions of the data previously provided by earlier reports developed during Part I, Phase II of the SPREE programs. Also reported are data obtained from full-scale tests, which were made available for this effort and which have been used to correlate subscale model test results developed during this program.

A design handbook will be issued at a later date, which can be used as a guide in the design of portions of launch facilities from which vehicles using solid rocket motors are to be launched. The handbook will be compiled from data developed and evaluated during the SPREE program.

These investigations were prompted by a need to develop supporting technology for launch facilities applicable to potential improvements of the Saturn IB and Saturn V space vehicle systems.

CONTENTS

		Page
Foreword		ii
Contents		iii thru xi
I.	Introduction	I-1
	A. Program Objectives	I-3
	B. Program Description	I-4 thru I-7
II.	Materials Evaluation (Group I)	II-1
	A. Group I Technical Objectives	II-1
	B. Test Configuration	II-1
	C. Procedure	II-3
	D. Instrumentation	II-4
	E. Results	II-4
	F. Analysis	II-6 thru II-24
III.	Test Facility	III-1
	A. Test Fixture	III-1
	B. Test Setups	III-2
	C. Instrumentation	III-3 thru III-12
IV.	Solid Rocket Motor Design	IV-1
	A. Design Considerations	IV-1
	B. Motor Description	IV-3
	C. Grains and Igniters	IV-4
	D. Motor Performance	IV-4 thru IV-16

V. Aluminum Content and Scale Effects (Group II) . . V-1

A. Group II Technical Objectives V-1

B. Test Articles V-2

C. Procedure V-3

D. Test Results . . . . . V-5 thru V-24

VI. Liftoff Acceleration Effects (Group III) VI-1

A. Group III Technical Objectives VI-1

B. Meaning of Acceleration Rate Terminology . . VI-1

C. Test Articles VI-2

D. Test Procedure VI-2

E. Results . . . . . VI-3 thru VI-13

VII. Special Evaluations (Group IV) VII-1

A. Group IV Technical Objectives VII-1

B. Test Articles VII-2

C. Test Procedure VII-3

D. Test Results . . . . . VII-3 thru VII-15

VIII. Multiple Motor Effects on Deflectors (Group V) . VIII-1

A. Group V Technical Objectives VIII-1

B. Test Articles VIII-1

C. Test Procedure VIII-2

D. Test Results . . . . . VIII-2 thru VIII-11

IX. Motor Exhaust Plume Characteristics (Group VI) . IX-1

A. Objective IX-1

B. Test Articles IX-1

C. Test Procedure IX-2

D. Test Results . . . . . IX-3 thru IX-12

X. Protective Materials Evaluation X-1

A. Technical Objectives X-1

B. Desirable Coating Properties X-1

C. Types and Characteristics of Coatings Investigated X-2

D. Environment X-2

E. Data Presentation X-3

F. Results and Discussion . . . . . X-3 thru X-22

XI. Conclusions XI-1

A. Deflector Coatings XI-1

B. Effect of Aluminum Content XI-1

C. Scale Effects XI-2

D. Liftoff Acceleration Effects XI-2

E. Effect of Rocket Motor Cant XI-3

F. Effect of Successive Firings XI-3

G. Refurbishability XI-3

H. Protective Coatings for GSE XI-3

XII. Recommendations for Future Studies XII-1

A. Scientific Investigations XII-1

B. Engineering Investigations . . . . . XII-3 and XII-4

XIII. References and Bibliography XIII-1

A. References XIII-1

B. Bibliography . . . . . XIII-1 thru XIII-6

Distribution

Figure

II-1 Group I Test Setup II-7

II-2 TM-1 Motor II-8

II-3 Chamber Pressure Time Histories, Runs 1 thru 6 . . . . . II-9

II-4 Flat Plate Deflector before Coating II-10

II-5 Ice Deflector Frame II-10

II-6 Flat Plate Deflector II-11

II-7 Ice Deflector II-12

II-8 Fondu Fyre WA-1 Deflector after Firing II-13

II-9 Fondu Fyre XB-1 Deflector after Firing II-13

II-10 Cracked Fondu Fyre WA-1 Deflector before Firing II-14

II-11 Cracked Fondu Fyre WA-1 Deflector after Firing II-14

II-12 Ice Deflector Just before Firing II-15

II-13 Ice Deflector after Firing II-15

II-14 Deflector Coated with Portland Cement Mix after Firing II-16

II-15 Refurbished Fondu Fyre WA-1 Deflector before Firing II-17

II-16 Refurbished Fondu Fyre WA-1 Deflector after Firing II-17

II-17 Erosion Resistance of Fondu Fyre and Portland Cement Mixes to Solid Propellant Motor Blast . II-18

III-1 SPREE Acceleration Control Test Fixture . . . III-4

III-2 Comparison of Typical Desired and Expected Liftoff Rates III-5

7

III-3	Cart Travel Time Histories, Runs 7 thru 27	III-6
III-4	SPREE Test Instrumentation	III-12
IV-1	13-sec Rocket Motor Schematic	IV-6
IV-2	24-sec Rocket Motor Schematic	IV-6
IV-3	13-sec Burntime Motor	IV-7
IV-4	24-sec Burntime Motor	IV-7
IV-5	Grain Assemblies	IV-8
IV-6	Chamber Pressure Time Histories, Runs 7 thru 27	IV-9
IV-7	Characteristic Alumina Deposit in Nozzle of 22% Aluminum SRM	IV-13
IV-8	Chamber Pressure Overlay for Motors with Varying Percents of Aluminum	IV-14
V-1	J Deflector	V-10
V-2	J Deflector Base Plate	V-11
V-3	Fondu Fyre WA-1 Compression Test Cylinders before and after Crushing	V-11
V-4	Coated Test Panel Sketch	V-12
V-5	Coated Panels Mounted in Place before Firing 7	V-13
V-6	Effect of Propellant Aluminum Content on Deflector Centerline Erosion	V-14
V-7	Effect of Rocket Motor Cant on Deflector Centerline Erosion	V-14
V-8	Launch Complex 40 Deflector Erosion after First Titan IIIC Firing	V-15

V-9	Comparison of Titan IIIC Full-Scale and Model Deflector Erosion	V-16
VI-1	Relationship between Liftoff Thrust-to-Weight Ratio and Nozzle Diameters Separation in 10 sec	VI-6
VI-2	Effect of Liftoff Acceleration on Deflector Centerline Erosion	VI-6
VI-3	Effect of Liftoff Thrust-to-Weight Ratio on Erosion of Several Deflector Coating Materials	VI-7
VI-4	Variation of Exhaust Plume Centerline Heat Transfer Coefficient with Distance from Nozzle Exit	VI-7
VI-5	Correlation of Heat and Weight Loss Ratios .	VI-8
VI-6	Correlation of Maximum Erosion Depth and Total Heat Ratios	VI-8
VI-7	Thickness Reduction of Two Umbilical Mast Protective Coatings during Simulated Liftoff	VI-9
VII-1	Effect of Rocket Motor Cant on Deflector Centerline Erosion	VII-5
VII-2	Effect of Successive Firings on Deflector Centerline Erosion	VII-6
VII-3	Erosion Resistance of Deflectors Coated with H-W Special Mix 13-65 and Fondu Fyre WA-1 . .	VII-7
VII-4	Deflector Coated with H-W Special Mix 13-65, before and after Firing 21	VII-8
VII-5	Fondu Fyre WA-1 Deflector after Firing 10 . .	VII-9
VII-6	Refurbished Deflector Effectiveness	VII-10
VII-7	Refurbished Deflector after Firing 22	VII-11

9

VI-1	J Deflector Erosion, Run 16	VI-10
VI-2	J Deflector Erosion, Run 18	VI-11
VI-3	J Deflector Erosion, Run 19	VI-12
VI-4	J Deflector Erosion, Run 20	VI-13
VII-1	J Deflector Erosion, Run 15	VII-12
VII-2	J Deflector Erosion, Run 17	VII-13
VII-3	J Deflector Erosion, Run 21	VII-14
VII-4	J Deflector Erosion, Run 22	VII-15
VIII-1	Wedge Deflector Erosion, Run 26, Side A and Side B	VIII-8
VIII-2	Wedge Deflector Erosion, Run 27, Side A and Side B	VIII-10
X-1	Ablative Materials Evaluation	X-7
X-2	Relative Performance of Protective Coatingings	X-22

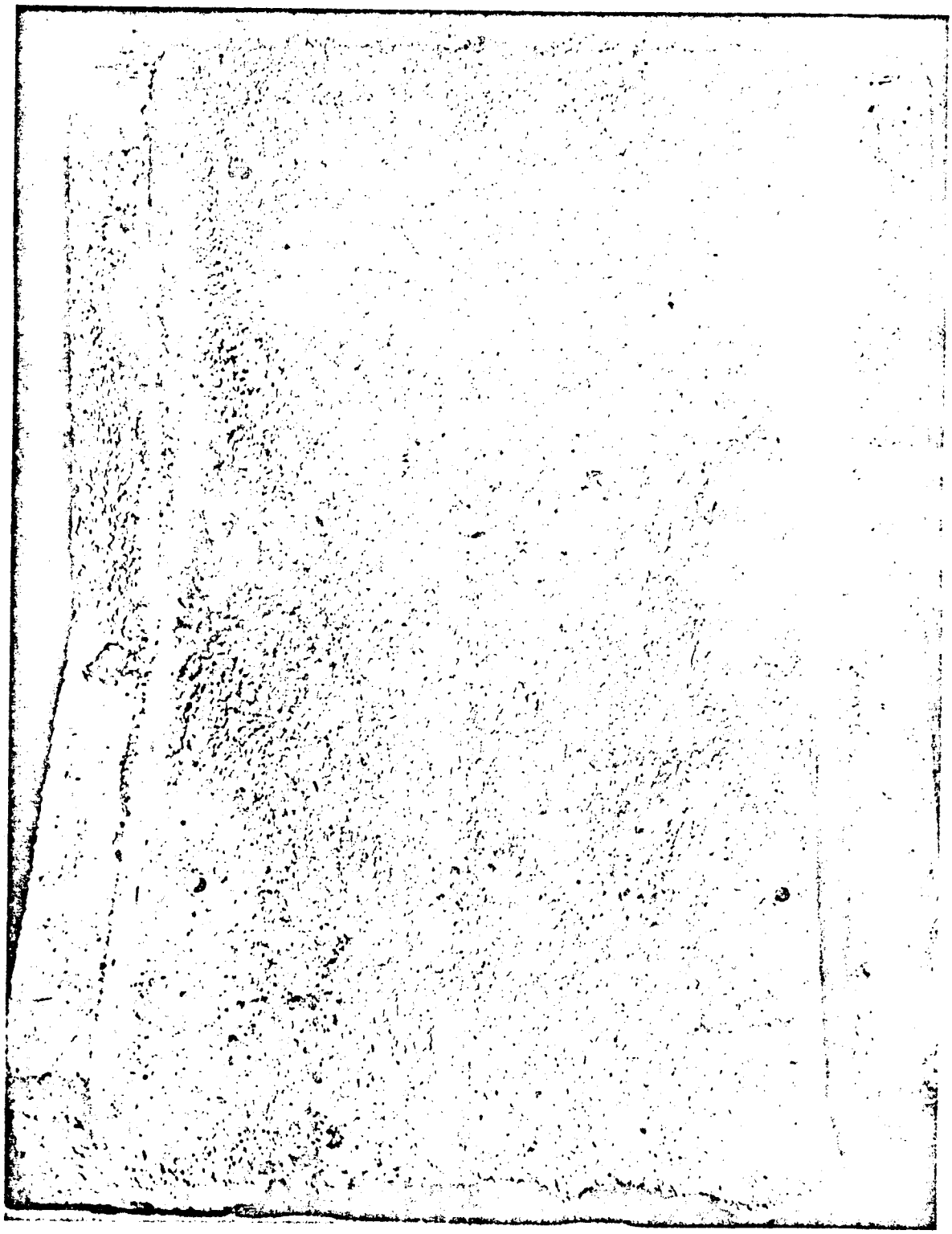

Fig. VII-5 Fondu Fyre-WA-1 Deflector after Firing 10

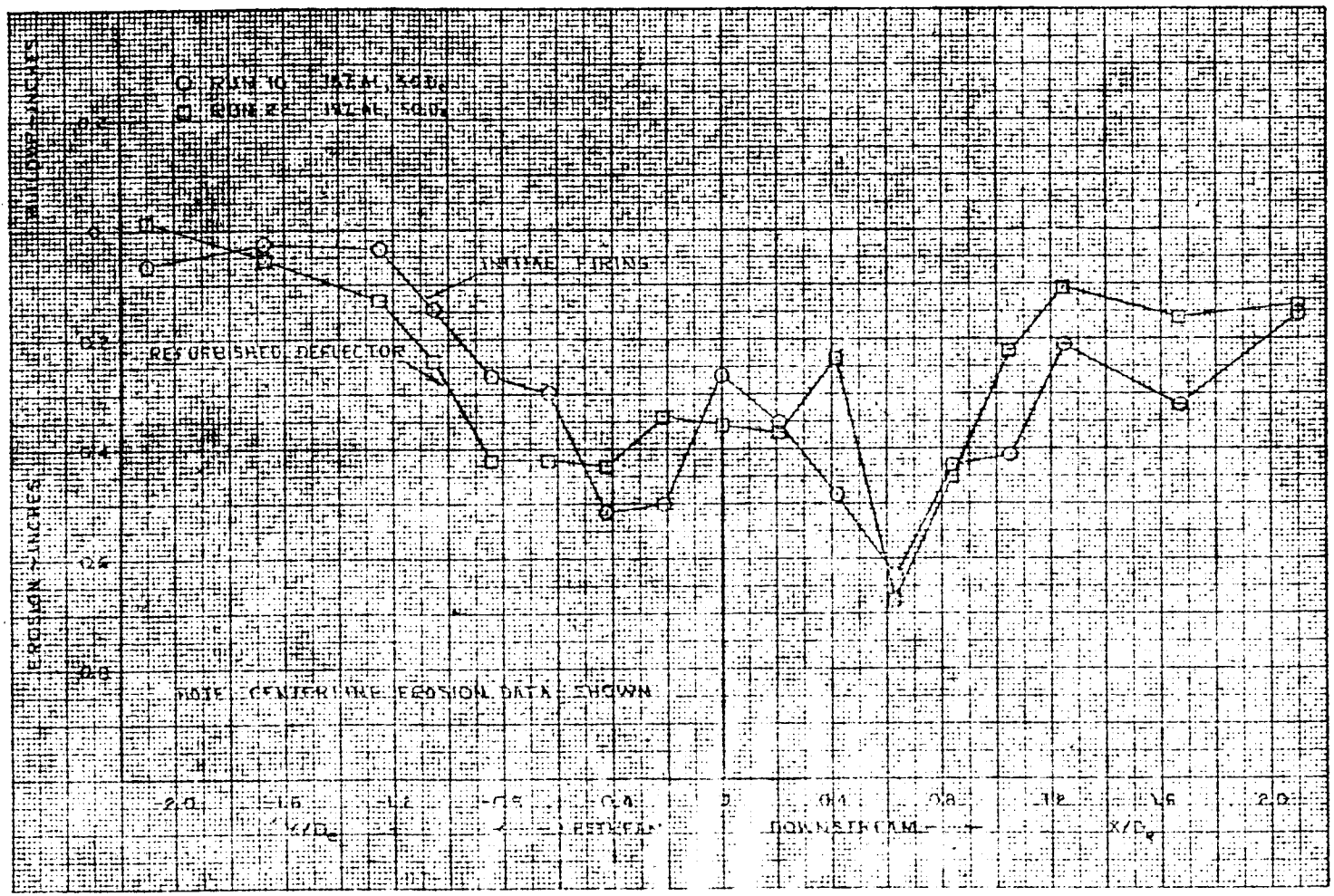

Fig. VII-6 Refurbi he D e r fectiveness

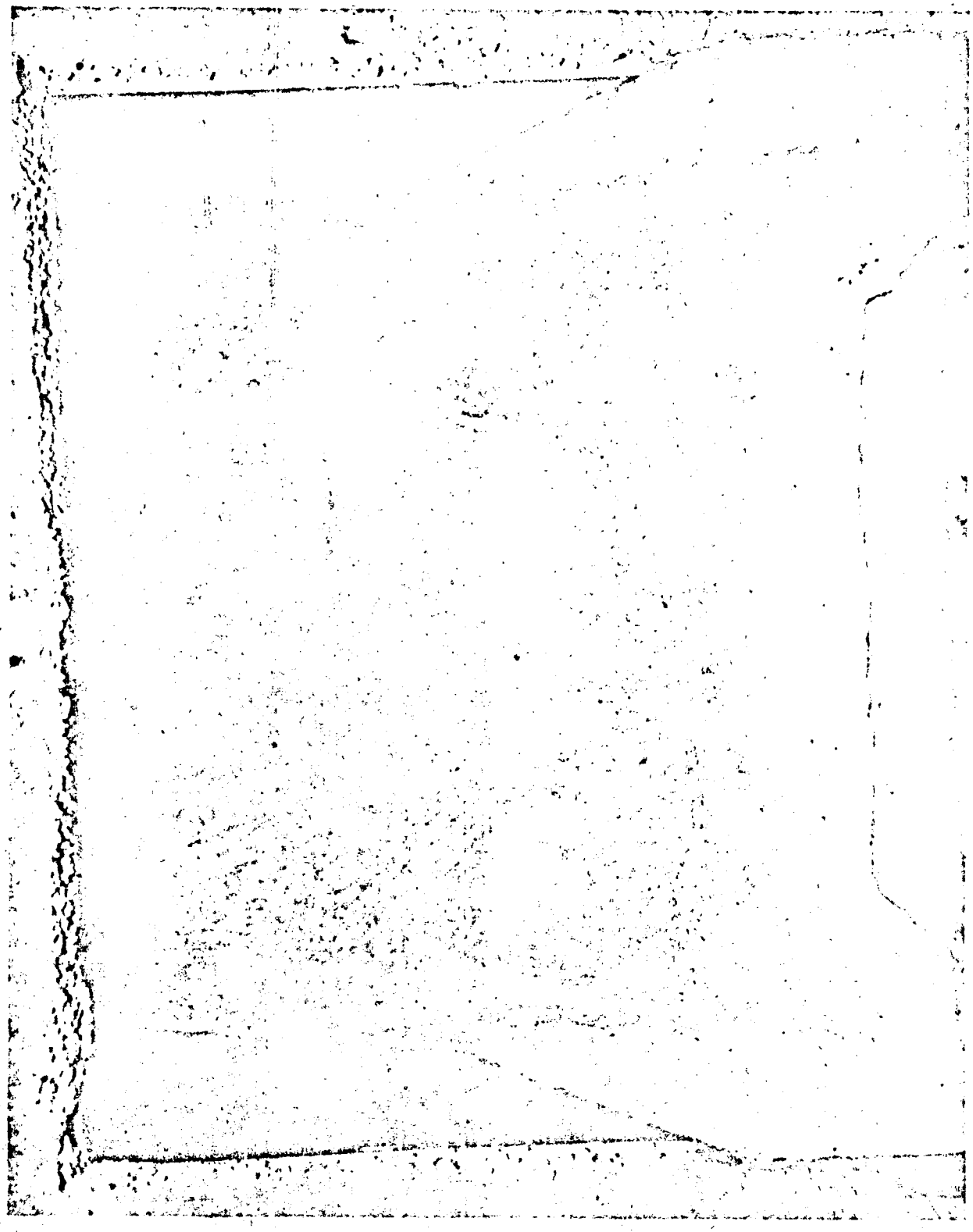

Fig. VII-7 Refurbished Deflector after Firing 22

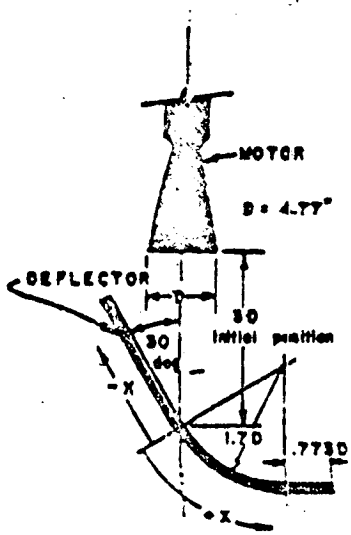

Table VII-1 J Deflector Erosion, Run 15

DEFLECTOR COATING: Fondu Fyre WA-1
LIFT-OFF RATE: 50 lb in 10 sec
GRAIN DATA:
% Al 18 ; ṁ 9.8 lb/sec
P_c (nom) 501 psi

Rocket motor canted 6 degrees in the +Y direction

COMMENTS

1. POUNDS OF DEFLECTOR COATING MATERIAL ERODED = 6.25
2. MAXIMUM EROSION DEPTH = 0.690 in.
3. LOCATION OF MAXIMUM EROSION $\frac{X}{D}$ = +0.63
   $\frac{Y}{D}$ = +0.63
4. COMPRESSIVE STRENGTH OF DEFLECTOR COATING = 9180 psi
5. Hold-down excessive (0.92 sec)

TOP OF DEFLECTOR

X/D	-1.47	-1.05	-0.63	-0.42	-0.21	0	+0.21	+0.42	+0.63	+1.05	+1.47
-2.10	+.010	-.005	+.002	-.010	+.010	+.036	+.048	+.100	+.067	-.020	+.065
-1.67	-.015	-.005	-.002	-.013	+.085	+.088	+.050	-.012	-.015	-.043	.000
-1.25	+.010	-.020	+.080	+.110	+.020	+.110	+.010	-.055	-.065	-.065	+.010
-1.05	+.050	+.015	-.020	+.025	.000	-.062	-.090	-.115	-.113	-.100	-.010
-0.84	+.085	+.050	-.105	-.055	-.170	-.170	-.170	-.135	-.135	-.120	+.010
-0.63	+.140	+.090	+.075	-.135	-.325	-.395	-.335	-.245	-.175	-.175	-.005
-0.42	+.140	+.180	.000	-.175	-.315	-.463	-.415	-.330	-.250	[illegible]	[illegible]
-0.21	+.110	+.125	+.015	-.191	-.313	-.435	-.517	-.450	-.270	[illegible]	[illegible]
℄-0 of motor	+.170	+.285	+.018	-.158	-.220	-.252	-.325	-.388	-.277	-.110	+.010
+0.21	+.140	+.198	-.050	-.200	-.220	-.225	-.335	-.435	-.415	-.200	-.085
+0.42	+.130	+.230	-.085	-.260	-.362	-.290	-.395	-.470	-.560	-.295	-.095
+0.63	+.095	+.165	-.115	-.405	-.470	-.500	-.500	-.565	-.690	-.430	-.095
+0.84	+.015	+.115	-.075	-.185	-.320	-.400	-.457	-.383	-.335	-.320	-.220
+1.05	-.010	+.110	-.082	-.175	-.240	-.405	-.443	-.440	-.357	-.295	-.195
+1.25	-.020	+.120	-.065	-.123	-.152	-.155	-.145	-.247	-.288	-.345	-.215
+1.67	-.050	-.080	-.120	-.190	-.260	-.285	-.275	-.325	-.390	-.265	-.210
+2.10	-.030	-.085	-.127	-.035	-.190	-.175	-.200	-.250	-.240	-.225	-.218

Y/D

℄ of motor

MEASUREMENTS ON DEFLECTOR SURFACE
(- VALUE, EROSION, + VALUE, BUILDUP)

3. Comparison of Erosion on Either Side of Wedge

Figure VIII-5 shows a comparison of erosion occurring on Sides A and B of the wedge used during Run 27. Note the excellent agreement. The data are indicative of the repeatability that can be expected from the SPREE tests providing cart travel is repeatable.

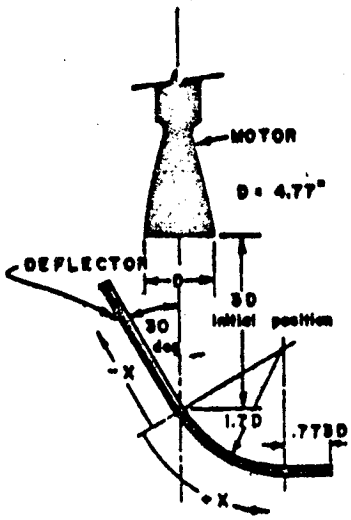

Table VII-2 J Deflector Erosion, Run 17

DEFLECTOR COATING: Fondu-Fyre WA-1
LIFT-OFF RATE: 50 lb in 10 sec
GRAIN DATA:
% AL 18 ; $\dot{m}$ 7.9 lb/sec
P_c (nom) 570 psi

Repeat firing on deflector used for Run #10

COMMENTS

1. POUNDS OF DEFLECTOR COATING MATERIAL ERODED = 5.75
2. MAXIMUM EROSION DEPTH = 0.855 in.
3. LOCATION OF MAXIMUM EROSION $\frac{X}{D}$ = +0.63
   $\frac{Y}{D}$ = -0.42
4. COMPRESSIVE STRENGTH OF DEFLECTOR COATING = 6040 psi

TOP OF DEFLECTOR

X/D	-1.47	-1.05	-0.63	-0.42	-0.21	0	+0.21	+0.42	+0.63	+1.05	+1.47
-2.10	+.035	+.065	+.045	-.010	-.020	+.015	+.070	+.005	+.045	-.010	-.010
-1.67	-.020	-.005	-.050	-.115	-.080	-.090	-.105	-.075	+.065	-.080	-.0[illegible]
-1.25	+.015	-.055	-.055	-.145	-.110	-.200	-.140	-.155	-.070	+.015	-.055
-1.05	-.115	+.050	-.065	-.145	-.225	-.260	-.190	-.140	-.115	-.050	+.090
-0.84	+.055	-.135	-.075	-.110	-.210	-.275	-.245	-.215	-.090	-.035	+.095
-0.63	-.040	-.125	-.060	-.245	-.345	-.535	-.315	-.215	-.095	-.110	+.110
-0.42	-.005	-.125	-.145	-.295	-.350	-.460	-.425	-.315	-.100	-.045	+.140
-0.21	+.055	-.080	-.150	-.390	-.445	-.495	-.475	-.405	-.260	-.090	+.065
℄-0 of motor	-.045	-.175	-.155	-.445	-.630	-.610	-.660	-.585	-.175	-.055	+.265
+0.21	-.010	-.105	-.015	-.425	-.580	-.520	-.465	-.465	-.355	+.025	-.060
+0.42	+.070	+.040	-.310	-.375	-.385	-.375	-.430	-.435	-.455	-.185	-.045
+0.63	-.120	-.025	-.705	-.855	-.725	-.485	-.530	-.525	-.810	-.200	-.040
+0.84	-.075	-.155	-.345	-.680	-.700	-.770	-.810	-.630	-.425	-.110	-.040
+1.05	-.210	-.125	-.195	-.395	-.405	-.500	-.450	-.415	-.265	-.115	-.170
+1.25	-.175	-.080	-.180	-.265	-.495	-.500	-.520	-.390	-.230	-.160	-.130
+1.67	-.195	-.155	-.215	-.220	-.155	-.165	-.140	-.290	-.250	-.155	-.125
+2.10	-.185	-.210	-.360	-.360	-.340	-.415	-.345	-.315	-.385	-.260	-.200

Y/D

℄ of motor

MEASUREMENTS ON DEFLECTOR SURFACE
(- VALUE, EROSION, + VALUE, BUILDUP)

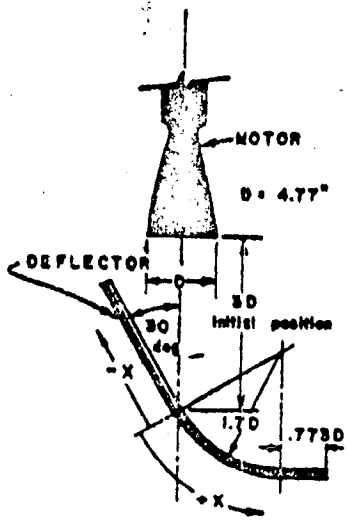

Table VII-3 J Deflector Erosion, Run 21

DEFLECTOR COATING: Harbison-Walker Special Mix 13-65
LIFT-OFF RATE: 50 De in 10 sec,
GRAIN DATA:
% AL 18 ; $\dot{m}$ 8.75 lb/sec
P_c (nom) 573 psi

TOP OF DEFLECTOR

X/D											
- 2.10	+.010	+.050	+.040	-.005	+.005	-.075	+.005	+.030	-.085	+.040	+.020
- 1.67	+.020	.000	-.155	-.085	-.055	-.150	-.095	-.080	+.010	+.030	-.030
- 1.25	-.005	-.035	-.035	-.155	-.285	-.195	-.165	-.140	-.025	+.005	+.010
- 1.05	+.020	-.015	-.075	-.205	-.320	-.370	-.235	-.220	-.125	-.010	.000
- 0.84	+.010	+.020	-.075	-.255	-.350	-.345	-.320	-.185	-.060	-.010	-.035
- 0.63	+.010	-.025	-.130	-.245	-.355	-.315	-.310	-.240	[illegible]	[illegible]	[illegible]
- 0.42	+.005	+.015	-.065	-.275	-.295	-.265	-.260	-.250	-.165	[illegible]	[illegible]
- 0.21	+.160	+.010	-.105	-.185	-.090	-.115	-.095	-.190	-.135	+.075	+.095
℄-0 of motor	+.015	-.030	-.125	-.240	-.335	-.245	-.300	-.240	-.135	-.050	-.025
+ 0.21	.000	-.070	-.235	-.375	-.295	-.325	-.330	-.360	-.245	-.085	-.015
+ 0.42	-.045	-.135	-.260	-.460	-.415	-.425	-.430	-.430	-.195	-.090	[illegible]
+ 0.63	-.010	-.065	-.100	-.240	-.355	-.290	-.275	-.170	-.080	+.035	-.060
+ 0.84	-.065	-.135	-.100	-.125	-.160	-.225	-.255	-.170	-.180	-.115	-.070
+ 1.05	-.120	-.185	-.260	-.175	-.190	-.170	-.180	-.155	-.180	-.145	-.290
+ 1.25	-.105	-.215	-.205	-.185	-.225	-.190	-.160	-.140	-.225	-.155	-.070
+ 1.67	-.045	-.105	-.125	-.120	-.205	-.205	-.125	-.205	-.200	-.145	-.085
+ 2.10	+.020	+.025	-.020	+.015	+.020	-.010	+.020	+.040	.000	+.020	+.035
Y/D	-1.47	-1.05	-0.63	-0.42	-0.21	0	+0.21	+0.42	+0.63	+1.05	+1.47

℄ of motor

MEASUREMENTS ON DEFLECTOR SURFACE
(- VALUE, EROSION, + VALUE, BUILDUP)

COMMENTS

1. POUNDS OF DEFLECTOR COATING MATERIAL ERODED = 4.50
2. MAXIMUM EROSION DEPTH = 0.460 in.
3. LOCATION OF MAXIMUM EROSION $\frac{X}{D}$ = +0.42
   $\frac{Y}{D}$ = -0.42
4. COMPRESSIVE STRENGTH OF DEFLECTOR COATING = 8180 psi
5. Considerable spalling evident

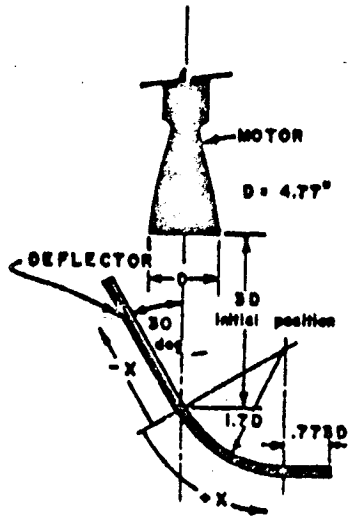

Table VII-4 J Deflector Erosion, Run 22

DEFLECTOR COATING: Fondu-Fyre WA-1 (Refurbished)
LIFT-OFF RATE: 50 De in 10 secs.
GRAIN DATA:
% AL 18, $\dot{m}$ 8.50 lb/sec
P_c (nom) 612 psi

COMMENTS

1. POUNDS OF DEFLECTOR COATING MATERIAL ERODED = 6.50
2. MAXIMUM EROSION DEPTH = 0.730 in.
3. LOCATION OF MAXIMUM EROSION $\frac{X}{D}$ = +0.63
   $\frac{Y}{D}$ = -0.42
4. COMPRESSIVE STRENGTH OF DEFLECTOR COATING = 6040 psi

TOP OF DEFLECTOR

X/D	-1.47	-1.05	-0.63	-0.42	-0.21	0	+0.21	+0.42	+0.63	+1.05	+1.47
-2.10	+.070	+.035	+.010	+.005	+.005	+.015	.000	-.010	+.055	+.045	+.065
-1.67	+.015	+.040	+.020	.000	-.095	-.055	-.025	+.015	+.050	+.040	+.080
-1.25	+.035	+.020	-.120	-.155	-.125	-.130	-.095	-.055	+.055	+.025	[illegible]
-1.05	+.030	-.315	-.010	-.160	-.255	-.240	-.265	-.125	.000	+.030	+.010
-0.84	+.065	+.010	+.110	-.085	-.400	-.420	-.350	-.135	-.105	+.075	+.160
-0.63	+.075	+.005	+.100	-.075	-.390	-.420	-.380	-.115	-.055	+.055	+.110
-0.42	+.165	+.020	-.205	-.395	-.540	-.430	-.275	-.320	-.115	+.115	+.085
-0.21	+.295	-.015	-.310	-.500	-.440	-.340	-.385	-.330	-.150	+.095	+.095
℄ of motor	+.210	+.280	+.200	-.520	-.355	-.355	-.375	-.400	-.240	+.030	+.070
+0.21	+.130	-.075	-.450	-.495	-.340	-.370	-.390	-.525	-.325	-.005	+.040
+0.42	+.090	-.125	-.385	-.450	-.485	-.235	-.435	-.580	-.230	-.065	+.025
+0.63	-.005	-.225	-.345	-.730	-.690	-.675	-.710	-.590	-.315	-.095	+.030
+0.84	-.045	-.140	-.200	-.245	-.420	-.450	-.350	-.260	-.175	-.105	-.105
+1.05	-.050	-.135	-.155	-.205	-.235	-.220	-.215	-.180	-.155	-.050	-.160
+1.25	-.150	-.085	-.125	-.145	-.135	-.105	-.125	-.100	-.130	-.075	-.135
+1.67	-.220	-.050	-.140	-.105	-.140	-.160	-.165	-.170	-.170	-.055	-.135
+2.10	-.180	-.065	-.125	-.105	-.090	-.140	-.125	-.145	-.105	-.165	-.125

Y/D

℄ of motor

MEASUREMENTS ON DEFLECTOR SURFACE
(- VALUE, EROSION; + VALUE, BUILDUP)

VIII. MULTIPLE MOTOR EFFECTS ON DEFLECTORS (GROUP V)

A. GROUP V TECHNICAL OBJECTIVES

Wedge deflector tests were made for two purposes -- to evaluate ridge erosion and to determine the effect of varying initial nozzle-to-deflector standoff distance. Ridge erosion was of interest because of the additive effects of the exhaust plumes impinging on the ridge. Standoff distance was varied because of the continuing need in Saturn improvement studies for information relative to the minimum acceptable standoff distance. Distances of 2.5 and 3.0 D_e were investigated.

As standoff distance is reduced for a given missile-wedge configuration, the wedge ridge gets progressively closer to the missile base until, at some point, the wedge contacts the base. To prevent this from occurring deflector height must be reduced by either increasing the impingement angle or increasing the ridge radius. Unfavorable factors affecting the airborne vehicle can result from an impingement angle increase, making it more desirable to increase the ridge radius. For tests made with the 3.0 D_e nozzle standoff distance, the ridge radius was 0.25 D_e; for the 2.5 D_e nozzle standoff distance tests, ridge radius was increased to 0.50 D_e. The increase in ridge radius reduced deflector height by an amount equal to the 0.50 D_e standoff distance reduction (Fig. VIII-1).

B. TEST ARTICLES

Two wedge deflectors were fabricated by modifying (shortening) the molds used for the J deflectors and making additional molds for the ridges. Wedge deflector base plates were similar to those used for the J deflectors but were also shortened. Both wedges were coated with reinforced Fondu Fyre WA-1, which was poured and cured in accordance with previously discussed practices. Each wedge was instrumented with a thermocouple on the backside of the Fondu Fyre coating. Figure VIII-2 is a wedge schematic.

The wedges were mounted to deflect motor exhaust to either side of the cart. The cart was ballasted (second firing only) to prevent its derailing from thrust loads. Figure VIII-3 shows the wedge deflector mounted on the cart.

C. TEST PROCEDURE

Base plates for each side of the wedge and the ridge were weighed before coating. Coated parts were weighed before and after testing. The grid established on the deflectors was similar to that established on the J deflectors and the target was at the same point relative to the tangency between curved and straight surfaces (0.06 D_e up along the deflector centerline). The distance between targets equaled the distance between rocket motor centerlines (16.25 in. or 3.40 D_e).

Runs were made at a 50 D_e in 10 sec separation rate with a 0.2 sec holddown. The procedure was similar to that employed for J deflector tests except that the pretensioning load established before testing was doubled. This was because of the greater thrust loads on the cart system from the two motors firing simultaneously.

D. TEST RESULTS

1. Ridge Erosion

Ridge erosion on the two tests was minimal. There was no measurable nose cap weight loss as a result of Firing 26 and a 0.50-lb weight loss was recorded as a result of Firing 27. From this it can be concluded that contemporary rocket motors separated 3.4 nozzle exit diameters laterally and firing parallel to each other do not present a centerline exhaust environment sufficiently severe to require the taking of special precautions for ridge protection. The ridge may be protected by the same coating as that used on the deflector.

2. Nozzle-to-Deflector Standoff Distance

The effect of varying initial nozzle-to-deflector standoff distance is shown in Fig. VIII-4 and Tables VIII-1 and VIII-2. As would be expected more erosion occurred for the smaller standoff distance (2.5 D_e). Erosion for the smaller standoff distance was not severe, however. Run 26 data are somewhat questionable since the cart derailed after approximately 6 ft of travel. The cart continued accelerating satisfactorily after derailment and misalignment was minimum, however.

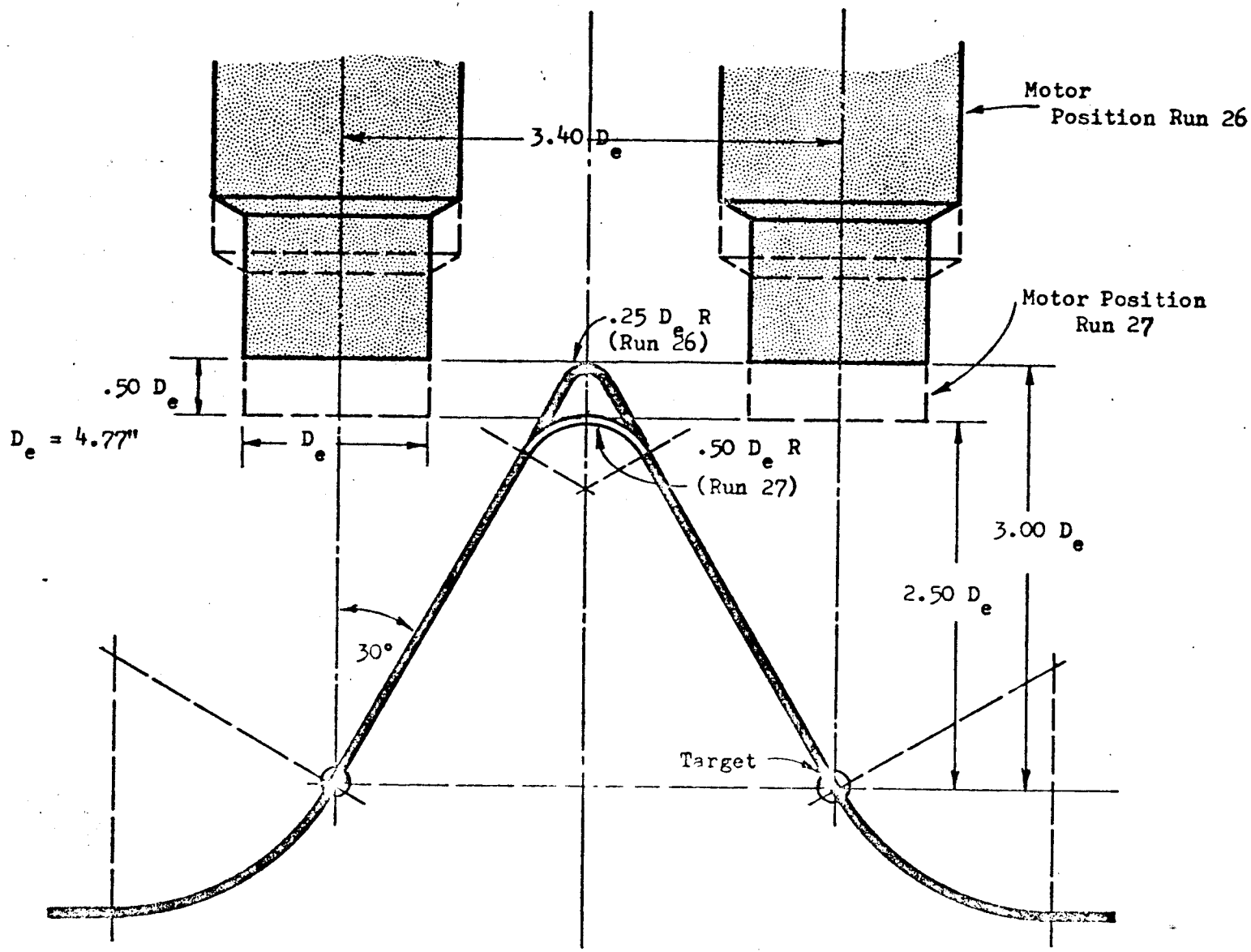

Fig. VIII-1 Wedge Deflector Used for Runs 26 and 27

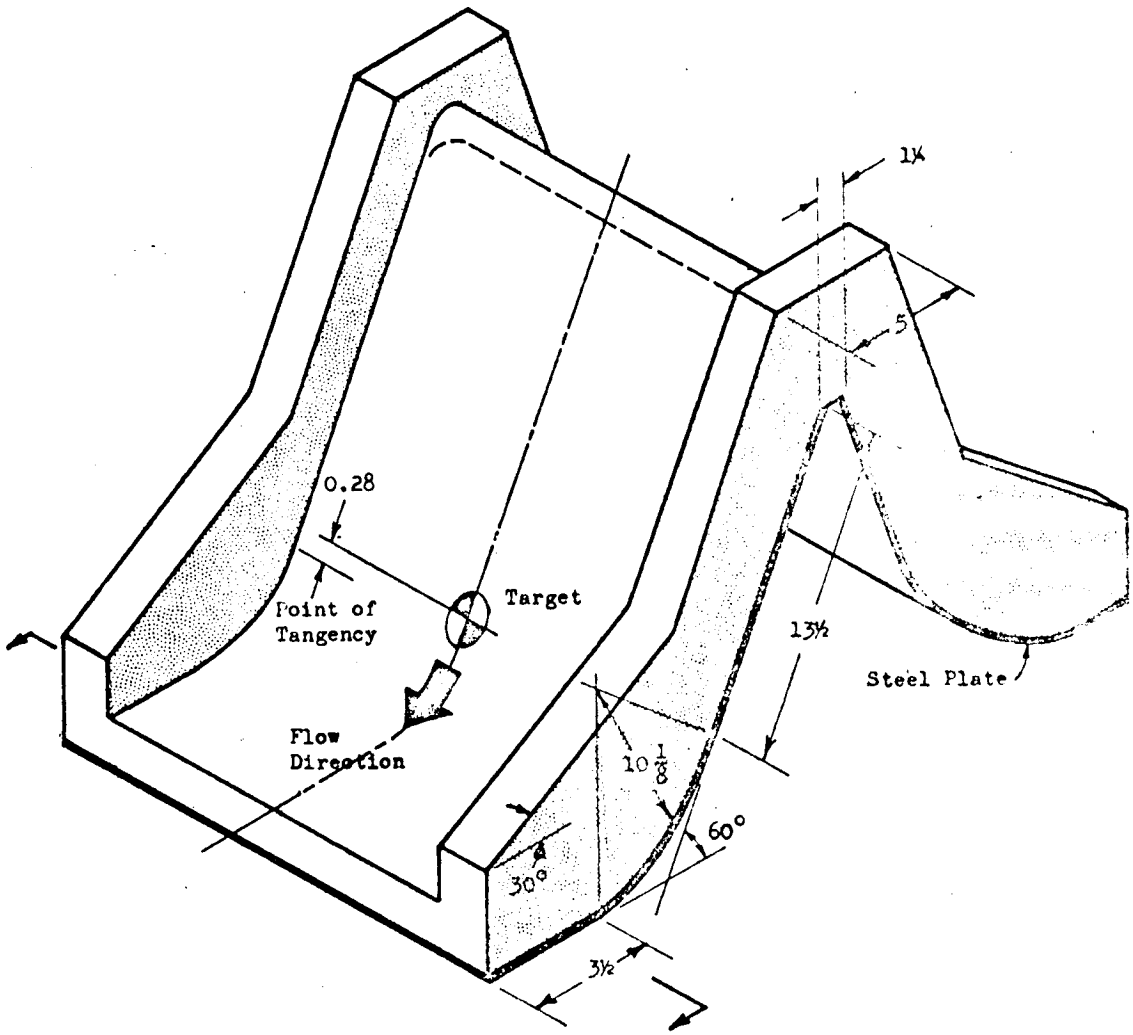

Note: All dimensions in inches

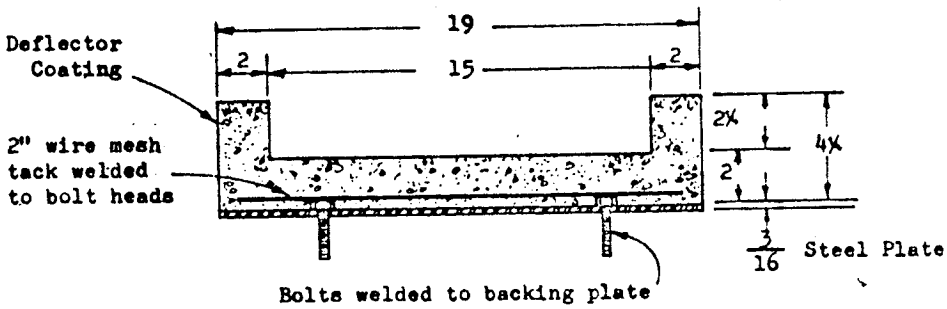

Fig. VIII-2 Wedge Deflector

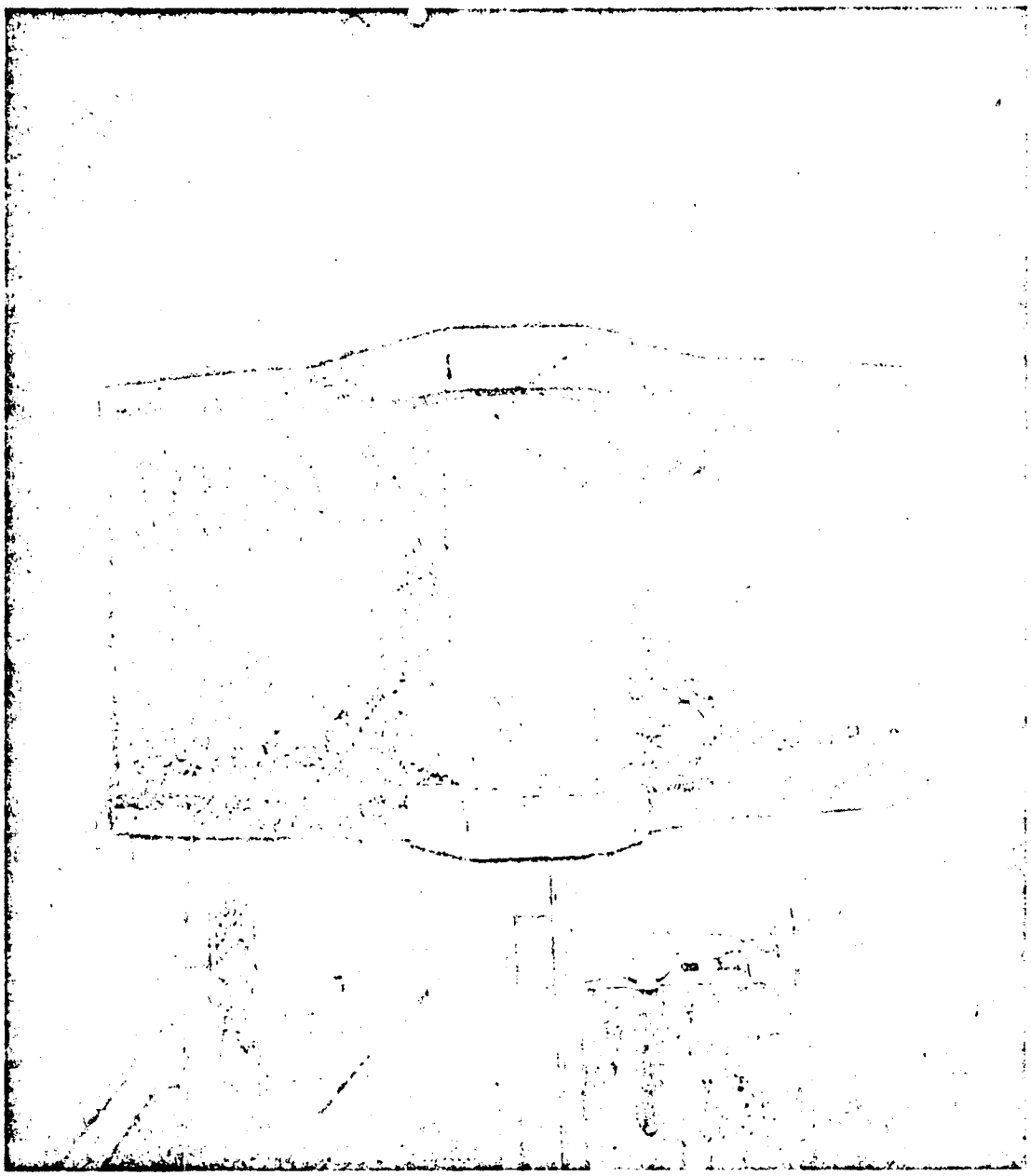

Fig. VIII-3 Wedge Deflector after Firing 27

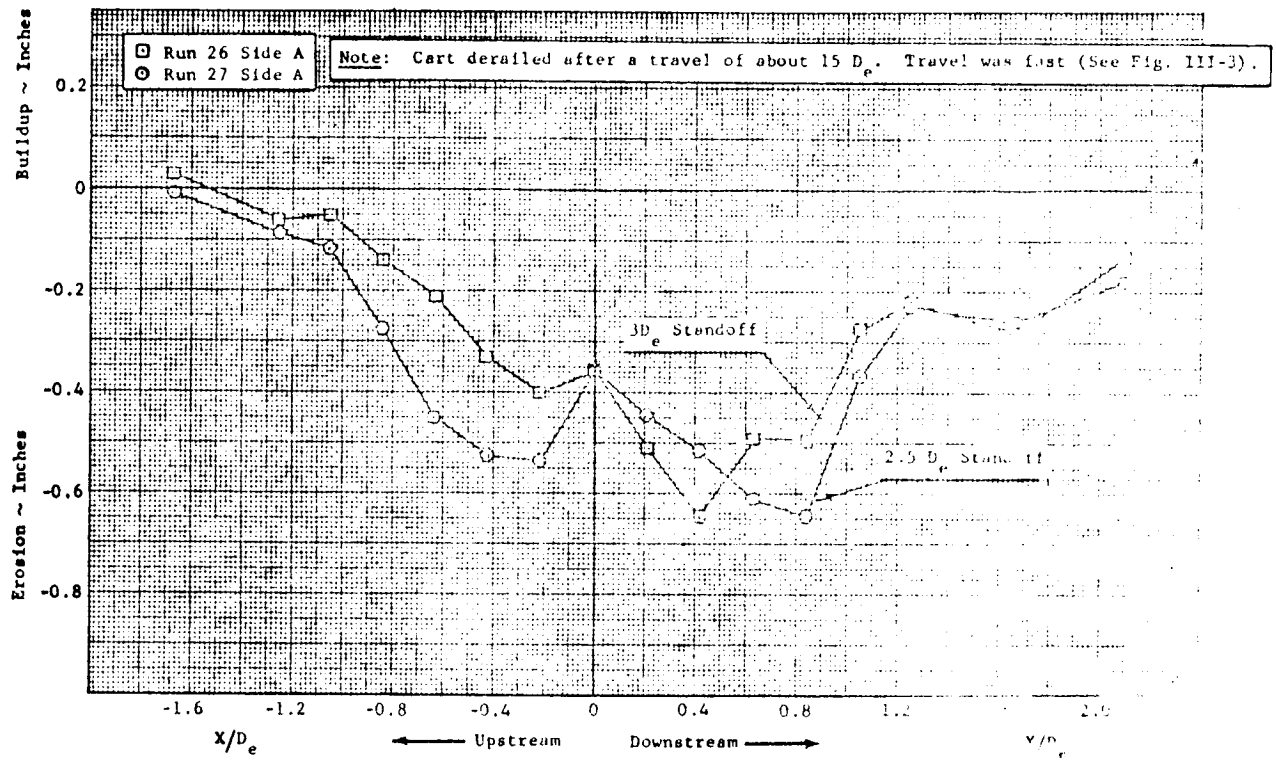

Fig. VIII-4 Effect of Varying Initial Nozzle-to-Deflector Standoff Distance

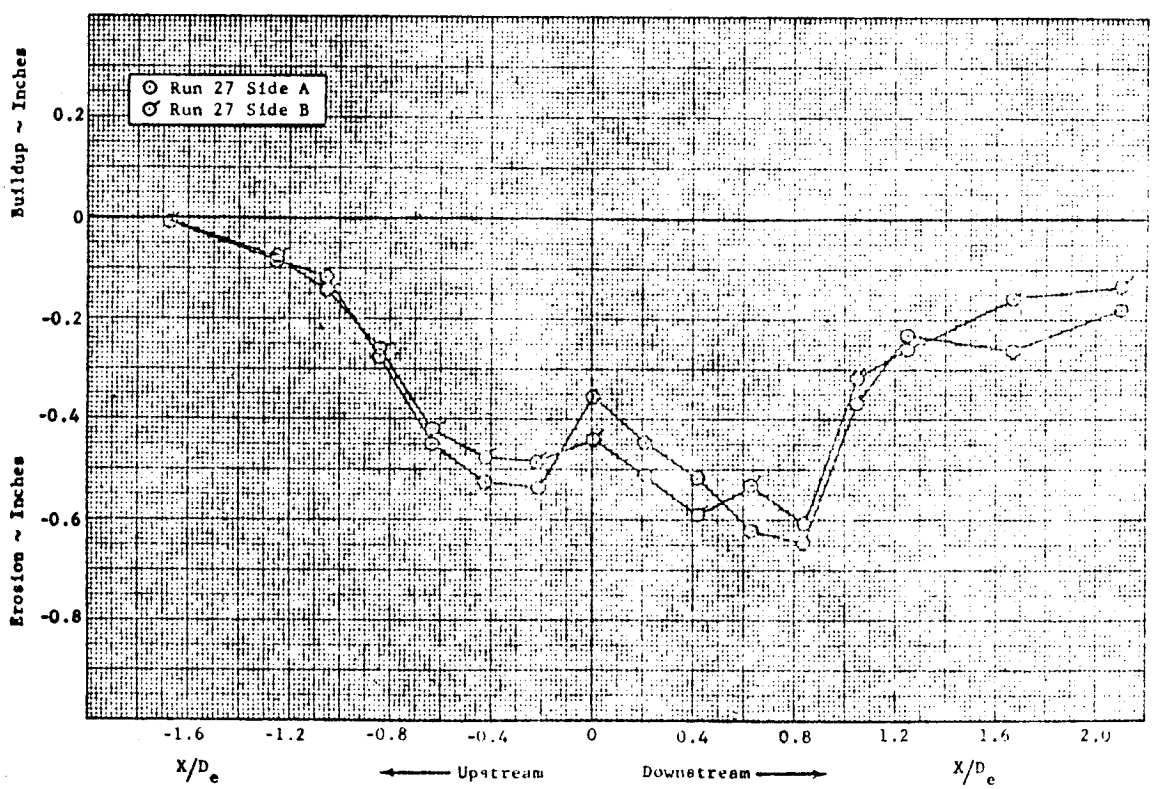

Fig. VIII-5 Data Repeatability as Illustrated by a Comparison of Wedge Deflector Centerline Erosion Profiles

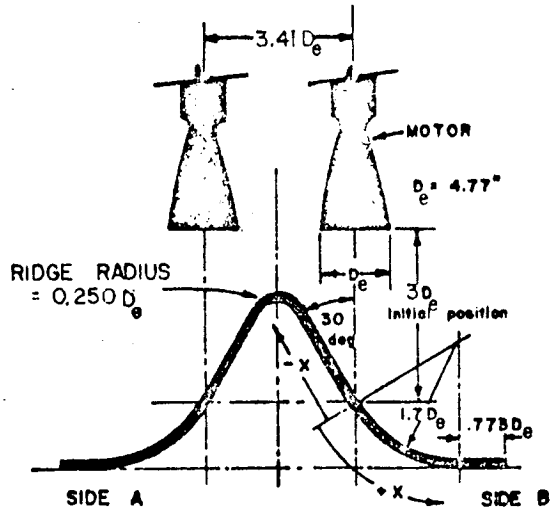

Table VIII-1 Wedge Deflector Erosion, Run 26, Side A and Side B

Side A

Deflector Coating: Fondu Fyre WA-1
Lift-Off Rate: 50 De in 10 sec
Grain Data:
% AL 18: m 8.02 lb/sec
P_c (nom) 593 psi

COMMENTS

1. POUNDS OF DEFLECTOR COATING MATERIAL ERODED = 5.00
2. MAXIMUM EROSION DEPTH = 0.650 in.
3. LOCATION OF MAXIMUM EROSION $\frac{X}{D}$ = +0.42
   $\frac{Y}{D}$ = -0.21
4. COMPRESSIVE STRENGTH OF DEFLECTOR COATING = 5260 psi
5. The cart derailed after approximately 6 ft of travel
6. Nose cap weight loss = 0 lbs.

TOP OF DEFLECTOR

X/D											
	+.040	+.035	-.010	-.045	+.045	+.030	+.010	-.010	-.045	+.025	-.015
- 1.67	+	+	+	+	+	+	+	+	+	+	+
	+.030	+.020	-.080	-.045	-.090	-.060	+.005	+.010	+.010	+.055	+.035
- 1.25	+	+	+	+	+	+	+	+	+	+	+
	-.005	-.010	-.080	-.120	-.140	-.050	-.070	-.030	+.015	+.010	+.050
- 1.05	+	+	+	+	+	+	+	+	+	+	+
	+.025	-.055	-.270	-.240	-.270	-.140	-.110	-.060	-.005	+.040	+.040
- 0.84	+	+	+	+	+	+	+	+	+	+	+
	+.035	-.005	-.215	-.270	-.350	-.210	-.140	.000	+.020	+.020	+.060
- 0.63	+	+	+	+	+	+	+	+	+	+	+
	-.010	-.090	-.295	-.370	-.420	-.330	-.225	-.060	+.020	.000	+.040
- 0.42	+	+	+	+	+	+	+	+	+	+	+
	-.060	-.040	-.280	-.390	-.390	-.400	-.230	-.150	-.100	-.010	-.015
- 0.21	+	+	+	+	+	+	+	+	+	+	+
	-.015	-.060	-.280	-.340	-.370	-.360	-.310	-.095	+.065	+.105	+.070
— ℄ —	+	+	+	+	+	+	+	+	+	+	+
of motor											
	-.125	-.195	-.460	-.495	-.485	-.510	-.475	-.260	-.125	.000	+.025
+ 0.21	+	+	+	+	+	+	+	+	+	+	+
	-.065	-.270	-.645	-.640	-.650	-.645	-.570	-.330	-.170	-.030	+.045
+ 0.42	+	+	+	+	+	+	+	+	+	+	+
	-.080	-.225	-.475	-.480	-.575	-.490	-.405	-.295	-.145	-.010	+.055
+ 0.63	+	+	+	+	+	+	+	+	+	+	+
	-.085	-.240	-.350	-.505	-.525	-.495	-.435	-.310	-.125	-.010	+.050
+ 0.84	+	+	+	+	+	+	+	+	+	+	+
	-.115	-.185	-.245	-.305	-.330	-.275	-.235	-.175	-.130	-.015	+.040
+ 1.05	+	+	+	+	+	+	+	+	+	+	+
	-.130	-.145	-.235	-.290	-.245	-.225	-.150	-.125	-.075	-.045	-.035
+ 1.25	+	+	+	+	+	+	+	+	+	+	+
	-.130	-.180	-.265	-.295	-.280	-.280	-.245	-.215	-.150	-.100	-.095
+ 1.67	+	+	+	+	+	+	+	+	+	+	+
+ 2.10	-.080	-.120	-.105	-.120	-.135	-.130	-.145	-.125	-.135	[illegible]	[illegible]
	+0.21	+0.42	+0.63	+1.05	+1.47		-1.47	-1.05	-0.63	-0.42	-0.[illegible]

0
℄ of motor

MEASUREMENTS ON DEFLECTOR SURFACE
(- VALUE, EROSION, + VALUE, BUILDUP)

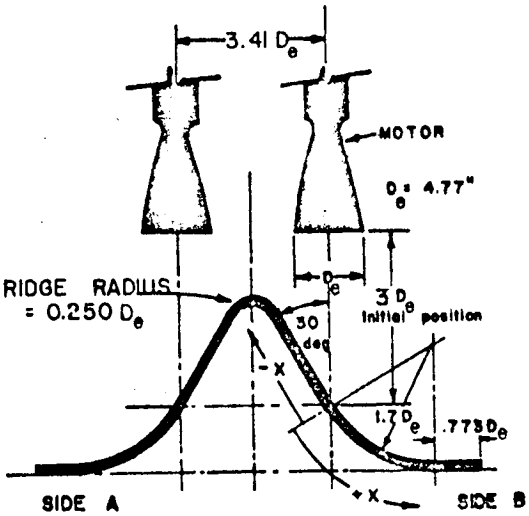

Table VIII-1 (concl)

Side B

Deflector Coating: Fondu-Fyre WA-1
Lift-Off Rate: 50 De in 10 sec
Grain Data:
% AL 18: m 8.43 lb/sec
P_c (nom) 585 psi

COMMENTS

1. POUNDS OF DEFLECTOR COATING MATERIAL ERODED = 5.50
2. MAXIMUM EROSION DEPTH = 0.800 in.
3. LOCATION OF MAXIMUM EROSION $\frac{X}{D}$ = +0.42
   $\frac{Y}{D}$ = +0.42
4. COMPRESSIVE STRENGTH OF DEFLECTOR COATING = 5260 psi

TOP OF DEFLECTOR

X/D											
- 1.67	-.010 +	+.035 +	+.025 +	-.005 +	-.030 +	-.035 +	-.045 +	-.035 +	-.015 +	-.025 +	+.095 +
- 1.25	-.035 +	-.045 +	-.020 +	-.040 +	-.030 +	-.060 +	-.120 +	-.115 +	-.060 +	-.065 +	+.055 +
- 1.05	-.025 +	-.045 +	-.040 +	-.040 +	-.070 +	-.095 +	-.155 +	-.075 +	-.065 +	-.035 +	+.050 +
- 0.84	+.040 +	-.015 +	-.030 +	-.040 +	-.120 +	-.150 +	-.255 +	-.180 +	-.150 +	-.065 +	-.010 +
- 0.63	-.050 +	-.030 +	-.060 +	-.055 +	-.065 +	-.150 +	-.190 +	-.165 +	-.135 +	-.100 +	-.025 +
- 0.42	-.025 +	+.010 +	-.070 +	-.075 +	-.105 +	-.230 +	-.340 +	-.355 +	-.345 +	-.135 +	.000 +
- 0.21	-.050 +	-.085 +	-.050 +	-.025 +	-.230 +	-.320 +	-.445 +	-.480 +	-.245 +	-.045 +	+.055 +
℄-0	-.015 +	+.050 +	+.025 +	-.100 +	-.265 +	-.375 +	-.440 +	-.460 +	-.360 +	-.040 +	+.050 +
℄ of motor + 0.21	+.015 +	+.045 +	-.075 +	-.165 +	-.305 +	-.465 +	-.455 +	-.425 +	-.425 +	-.090 +	+.030 +
+ 0.42	+.080 +	-.035 +	-.215 +	-.255 +	-.485 +	-.630 +	-.695 +	-.800 +	-.655 +	-.220 +	-.070 +
+ 0.63	.000 +	-.015 +	-.140 +	-.265 +	-.550 +	-.655 +	-.610 +	-.555 +	-.495 +	-.165 +	-.095 +
+ 0.84	+.090 +	+.170 +	-.100 +	-.360 +	-.405 +	-.610 +	-.600 +	-.575 +	-.480 +	-.150 +	-.040 +
+ 1.05	-.030 +	.000 +	-.140 +	-.180 +	-.400 +	-.380 +	-.510 +	-.570 +	-.515 +	-.140 +	-.070 +
+ 1.25	-.135 +	-.015 +	-.060 +	-.110 +	-.165 +	-.225 +	-.245 +	-.305 +	-.410 +	-.100 +	-.165 +
+ 1.67	-.050 +	-.100 +	-.130 +	-.195 +	-.150 +	-.195 +	-.185 +	-.235 +	-.105 +	-.135 +	-.145 +
+ 2.10	-.125 +0.21	-.130 +0.42	-.110 +0.63	-.105 +1.05	-.150 +1.47	-.120 -1.47	-.140 -1.05	-.105 -0.63	-.030 -0.42	-.080 -0.21	-.165

0
℄ of motor

MEASUREMENTS ON DEFLECTOR SURFACE
(- VALUE, EROSION, + VALUE, BUILDUP)

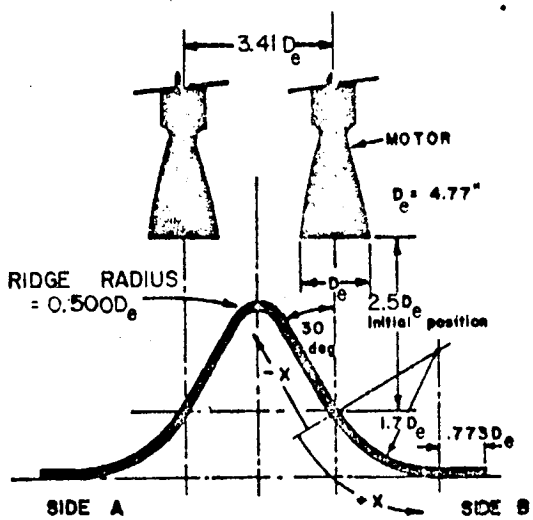

Table VIII-2 Wedge Deflector Erosion, Run 27, Side A and Side B

Side A

Deflector Coating: Fondu Fyre WA-1
Lift-Off Rate: 50 De in 10 sec.
Grain Data:
% AL 18: in 7.64 lb/sec
P_c (nom) 580 psi

COMMENTS

1. POUNDS OF DEFLECTOR COATING MATERIAL ERODED = 5.00 lb
2. MAXIMUM EROSION DEPTH = 0.660 in.
3. LOCATION OF MAXIMUM EROSION $\frac{X}{D}$ = +0.63
   $\frac{Y}{D}$ = -0.21
4. COMPRESSIVE STRENGTH OF DEFLECTOR COATING = 5420 psi
5. Nose cap weight loss = 0.50 lbs.

TOP OF DEFLECTOR

X/D											
- 1.67	-.005 +	-.035 +	-.030 +	-.015 +	-.020 +	-.005 +	+.015 +	+.015 +	+.030 +	+.100 +	+.095 +
- 1.25	-.020 +	-.090 +	-.105 +	-.095 +	-.060 +	-.085 +	-.055 +	+.005 +	+.035 +	+.120 +	+.060 +
- 1.05	+.010 +	-.145 +	-.060 +	-.095 +	-.095 +	-.115 +	-.055 +	-.030 +	+.055 +	+.075 +	+.055 +
- 0.84	-.015 +	-.020 +	-.025 +	-.110 +	-.195 +	-.275 +	-.180 +	-.120 +	-.010 +	+.025 +	-.050 +
- 0.63	-.030 +	-.030 +	-.075 +	-.220 +	-.325 +	-.450 +	-.370 +	-.185 +	-.105 +	+.005 +	-.015 +
- 0.42	-.025 +	-.045 +	-.085 +	-.340 +	-.475 +	-.525 +	-.515 +	-.360 +	-.120 +	+.010 +	.000 +
- 0.21	-.030 +	-.050 +	-.110 +	-.440 +	-.505 +	-.535 +	-.505 +	-.365 +	.000 +	.000 +	-.020 +
℄-0 of motor	-.080 +	-.025 +	-.160 +	-.355 +	-.425 +	-.355 +	-.535 +	-.445 +	-.205 +	+.020 +	-.020 +
+ 0.21	-.085 +	-.080 +	-.315 +	-.305 +	-.400 +	-.445 +	-.470 +	-.535 +	-.325 +	-.010 +	+.045 +
+ 0.42	-.080 +	-.070 +	-.460 +	-.640 +	-.565 +	-.515 +	-.425 +	-.640 +	-.430 +	+.010 +	+.085 +
+ 0.63	-.085 +	-.150 +	-.360 +	-.520 +	-.660 +	-.620 +	-.620 +	-.610 +	-.385 +	-.135 +	-.100 +
+ 0.84	-.095 +	-.080 +	-.260 +	-.520 +	-.615 +	-.645 +	-.620 +	-.560 +	-.300 +	-.115 +	-.095 +
+ 1.05	-.050 +	-.160 +	-.190 +	-.265 +	-.355 +	-.365 +	-.405 +	-.325 +	-.240 +	-.150 +	-.070 +
+ 1.25	-.135 +	-.150 +	-.215 +	-.260 +	-.210 +	-.230 +	-.250 +	-.260 +	-.225 +	-.200 +	-.155 +
+ 1.67	-.090 +	-.130 +	-.255 +	-.245 +	-.230 +	-.260 +	-.225 +	-.265 +	-.310 +	-.155 +	-.150 +
+ 2.10	-.090 +0.21	-.155 +0.42	-.125 +0.63	-.150 +1.05	-.090 +1.47	-.180	-.185 -1.47	-.125 -1.05	-.190 -0.63	-.185 -0.42	-.180 -0.21

0
℄ of motor

MEASUREMENTS ON DEFLECTOR SURFACE
(- VALUE, EROSION, + VALUE, BUILDUP)

IX. MOTOR EXHAUST PLUME CHARACTERISTICS (GROUP VI)

Considerable analytical work has been done toward defining the temperature and pressure distributions in aluminized solid propellant rocket motor exhaust plumes. There has been little experimental verification of this work, however, because of the difficulty of probing the plumes. The high temperature erosive expellant from aluminized solids has presented a formidable environment for even the best designed temperature-pressure rakes and the alumina particles have clogged pressure tubes and distorted thermocouple readings. The planned use of a propellant containing only 7% aluminum for the SPREE Group II tests presented a plume probe opportunity with reasonable success assurance. Consequently, the Group VI test series was incorporated into the SPREE program.

A. OBJECTIVE

The objective of the Group VI tests was to make traversing plume probes of two single and one dual motor firing. The first single plume probe was to establish temperature and pressure limits and generally explore possible measurement or rake problems. Improved measurement accuracy was expected on subsequent probes. Another objective was to obtain data in the merging plume area for comparison with single plume data and to provide an insight into how the temperatures and pressures add.

B. TEST ARTICLES

Two rakes were fabricated for Group VI tests, one 24-in. long and the other 42-in. long. Both were 1-in. thick and had a 0.5-in. nose radius. The shorter rake was for the single plume probes and was instrumented with eight pressure pickups and eight thermocouples. Four of the thermocouples were tungsten-tungsten rhenium and four chromel-alumel. The longer rake for the dual plume probe was instrumented with 13 pressure pickups and 13 thermocouples, nine of which were tungsten-tungsten rhenium. The remaining were chromel-alumel. Figures IX-1 and IX-2 are rake sketches showing pressure and temperature pickup locations and designations.

Each rake consisted of a steel core protected by a graphite shield. All instrumentation leads and pressure tubes exited from the end farthest from the plume centerline. Pressure transducers were housed in a box attached to the cart near the rake end. Pressure tube lengths were minimized to cut down lag. Each transducer was wrapped in acoustic deadening material to reduce responses from noise. Galvanometers having a 6-cps response were used for pressure readout. Figures IX-3 and IX-4 show the rake installations on the cart.

Rocket motors for the dual plume probe were placed side by side with parallel thrust axes 16.25-in. apart. Figure IX-5 shows the motors firing during Run 25.

C. TEST PROCEDURE

The first single plume probe was made by cantilevering the rake from a holding fixture at the edge of the cart. This fixture was affixed so that the rake leading edge was just 8 D_e from the exit of the rocket motor nozzle when the cart was drawn up against the stops. Swing arm gearing was the same as that used for the 50 D_e in 10-sec runs. The motor ignition switch was positioned for a 0.2-sec holddown. Thus cart travel for the first plume probe, and in fact for all three probes, was 47 D_e in 9.8 sec. Travel at this rate minimized the effect of pressure sensing lag since the cart was moving slowly when the pressures were changing most rapidly. Cart speed, on the other hand, was rapid enough to allow good plume coverage. It was not necessary to pretension the holdback cable since thrust loads on the cart were light.

During the first firing (Run 23), the graphite shielding was stripped from the tip of the rake (Fig. IX-6), and the rake was bent slightly downward and aft. Since the steel core was exposed at the tip, it was theorized that gases got between the core and the shield creating thermal and mechanical stresses that cracked the graphite.

A new graphite shield that extended beyond and completely covered the core tip was fabricated for Run 24. In addition, the rake was braced at the center with steel angle iron. The angle iron was thermally protected. The initial position of the rake was again set at 8 D_e, and the motor ignition switch was set for a 0.2-sec holddown.

Figure IX-7 is a Run 24 postfiring photograph. Note that again the rake tip was lost and the steel supporting members were burned through.

Because of the tip failure, the rake for the two-plume probe (Run 25) was set at an initial position 12 D_e from the nozzle exit. The two supports extending into the plume were 1-in. heavy wall steel pipe. The pipe was thermally protected by 3/4 in. thick panelyte, the same material used for the rocket motor nozzle entrance rings. Figure IX-4 is a Run 25 prefiring photograph. The postfiring condition of the rake is shown in Fig. IX-8.

D. TEST RESULTS

1. Single Plume Probes

Despite what appears to be serious rake damage, there was only one instrumentation dropout during Run 23 and two dropouts during Run 24, and good pressure and temperature data were obtained. The pressure data are shown in Fig. IX-9 as isobars that have been nondimensionalized to broaden the scope of applicability. The isobars represent ratios of measured pressure in psi above atmospheric to chamber pressure in absolute units. Exhaust plume stagnation pressures can be evaluated by simply multiplying the ratios given by chamber pressure. The data are applicable for chamber pressures ranging from 500 to 750 psia.

Exhaust plume temperature data as obtained by each one of the thermocouples are given in Fig. IX-10. Isotherms are shown in Fig. IX-11. The isobars and isotherms were obtained by averaging data from Runs 23 and 24.

2. Dual Plume Probe

While the rocket motors were placed as close together as physically possible for the dual plume probe (3.40 D_e) apart center-to-center, the plumes were too far apart laterally to intermix to any great extent and the temperature and pressure environment at the cluster centerline was much less severe than the environment at the centerline of individual plumes. This fact is depicted in the isobars and isotherms shown in Fig. IX-12 and IX-13.

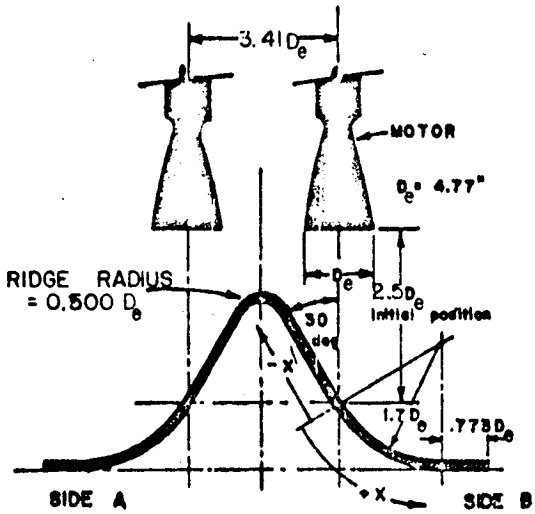

Table VIII-2 (concl)

Side B

Deflector Coating: Fondu Fyre WA-1
Lift-Off Rate: 50 De in 10 sec
Grain Data:
% AL 18: in 7.42 lb/sec
P_c (nom) 560 psi

COMMENTS

1. POUNDS OF DEFLECTOR COATING MATERIAL ERODED = 4.25 lb
2. MAXIMUM EROSION DEPTH = 0.730 in.
3. LOCATION OF MAXIMUM EROSION $\frac{X}{D}$ = +0.42
   $\frac{Y}{D}$ = -0.42
4. COMPRESSIVE STRENGTH OF DEFLECTOR COATING = 5420 psi

TOP OF DEFLECTOR

X/D											
	+.105	+.060	+.010	+.010	-.005	-.055	+.005	-.010	+.040	+.035	+.030
- 1.67	+	+	+	+	+	+	+	+	+	+	+
	+.085	-.025	-.045	-.015	-.045	-.075	-.110	-.065	-.040	-.040	.000
- 1.25	+	+	+	+	+	+	+	+	+	+	+
	+.065	.000	-.050	-.085	-.090	-.145	-.130	-.055	-.035	-.025	-.040
- 1.05	+	+	+	+	+	+	+	+	+	+	+
	-.045	-.060	-.060	-.140	-.215	-.260	-.255	-.095	-.045	-.030	.000
- 0.84	+	+	+	+	+	+	+	+	+	+	+
	-.050	-.045	-.090	-.250	-.360	-.420	-.365	-.240	-.110	-.040	-.070
- 0.63	+	+	+	+	+	+	+	+	+	+	+
	-.015	+.005	-.105	-.310	-.455	-.475	-.425	-.270	-.080	-.040	-.055
- 0.42	+	+	+	+	+	+	+	+	+	+	+
	-.015	-.035	-.135	-.375	-.505	-.485	-.515	-.345	-.090	-.010	-.085
- 0.21	+	+	+	+	+	+	+	+	+	+	+
	-.080	-.020	-.115	-.435	-.520	-.440	-.445	-.345	-.050	+.005	-.065
— ℄-0 — of motor	+	+	+	+	+	+	+	+	+	+	+
	+.025	-.020	-.195	-.515	-.490	-.510	-.530	-.570	-.330	-.105	-.065
+ 0.21	+	+	+	+	+	+	+	+	+	+	+
	+.020	-.075	-.635	-.730	-.610	-.590	-.605	-.680	-.330	-.065	.000
+ 0.42	+	+	+	+	+	+	+	+	+	+	+
	+.015	-.025	-.210	-.560	-.495	-.530	-.565	-.470	-.185	+.010	-.005
+ 0.63	+	+	+	+	+	+	+	+	+	+	+
	-.040	-.065	-.210	-.385	-.590	-.605	-.635	-.510	-.245	-.035	.000
+ 0.84	+	+	+	+	+	+	+	+	+	+	+
	-.060	-.080	-.185	-.245	-.290	-.315	-.305	-.290	-.210	-.075	+.025
+ 1.05	+	+	+	+	+	+	+	+	+	+	+
	-.035	-.130	-.205	-.260	-.250	-.260	-.335	-.215	-.140	-.125	-.060
+ 1.25	+	+	+	+	+	+	+	+	+	+	+
	-.190	-.165	-.250	-.300	-.315	-.155	-.300	-.300	-.305	-.130	-.075
+ 1.67	+	+	+	+	+	+	+	+	+	+	+
+ 2.10	-.115	-.180	-.130	-.090	-.185	-.135	-.115	-.100	-.115	-.090	-.135
Y/D	+0.21	+0.42	+0.63	+1.05	+1.47		-1.47	-1.05	-0.63	-0.42	-0.21

0
℄ of motor

MEASUREMENTS ON DEFLECTOR SURFACE
(- VALUE, EROSION, + VALUE, BUILDUP)

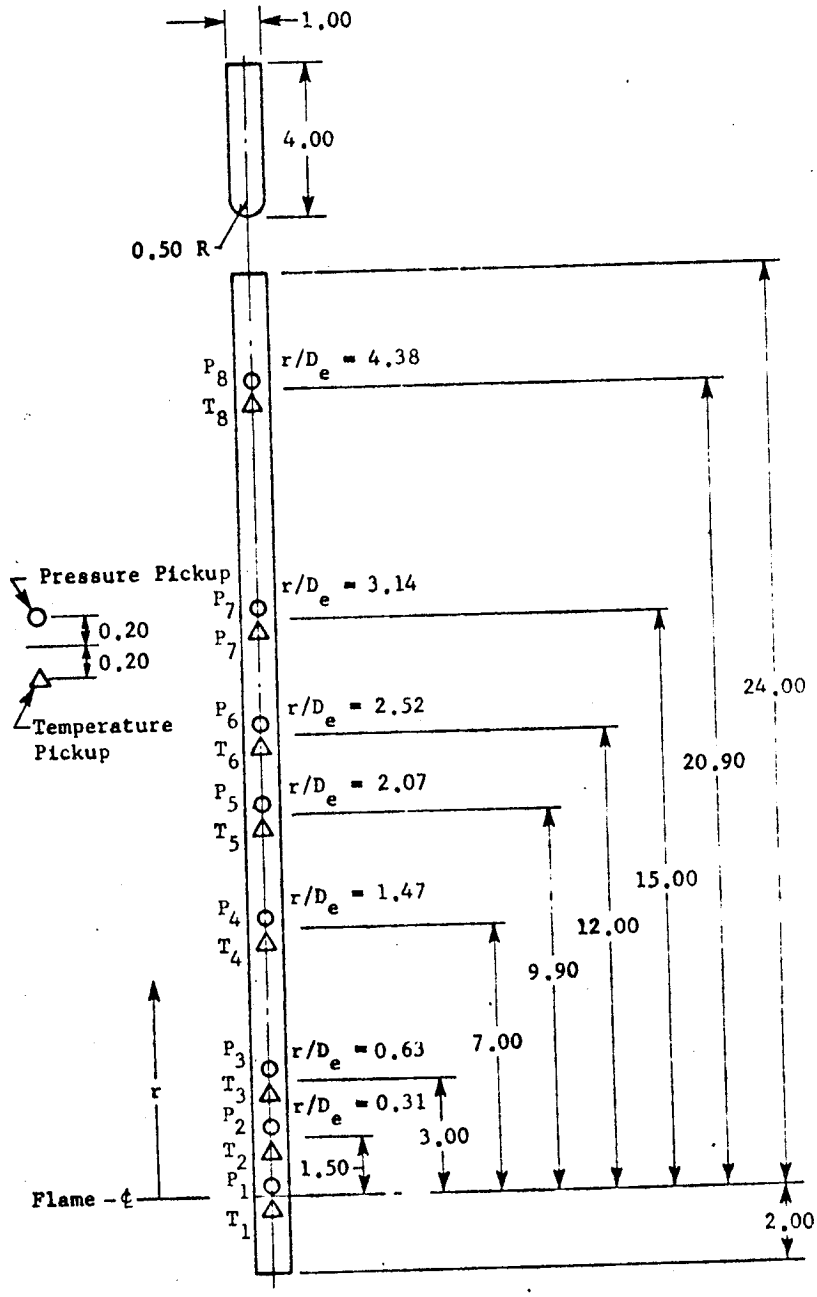

Note: Thermocouples T_1 thru T_4 are Tungsten-Tungsten Rhenium; thermocouples T_5 thru T_8 are Chromel-Alumel.

Fig. IX-1 Single Plume Rake Pressure and Temperature Pickup Locations and Designations

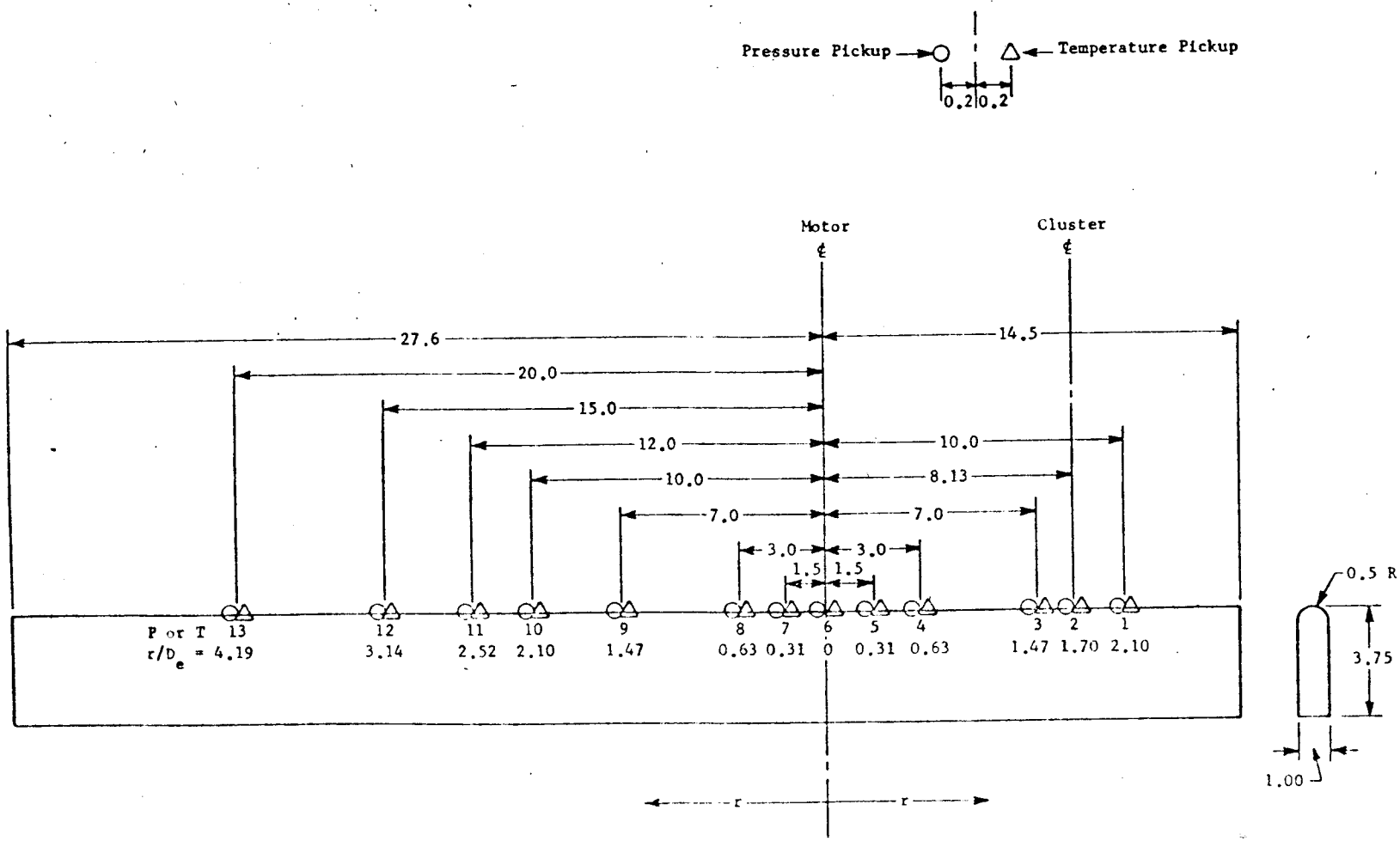

Fig. IX-2 Dual Motor Firing Rake Pressure and Temperature Pickup Locations and Designations

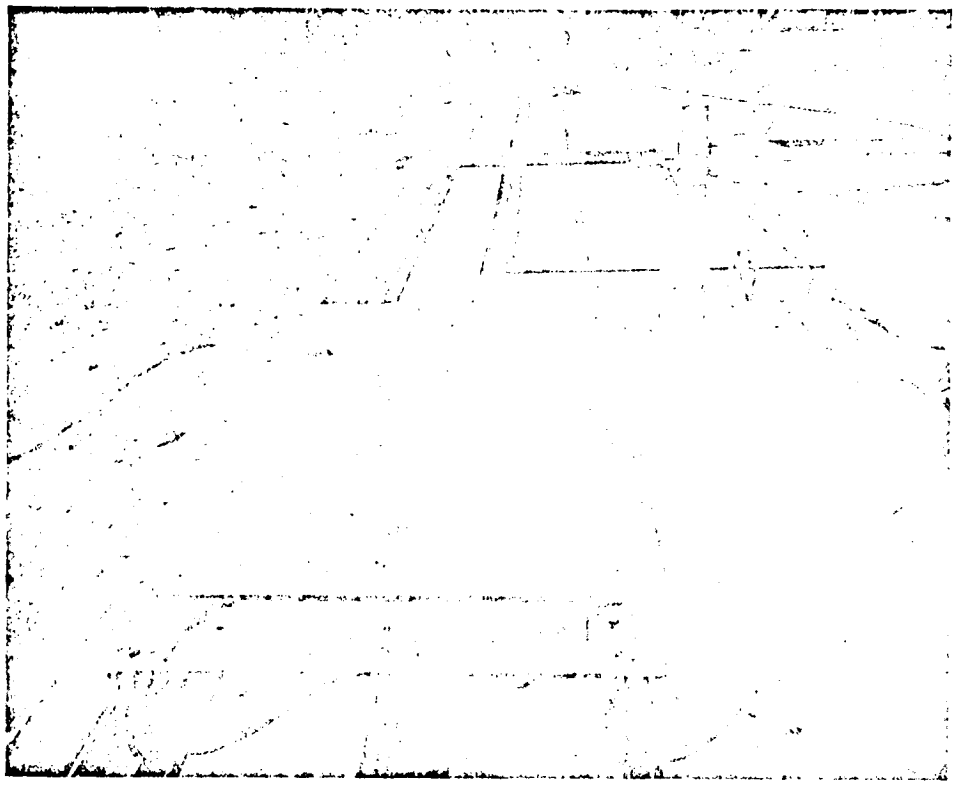

Fig. IX-3 Single Plume Rake Installed on Cart before Firing 23

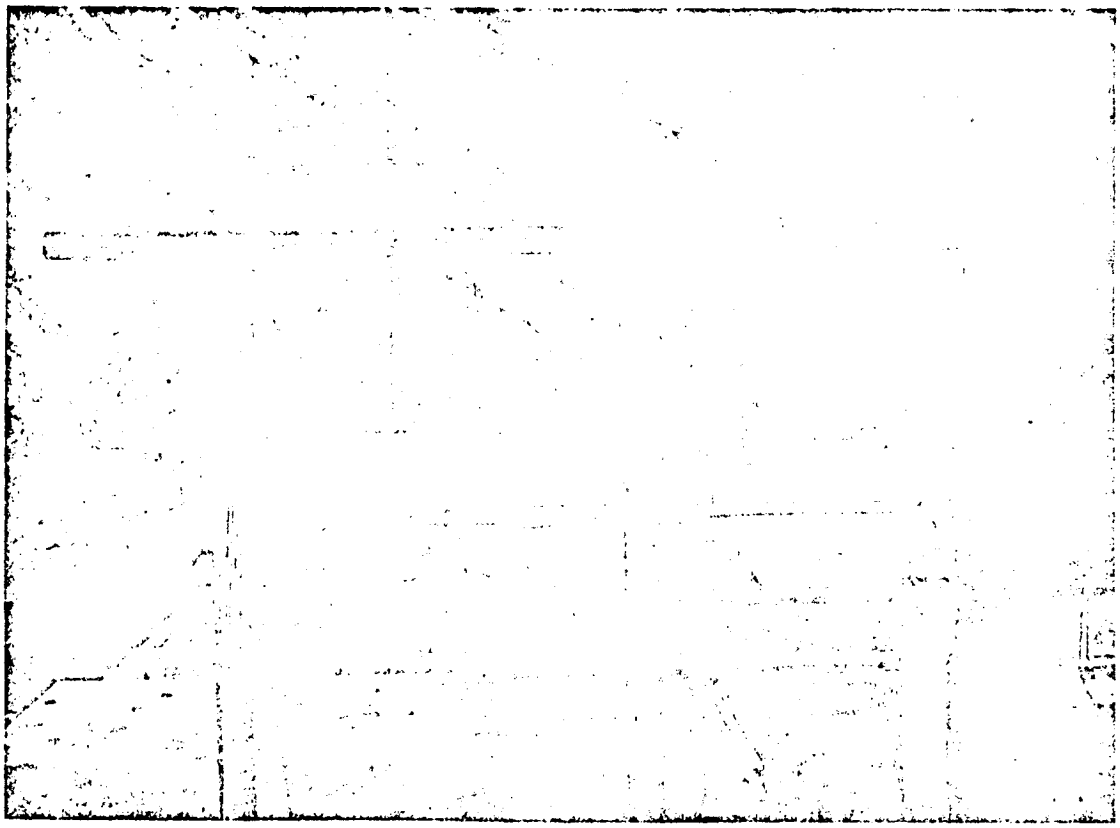

Fig. IX-4 Dual Plume Rake Installed on Cart before Firing 25

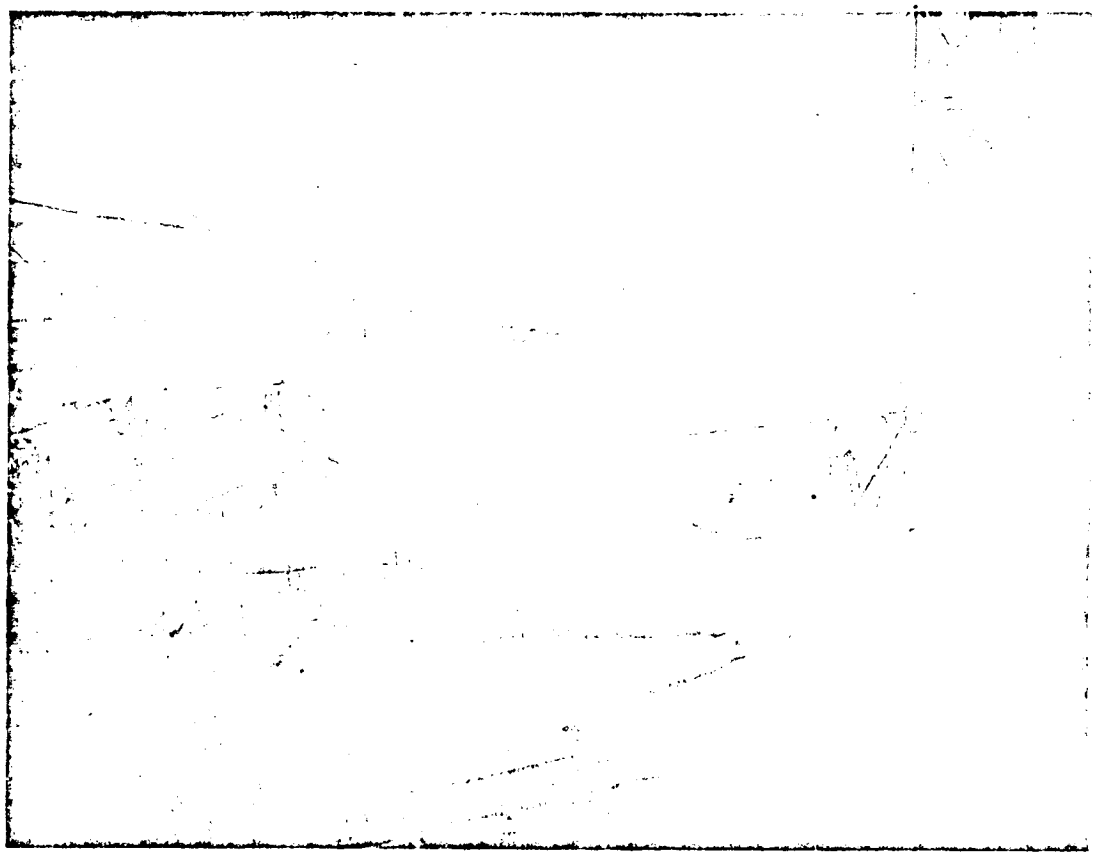

Fig. IX-5 Rocket Motors Firing during Run 25

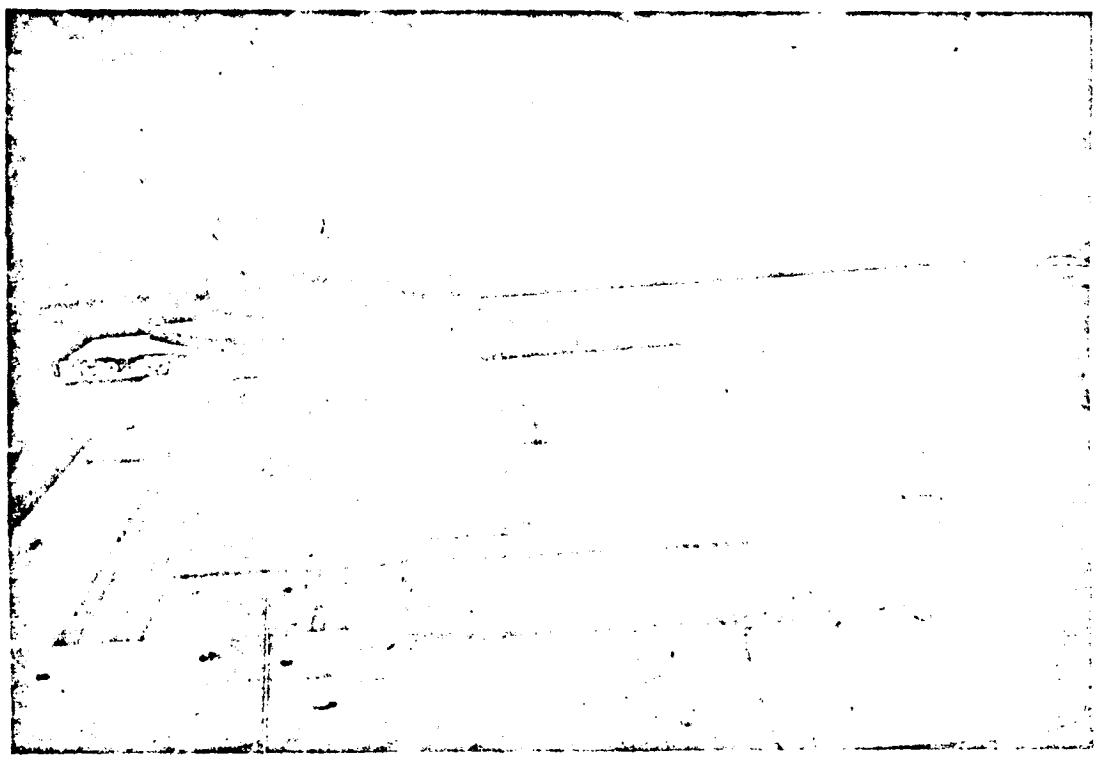

Fig. IX-6 Single Plume Rake after Firing 23

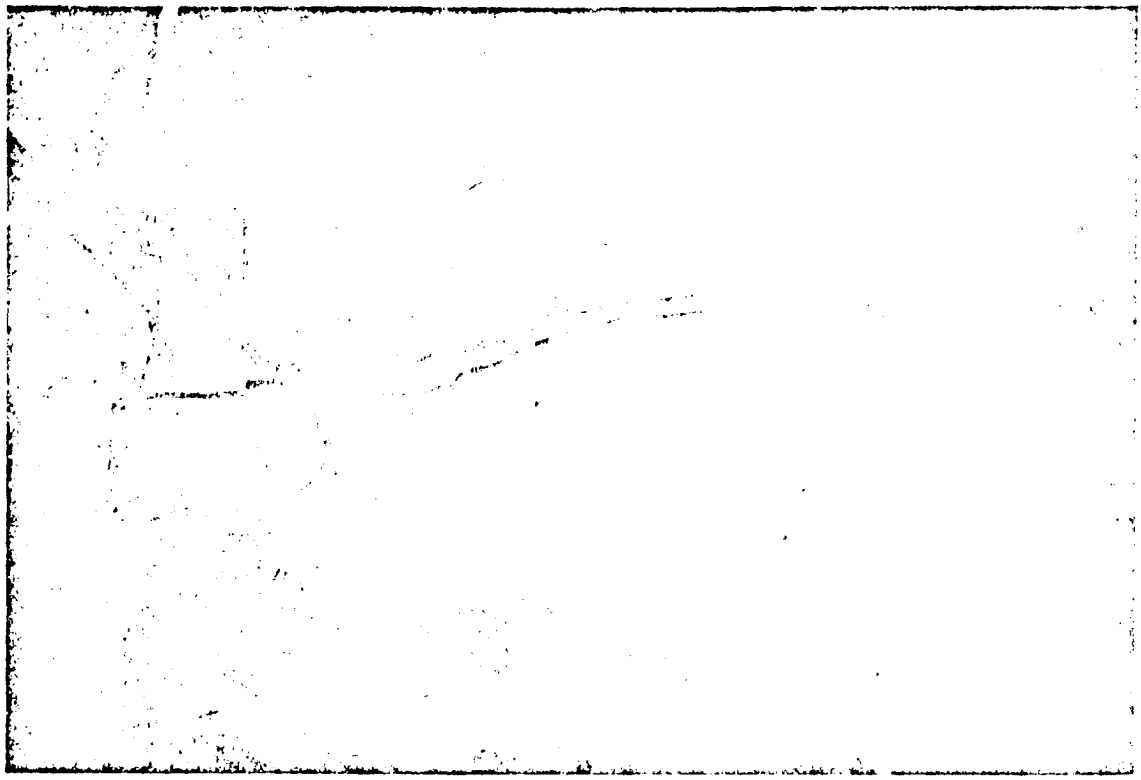

Fig. IX-7 Single Plume Rake after Firing 24

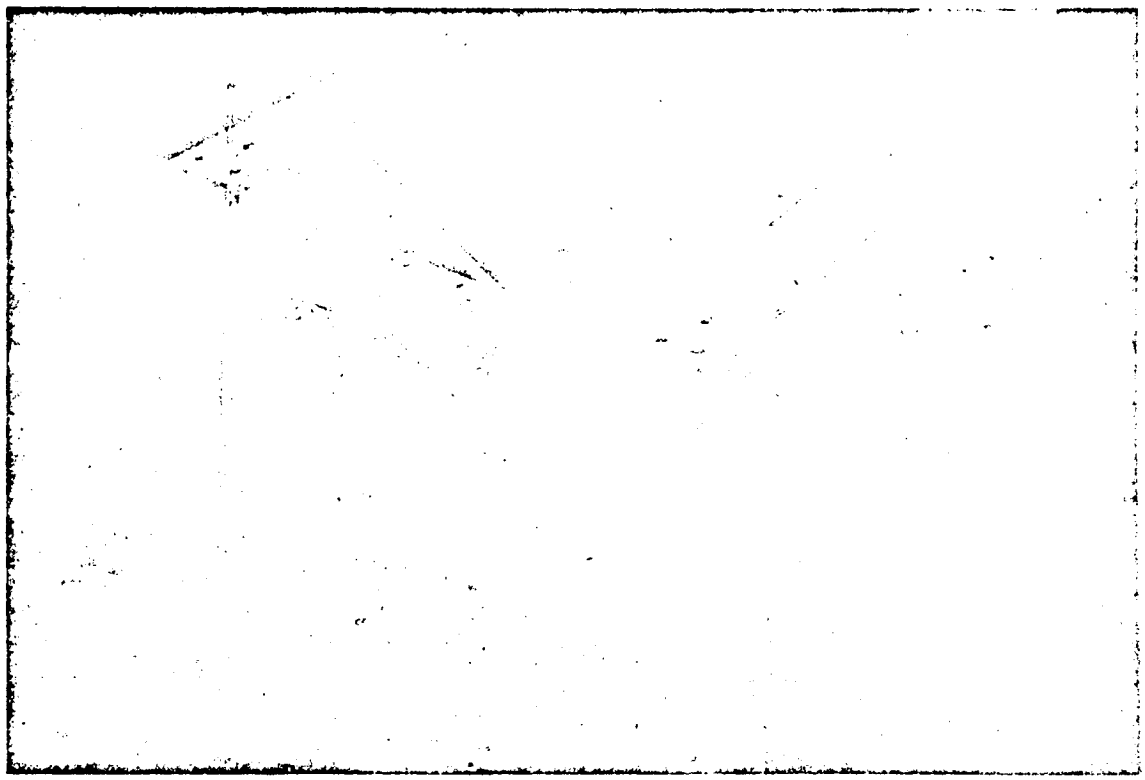

Fig. IX-8 Dual Plume Rake after Firing 25

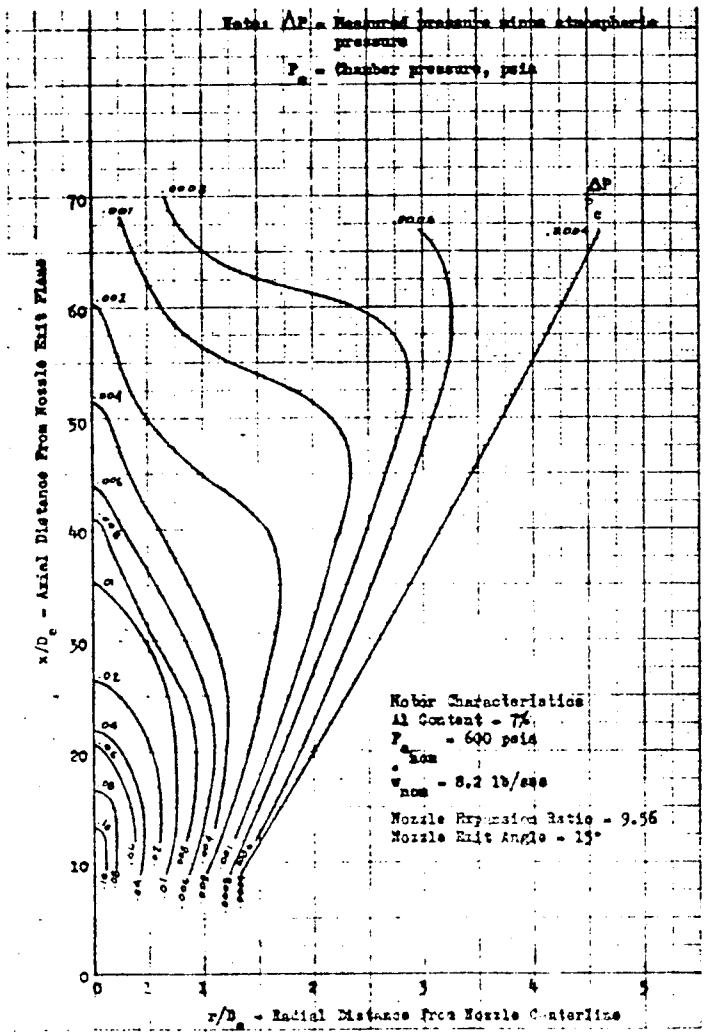

Fig. IX-9 Exhaust Plume Pressure Profile

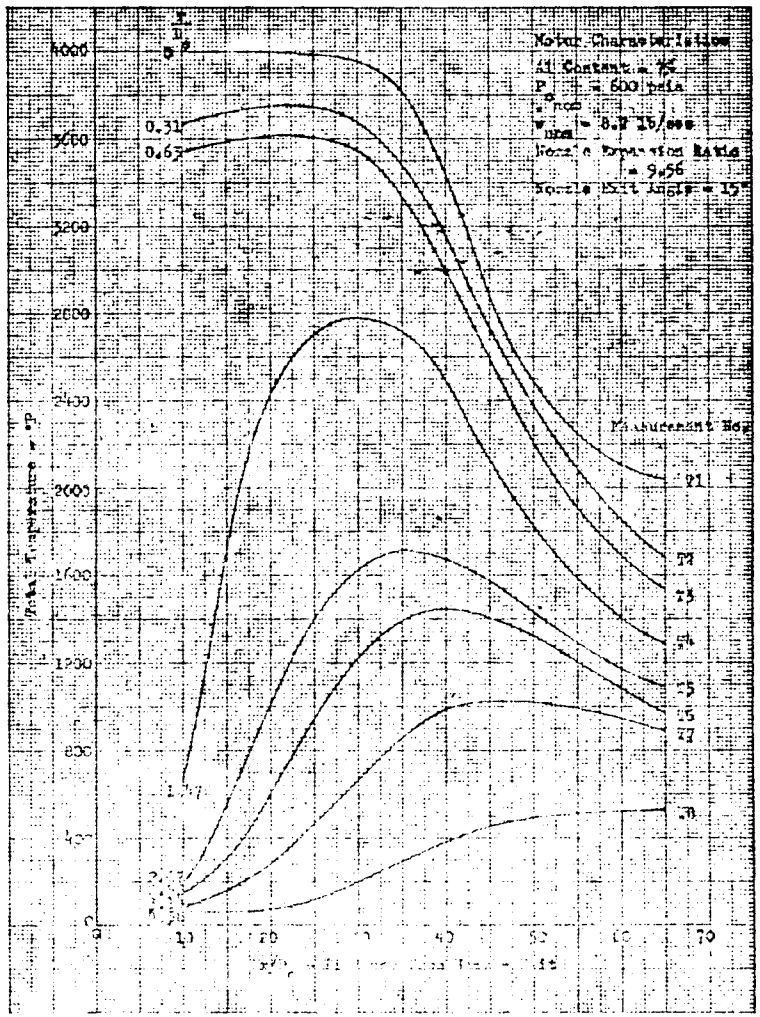

Fig. IX 10 Single Plume Temperature Data

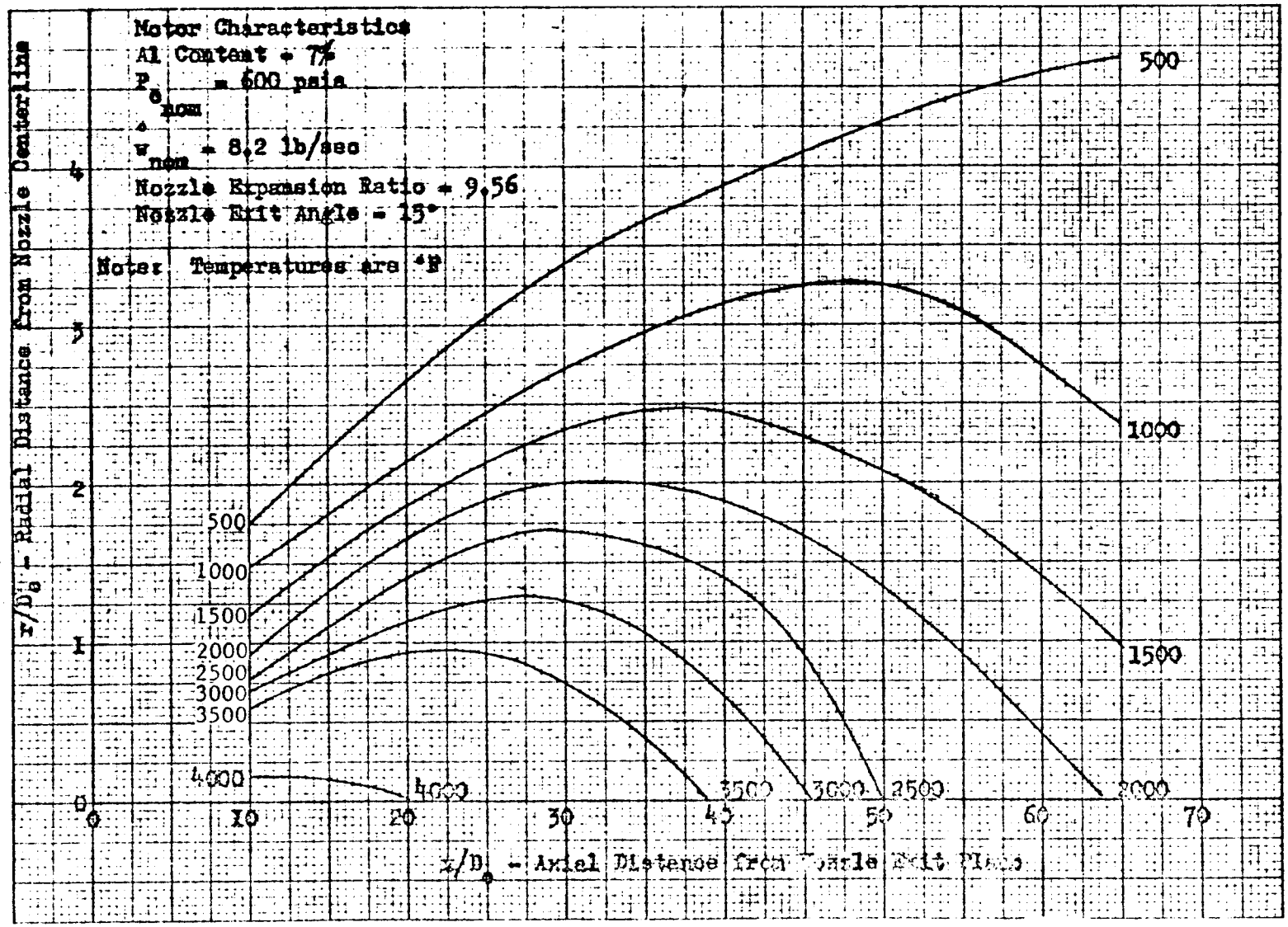

Fig. IX-11 Exhaust Plume Temperature Profile

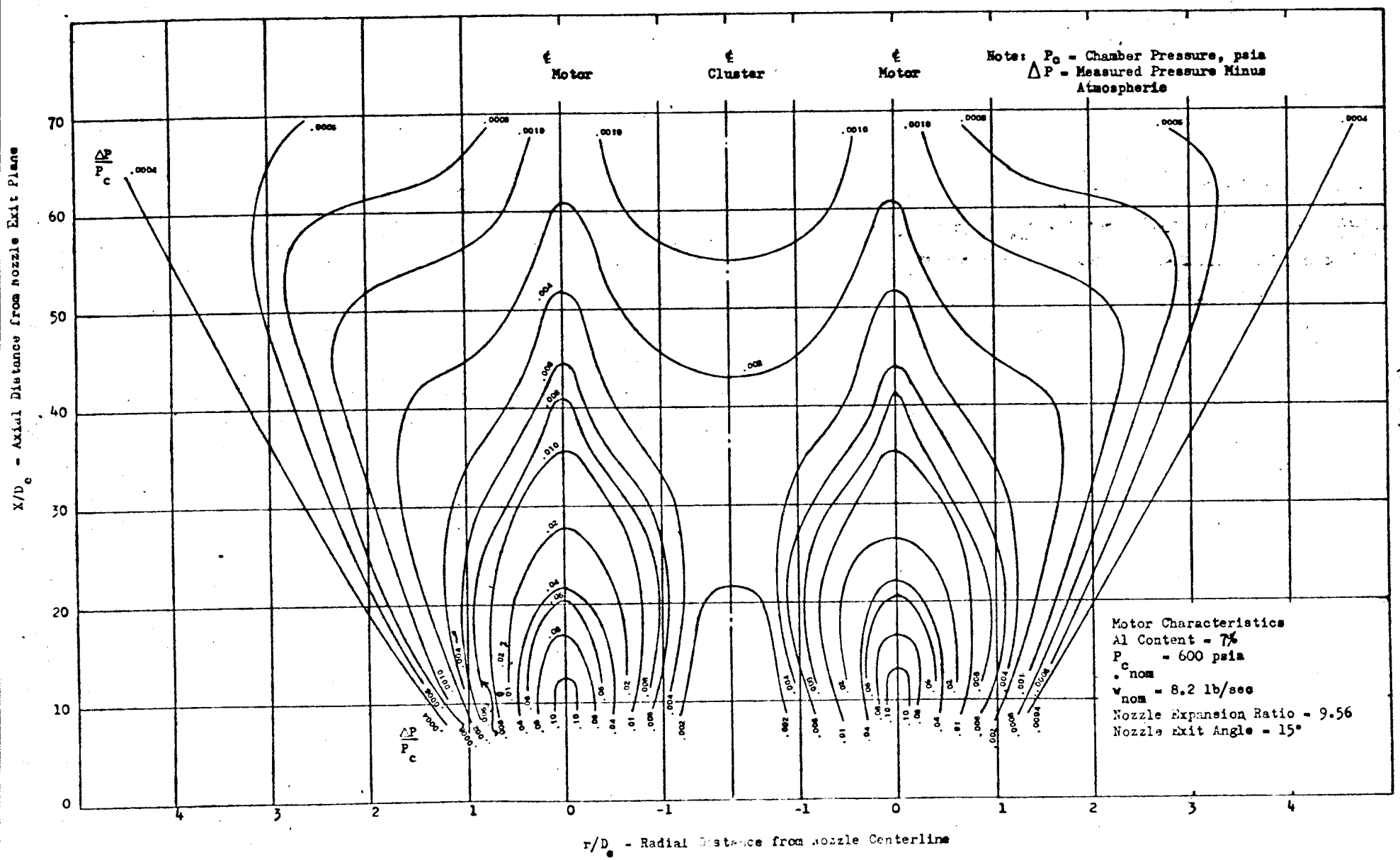

Fig. IX-12 Dual Motor Exhaust Plume Pressure Profile

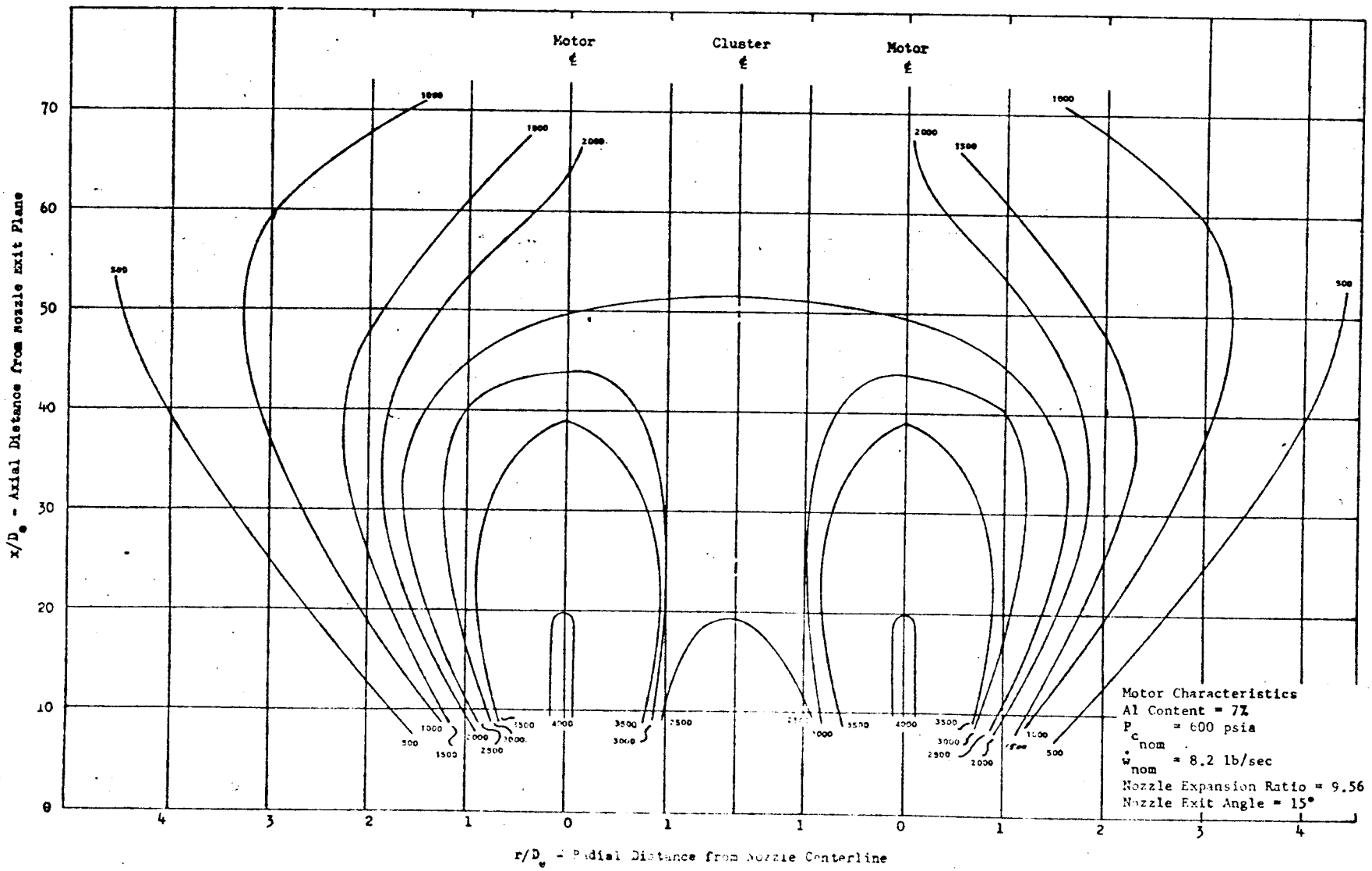

Fig. IX-13 Dual Motor Exhaust Plume Temperature Profile

X. PROTECTIVE MATERIALS EVALUATION

A. TECHNICAL OBJECTIVES

Objective of the protective materials evaluation was to find the best currently available material for protecting structures exposed to, but not directly impinged upon, by SRM exhaust products. Included among such structures are umbilical masts and launch mount frameworks.

B. DESIRABLE COATING PROPERTIES

Many structures needing thermal protection are massive and must be transported from a vertical assembly building to the launch pad. The several million pound Saturn V mobile launcher, for instance, poses a formidable moving problem. The protective coating on such a structure should not add substantially to the problem and, therefore, should offer maximum thermal protection at a weight minimum. Desirable coating properties in addition to low density are discussed in the following paragraph.

Since ground support equipment (GSE) thermal protective coatings will be applied in one thick layer (hopefully) and primarily to vertical surfaces, they must be viscous and set rapidly to prevent sagging. They must be easy to apply, easy to refurbish, have good adhesion characteristics, be compatible with propellants, weather well, and be somewhat elastic to prevent cracking when the primary structure to which they are attached is temporarily deformed. Thermal conductivity must be low and resistance to thermal and acoustic shock high. They must not support combustion and should hold up well under the high temperature erosive environment of an aluminized SRM; and finally, the cost must be low.

C. TYPES AND CHARACTERISTICS OF COATINGS INVESTIGATED

Two basic coating types were investigated: epoxy resins (with various fillers) and silicone rubbers. The thermal degradation of each of these organic coatings produces gases that absorb and carry away heat. The ablative process reduces the heat conducted to the remainder of the coating and protects the organic substrate from the high temperature environment.

Epoxy resins char and the char provides a porous rigid mass through which gas products can pass. This process is called transpiration and provides an additional means of cooling. The char is also a good infrared emitter. Dynatherm E-300, an excellent epoxy-type material, has additional transpiration formulated in the coating in the form of subliming inorganic oxides. It also contains glasses that soften and retain some of the char for future launches.

Silicones char if the organic portion contains phenyl groups. Methyl silicones will not char. Whipple (Ref 3) has shown that in a high heat flux and high shear environment both the mass loss and erosion rate of silicone elastomers decrease as phenyl content rises to a point where no further improvement is noted. Dow Corning Q90-006 is a silicone that was found to develop a char. Furthermore, it contains iron oxide; which is a good emitter of infrared radiation, and thereby offers additional cooling.

D. ENVIRONMENT

The pressure and temperature environment to which SPREE test panels were exposed was representative of the environment to which an umbilical mast would be subjected. A 1.5 D_e mast-to-plume separation was established for most tests. This is approximately the separation between the midpoint of the Titan IIIC umbilical mast and the centerline of the 120-in. SRMs. Results of measurements to determine the mast pressure and heating rate variation during liftoff are shown in Fig. X-1 and X-2. SPREE heating rate data shown in Fig. X-2 agree well with similar data obtained during a Titan IIIC launch.

E. DATA PRESENTATION

Data obtained during each test firing are presented in Table X-1. This table gives the location of each test panel including the location of instrumentation on the panels; coating weights and thicknesses before and after exposure to exhaust gases; coating weight, thickness, and volume losses; maximum coating backside temperature rise data; maximum pressures; and heating rates. Figure X-3 was prepared to show the initial rocket motor nozzle exit plane position relative to the ground plane at the base of the umbilical mast.

Table X-2 classifies each coating tested according to the type of ablative material (i.e., whether an epoxy or silicone) and summarizes weight and volume loss data in a gross manner. The best performing materials are shown at the top of the table with successively poorer performing materials listed below.

F. RESULTS AND DISCUSSION

Three outstanding materials were recognized as a result of the testing: Martyte WN-1, Dynatherm E-300, and Dow Corning Q-90-006. The top two performers (Martyte WN-1 and Dynatherm E-300) were epoxies. These were the lowest cost and most easily applied materials, although large scale applications using the required patty-cake process would be time consuming. There was essentially no difference in the ease with which Dynatherm or Martyte could be applied.

Martyte formulation changes were made to study the effects of formulation on applicability. The basic difference between the formulations involved the amount of reactive diluent added. Increasing the amount of diluent provided a more homogeneous, more easily applied coating, and reduced the brittleness and the performance variation between like samples. However, the larger quantity of diluent reduced heat distortion temperature. Martyte WN-2 and WN-3 possessed more reactive diluent and performed more poorly than WN-1. Epoxy resins with higher heat distortion temperatures may be more resistive to material loss.

Martyte WN-11 had a greater ratio of epoxy resin to ceramic filler. The quantity of filler does not appear critical since WN-11 performed about the same as WN-3, which had the standard amount of ceramic filler. Reducing the filler content in Martyte will improve coating applicability.

Separation rates of less than 35 D_e in 10 sec produced very large coating weight and volume losses. It would be well to provide greater clearance between SRM exhaust products and GSE at these very low liftoff acceleration rates.

Future work involving the development of superior thermal protective coatings should involve subliming materials, reactive diluents for epoxies, high infrared emittance materials, high heat distortion temperatures in epoxies, and efforts to improve coating applicability and reduce coating costs.

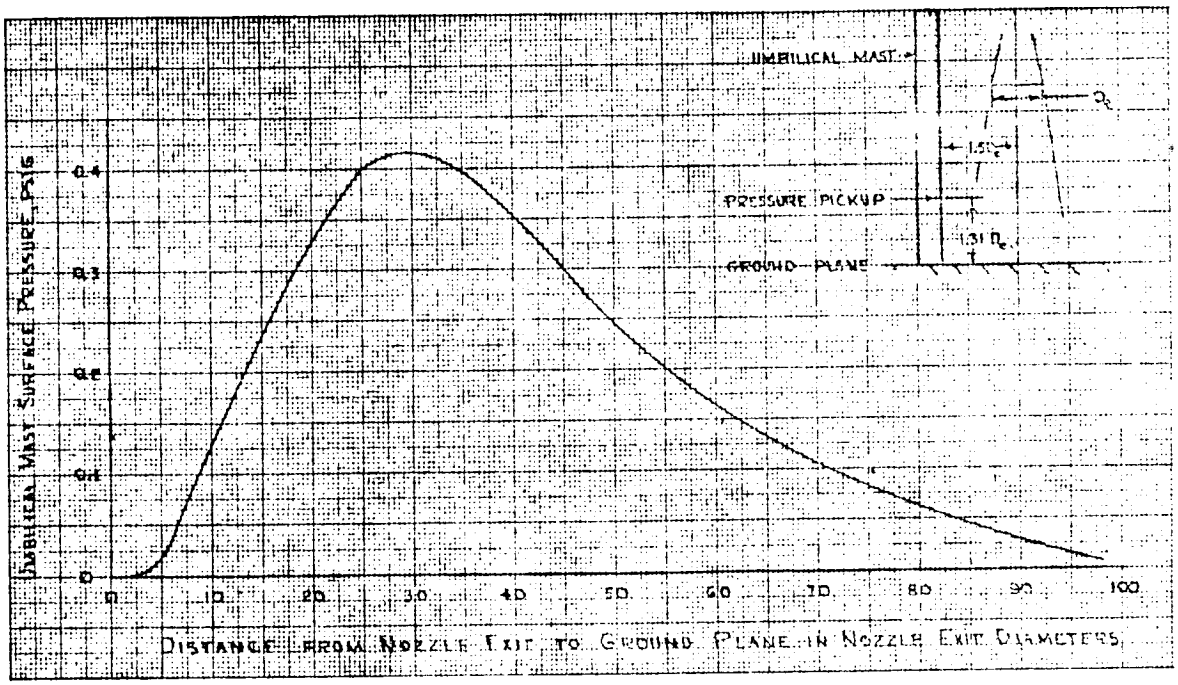

Fig. X-1 Variation of Umbilical Mast Surface Pressure during Liftoff

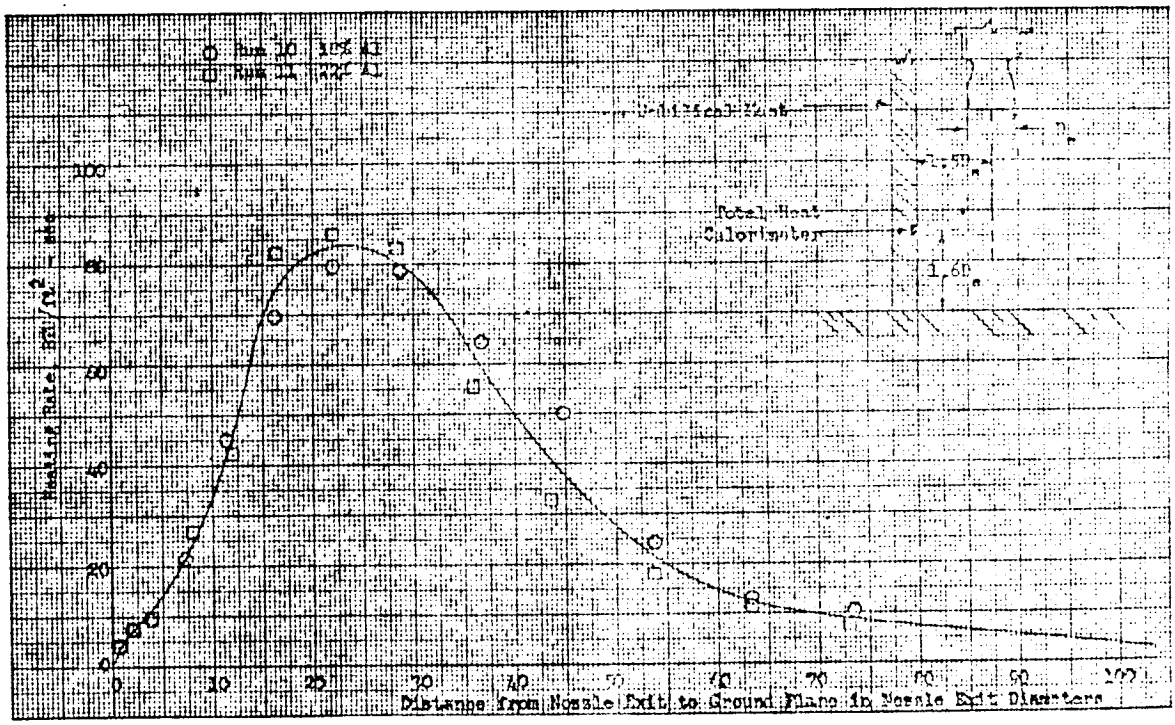

Fig. X-2 Umbilical Mast Heating Environment during Liftoff

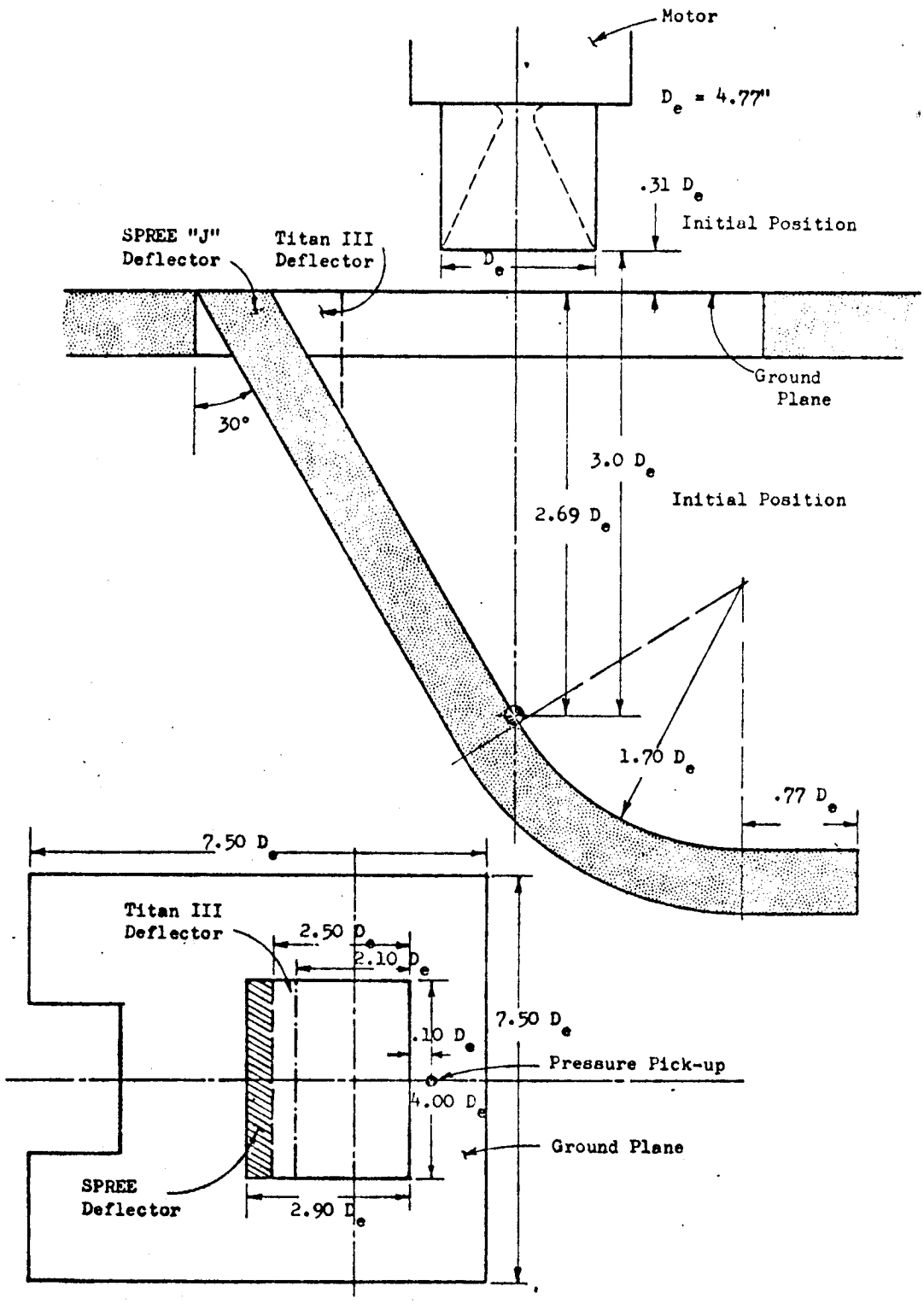

Fig. X-3 Ground Plane and J Deflector Schematic

Table X-1 Ablative Materials Evaluation

% Aluminum 18 RUN Nº 7

Separation Rate 130 D_e in 10 seconds

Distance, Coated Plate Face to Motor ℄ 1.5 D_e

Calorimeter Location X/D_e = 1.10, Y/D_e = 0

Pressure Tap Locations 1) X/D_e = 0.42 Y/D_e = 0

2) X/D_e = 1.31 Y/D_e = 0

Note: Cart Travel Malfunction

TOP OF TOWER

	A	B	C
2	1. 7A-2 2. Dow Corning Q 30-121 3. 56.2 gm 4. 41.9 gm 5. 14.3 gm 6. - in 7. - in 8. - in 9. 0.81 in^3 10 17 °F 11. - psig	1. 7B-2 2. Martyte 3. 111.2 gm 4. 90.5 gm 5. 20.7 gm 6. - in 7. - in 8. - in 9. 0.84 in^3 10 - °F 11. - psig 12 84 Btu./Ft^2-sec.	1. 7C-2 2. Fuller 190 J-4 3. 76.9 gm 4. 58.7 gm 5. 18.2 gm 6. - in 7. - in 8. - in 9. 1.27 in^3 10 - °F
1	1. 7A-1 2. Dow Corning Q 20-103-2 3. 69.9 gm 4. 48.4 gm 5. 21.5 gm 6. - in 7. - in 8. - in 9. 0.90 in^3 10 - °F 11 - psig	1. 7B-1 2. Martyte 3. 99.4 gm 4. 63.7 gm 5. 35.7 gm 6. - in 7. - in 8. - in 9. 1.45 in^3 10 - °F 11. 1.76 psig 12 - Btu./Ft^2-sec.	1. 7C-1 2. General Electric RTV 757 3. 76.9 gm 4. 57.5 gm 5. 19.4 gm 6. - in 7. - in 8. - in 9. 1.69 in^3 10 - °F 11 - psig

$+\frac{X}{D_e}$

GROUND PLANE

$-\frac{Y}{D_e}$ $+\frac{Y}{D_e}$

Flame ℄

LEGEND

1. Panel Designation: Run Nº and Panel Location (as B-1)
2. Coating Material
3. Coating Weight Before Firing, gm.
4. Coating Weight After Firing, gm.
5. Coating Weight Loss, gm.
6. Coating Thickness Before Firing, in
7. Coating Thickness After Firing, in
8. Coating Thickness Reduction, in
9. Coating Volume Loss, in^3
10. Maximum Backside Temperature, °F Rise
11. Maximum Pressure, psig
12. Maximum Heat Flux, Btu./Ft^2-sec.

Table X-1 (cont)

ABLATIVE MATERIALS EVALUATION

% Aluminum 22 RUN № 8

Separation Rate 130 D_e in 10 seconds

Distance, Coated Plate Face to Motor ℄ 1.5 D_e

Calorimeter Location X/D_e = 1.10 , Y/D_e = 0

Pressure Tap Locations 1) X/D_e = 0.42 Y/D_e = 0

2) X/D_e = 1.31 Y/D_e = 0

TOP OF TOWER

	A	B	C
L	1. 8A-2 2. Dynatherm E-300 3. 63.0 gm 4. 59.1 gm 5. 3.9 gm 6. - in 7. - in 8. - in 9. 0.20 in^3 10. - °F 11. - psig	1. 8B-2 2. Martyte 3. 115.0 gm 4. 97.3 gm 5. 17.7 gm 6. - in 7. - in 8. - in 9. 0.72 in^3 10. - °F 11. 0.72 psig 12. 84 Btu./Ft^2-sec.	1. 8C-2 2. Fuller 190 J-4 3. 83.6 gm 4. 71.6 gm 5. 12.0 gm 6. - in 7. - in 8. - in 9. 0.84 in^3 10. - °F
L	1. 8A-1 2. Dow Corning Q 93-019 3. 66.0 gm 4. 52.1 gm 5. 13.9 gm 6. - in 7. - in 8. - in 9. 0.65 in^3 10. - °F 11. - psig	1. 8B-1 2. Martyte 3. 123.0 gm 4. 98.8 gm 5. 24.2 gm 6. - in 7. - in 8. - in 9. 0.98 in^3 10. - °F 11. 0.72 psig 12. - Btu./Ft^2-sec.	1. 8C-1 2. Raytheon RPR 2138 3. 97.4 gm 4. 82.9 gm 5. 14.5 gm 6. - in 7. - in 8. - in 9. 0.59 in^3 10. - °F 11. - psig

$+\frac{X}{D}$

GROUND PLANE

$-\frac{Y}{D_e}$ $+\frac{Y}{D_e}$

Flame ℄

LEGEND

1. Panel Designation: Run № and Panel Location (as B-1)
2. Coating Material
3. Coating Weight Before Firing, gm.
4. Coating Weight After Firing, gm.
5. Coating Weight Loss, gm.
6. Coating Thickness Before Firing, in
7. Coating Thickness After Firing, in
8. Coating Thickness Reduction, in
9. Coating Volume Loss, in^3
10. Maximum Backside Temperature, °F R
11. Maximum Pressure, psig
12. Maximum Heat Flux, Btu./Ft^2-sec.

Table X-1 (cont)

ABLATIVE MATERIALS EVALUATION

% Aluminum 14 RUN Nº 9

Separation Rate 50 D_e in 10 seconds

Distance, Coated Plate Face to Motor ℄ 1.5 D_e

Calorimeter Location X/D_e = 1.10 , Y/D_e = 0

Pressure Tap Locations 1) X/D_e = 0.42 Y/D_e = 0

2) X/D_e = 1.31 Y/D_e = 0

TOP OF TOWER

	A	B	C
2	1. 9A-2 2. General Electric RTV 757 3. 69.9 gm 4. 59.6 gm 5. 10.3 gm 6. - in 7. - in 8. - in 9. 0.90 in^3 10 98 °F 11. - psig	1. 9B-2 2. Raytheon RPR 2140 3. 46.3 gm 4. 43.7 gm 5. 2.6 gm 6. - in 7. - in 8. - in 9. 0.10 in^3 10 - °F 11. 0.56 psig 12 77 Btu./$Ft.^2$-sec.	1. 9C-2 2. General Electric RTV 511 3. 67.7 gm 4. 56.5 gm 5. 11.2 gm 6. - in 7. - in 8. - in 9. 0.57 in^3 10 - °F
1	1. 9A-1 2. Raytheon RPR 2156 3. 4212 gm 4. 36.4 gm 5. 5.8 gm 6. - in 7. - in 8. - in 9. 0.37 in^3 10 29. °F 11 - psig	1. 9B-1 2. Martyte 3. 116.5 gm 4. 88.7 gm 5. 27.8 gm 6. - in 7. - in 8. - in 9. 1.13 in^3 10 45. °F 11. 1.23 psig 12 - Btu./$Ft.^2$-sec.	1. 9C-1 2. Fuller Fulblate 878 Type II 3. 58.6 gm 4. 43.5 gm 5. 15.1 gm 6. - in 7. - in 8. - in 9. 0.84 in^3 10 156. °F 11 - psig

$+\frac{X}{D_e}$

GROUND PLANE

$-\frac{Y}{D_e}$ $+\frac{Y}{D_e}$

Flame ℄

LEGEND

1. Panel Designation: Run Nº and Panel Location (as B-1)
2. Coating Material
3. Coating Weight Before Firing, gm.
4. Coating Weight After Firing, gm.
5. Coating Weight Loss, gm.
6. Coating Thickness Before Firing, in
7. Coating Thickness After Firing, in
8. Coating Thickness Reduction, in
9. Coating Volume Loss, in^3
10. Maximum Backside Temperature, °F Rise
11. Maximum Pressure, psig
12. Maximum Heat Flux, Btu./$Ft.^2$-sec.

Table X-1 (cont)

ABLATIVE MATERIALS EVALUATION

% Aluminum 18 RUN Nº 10

Separation Rate 50 D_e in 10 seconds

Distance, Coated Plate Face to Motor ℄ 1.5 D_e

Calorimeter Location X/D_e = 0.63, Y/D_e = 0

Pressure Tap Locations 1) X/D_e = 0.47 Y/D_e = 0

2) X/D_e = 0.47 Y/D_e = 0.63

TOP OF TOWER

	A	B	C
2.	1. 10 A-2 2. Ratheon RPR 2141 3. 57.9 gm 4. 52.9 gm 5. 5.0 gm 6. - in 7. - in 8. - in 9. 0.22 in^3 10. - °F 11. - psig	1. 10 B-2 2. Ratheon RPR 2141 3. 59.4 gm 4. 49.9 gm 5. 9.5 gm 6. - in 7. - in 8. - in 9. 0.41 in^3 10. - °F 11. - psig 12. - Btu./Ft^2-sec.	1. 10 C-2 2. Ratheon RPR 2156 3. 41.7 gm 4. 37.1 gm 5. 4.6 gm 6. - in 7. - in 8. - in 9. 0.30 in^3 10. - °F -
1.	1. 10 A-1 2. Martyte WN 2-1 3. 125.4 gm 4. 100.6 gm 5. 24.8 gm 6. - in 7. - in 8. - in 9. 1.01 in^3 10. - °F 11. 1.20 psig	1. 10 B-1 2. Martyte WN2-2 3. 116.6 gm 4. 95.1 gm 5. 21.5 gm 6. - in 7. - in 8. - in 9. 0.88 in^3 10. - °F 11. 1.29 psig 12. 80 Btu./Ft^2-sec.	1. 10 C-1 2. Martyte WN 3-2 3. 124.0 gm 4. 100.6 gm 5. 23.4 gm 6. - in 7. - in 8. - in 9. 0.95 in^3 10. - °F 11. - psig

$+\frac{X}{D_e}$

GROUND PLANE

$-\frac{Y}{D_e}$ $+\frac{Y}{D_e}$

Flame ℄

LEGEND
1. Panel Designation: Run Nº and Panel Location (as B-1)
2. Coating Material
3. Coating Weight Before Firing, gm.
4. Coating Weight After Firing, gm.
5. Coating Weight Loss, gm.
6. Coating Thickness Before Firing, in
7. Coating Thickness After Firing, in
8. Coating Thickness Reduction, in
9. Coating Volume Loss, in^3
10. Maximum Backside Temperature, °F Rise
11. Maximum Pressure, psig
12. Maximum Heat Flux, Btu./Ft^2-sec.

Table X-1 (cont)

ABLATIVE MATERIALS EVALUATION

% Aluminum 18 RUN № 10

Separation Rate 50 D_e in 10 seconds

Distance, Coated Plate Face to Motor ℄ 1.5 D_e

Calorimeter Location X/D_e = 0.63, Y/D_e = 0

Pressure Tap Locations 1) X/D_e = 0.47 Y/D_e = 0

2) X/D_e = 0.47 Y/D_e = 0.63

TOP OF TOWER

	A	B	C
2.	1. 10 A-2 2. Ratheon RPR 2141 3. 57.9 gm 4. 52.9 gm 5. 5.0 gm 6. - in 7. - in 8. - in 9. 0.22 in^3 10. - °F 11. - psig	1. 10 B-2 2. Ratheon RPR 2141 3. 59.4 gm 4. 49.9 gm 5. 9.5 gm 6. - in 7. - in 8. - in 9. 0.41 in^3 10. - °F 11. - psig 12. - Btu./Ft^2-sec.	1. 10 C-2 2. Ratheon RPR 2156 3. 41.7 gm 4. 37.1 gm 5. 4.6 gm 6. - in 7. - in 8. - in 9. 0.30 in^3 10. - °F -
1.	1. 10 A-1 2. Martyte WN 2-1 3. 125.4 gm 4. 100.6 gm 5. 24.8 gm 6. - in 7. - in 8. - in 9. 1.01 in^3 10. - °F 11. 1.20 psig	1. 10 B-1 2. Martyte WN2-2 3. 116.6 gm 4. 95.1 gm 5. 21.5 gm 6. - in 7. - in 8. - in 9. 0.88 in^3 10. - °F 11. 1.29 psig 12. 80 Btu./Ft^2-sec.	1. 10 C-1 2. Martyte WN 3-2 3. 124.0 gm 4. 100.6 gm 5. 23.4 gm 6. - in 7. - in 8. - in 9. 0.95 in^3 10. - °F 11. - psig

$+\frac{X}{D_e}$

GROUND PLANE

$-\frac{Y}{D_e}$ $+\frac{Y}{D_e}$

Flame ℄

LEGEND
1. Panel Designation: Run № and Panel Location (as B-1)
2. Coating Material
3. Coating Weight Before Firing, gm.
4. Coating Weight After Firing, gm.
5. Coating Weight Loss, gm.
6. Coating Thickness Before Firing, in
7. Coating Thickness After Firing, in
8. Coating Thickness Reduction, in
9. Coating Volume Loss, in^3
10. Maximum Backside Temperature, °F Rise
11. Maximum Pressure, psig
12. Maximum Heat Flux, Btu./Ft^2-sec.

Table X-1 (cont)

ABLATIVE MATERIALS EVALUATION

% Aluminum 22 RUN Nº 11

Separation Rate 50 D_e in 10 seconds

Distance, Coated Plate Face to Motor ℄ 1.5 D_e

Calorimeter Location X/ D_e = 0.68 , Y/ D_e = 0

Pressure Tap Locations 1) X/D_e = 0.47 Y/D_e = 0

2) X/D_e = 0.47 Y/D_e = 0.63

TOP OF TOWER

	A	B	C
2	1. 11A-2 2. Mild Steel 3. 311.5 gm 4. 312.6 gm 5. 1.1 (Gain) gm 6. - in 7. - in 8. - in 9. - in^3 10 1200 (Est) °F 11. - psig	1. 11B-2 2. Mild Steel 3. 311.5 gm 4. 312.2 gm 5. 0.7 (Gain) gm 6. - in 7. - in 8. - in 9. - in^3 10 1200 (Est) °F 11 - psig 12 - Btu./Ft^2-sec.	1. 11C-2 2. Raytheon PPR 2140 3. 43.6 gm 4. 34.5 gm 5. 9.1 gm 6. - in 7. - in 8. - in 9. 0.36 in^3 10 76. °F
1	1. 11 A-1 2. Dow Corning Q 90-006 3. 104.4 gm 4. 91.5 gm 5. 12.9 gm 6. - in 7. - in 8. - in 9. 0.53 in^3 10 149. °F 11 - psig	1. 11 B-1 2. Dow Corning Q 90-006 3. 99.9 gm 4. 91.9 gm 5. 8.0 gm 6. - in 7. - in 8. - in 9. 0.33 in^3 10 - °F 11. - psig 12 86 Btu./Ft^2-sec.	1. 11 C-1 2. Martyte WN-11-1 3. 116.8 gm 4. 89.2 gm 5. 27.6 gm 6. - in 7. - in 8. - in 9. 1.12 in^3 10 121. °F 11 - psig

$+\frac{X}{D_e}$

GROUND PLANE

$-\frac{Y}{D_e}$ $+\frac{Y}{D_e}$

Flame ℄

LEGEND

1. Panel Designation: Run Nº and Panel Location (as B-1)
2. Coating Material
3. Coating Weight Before Firing, gm.
4. Coating Weight After Firing, gm.
5. Coating Weight Loss, gm.
6. Coating Thickness Before Firing, in
7. Coating Thickness After Firing, in
8. Coating Thickness Reduction, in
9. Coating Volume Loss, in^3
10. Maximum Backside Temperature, °F Rise
11. Maximum Pressure, psig
12. Maximum Heat Flux, Btu./Ft^2-sec.

Table X-1 (cont)

ABLATIVE MATERIALS EVALUATION

% Aluminum 7 RUN № 12

Separation Rate 50 D_e in 10 seconds

Distance, Coated Plate Face to Motor ℄ 1.5 D_e

Calorimeter Location X/D_e = 1.10, Y/D_e = 0

Pressure Tap Locations 1) X/D_e = 1.31 Y/D_e = 0

2) X/D_e = 1.31 Y/D_e = 0.63

TOP OF TOWER

	A	B	C
2.	1. 12 A-2 2. Fuller Korblate II-190-1-2 3. 53.4 gm 4. 46.8 gm 5. 6.6 gm 6. - in 7. - in 8. - in 9. 0.59 in^3 10. 50 (Est.) °F 11. 0.43 psig	1. 12 B-2 2. Fuller Korblate II-190-1-2 3. 53.2 gm 4. 50.6 gm 5. 2.6 gm 6. - in 7. - in 8. - in 9. 0.23 in^3 10. - °F 11. 0.43 psig 12. 75 Btu./Ft^2-sec.	1. 12 C-2 2. Martyte EN 3-1 3. 114.5 gm 4. 104.6 gm 5. 9.9 gm 6. - in 7. - in 8. - in 9. 0.40 in^3 10. 50 (Est.) °F
1.	1. 12 A-1 2. Mild Steel 3. 303.5 gm 4. 303.8 gm 5. 0.3 (Gain) gm 6. - in 7. - in 8. - in 9. - in^3 10. - °F 11. - psig	1. 12 B-1 2. Mild Steel 3. 300.4 gm 4. 300.4 gm 5. 0 gm 6. - in 7. - in 8. - in 9. - in^3 10. 345 °F 11. - psig 12. - Btu./Ft^2-sec.	1. 12 C-1 2. Martyte EN 1-1 3. 124.3 gm 4. 108.8 gm 5. 15.5 gm 6. - in 7. - in 8. - in 9. 0.63 in^3 10. - °F 11. - psig

$+\frac{X}{D_e}$

GROUND PLANE

$-\frac{Y}{D_e}$ $+\frac{Y}{D_e}$

Flame ℄

LEGEND

1. Panel Designation: Run № and Panel Location (as B-1)
2. Coating Material
3. Coating Weight Before Firing, gm.
4. Coating Weight After Firing, gm.
5. Coating Weight Loss, gm.
6. Coating Thickness Before Firing, in
7. Coating Thickness After Firing, in
8. Coating Thickness Reduction, in
9. Coating Volume Loss, in^3
10. Maximum Backside Temperature, °F Rise
11. Maximum Pressure, psig
12. Maximum Heat Flux, Btu./Ft^2-sec.

Table X-1 (cont)

ABLATIVE MATERIALS EVALUATION

% Aluminum 14 RUN № 14

Separation Rate 130 D_e in 10 seconds

Distance, Coated Plate Face to Motor ℄ 1.25 D_e

Calorimeter Location X/D_e = 0.68, Y/D_e = 0

Pressure Tap Locations 1) X/D_e = 0.47 Y/D_e = 0

2) X/D_e = 0.47 Y/D_e = +0.63

Rocket motor canted 6-deg. in +Y direction

TOP OF TOWER

	A	B	C
1.	14 A-1	14 B-1	14 C-1
2.	Martyte WN 1-2	Martyte WN-3	Martyte WN-3
3.	120.5 gm	99.0 gm	109.3 gm
4.	119.2 gm	90.9 gm	100.3 gm
5.	1.3 gm	8.1 gm	9.0 gm
6.	- in	- in.	- in
7.	- in	- in	- in
8.	- in	- in	- in
9.	0.05 in^3	0.33 in^3	0.37 in^3
10	70 (Est.) °F	- °F	70 (Est.) °F
11	- psig	0.45 psig	0.50 psig
12		56. Btu./Ft^2-sec.	

L

$+\frac{X}{D_e}$

GROUND PLANE

$-\frac{Y}{D_e}$ $+\frac{Y}{D_e}$

Flame ℄

LEGEND

1. Panel Designation: Run № and Panel Location (as B-1)
2. Coating Material
3. Coating Weight Before Firing, gm.
4. Coating Weight After Firing, gm.
5. Coating Weight Loss, gm.
6. Coating Thickness Before Firing, in
7. Coating Thickness After Firing, in
8. Coating Thickness Reduction, in
9. Coating Volume Loss, in^3
10. Maximum Backside Temperature, °F Rise
11. Maximum Pressure, psig
12. Maximum Heat Flux, Btu./Ft^2-sec.

Table X-1 (cont)

ABLATIVE MATERIALS EVALUATION

% Aluminum 18 RUN Nº 15

Seperation Rate 50 D_e in 10 seconds

Distance, Coated Plate Face to Motor ℄ 1.25 D_e

Calorimeter Location X/D_e = 0.68 , Y/D_e = 0

Pressure Tap Locations 1) X/D_e = 0.47 Y/D_e = 0

2) X/D_e = 0.47 Y/D_e = +0.63

Rocket motor canted 6-deg. in + Y direction

TOP OF TOWER

	A	B	C
1.	15 A-1	15 B-1 (Retest of 14 B-1)	15 C-1
2.	Martyte WN 1-2	Martyte WN-3	Martyte WN-3
3.	119.2 gm	90.9 gm	100.3 gm
4.	112.1 gm	78.9 gm	77.8 gm
5.	7.1 gm	12.0 gm	22.5 gm
6.	- in	- in	- in
7.	- in	- in	- in
8.	- in	- in	- in
9.	0.29 in^3	0.49 in^3	0.92 in^3
10	95 (Est.) °F	- °F	95 (Est.) °F
11	- psig	0.26 psig	0.53 psig
12		60.6 Btu./Ft^2-sec.	

$+\frac{X}{D_e}$

GROUND PLANE

$-\frac{Y}{D_e}$ $+\frac{Y}{D_e}$

Flame ℄

LEGEND

1. Panel Designation: Run Nº and Panel Location (as B-1)
2. Coating Material
3. Coating Weight Before Firing, gm.
4. Coating Weight After Firing, gm.
5. Coating Weight Loss, gm.
6. Coating Thickness Before Firing, in
7. Coating Thickness After Firing, in
8. Coating Thickness Reduction, in
9. Coating Volume Loss, in^3
10. Maximum Backside Temperature, °F Rise
11. Maximum Pressure, psig
12. Maximum Heat Flux, Btu./Ft^2-sec.

DISTRIBUTION

Copies	To
1 thru 10 and one unbound reproducible	Contracting Officer Kennedy Space Center National Aeronautics and Space Administration John F. Kennedy Space Center, Florida 32899
11	New Technology Representative Counsel for Patent Material Kennedy Space Center National Aeronautics and Space Administration John F. Kennedy Space Center, Florida 32899
12 thru 61	Martin Company Denver Division Denver, Colorado 80201 Attn: Libraries Section

Table X-1 (cont)

ABLATIVE MATERIALS EVALUATION

% Aluminum 18 RUN NO 16

Separation Rate 100 D_e in 10 seconds

Distance, Coated Plate Face to Motor ℄ 1.5 D_e

Calorimeter Location X/D_e = 1.10, Y/D_e = 0

Pressure Tap Locations 1) X/D_e = 0.47 Y/D_e = 0

2) X/D_e = 1.31 Y/D_e = 0

TOP OF TOWER

	A	B	C
2.	1. 16 A-2 2. Dow Corning Q 90-006 3. 92.7 gm 4. 86.3 gm 5. 6.4 gm 6. 0.219 in 7. 0.187 in 8. 0.032 in 9. 0.26 in^3 10 45. (Est.) °F 11. - psig	1. 16 B-2 2. Martyte WN-3 3. 92.5 gm 4. 80.9 gm 5. 11.6 gm 6. 0.281 in 7. 0.234 in 8. 0.047 in 9. 0.47 in^3 10 - °F 11. .40 psig 12. 77.8 Btu./Ft^2-sec.	1. 16 C-2 2. Raytheon PPR 2140 3. 37.0 gm 4. 30.6 gm 5. 6.4 gm 6. 0.188 in 7. 0.141 in 8. 0.047 in 9. 0.25 in^3 10 56 °F
4	1. 16 A-1 2. Dow Corning Q 90-006 3. 88.1 gm 4. 81.8 gm 5. 6.3 gm 6. 0.234 in 7. 0.219 in 8. 0.015 in 9. 0.26 in^3 10 60 (Est.) °F 11. - psig	1. 16 B-1 2. Martyte WN-3 3. 109.3 gm 4. 95.3 gm 5. 14.0 gm 6. 0.313 in 7. 0.219 in 8. 0.094 in 9. 0.57 in^3 10 63 (Est) °F 11. 1.30 psig 12. - Btu./Ft^2-sec.	1. 16 C-1 2. Raytheon PPR 2140 3. 36.1 gm 4. 28.9 gm 5. 7.2 gm 6. 0.188 in 7. 0.141 in 8. 0.047 in 9. 0.20 in^3 10 80 (Est) °F 11. - psig

$+\frac{X}{D_e}$

GROUND PLANE

$-\frac{Y}{D_e}$ $+\frac{Y}{D_e}$

Flame ℄

LEGEND

1. Panel Designation: Run No and Panel Location (ex B-1)
2. Coating Material
3. Coating Weight Before Firing, gm.
4. Coating Weight After Firing, gm.
5. Coating Weight Loss, gm.
6. Coating Thickness Before Firing, in
7. Coating Thickness After Firing, in
8. Coating Thickness Reduction, in
9. Coating Volume Loss, in^3
10. Maximum Backside Temperature, °F Rise
11. Maximum Pressure, psig
12. Maximum Heat Flux, Btu./Ft^2-sec.

Table X-1 (cont)

ABLATIVE MATERIALS EVALUATION

% Aluminum 18 RUN Nº 17

Separation Rate 50 D_e in 10 seconds

Distance, Coated Plate Face to Motor ℄ 1.5 D_e

Calorimeter Location X/D_e = - , Y/D_e = -

Pressure Tap Locations 1) X/D_e = - Y/D_e = -

2) X/D_e = - Y/D_e = -

TOP OF TOWER

	A	B	C
2	1. 17 A-2 2. Fuller Fulblate 878 Type I 3. 62.5 gm 4. - gm 5. - gm 6. - in 7. - in 8. - in 9. - in^3 10 - °F 11. psig	1. 17 B-2 2. Fuller Fulblate 878 Type I 3. 63.5 gm 4. 46.4 gm 5. 17.1 gm 6. - in 7. - in 8. - in 9. 0.99 in^3 10 - °F 11. - psig 12 - Btu./Ft^2-sec.	1. 17 C-2 2. Fuller Fulblate 873 Type I 3. 65.4 gm 4. - gm 5. - gm 6. - in 7. - in 8. - in 9. - in^3 10 - °F
1	1. 17 A-1 2. Fuller Fulblate 878 Type II 3. 66.2 gm 4. 47.0 gm 5. 19.2 gm 6. - in 7. - in 8. - in 9. 1.06 in^3 10 - °F 11 - psig	1. 17 B-1 2. Fuller Fulblate 878 Type II 3. 65.6 gm 4. 46.1 gm 5. 19.5 gm 6. - in 7. - in 8. - in 9. 1.08 in^3 10 - °F 11. - psig 12 - Btu./Ft^2-sec.	1. 17 C-3 2. Fuller Fulblate 878 Type II 3. 66.3 gm 4. 49.1 gm 5. 17.2 gm 6. - in 7. - in 8. - in 9. 0.95 in^3 10 - °F 11 - psig

$+\frac{X}{D_e}$

GROUND PLANE

$-\frac{Y}{D_e}$ $+\frac{Y}{D_e}$

Flame ℄

LEGEND

1. Panel Designation: Run Nº and Panel Location (as B-1)
2. Coating Material
3. Coating Weight Before Firing, gm.
4. Coating Weight After Firing, gm.
5. Coating Weight Loss, gm.
6. Coating Thickness Before Firing, in
7. Coating Thickness After Firing, in
8. Coating Thickness Reduction, in
9. Coating Volume Loss, in^3
10. Maximum Backside Temperature, °F Rise
11. Maximum Pressure, psig
12. Maximum Heat Flux, Btu./Ft^2-sec.

Table X-1 (cont)

ABLATIVE MATERIALS EVALUATION

% Aluminum 18 RUN № 18

Separation Rate 35 D_e in 10 seconds

Distance, Coated Plate Face to Motor ℄ 1.5 D_e

Calorimeter Location X/D_e = 0.68, Y/D_e = 0

Pressure Tap Locations 1) X/D_e = 0.42 Y/D_e = 0

2) X/D_e = - Y/D_e = -

TOP OF TOWER

	A	B	C
1.	18 A-1	18 B-1	18 C-1
2.	Dow Corning Q 90-006	Martyte WN-3	Ratheon RPR 2140
3.	94.3 gm	111.7 gm	35.1 gm
4.	78.5 gm	73.7 gm	15.2 gm
5.	15.8 gm	38.0 gm	19.9 gm
6.	0.2344 in	0.3125 in	0.1875 in
7.	0.1875 in	0.1875 in	0.1094 in
8.	0.0469 in	0.1250 in	0.0781 in
9.	0.65 in^3	1.55 in^3	0.20 in^3
10.	140 (Est) °F	- °F	275. (Est) °F
11.	- psig	1.24 psig	- psig
12.		118.5 Btu./Ft^2-sec.	

L

$+\frac{X}{D_e}$

GROUND PLANE

$-\frac{Y}{D_e}$ $+\frac{Y}{D_e}$

Flame ℄

LEGEND

1. Panel Designation: Run № and Panel Location (as B-1)
2. Coating Material
3. Coating Weight Before Firing, gm.
4. Coating Weight After Firing, gm.
5. Coating Weight Loss, gm.
6. Coating Thickness Before Firing, in
7. Coating Thickness After Firing, in
8. Coating Thickness Reduction, in
9. Coating Volume Loss, in^3
10. Maximum Backside Temperature, °F Rise
11. Maximum Pressure, psig
12. Maximum Heat Flux, Btu./Ft^2-sec.

Table X-1 (cont).

ABLATIVE MATERIALS EVALUATION

% Aluminum 18 RUN № 19

Separation Rate 25 D_e in 10 seconds

Distance, Coated Plate Face to Motor ℄ 1.5 D_e

Calorimeter Location X/D_e = 0.68, Y/D_e = 0

Pressure Tap Locations 1) X/D_e = 0.47 Y/D_e = 0

2) X/D_e = - Y/D_e = -

TOP OF TOWER

	A	B	C
1.	19 A-1	19 B-1	19 C-1
2.	Dow Corning Q 90-006	Martyte WN-3	Raytheon PPR 2140
3.	84.7 gm	108.1 gm	34.7 gm
4.	60.2 gm	60.0 gm	20.6 gm
5.	24.5 gm	48.1 gm	14.1 gm
6.	0.1875 in	0.3125 in	0.1875 in
7.	0.1406 in	0.1562 in	0.1250 in
8.	0.0469 in	0.1563 in	0.0625 in
9.	1.01 in^3	1.96 in^3	0.56 in^3
10.	- °F	- °F	- °F
11.	- psig	1.28 psig	- psig
12.		115.0 Btu./$Ft.^2$-sec.	

GROUND PLANE

$-\frac{Y}{D_e}$ $+\frac{Y}{D_e}$ $+\frac{X}{D_e}$

Flame ℄

LEGEND
1. Panel Designation: Run № and Panel Location (as B-1)
2. Coating Material
3. Coating Weight Before Firing, gm.
4. Coating Weight After Firing, gm.
5. Coating Weight Loss, gm.
6. Coating Thickness Before Firing, in
7. Coating Thickness After Firing, in
8. Coating Thickness Reduction, in
9. Coating Volume Loss, in^3
10. Maximum Backside Temperature, °F Rise
11. Maximum Pressure, psig
12. Maximum Heat Flux, Btu./$Ft.^2$-sec.

Table X-1 (cont)

ABLATIVE MATERIALS EVALUATION

% Aluminum 18 RUN № 20

Separation Rate 15 D_e in 10 seconds

Distance, Coated Plate Face to Motor ℄ 1.5 D_e

Calorimeter Location X/D_e = 0.68, Y/D_e = 0

Pressure Tap Locations 1) X/D_e = 0.47 Y/D_e = 0

2) X/D_e = - Y/D_e = -

TOP OF TOWER

	A	B	C
1.	20 A-1	20 B-1	20 C-1
2.	Dow Corning Q 90-006	Martyte WN-3	Raytheon RFR 2140
3.	89.6 gm	100.7 gm	31.5 gm
4.	64.6 gm	36.9 gm	5.5 gm
5.	25.0 gm	63.8 gm	26.0 gm
6.	0.2344 in	0.2812 in	0.1719 in
7.	0.1563 in	0.0938 in	0.0313 in
8.	0.0781 in	0.1874 in	0.1406 in
9.	1.03 in^3	2.60 in^3	1.04 in^3
10	160 (Est) °F	- °F	228 °F
11	- psig	1.28 psig	- psig
12		129.0 Btu./Ft.^{2}-sec.	

L

$+\frac{X}{D_e}$

GROUND PLANE

$-\frac{Y}{D_e}$ $+\frac{Y}{D_e}$

Flame ℄

LEGEND

1. Panel Designation: Run № and Panel Location (as B-1)
2. Coating Material
3. Coating Weight Before Firing, gm.
4. Coating Weight After Firing, gm.
5. Coating Weight Loss, gm.
6. Coating Thickness Before Firing, in
7. Coating Thickness After Firing, in
8. Coating Thickness Reduction, in
9. Coating Volume Loss, in^3
10. Maximum Backside Temperature, °F Rise
11. Maximum Pressure, psig
12. Maximum Heat Flux, Btu./Ft.^{2}-sec.

Table X-1 (cont)

ABLATIVE MATERIALS EVALUATION

% Aluminum 18 RUN № 21

Separation Rate 50 D_e in 10 seconds

Distance, Coated Plate Face to Motor ℄ 1.5 D_e

Calorimeter Location X/D_e = - , Y/D_e = -

Pressure Tap Locations 1) X/D_e = 0.47 Y/D_e = 0

2) X/D_e = - Y/D_e = -

TOP OF TOWER

	A	B	C
1.	21 A-1	21 B-1	21 C-1
2.	Dow Corning Q 90-006	Martyte	Raytheon RPP 2140
3.	90.8 gm	98.8 gm	32.9 gm
4.	75.5 gm	67.9 gm	19.7 gm
5.	15.3 gm	30.9 gm	13.2 gm
6.	0.2188 in	0.2656 in	0.1719 in
7.	0.1875 in	0.1563 in	0.0938 in
8.	0.0313 in	0.1093 in	0.0781 in
9.	0.63 in^3	1.26 in^3	0.53 in^3
10.	130 (Est) °F	120 (Est) °F	100 °F
11.	- psig	1.35 psig	- psig
12.		- Btu./Ft^2-sec.	

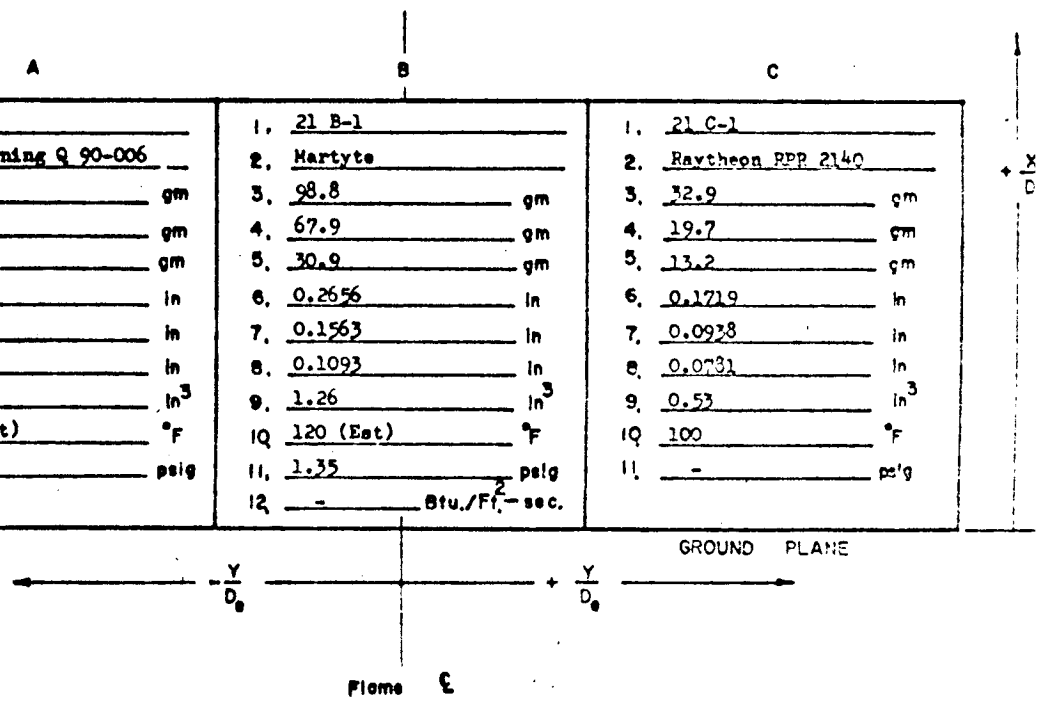

LEGEND

1. Panel Designation: Run № and Panel Location (as B-1)
2. Coating Material
3. Coating Weight Before Firing, gm.
4. Coating Weight After Firing, gm.
5. Coating Weight Loss, gm.
6. Coating Thickness Before Firing, in
7. Coating Thickness After Firing, in
8. Coating Thickness Reduction, in
9. Coating Volume Loss, in^3
10. Maximum Backside Temperature, °F Rise
11. Maximum Pressure, psig
12. Maximum Heat Flux, Btu./Ft^2-sec.

Table X-1 (concl)

ABLATIVE MATERIALS EVALUATION

% Aluminum 18 RUN № 22

Separation Rate 50 D_e in 10 seconds

Distance, Coated Plate Face to Motor ℄ 1.5 D_e

Colorimeter Location X/D_e = - , Y/D_e = -

Pressure Tap Locations 1) X/D_e = 0.47 Y/D_e = 0

2) X/D_e = - Y/D_e = -

TOP OF TOWER

	A	B	C
1.	22 A-1	22 B-1	22 C-1
2.	Martyte MN-7-1	Dynatherm E-300	Dynatherm E-300
3.	130.8 gm	90.1 gm	94.8 gm
4.	102.0 gm	82.8 gm	86.9 gm
5.	28.8 gm	7.3 gm	7.9 gm
6.	0.3125 in	0.3125 in	0.3125 in
7.	0.2187 in	0.2656 in	0.2812 in
8.	0.0938 in	0.0469 in	0.0313 in
9.	1.17 in^3	0.37 in^3	0.40 in^3
10.	120 (Est) °F	120 (Est) °F	120 (Est) °F
11.	- psig	.99 psig	- psig
12.		- Btu./Ft^2-sec.	

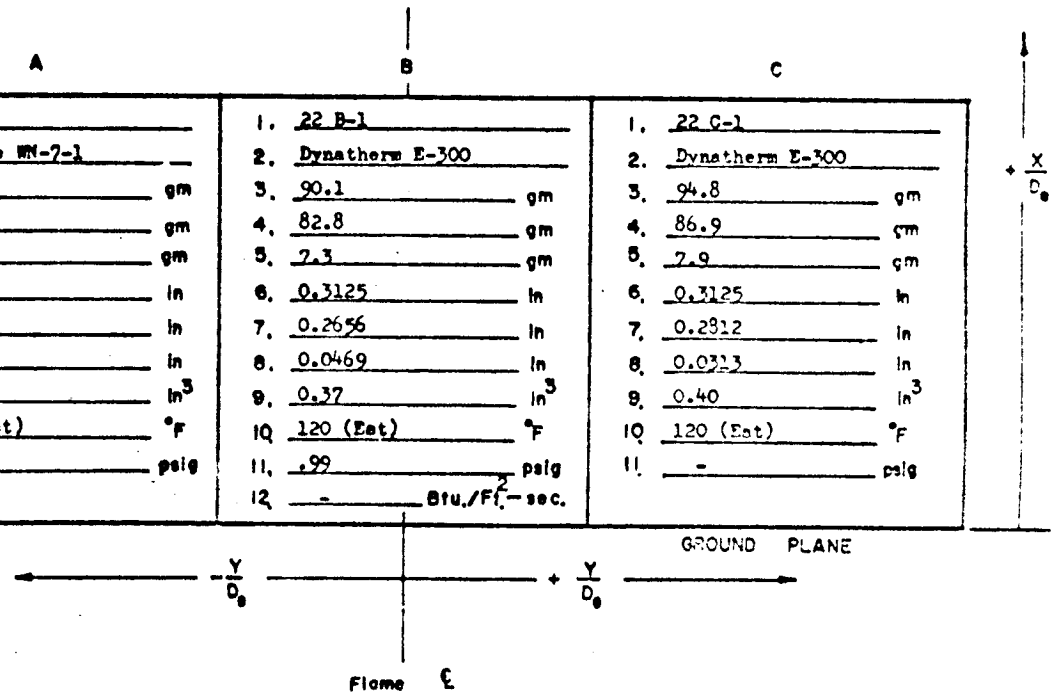

LEGEND

1. Panel Designation: Run № and Panel Location (as B-1)
2. Coating Material
3. Coating Weight Before Firing, gm
4. Coating Weight After Firing, gm
5. Coating Weight Loss, gm.
6. Coating Thickness Before Firing, in
7. Coating Thickness After Firing, in
8. Coating Thickness Reduction, in
9. Coating Volume Loss, in^3
10. Maximum Backside Temperature, °F Rise
11. Maximum Pressure, psig
12. Maximum Heat Flux, Btu./Ft^2-sec.

Table X-2 Relative Performance of Protective Coatings

Ablative Material		Number of Samples	Loss in Weight (%)		Loss in Volume (%)	
Name	Type		Mean	Range	Mean	Range
Martyte WN-1	Epoxy	3	6.5	1.1 to 12.4	4.3	0.74 to 5.3
Dynatherm E-300	Subliming Epoxy	4	6.8	4.2 to 8.3	5.6	3.5 to 6.9
Dow Corning Q90-006 Separation Rate $\geq$ 35 D_e	Silicone	6	11.4	6.9 to 16.9	7.6	4.6 to 11.1
Separation Rate < 35 D_e		2	28.4		19.25	
Martyte WN-7	Epoxy	2	15.62		10.42	
Raytheon RPR 2141	Epoxy	2	12.3		10.2	
Raytheon RPR 2138	Epoxy	1	14.9		10.0	
Raytheon RPR 2156	Elastomeric	2	12.35		11.2	
Martyte WN-11	Epoxy	2	18.0		12.0	
Martyte WN-263 Separation Rate $\geq$ 35 D_e	Epoxy	12	19.0	8.1 to 34.0	12.7	5.4 to 23.0
Separation Rate < 35 D_e		2	54.0		36.4	
Fuller Korblate II-190-L	Silicone-Cork	2	8.7		12.7	
GE RTV 511	Silicone	1	16.5		14.0	
Martyte	Epoxy	6	24.1	15.4 to 31.3	16.1	10.3 to 24.0
Dow Corning Q93-019	Silicone	1	21.1		16.2	
Raytheon RPR 2140 Separation Rate $\geq$ 35 D_e	Elastomeric	6	26.7	5.6 to 56.7	17.6	3.7 to 37.0
Separation Rate < 35 D_e		2	61.6		40.0	
Dow Corning Q2-0103	Silicone	1	30.7		21.2	
Fuller 190J-4	Epoxy	2	23.6		21.75	
Dow Corning Q3-0121	Silicone	1	25.5		24.0	
Fulblate 878 Type II	Epoxy	2	26.4		24.0	
Fulblate 878 Type I	Epoxy	3	28.2	25.9 to 29.7	26.9	24.7 to 28.3
GE RTV 757	Foaming Silicone	2	20.0		28.5	

XI. CONCLUSIONS

A. DEFLECTOR COATINGS

Five deflector coatings were evaluated: Fondu Fyre WA-1, Fondu Fyre XB-1, Portland cement concrete, H-W Harcast ES, and H-W Special Mix 13-65. Of the five coatings, Fondu Fyre WA-1 was selected as the best all around coating for large-scale applications. Selection was based on performance, cost, and ease by which a satisfactory pour and cure can be effected. Though Fondu Fyre XB-1 and H-W Special Mix 13-65 eroded less under a given environment, they had undesirable spalling characteristics and cost considerably more than Fondu Fyre WA-1. Fondu Fyre WA-1 could be poured and cured without cracking under a wider latitude of conditions than XB-1. When cracked, Fondu Fyre WA-1 exhibited a self-healing tendency, and it could be refurbished easily.

B. EFFECT OF ALUMINUM CONTENT

The effect of propellant aluminum content on deflector erosion is not clearly discernible for propellants with common oxidizers and binders for aluminum contents varying between 14 and 22%. Considerably less erosion was experienced, and is to be expected, with 7% aluminum grains that produce lower chamber temperatures.

Deflector coatings that melt when fired upon are eroded primarily as a result of thermal effects. Fondu Fyre WA-1, the coating used to evaluate aluminum content effects, eroded as a result of surface melting. Thus, it is not surprising that the effect of aluminum content was not discernible in the 14 to 22% aluminum range, since motor chamber temperatures were nearly the same.

If propellant oxidizers and binders are varied to derive peak performance from grains with varying percentages of aluminum, the grain producing the greatest caloric output (probably the one with the greatest percentage of aluminum) will cause the greatest Fondu Fyre WA-1 erosion. Deflector coatings that do not melt when exposed to solid rocket motor exhaust will probably be eroded predominately by a mechanical means related to exhaust gas kinetic energy.

C. SCALE EFFECTS

From the limited data obtained it appears that full-scale erosion depths can be predicted somewhat conservatively but quite accurately via model tests. The technique requires that full-scale separation rates in terms of nozzle diameters per unit of time be matched with the model. Proper rocket motor and deflector scaling is, of course, a requirement. A model deflector coating that is cast instead of gunited, as is done in full-scale applications, will be less dense and therefore slightly more vulnerable to erosion. The crater in the model deflector will be about the same depth as full-scale but the foot print will be reduced by the nozzle-scale relationship. Because of this, gas flow in the model crater will follow a different path than in the full-scale crater and this will tend to cause slightly greater model erosion. Maximum measured erosion on a model Titan IIIC flame deflector was 0.6 in., where, maximum full-scale erosion was 0.5 in.

D. LIFTOFF ACCELERATION EFFECTS

Liftoff acceleration has a very significant effect on deflector erosion. The effect on a Fondu Fyre WA-1 deflector is roughly proportional to the total heat incident on the deflector, which in turn is a function of dwell time. If erosion data, for one vehicle liftoff acceleration, and exhaust plume pressures and temperatures are known, accurate erosion predictions can be made for other liftoff accelerations. In the absence of exhaust plume data and for liftoffs involving a given SRM, erosion is approximately inversely proportional to the square root of separation acceleration in diameters per unit time. For example, if

$\delta_X / D_e = 22$ = maximum erosion depth for a separation rate of 22 nozzle exit diameters in 10 sec,

and

$\delta_X / D_e = 47$ = maximum erosion depth for a separation rate of 47 nozzle exit diameters in 10 sec,

then,

$$\frac{\delta_X / D_e = 22}{\delta_X / D_e = 47} \approx \sqrt{\frac{47}{22}}.$$

This inverse square root relationship applies not only to deflector erosion problems but also to the erosion of umbilical mast protective coatings.

E. EFFECT OF ROCKET MOTOR CANT

Rocket motor cant reduces deflector erosion but the percentage reduction for a typical 6-deg cant situation was not determined to any degree of accuracy. From the limited data available, it looked like a 6-deg cant reduces erosion from 8 to 33%.

F. EFFECT OF SUCCESSIVE FIRINGS

A second firing on a Fondu Fyre WA-1 deflector produced 38% more erosion than was incurred as a result of the first firing.

G. REFURBISHABILITY

Fondu Fyre WA-1 can be refurbished by simply wire brushing away loose scale and by packing wet mix into the crater under pressure. Epoxy can be applied to the area to be refurbished before packing in the wet mix but this would seem unnecessary on the basis of the results obtained without epoxy.

H. PROTECTIVE COATINGS FOR GSE

Protective coatings for GSE (except in direct impingement areas) should be low density, low cost, and should be able to be applied easily. Epoxy resins filled with a ceramic were superior to silicones. Martyte and Dynatherm E-300 were the best of the 17 candidate materials evaluated.

XII. RECOMMENDATIONS FOR FUTURE STUDIES

A review of data obtained during the SPREE program has resulted in identifying certain key investigations that should subsequently be performed. Although the SPREE program produced a large amount of engineering data essential for design of deflectors, launch decks, umbilical towers, and other support equipment that may be exposed to the launch environments of solid propellant rocket motors, it was not planned to develop optimizing design criteria. The SPREE data were accrued from scale model tests that generally present more severe results than those encountered under actual full-scale conditions. Only limited reconciliation with full-scale data was possible due to the limited amount of usable data available from full-scale firings. Major future emphasis should, therefore, be placed on providing proper and adequate instrumentation of full-scale launch operations of all size categories of solid motors to supplement the effects prediction models developed during the SPREE program. The recommendations presented here are grouped into scientific and engineering investigations.

A. SCIENTIFIC INVESTIGATIONS

Data derived from these programs will ultimately allow development of environmental and effects prediction models as a function of more basic rocket motor characteristics and exhaust parameters than those used in current technology. The result of these more generalized solutions will allow application of design data without the constraints of a single or a narrow selection of specific launch facility configurations.

1. Near-Exit Plane External Ballistics Data

Little experimental data are available in terms of temperature and pressure distributions in the exhaust jet stream of solid rocket motors. Most of the data available pertain to jet stream characteristics downstream of the sonic point. What data are available have been analytically extrapolated from internal ballistics analyses. Experimental data are required to allow more accurate definition of particle compositions and velocities as a function of chamber pressure, chamber temperature, and nozzle expansion ratio.

2. Particle Sizes, Distribution, and Solidity

Data pertaining to alumina particle sizes, distribution, and solidity in solid motor exhaust gases are required to theoretically evaluate the results of scale model tests. These data are imperative for specific impulse and thrust coefficient scaling. A knowledge of where in the jet stream particles come into existence as solids would allow better description of plume characteristics. These data should be obtained for various chamber pressures and temperatures, for different propellant formulations, and for several thrust ranges of motors under varying expansion ratios.

3. Particle Velocities, Temperatures, and Paths in Exhaust Jets

Certain assumptions are necessary with regard to particle drag and heat transfer coefficients in a stream whose velocity and temperature vary along the length. Accurate definition of particle characteristics would permit more accurate assumptions and the development of a mathematical model that would allow a greater understanding of particle impact and erosion effects on hot surfaces. Particle impact is the most fundamental difference between the effects of liquid engine and solid rocket motor exhaust gases.

4. Grain Particle Size Effects

The size of aluminum particles introduced into solid propellant formulations varies from 5 to 70 microns in a random distribution. The question arises as to whether the size of the alumina particles in the exhaust stream are a function of the size of the aluminum particles in the grain itself. If there is an interdependence such that smaller aluminum particles result in small alumina particles and these in turn result in reduced effects on launch facilities, it may be technically reasonable to specify more stringent control of aluminum particle sizes in solid rocket propellants. This control may also produce improved performance of the solid rocket. A relatively simple test program should be established where erosion of a selected material is evaluated against the exhaust products of a standard rocket motor where size of aluminum particles is the only variable.

B. ENGINEERING INVESTIGATIONS

These investigations are aimed at expanding the use of SPREE data for applications more adaptable to variances in configuration details of launch facilities.

1. Flow Field of Deflected Jets

It is occasionally necessary to install some launch equipment in the direct path of a deflected exhaust stream. Current design philosophy assumes that the effects of the deflected exhaust are identical to a direct impingement condition. Frequently, unexpected damage to facilities is incurred that cannot be readily explained by this extrapolation process. Temperature and pressure measurements should be made to better identify the characteristics of deflected exhaust streams.

2. Water Cooling of Ablative Deflectors

During the course of the SPREE tests, it was observed that when a deflector was moist before exposure to hot exhaust products, erosion was reduced. It appears, therefore, that refurbishment of ablative deflectors can be reduced if water is introduced onto the deflector before or during exposure to solid rocket motor exhaust products. A complete investigation is merited to optimize the methods for wetting deflectors and to determine potential refurbishment cost savings.

3. Dual Jet Impingement Investigations

With the advent of solid motor strap-on configurations of liquid propellant launch vehicles, complex exhaust plumes are possible. This is particularly true when the liquid and solid motors are ignited before vehicle liftoff. With these configurations, the liquid engines are ignited first with solid rocket motors being ignited just before liftoff. With the large comparative thrust of the liquid engines, the exhaust stream could deflect the solid motor exhaust so that minimal effect is felt by the deflector. The cold-jet test program of SPREE demonstrated the effectiveness of a diversion jet that is approximately the magnitude of the jet to be diverted. Analyses and tests should be performed to evaluate the interaction of solid and liquid jets.

4. Development of New Protective Materials

Adequate testing has now been accomplished to identify desirable characteristics of protective deflector coatings. Until such time as detailed quantitative chemical and mechanical properties can be specified, it will be necessary to evaluate new coatings by means of tests. This should be undertaken, however, only if costs of these new materials, including installation and refurbishment, are lower than the Fondu Fyre WA-1 now shown to be adequate for the launch facility applications, or if new generations of launch vehicles produce a considerably more severe exhaust gas environment than contemporary vehicles necessitating an improved deflector coating.

5. Ignition Overpressure Pulse Investigations

The magnitude of the pressure pulse generated at solid rocket motor ignition can be large (greater than 7 psig). This pressure condition is centralized in the vicinity of the engine compartment and presents a primary concern for vehicle engine compartment design and liquid vehicle tank bottoms. The magnitude of the pulse is a function of launch duct geometry, the deflector configuration, and separation distance between the exit plane of the rocket motor and the first point of impingement of the exhaust gases. Previous analyses indicate that mathematical models to predict the phenomena are overly sensitive to detailed configuration effects. It, therefore, will be necessary to perform scale model tests to measure the overpressure pulse for new and untried vehicle-launch facility configurations.

XIII. REFERENCES AND BIBLIOGRAPHY

A. REFERENCES

1. E. Lays and others: Solid Propellant Rocket Exhaust Effects (SPREE) and Methods of Attenuation, Phase II Final Report, Martin CR-64-87 (Vol I). Martin Company, Denver, Colorado, December 1964.

2. D. Conn: Martin-Denver Inter-Department Communication 0494-WTR-4, Martin Company, Denver, Colorado, March 1965.

3. Clyde L. Whipple: "Elastomeric Silicones for Aerospace Insulation". (Section 1 - Ablative Materials), presented at the Eighth National Symposium, SAMPE, May 1965.

B. BIBLIOGRAPHY

A Brief Study of Flame Deflection. Aerojet-General Report 1323. August 1957.

Analysis of the Flow of Gas Particle Mixtures in Two-Dimensional and Axisymmetric Nozzles. NASA Accession N63-11959. (Also Aerojet-General Report 0162-01TN-16).

Anderson, A. and Johns, F.: Nondimensional Characteristics of Free and Deflected Supersonic Jets Exhausting with Quiescent Air. NADC-ED-54-01-25, March 1954.

Augur, W.L., Richter, F. E., and Allen, A. W.: Critical Literature Survey of Missile Blast Resistant Materials. University of Illinois Report No. 6-1, August 1965.

Bailey, W. S.: "Gas Particle Flow in an Axisymmetric Nozzle." ARS Journal, Vol 31, June 1961, p 793.

Baxter, A.: The Influence of Jet Properties on the Design of Uncooled Deflector Surfaces. ARS Report 625-58, June 1958.

Ellis, H. B.: Design Information for Uncooled Flame Deflectors. Aerojet-General Report 1286, July 1957.

Evans, R. and Sparks, O.: Launch Deflector Design Criteria and Their Application to the Saturn C-1 Deflector. MIN-LOD-DL-5-62, April 1962.

Exhaust Blast Effect Studies for Large Super Boosters. Technical Report No. 1-21 (Interim Report), U.S. Army Engineer Division, Ohio River Division, January 1962.

Exhaust Diffusers for Rocket Engines. NASA Accession N62-10666. (Also Jet Propulsion Laboratory Report TR-32-210).

Exhaust Duct and Flame Deflectors - Literature Survey and Preliminary Design Estimates. Aerojet-General Report 1178, October 1956.

Exhaust Effects on Launching System. Aerojet-General Report 1515.

Flame Deflector Full-Scale Evaluation. Aerojet-General Report 1516, January 1959.

Flame Deflector Scale Model Evaluation. Aerojet-General Report 1457, August 1956.

Friedlander, S. K.: "Particle Impaction on Spheres at High Mach Numbers." ARS Journal, Vol 29, No. 4, April 1959.

Gilbert, M., Davis, D., and Altman, D.: "Velocity Lag of Particles in Linearly Accelerated Combustion Gases." Jet Propulsion, Vol 25, 1955, p 26.

Gilbert, M., Allport, J., and Dunlap, R.: "Dynamics and Two-Phase Flow in Rocket Nozzles." ARS Journal, Vol 32, No. 12, December 1962, p 1929 and 1930.

Glauz, R. D.: "Combined Subsonic-Supersonic Gas-Particle Flow." ARS Preprint 1717-61, April 1961. (Also ARS Journal, Vol 32, No. 5, May 1962, p 7[illegible]3).

Henderson, L. F.: The Impingement of a Supersonic Jet on a Flat Plate. Australian Defense Scientific Service, Mechanical Engineering Note 238.

Hogland, R., and Saarlas, M.: Expansion Nozzles for Gas Particle Flows. Aeronutronics Report C-1232, April 1961.

Hoglund, R.F.: "Recent Advances in Gas-Particle Nozzle Flows." ARS Journal, Vol 32, No. 5, May 1962, p 662 thru 671.

Hoyt, J.: "A Study of Supersonic Jet Deflection." University of California, January 1962.

Hypervelocity Impact of Solid Particles Against Solids. AEDC TDR-62-202. (Also NASA Accession N62-17867).

Ingebo, R. D.: Drag Coefficients for Droplets and Solid Spheres in Clouds Accelerating in Airstreams. NACA TN 3762, 1956.

Kavanu, L. L.: "Heat Transfer from Spheres to a Rarefied Gas in Subsonic Flow." ASME Transactions, Vol 77, 1955, p 617.

Kliegel, J. R., and Nickerson, G. R.: "Flow of Gas-Particle Mixtures in Axially Symmetric Nozzles." ARS Preprint 1713-61, April 1961.

Kliegel, J. R.: One Dimensional Flow of a Gas Particle System. Space Technology Laboratories, TR 59-0000-00746, 1959. (Also IAS Preprint 60-5, January 1960, or JAS, March 1960).

Kronig, R., and Buijsten, J.: "On the Theory of the Heat and Mass Transfer from a Sphere in a Flow Medium at Low Values of Reynolds Number." Journal of Applied Scientific Research. Vol A2, 1951, p 439.

Kurtovich, D. D., and Pinson, G. T.: "Exhaust Heat Radiation of Aluminized Solid Rockets." Space/Aeronautics, July 1961.

Kynch, G.: "Effective Viscosity of Suspension of Spherical Particles." Proceedings of the Royal Society of London, Series A, 25 September 1956.

Locke, S. R., et al: "Development of Materials for Solid Propellant Rocket Blast Deflectors." Society of Automotive Engineers, Report 579C, October 1962.

Lype, E. F.: "One Dimensional Analysis of Non-Isentropic Two-Phase Flow." ARS Preprint 1605-61, February 1961.

Metzger, D. E.: Spot Cooling and Heating of Surfaces with High Velocity Impinging Air Jets. NASA Accession N62-13683. (Also Stanford University Technical Report 52, April 1962.)

Morgenthaler, J. H.: "Analysis of Two-Phase Flow in Supersonic Exhausts." ARS Preprint 1715-61, April 1961.

NOVA Launch Facilities Study. NASA-CR-62-7 (Vol I, II, and III). Martin Company, Denver, Colorado, March 1963.

Pack, D. C., and Roberts, L.: "Flow of an Inviscid Supersonic Jet Past and Infinite Wedge." The Philosophical Magazine, Series 7, Vol 44, May 1953, p 352 and 561 thru 563.

Perry, K. P.: "The Heat Transfer by Convection from a Hot Gas Jet to a Plane Surface." Proceedings of the Institute of Mechanical Engineers, London, Vol 68, No. 30, 1954, p 775 thru 780. (Also Chartered Mechanical Engineer, April 1954, p 207).

Pershing Blast Deflector Materials Development Program. OR 3172, Martin Company, Orlando, Florida, March 1963.

Pershing Sub-Scale Blast Deflector Loads and Environment Tests. OR 2315. Martin Company, Orlando, Florida, January 1962.

Pickford, R. S.: Design of Uncooled Flame Deflectors. ARS Report 582-58, March 1958.

Rannie, W. D.: "Perturbation Analysis of One-Dimensional Heterogeneous Flow in Rocket Nozzles." Progress in Astronautics and Rocketry, Vol 6.

Reinhardt, T. F.: The Problem of Cooling a Rocket Jet Deflector. ARS Report 107-53.

Scherling, A.: "Saturn V Flame Deflector Tests." (NASA Unpublished Data.)

Sehgal, R.: An Experimental Investigation of a Gas Particle System. TR 32-238. Jet Propulsion Laboratory, March 1962. (Also NASA N62-11504, AD 274-314).

Smith, S. R., et al.: Temperature and Composition Measurements in Rocket Exhaust Gases. Naval Ordnance Station Report NOTS 1347, March 1956.

Solid Propellant Rocket Exhaust Effects (SPREE) and Methods of Attenuation, Phase I Report - Updated Version. Martin-CR-64-84, Vol II, Martin Company, Denver, Colorado, December 1964.

Soo, S. R.: "Experimental Determination of Statistical Properties to Two-Phase Turbulent Motion." ASME Transactions - Journal of Basic Engineering, Vol 82, Series D, September 1960.

Taylor, T. D.: "Theoretical Analysis of Heat, Mass, and Momentum Transfer at Low Reynolds Numbers." PhD Thesis, University of California, Berkeley, California, 1962.

Thor IDC Flame Deflector and Uncooled Flat Dome Deflector. Aerojet-General Report 1460.

Torobin, L. B. and Gauvin, W. H.: "Fundamental Aspects of Solids - Gas Flow." Canadian Journal of Chemical Engineering (in 5 parts), Vol 37, p 129, 167, 224 and Vol 38.

Tourin, R. H., et al.: Infrared Radiation of Flames. Warner and Swasey Company, AFCR 2-1071, 1962. (Also NASA Accession N62-16304).

Travis, L. P.: Heat Transfer and Particle Trajectories in Solid-Rocket Nozzles. Aerojet-General Report 0162-01TN-17. (Also AFBSD Technical Note BSD-TDR-62-165, October 1962.)

Ungar, E. W.: "Particle Impacts on the Melt Layer of an Ablating Body." ARS Journal, Vol 30, No. 9, September 1960.

Warren, W., Jr: "Static Pressure Variation in Compressible Free Jets." Journal of Applied Science, March 1955.

Williamson, C. P.: The Effect of Six Pershing Missile Launchings on the EL-GMI Blast Deflector. Martin Company, Orlando, Florida.

Zabrodskii, S.: The Coefficient of Resistance of a Solid Particle in a Gas Flow. NASA 62-10297.

Brown, B.: "Particle Velocity Lag in Metalized Propellants." ARS Preprint 1607-61, February 1961.

Brown, B. and McArty, K. P.: "Particle Size of Condensed Oxides from Combustion of Metalized Solid Propellants." Proceedings of the 8th International Combustion Symposium. Williams and Williams Company, Baltimore, Maryland, 1962.

Carlson, D. J.: "Experimental Determination of Thermal Lag in Gas-Particle Nozzle Flow." ARS Journal, July 1962.

Carlson, D. J.: "Static Temperature Measurements in Hot Gas - Particle Flows." Temperature, Its Measurement and Control in Science and Industry, Reinhold Publishing Company, New York, New York, 1962.

Carrier, G. F.: "Shock Waves in a Dusty Gas." Journal Fluid Mechanics, Vol 4, 1958, p 376.

Chernov, A. P.: The Effect of Solid Admixtures on the Velocity of Motion of a Free Dusty Air Jet. Translation NACA TM 1430, 1957.

Coefficient of Resistance of a Solid Particle in a Gas Flow. NASA Accession N62-10297.

Cody, J. C.: Evaluation of Heat Flux History on Leading Edge of Pershing Blast Deflector. SAM 541-65-16, Martin Company, Orlando, Florida, May 1962.

Corrsin, S. and Lumley, J.: "On the Equation of Motion for a Particle in Turbulent Flow." Applied Science Research, Section A, No. 2 and 3, 1956, p 114 thru 116.

Deflector Erosion Life-Scale Model Evaluation. Aerojet-General Report 1493, August 1958.

Design Information for Uncooled Flame Deflectors. Aerojet-General Report 1286, July 1957.

Drake, R. M. and Bocker, G. H.: "Heat Transfer from Spheres to a Rarefied Gas in Supersonic Flow." ASME, Transactions, Vol 74, 1952, p 1251.

Effects on Adjacent Surfaces from the Firing of Rocket Jets. NASA Accession N62-64324. (Also NACA RML 57D19A).

VIII-1	Wedge Deflector Used for Runs 26 and 27 . .	VIII-4
VIII-2	Wedge Deflector	VIII-5
VIII-3	Wedge Deflector after Firing 27	VIII-6
VIII-4	Effect of Varying Initial Nozzle-to-Deflector Standoff Distance	VIII-7
VIII-5	Data Repeatability as Illustrated by a Comparison of Wedge Deflector Centerline Erosion Profiles	VIII-7
IX-1	Single Plume Rake Pressure and Temperature Pickup Locations and Designations	IX-4
IX-2	Dual Motor Firing Rake Pressure and Temperature Pickup Locations and Designations . .	IX-5
IX-3	Single Plume Rake Installed on Cart before Firing 23	IX-6
IX-4	Dual Plume Rake Installed on Cart before Firing 25	IX-6
IX-5	Rocket Motors Firing during Run 25	IX-7
IX-6	Single Plume Rake after Firing 23	IX-7
IX-7	Single Plume Rake after Firing 24	IX-8
IX-8	Dual Plume Rake after Firing 25	IX-8
IX-9	Exhaust Plume Pressure Profile	IX-9
IX-10	Single Plume Temperature Data	IX-9
IX-11	Exhaust Plume Temperature Profile	IX-10
IX-12	Dual Motor Exhaust Plume Pressure Profile .	IX-11
IX-13	Dual Motor Exhaust Plume Temperature Profile	IX-12

X-1 Variation of Umbilical Mast Surface Pressure during Liftoff X-5

X-2 Umbilical Mast Heating Environment during Liftoff X-5

X-3 Ground Plane and J Deflector Schematic X-6

Table

I-1 Run Schedule I-7

II-1 Properties of Fondu Fyre II-19

II-2 Approximate Chemical Analysis of Fondu Fyre (%) II-19

II-3 Flat Plate Erosion, 30-deg Deflector, Run 1 . II-20

II-4 Flat Plate Erosion, 30-deg Deflector, Run 2 . II-21

II-5 Flat Plate Erosion, 30-deg Deflector, Run 3 . II-22

II-6 Flat Plate Erosion, 30-deg Deflector, Run 5 . II-23

II-7 Flat Plate Erosion, 30-deg Deflector, Run 6 . II-24

IV-1 Propellant Formulations IV-2

IV-2 Predicted Motor Performance IV-15

IV-3 Actual Motor Performance IV-16

V-1 J Deflector Erosion, Run 7 . . . . . V-17

V-2 J Deflector Erosion, Run 8 . . . . . V-18

V-3 J Deflector Erosion, Run 9 . . . . . V-19

V-4 J Deflector Erosion, Run 10 . . . . . V-20

V-5 J Deflector Erosion, Run 11 . . . . . V-21

V-6 J Deflector Erosion, Run 12 . . . . . V-22

V-7 J Deflector Erosion, Run 13 . . . . . V-23

V-8 J Deflector Erosion, Run 14 . . . . . V-24

I. INTRODUCTION

The solid propellant rocket exhaust effects (SPREE) program was initiated to define the exhaust characteristics of solid propellant rockets and to determine the effects of their exhaust products on certain key elements of the launch facilities. The results of the program will allow formulation of criteria that can be used in providing adequate protection of the launch facilities from potentially damaging effects of the rocket exhaust plume.

Although data are available pertaining to liquid rocket engine exhaust characteristics and their effects, similar data have not been evolved for solid rocket motors. This has been due to the relatively limited number of instrumented solid vehicle launch experiences and the complete lack of such experience data from captive firing programs. This latter condition results from the fact that solid propellant motors are captive tested in such an attitude that they exhaust directly into the atmosphere and thereby minimize complicated facility requirements. The limited available data indicate that the effects of solid propellant exhausts are much more damaging on facilities than exhaust products from equivalent liquid engines. With these factors at hand, the SPREE program was initiated.

The program was planned to be implemented in several phases. During the Phase I program, primary emphasis was placed on searching and reviewing literature and available test data, performing theoretical and design analyses that could allow prediction of plume environmental characteristics, their effects on various key elements of the launch facilities, and the evaluation of available protective materials that could be used to minimize damage to facilities. A test program using small-scale solid rocket motors to obtain empirical data on exhaust characteristics and heating and erosion effects was recommended as a result of the Phase I program. Several unique deflector concepts requiring experimental data for evaluation were also suggested, but the expense of a test program involving hot-jet rocket motors did not seem warranted for their initial evaluation.

A compromised test program was established to minimize costs. This program, known as SPREE Phase II, Part I, was implemented and consisted of many cold-jet and 30 hot-jet tests. The broad objective of the Phase II program was that of testing and verifying the theoretical evaluations generated during the Phase I program. Detailed objectives included:

1) Development of insight into motor size scaling effects in terms of deflector erosion;

2) Determination of effects of propellant aluminum content on deflector materials;

3) Determination of the effects of motor chamber pressure on deflector materials;

4) Evaluation of new deflector configurations;

5) Evaluation of deflector materials in both the impingement and near-parallel flow regions;

6) Evaluation of rocket exhaust properties.

Results from the Phase II program indicated that the predication models developed during SPREE Phase I are within reasonable limits of accuracy. One anomaly, however, was uncovered during the hot-firing program relating to the effect of aluminum content on erosion rates. Within the variation of aluminum contents examined, only minor effects due to changes in aluminum content were realized. This led to the conclusion that the erosion rates of solid motors are not linearly related to the aluminum content of the motor. Furthermore, the effects of aluminum content must change rapidly below the 14% levels examined during the test program. It was further revealed that the liftoff acceleration rates had a profound effect on total erosion and may present the most significant exhaust plume variable for evaluation of effects on facilities. Evaluation of deflector materials indicated that cheap, trowelable concrete-type refractory materials are significant contenders as practical deflector materials. The more expensive and difficult to install cast refractory materials appeared to be less desirable for deflector coating applications. A material known as Fondu Fyre WA-1 was determined to be the most suited as an economical, durable, and easily maintainable protective material.

At the end of the SPREE Phase II, Part I program it was concluded that it was possible to develop a handbook that would be useful in the design of deflectors and the selection of protective coatings for launch facility elements that are subjected to exhaust environments. This handbook will be aimed at providing practical and usable data rather than pure analytical and theoretical criteria.

It was subsequently determined that Phase II, Part II of the SPREE program should be conducted for the purpose of providing a handbook. To achieve this goal, 27 hot-jet firings were scheduled to provide additional data. This report presents the data evolved as a result of these firings.

A. PROGRAM OBJECTIVES

The primary objective of SPREE Phase II, Part II, is to develop a handbook that will provide exhaust environmental data necessary for the design of launch facilities, criteria for the selection of deflector coatings (their maintenance and repair), and criteria for the selection of protective materials for those elements of the launch complex that would be damaged by SRM exhaust. To achieve this ultimate objective, additional empirical data from hot-jet firing tests were required to satisfy the following detailed technical objectives:

1) Evaluate and select deflector coating materials that provide adequate deflector protection and will be economical to apply as well as economical to maintain and refurbish;

2) Evaluate and select materials that will economically provide protection of launch site structures from exhaust plume products;

3) Determine heating and pressures on launch site structures due to impingement of exhaust products of single and clustered solid propellant rocket motors;

4) Measure effects of clustered solid propellant rocket motors;

5) Determine exhaust characteristics of clustered solid propellant rocket motors;

6) Determine the effect of booster thrust-to-weight ratio on deflector erosion and launch complex heating;

7) Further verify and modify scaling laws developed in the Phase I and Phase II, Part I program. This objective relied on using Titan IIIC flight data as the basis for obtaining full-scale effects data against which the scaling laws may be validated.

B. PROGRAM DESCRIPTION

The program initially established seven groups of tests that required 24 test firings. During the course of detailed development of the program to provide maximum required data, the program was revised to consist of six groups of tests and a total of 27 individual test firings.

The first group of six single motor firings was conducted using very short (4 sec) burning time rocket motors to allow evaluation and selection of deflector coating materials under static holddown conditions.

The second group of single motor firings consisting of eight runs with liftoff acceleration simulated, was conducted primarily to obtain deflector erosion rates as a function of aluminum content in solid propellant grains. A secondary objective was introduced into this test group to allow correlation of the subscale data being developed during the SPREE program with actual full-scale facility effects data derived from the launch of the Titan IIIC space vehicle. The instrumentation used during the first launch was closely coordinated with that employed for the SPREE program.

The third test group consisted of four single motor firings and provided erosion effects data as a function of liftoff acceleration. Again, an attempt was made to correlate SPREE subscale effects data with actual full-scale Titan IIIC data.

Test group four, consisting of four single motor firings under simulated liftoff conditions, had several detailed objectives. The degree of erosion on a deflector exposed to a second liftoff without refurbishment was evaluated. Also, the procedure and methodology for refurbishment of deflectors was evaluated and validated. To provide more realistic correlation to actual vehicle launch configurations, deflector erosion measurements were made with a simulated liftoff and the cant angle of the engine adjusted to 6 deg off vehicle centerline.

The fifth group of tests consisted of two dual motor firings with liftoff simulated, for the purpose of determining erosion measurements on coated wedge deflectors. Of particular interest during these two runs were the effects on erosion of the deflector of varying the distance of the deflector from the exit plane of the solid motors at the start of liftoff. Also, of major importance was the measurement of erosion of the deflector ridge due to convergence of the exhaust plumes of two engines.

Test group six consisted of three firings with the objective of measuring plume temperatures and pressures over the full length of both single and dual engine exhaust plumes.

A summary schedule for all of the hot-jet firings is shown in Table I-1. Also shown are some of the important characteristics of each of the test firings.

Text resumes on Page I-7

II. MATERIALS EVALUATION (GROUP I)

A. GROUP I TECHNICAL OBJECTIVES

Group I tests were made to evaluate the performance of several candidate deflector coating materials in order to select a material for the J deflector tests. The materials were evaluated for:

1) Resistance to erosion;

2) Spall resistance;

3) Resistance to cracking;

4) Cost;

5) Ease by which a satisfactory pour and cure can be effected;

6) Ease of refurbishment.

Three materials were evaluated: a Portland cement mix similar to that used for the Titan IIIC flame deflector; Fondu Fyre WA-1, now being used by NASA on Saturn deflectors (Complexes 34 and 37B); and Fondu Fyre XB-1, a higher cost deflector coating material that has been recommended as a topping for Fondu Fyre WA-1. The performance of an ice deflector was also evaluated. Table I-1 lists the specific runs made in pursuit of these objectives.

B. TEST CONFIGURATION

The apparatus used for the Group I tests consisted of a fixed rocket motor holding fixture, United Technology Corporation (UTC) TM-1 rocket motors, flat plate deflectors, and a deflector holding fixture. The motor holding fixture was mounted on jacks to facilitate alignment. The deflectors were oriented at a 30-deg angle relative to the rocket motor centerline and positioned so that the distance along the motor centerline between the nozzle exit plane and the deflector equaled three nozzle exit diameters. The motors were fired upward. Figure II-1 shows the test setup. A description of the rocket motor and individual deflectors is presented in the following paragraphs.

1. UTC TM-1 Motors

The UTC TM-1 motors were reloadable. The motor case was SAE 4130 Condition-A steel and the nozzle insert was a high density graphite used to minimize throat erosion. Nozzle throats were nominally 1.00-in. diameter and the exits were 2.84-in. diameter giving an 8:1 expansion ratio. The nozzle exit angle was 17.5 deg. The propellant formulation was a PBAN-type with 15% by weight of aluminum particles. The igniter was boron-potassium-nitrate. Motor chamber pressure was a nominal 650 psia and burn time was 4.3 sec. Figure II-2 shows the UTC TM-1 motor. Figure II-3 shows chamber pressure time histories for Runs 1 thru 6.

2. Deflectors

A total of six flat plate deflectors were evaluated. Each deflector, with the exception of the ice deflector, consisted of a 3/16-in. steel base plate 15-in. wide and 20-in. long with 3/16- by 1 1/2-in. side plates. A 2-in. wire mesh was affixed to the deflector base plate approximately 3/8-in. from the bottom. The ice deflector had a 3/16x15x20-in. steel base to which 3/16x12x20-in. side plates were welded. Carriage bolts were affixed to the base plate to hold the ice in place. A paper honeycomb was provided to facilitate erosion measurements. Figures II-4 and II-5 show the two types of deflectors used before coating. Figure II-6 and II-7 are deflector schematics.

Three types of concrete were evaluated as candidate deflector coating materials. These were Fondu Fyre WA-1, Fondu Fyre XB-1, and a Portland cement mix. The Fondu Fyre mixes are a product of Pryor and Giggey Company, Whittier, California. Fondu Fyre is a premixed combination of selected refractory aggregates and a hydraulic setting binder. According to its manufacturer, Fondu Fyre WA-1 was designed for use as a shielding from radiant heat and short duration flame impingement in all areas of launch buckets and flame deflectors. Fondu Fyre XB-1 was designed as a highly resistant topping for WA-1 in flame impingement areas. Some of the properties of Fondu Fyre WA-1 and XB-1 are given in Table II-1. Chemical composition data are given in Table II-2.

The Portland cement mix was comprised of one part by weight of Portland cement and four parts of crushed fine quartzite aggregate screened in accordance with specifications established for the sizing of aggregate for the full-scale Titan IIIC flame deflector. Grading was within the following limits:

Total Passing	Weight (%)
3/8-in. sieve	100
No. 4 sieve	95 to 100
No. 8 sieve	65 to 90
No. 16 sieve	45 to 75
No. 30 sieve	30 to 50
No. 50 sieve	10 to 22
No. 100 sieve	2 to 8

C. PROCEDURE

Each deflector base plate was weighed before coating. The Portland cement and aggregate were also weighed and proportioned. Dry coating material for each deflector was weighed and mixed with a proportioned quantity of water to assure uniformity of deflectors with like coatings but cast at different times. All deflectors were cured under high humidity conditions in an environmental chamber.

After the deflectors were removed from the environmental chamber, they were allowed to dry out, smoothed with a carborundum wheel and were then weighed. A grid was established on each deflector and the thickness measured at grid intersection points. Targets were marked on the deflector longitudinal centerlines 8 inches from the upstream end. Deflector mounting was so that the rocket motor centerline intersected the target and formed a 30-deg angle with the deflector longitudinal centerline. Distance from the nozzle exit plane to the target was set at three nozzle exit diameters.

After a firing, each deflector was wire brushed to remove loose material and weighed. The grid was reestablished and thickness measured at grid intersection points. Weight loss and thickness reduction data provided the desired erosion information. It was planned to determine eroded volume from weight loss and coating

density data, but the weight data were of too limited accuracy for satisfactory volume computations.

D. INSTRUMENTATION

The only instrumentation involved in Group I tests was a thermocouple for measuring the backside temperature of the deflector coating and a rocket motor chamber pressure pickup. The thermocouple data showed an insignificant backside temperature rise on all tests (less than 10°F) and are not reported in this document.

E. RESULTS

The results of Group I tests are given in the following paragraphs according to run number.

Run 1 - Maximum erosion on the Fondu Fyre WA-1 deflector was 0.635 in. and occurred at points approximately 0.35 D_e (nozzle exit diameters) downstream along the deflector surface from the target and 0.35 D_e to the side of the deflector longitudinal centerline. The erosion appeared to result from surface melting rathrather than sandblasting. There was no evidence of surface spalling. Figure II-8 shows the characteristic erosion pattern. Table II-3 shows the results of erosion measurements.

Run 2 - Maximum erosion on the Fondu Fyre XB-1 deflector was 0.478 in. and occurred approximately 0.35 D_e upstream along the deflector longitudinal centerline. The degradation resulted from surface melting and spalling. Note the large spall area in the upper left-hand corner of Fig. II-9. Movies of this firing revealed that the spalling occurred as the motor was burning out. Table II-4 shows the results of erosion measurements.

Run 3 - The purpose of this run was to see if a crack in a Fondu Fyre WA-1 surface in a high shear flow region would propagate or in any way contribute to the loss of a substantial quantity of deflector surface material. A 0.050-in. artificial crack was built into a deflector 1.13 D_e downstream from the target (Fig. II-10). It penetrated as far as, but not beyond, the wire mesh reinforcement. Results of the firing on this deflector are shown in Fig. II-11. Note that melt from the eroded area flowed into, and sealed, the crack. There were no ill effects evident attributable to the crack. Maximum erosion depth was 0.615 in. Point of occurrence was 0.7 D_e downstream along the surface and 0.35 D_e off the centerline. Table II-5 shows the results of erosion measurements.

Run 4 - The high heats of fusion and vaporization of water coupled with ready availability and negligible cost lead to the suggestion by customer personnel that we evaluate an ice deflector. Several investigators applied a blow torch to a cake of ice and to their amazement found it quite resistant to the heat for short exposure times. This led to visions of ice deflectors coated in a manner similar to that in which an artificial ice skating rink might be coated, and launch facilities in polar regions. The ice deflector run was added to the SPREE program in an effort to put an end to the ice question.

Figure II-12 shows the 12-in. ice block mounted in place before firing. Note the paper honeycomb imbedded in the ice to facilitate erosion measurements. Postfiring photographs are shown in Fig. II-13.

Movies of the test showed that shortly after motor ignition the ice split longitudinally approximately along the centerline. One-half of the ice block fell onto the rocket motor and the other half was ejected about 10 ft from the holding fixture. It appeared that cratering due to the heat was responsible for an increase in the thrust force transmitted to the ice block. The force built to a level sufficient to tear the ice from the carriage bolts holding it in place. The paper honeycomb probably weakened the block forming the concentration point for the longitudinal split. Depth of the pocket formed due to approximately 2-sec exposure to the rocket blast was about 6 in.

Run 5 - Maximum erosion of the Portland cement-quartzite mix was 0.972 in. Point of occurrence was on the target. Figure II-14 is a postfiring photograph. Note the exposed wire reinforcing and spall areas. Table II-6 shows the results of erosion measurements.

Run 6 - The deflector used during Run 1 was refurbished for this run. Preparation for refurbishment involved wire brushing to get rid of the loose scale, chiseling off buildup material, and sandblasting. The Fondu Fyre to be added was mixed with water and simply placed in the area to be refurbished under pressure much as a gunned mixture would be applied in a full-scale application. After curing, the deflector was smoothed with a carborundum wheel. Figure II-15 is a prefiring photograph of the refurbished deflector.

Figure II-16 is a postfiring photo. Note that the refurbished area held up well. Maximum erosion was 0.679 in. and occurred 0.35 D_e downstream and 0.35 D_e to the side of the target. No spalling was evident. Table II-7 shows the results of erosion measurements.

F. ANALYSIS

Figure II-17 shows the centerline erosion profiles of each of the deflectors tested. From these profiles it is evident that Fondu Fyre XB-1 had the greatest resistance to erosion of the materials evaluated, followed by Fondu Fyre WA-1 and the Portland cement mix. Fondu Fyre WA-1 performed almost as well as the XB-1 and the Portland cement mix performed much more poorly than either of the other two candidates.

It was learned during the pouring of the Fondu Fyre deflectors that more care must be exercised in curing XB-1 than WA-1. The first XB-1 deflector cracked when water soaked pads that were being used for cure dried out over the weekend. Pads on the WA-1 deflector also dried out but the WA-1 did not crack. No cracking problem was encountered with either material during environmental chamber cures at 95% humidity and 95 to 100°F.

Besides the tendency to crack during cure if proper conditions are not maintained, Fondu Fyre XB-1 had a spalling tendency (Fig. II-9) not exhibited by WA-1. Fondu Fyre WA-1 stood up well under the crack propagation test and no problem was encountered with refurbishment. Cost of WA-1 is about 30% of the cost of XB-1. Because of the foregoing, Fondu Fyre WA-1 was selected for more extensive testing during the balance of the program.

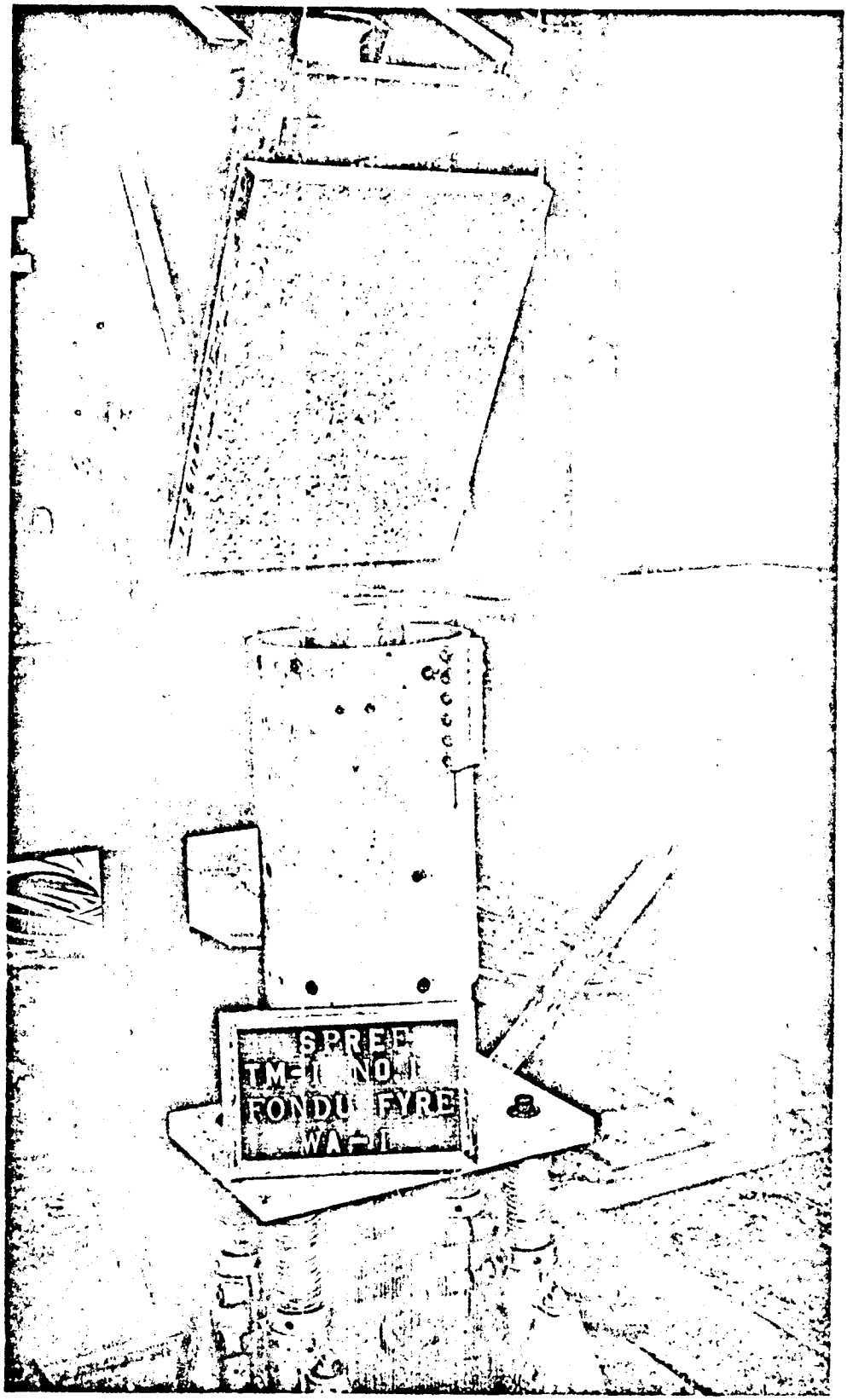

Fig. II-1 Group I Test Setup

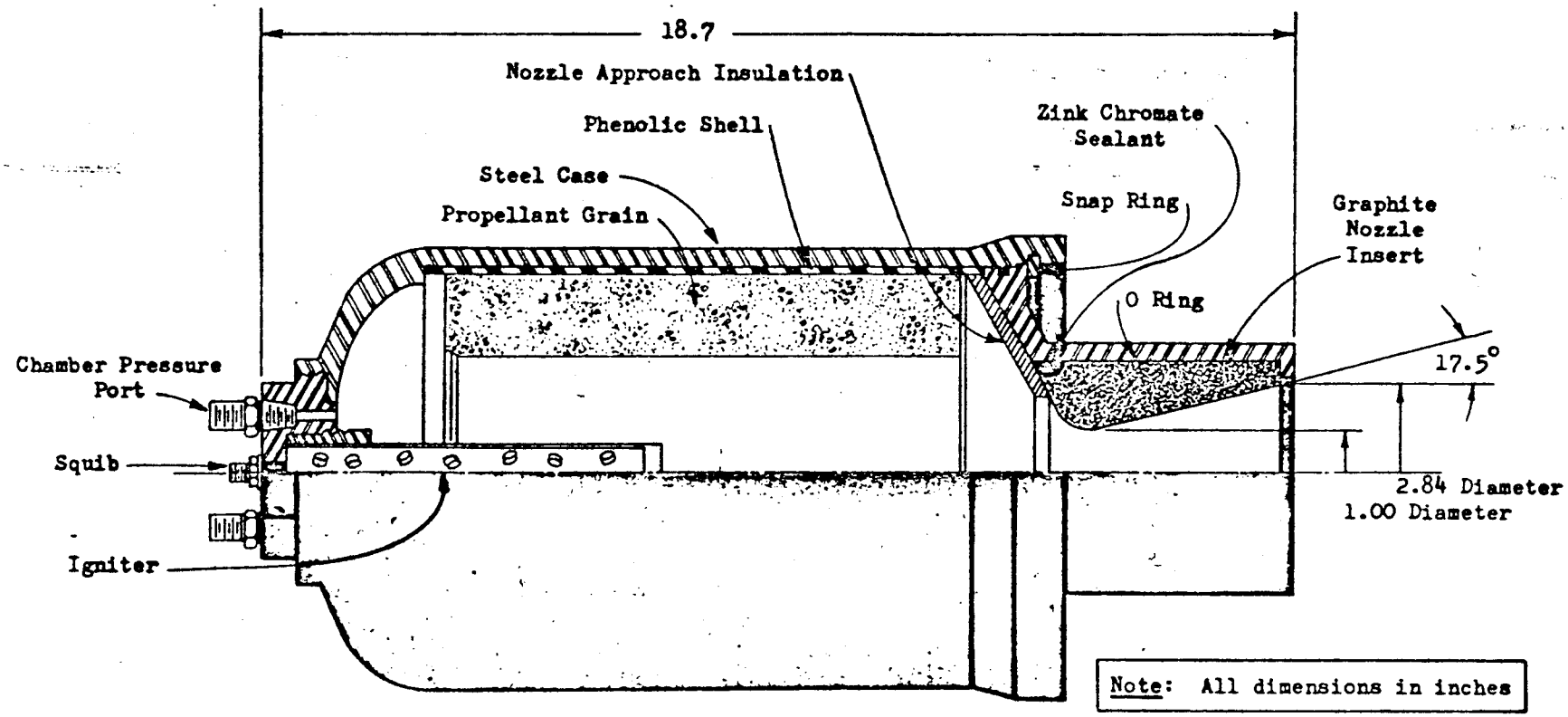

Fig. II-2 TM-1 Motor

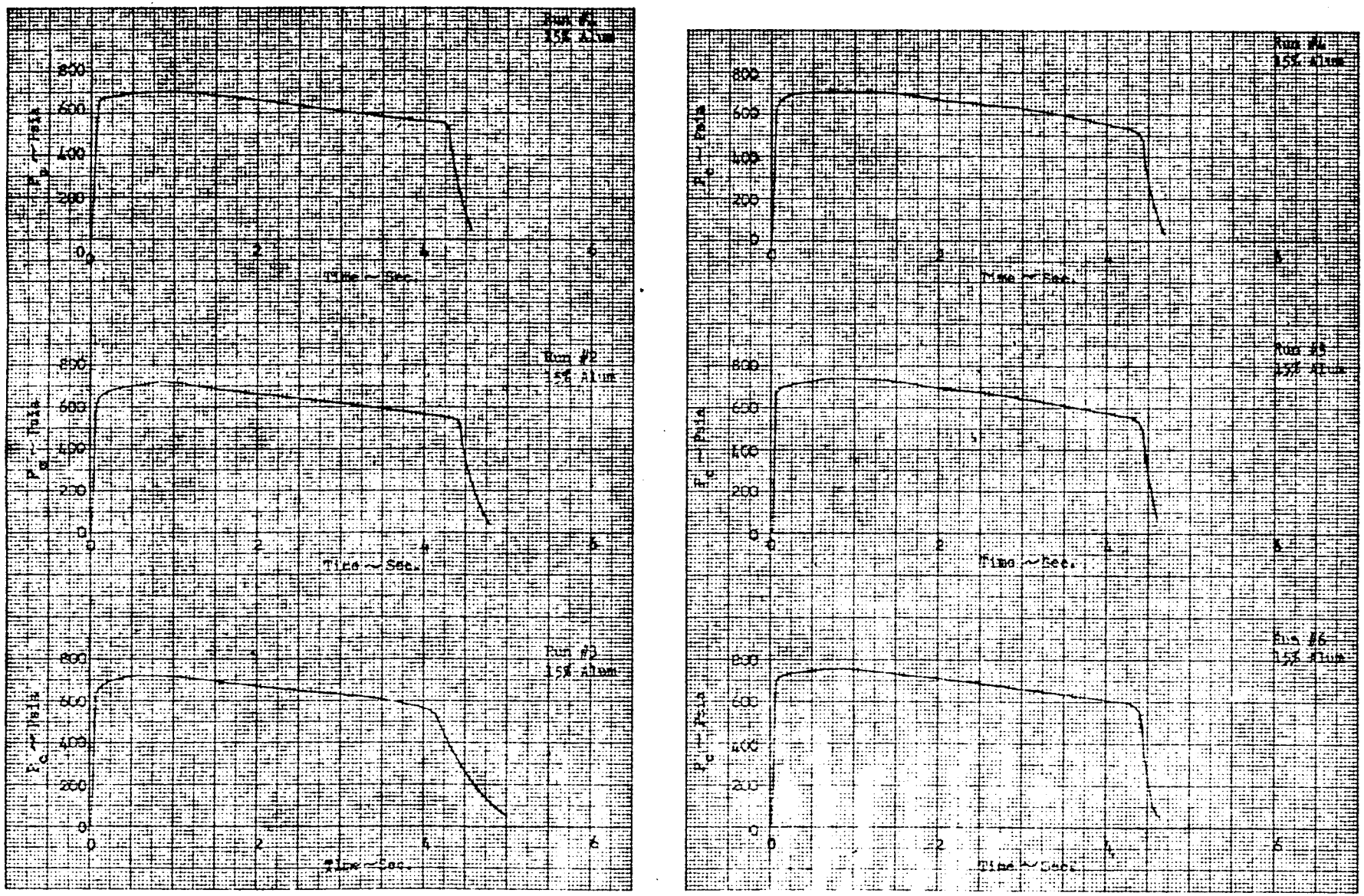

Fig. II-3 Chamber Pressure Time Histories, Runs 1 thru 6

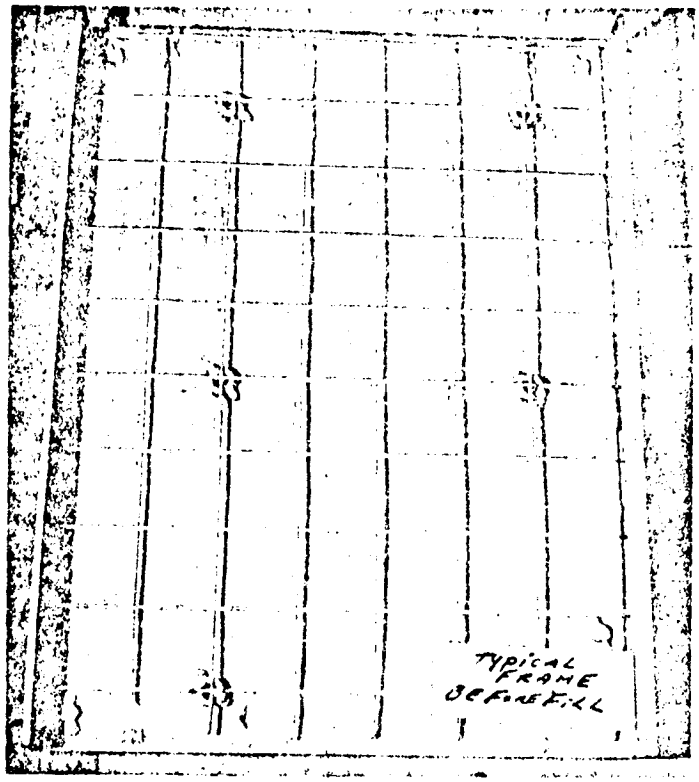

Fig. II-4 Flat Plate Deflector before Coating

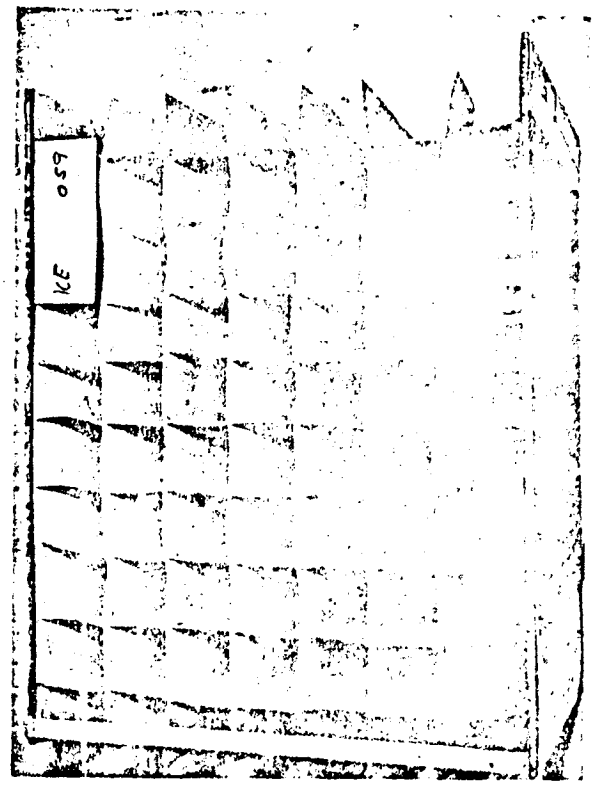

Fig. II-5 Ice Deflector Frame

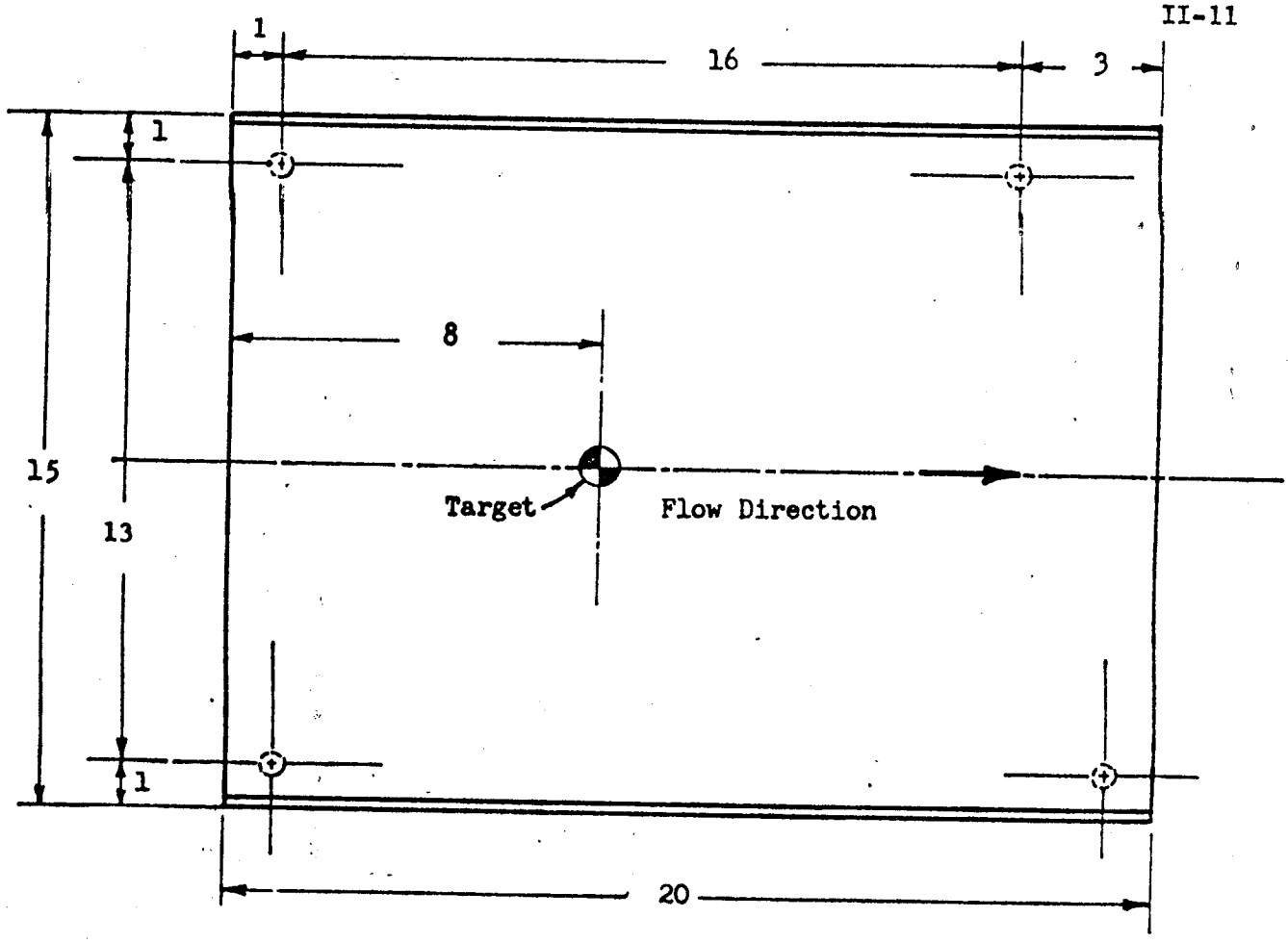

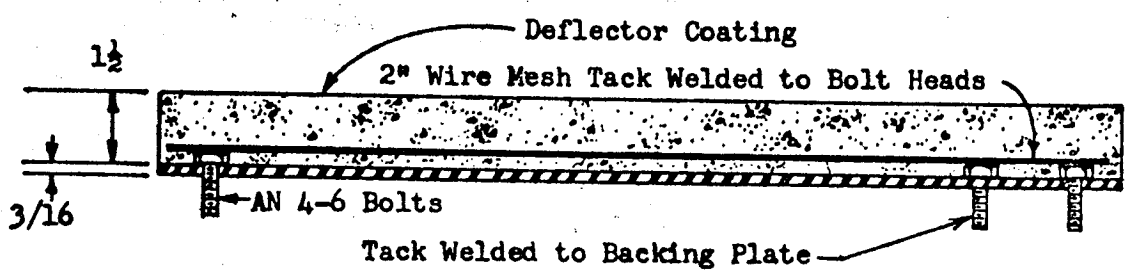

Fig. II-6 Flat Plate Deflector

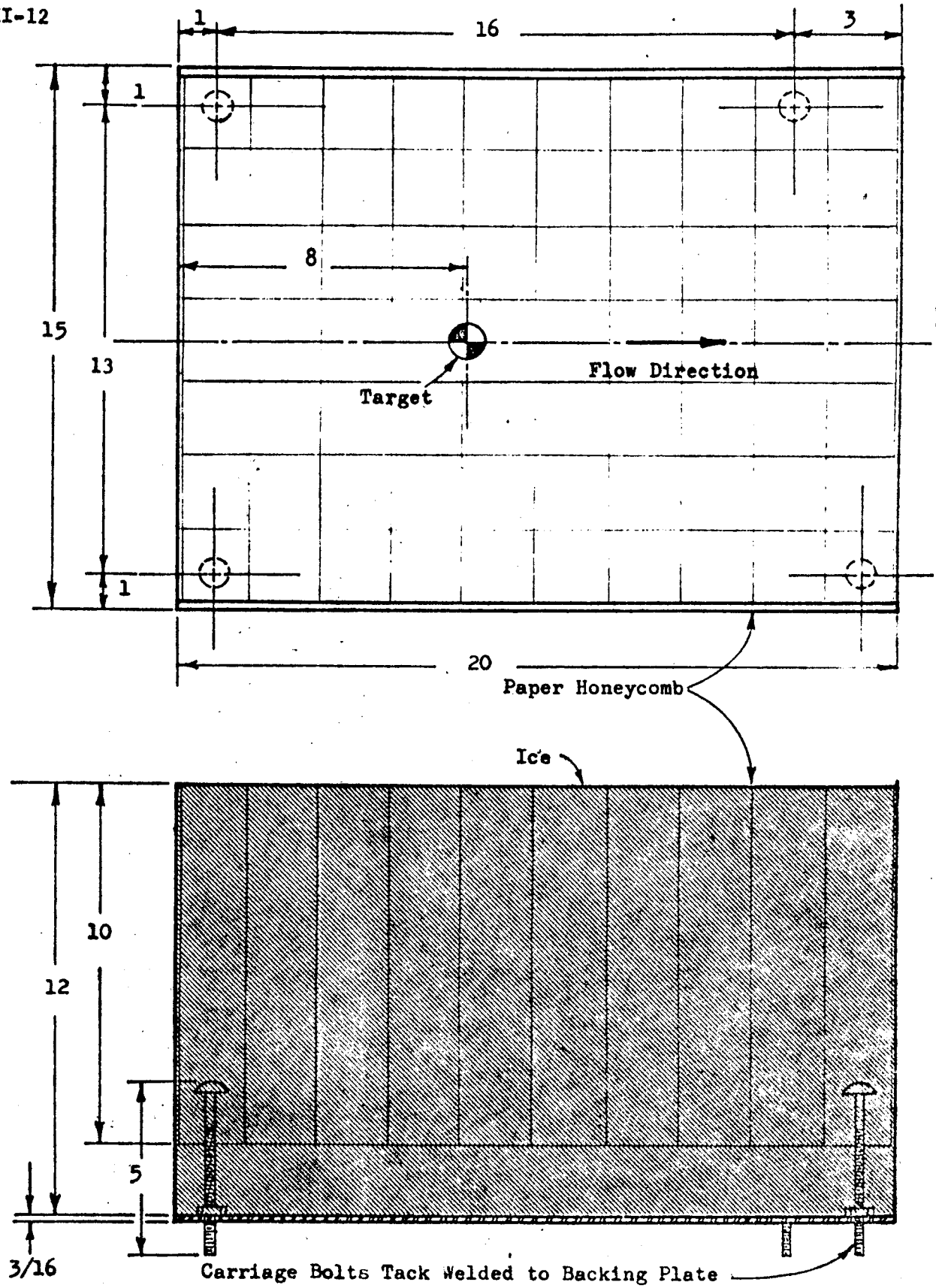

Fig. II-7 Ice Deflector

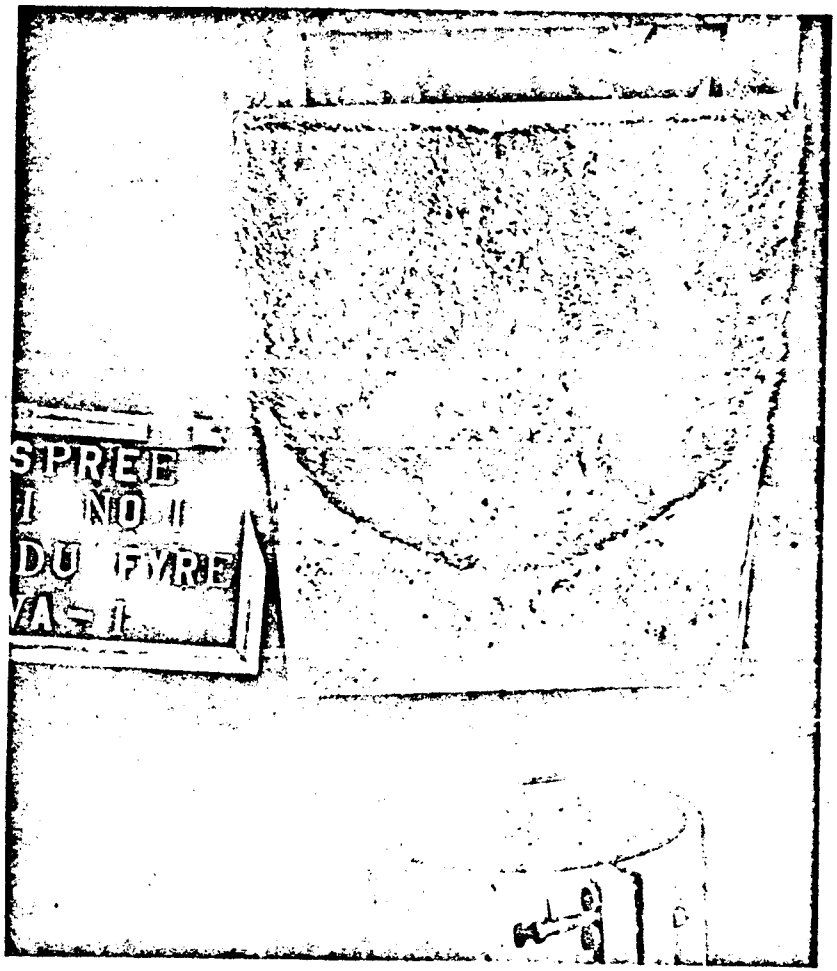

Fig. II-8 Fondu Fyre WA-1 Deflector after Firing

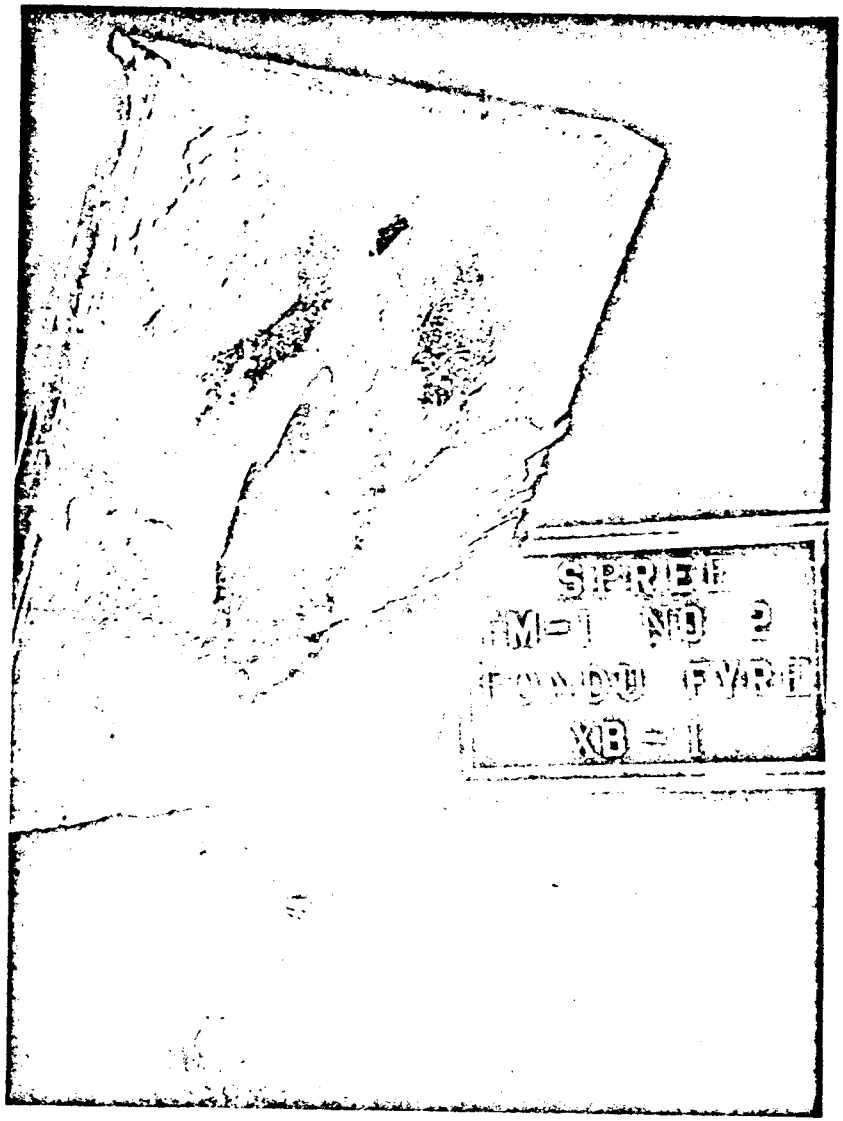

Fig. II-9 Fondu Fyre XB-1 Deflector after Firing

DISTRIBUTION

Copies	To
1 thru 10 and one unbound reproducible	Contracting Officer Kennedy Space Center National Aeronautics and Space Administration John F. Kennedy Space Center, Florida 32899
11	New Technology Representative Counsel for Patent Material Kennedy Space Center National Aeronautics and Space Administration John F. Kennedy Space Center, Florida 32899
12 thru 61	Martin Company Denver Division Denver, Colorado 80201 Attn: Libraries Section

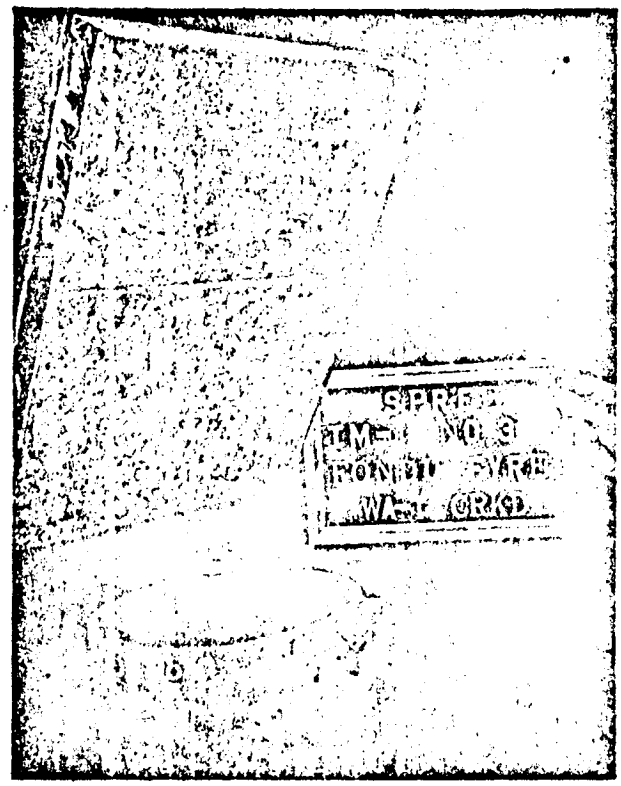

Fig. II-10 Cracked Fondu Fyre WA-1 Deflector before Firing

Fig. II-11 Cracked Fondu Fyre WA-1 Deflector after Firing

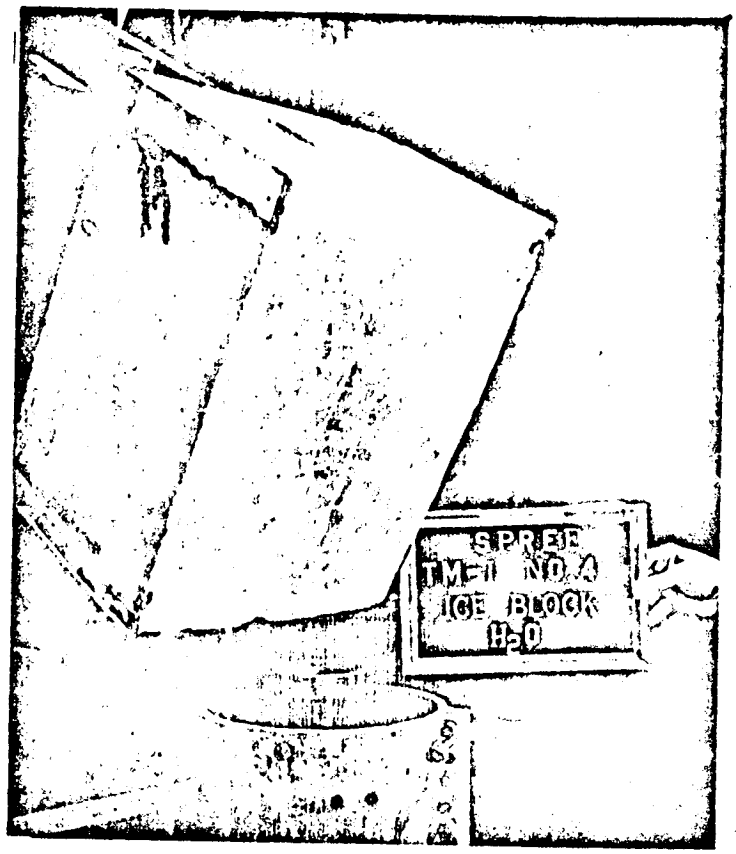

Fig. II-12 Ice Deflector Just before Firing

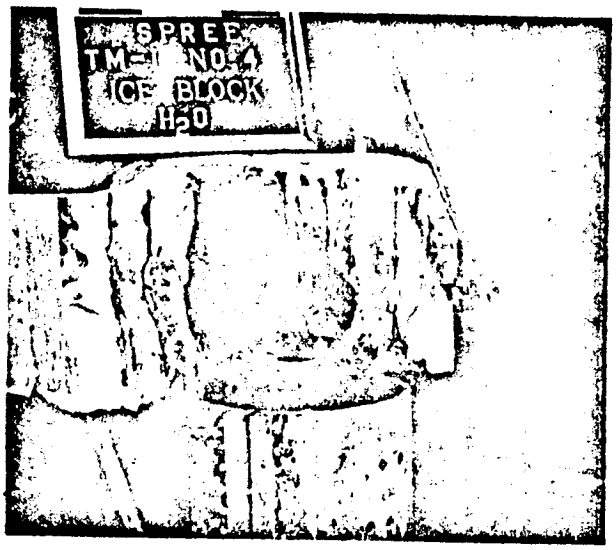

(a)

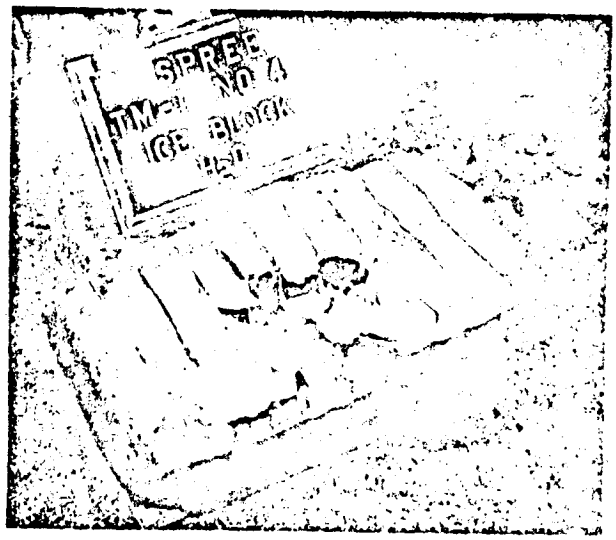

(b)

Fig. II-13 Ice Deflector after Firing

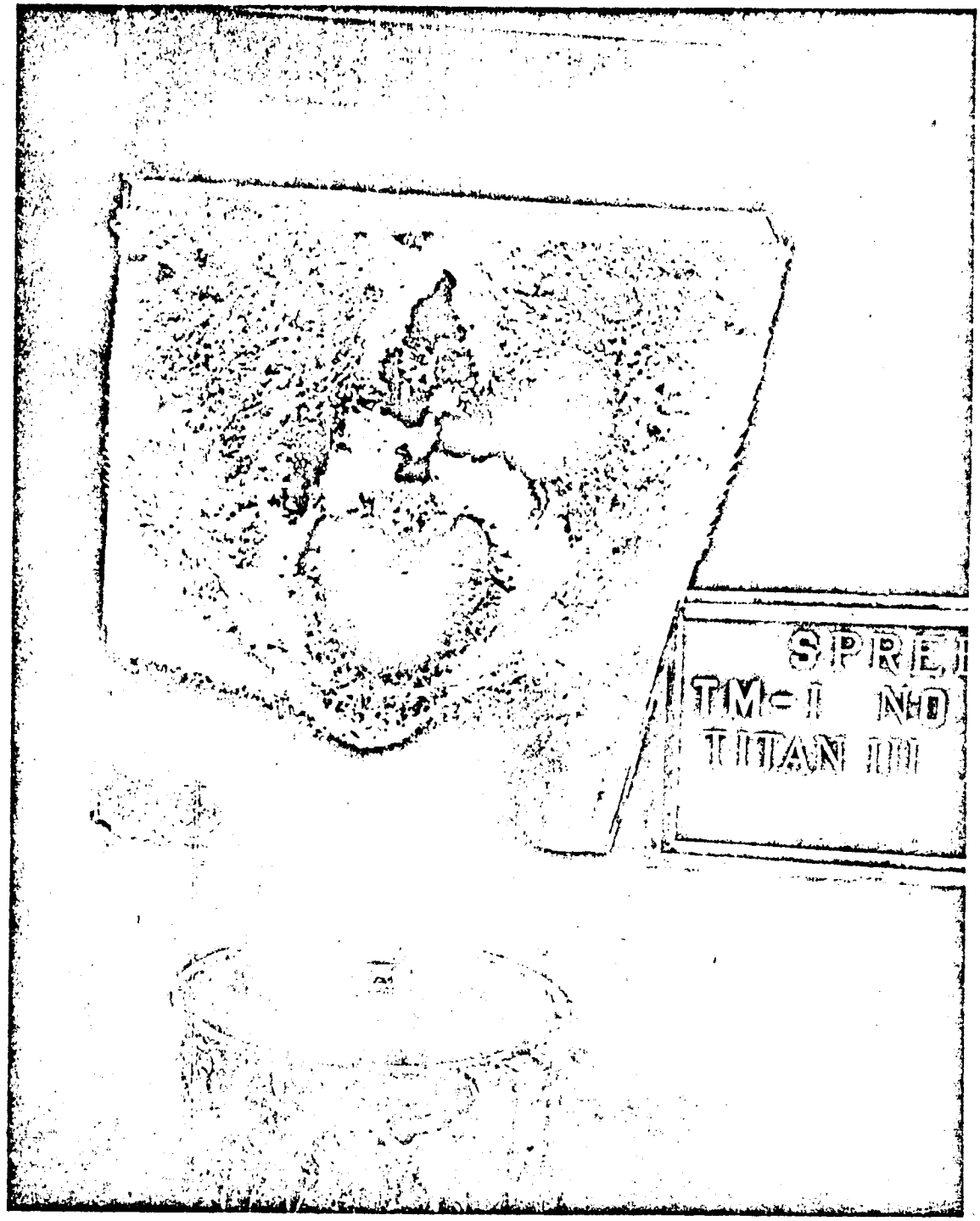

Fig. II-14 Deflector Coated with Portland Cement Mix after Firing

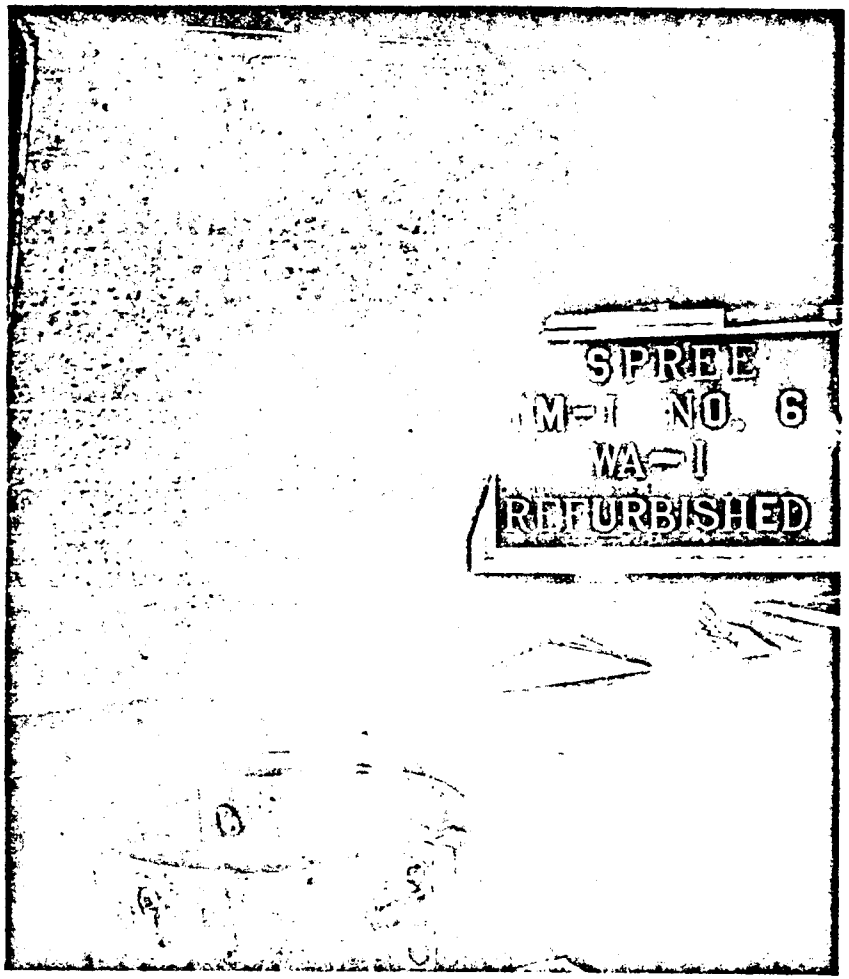

Fig. II-15 Refurbished Fondu Fyre WA-1 Deflector before Firing

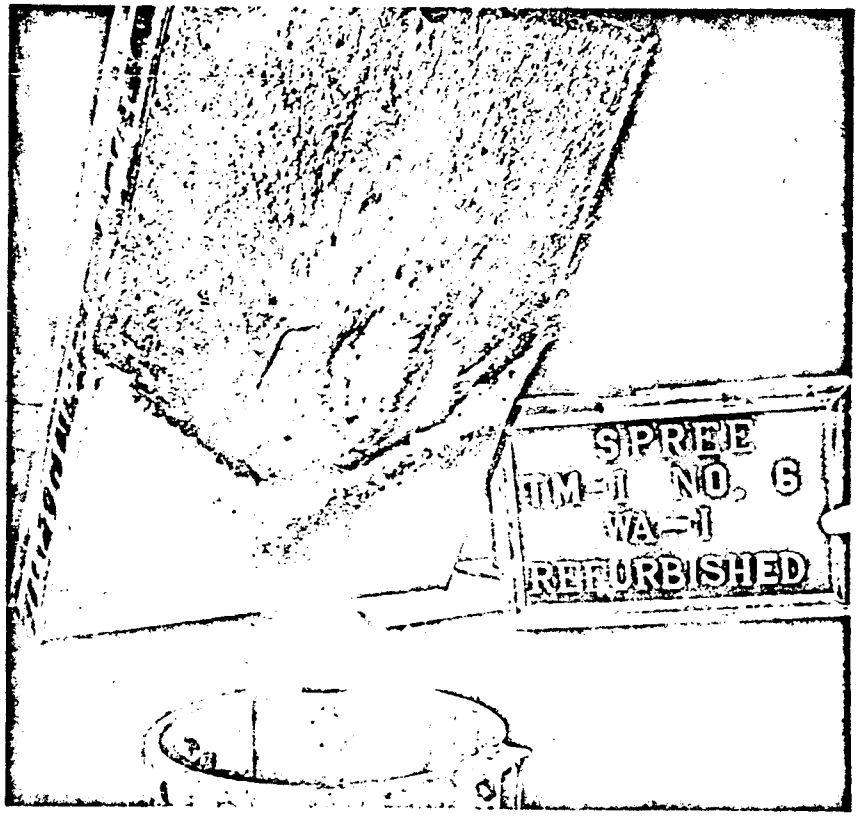

Fig. II-16 Refurbished Fondu Fyre WA-1 Deflector after Firing

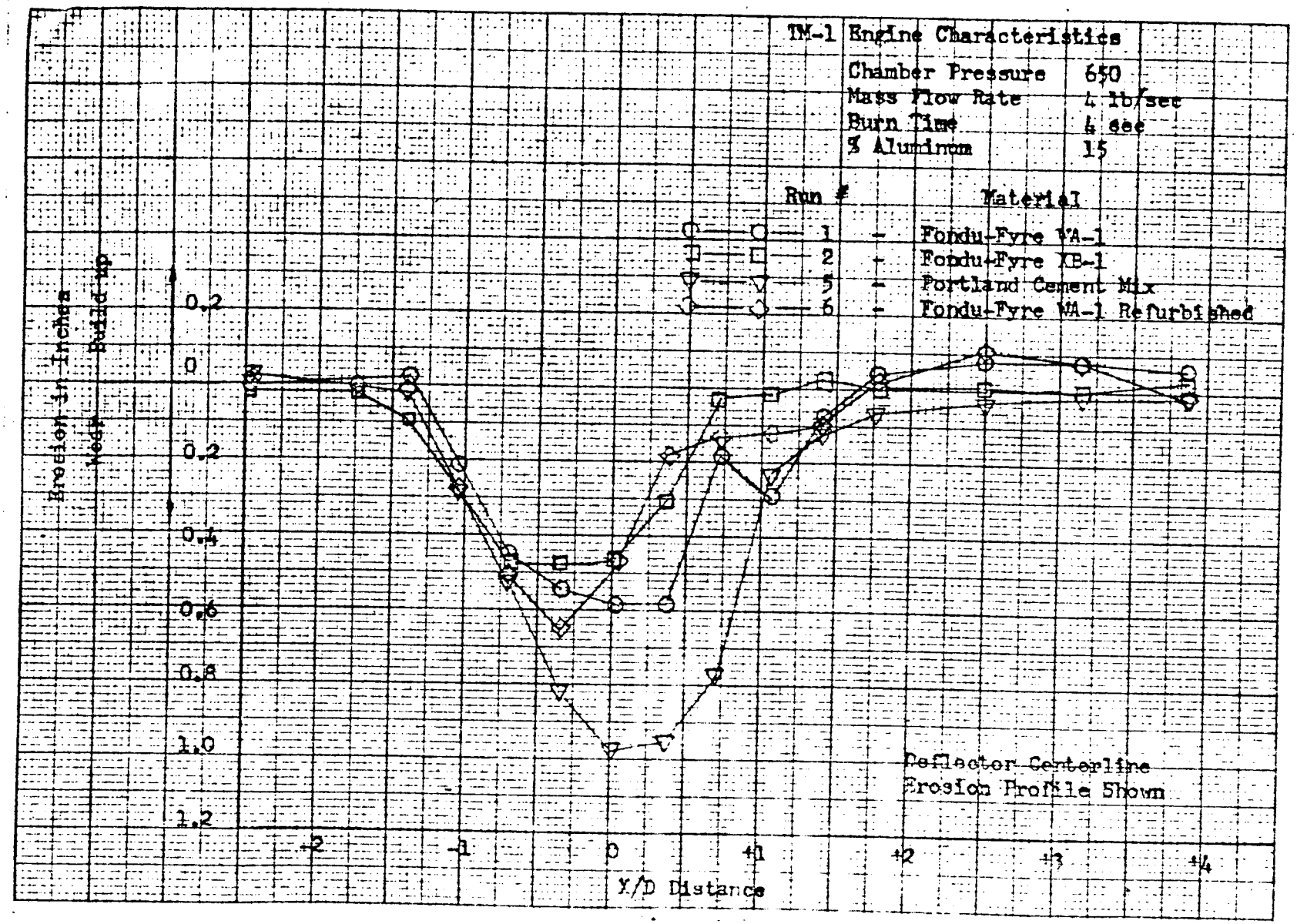

Fig. II-17 Erosion Resistance of Fondu Fyre an P rtland Cement Mixes to Solid Propellant Motor Blast

Table II-1 Properties of Fondu Fyre

	WA-1	XB-1
Density (lb/ft^3)	115	180
Compressive Strength (psi @ 7 days)*	5000	3000
Transverse Bending	916	430
Modulus of Elasticity (10^6 psi @ 7 days)	4.3	4.3
Porosity (%)	16	25
Coefficient of Thermal Expansion (in. x 10^{-6}/°F)	5.6	5.6
Coefficient of Thermal Conductivity (Btu/hr/ft^2/°F/in.)	3.5-4.5	11-13
Specific Heat (Btu/lb°F) estimated at 0°C	0.185	0.145
Approximate cost ($ per cwt)	$5.33	$18.50

*See actual compressive strength of test cylinders evaluated during SPREE testing. Table V-3 and subsequent.

Table II-2 Approximate Chemical Analysis of Fondu Frye (%)

WA-1		XB-1	
SiO_2	34.0	ZrO_2	53.0
Fe_2O_3	11.5	SiO_2	27.0
Al_2O_3	26.5	Al_2O_3	16.0
FeO	1.2	CaO	3.6
CaO	20.1	Fe_2O_3, MgO, Na_2O	0.4
TiO_2	0.5		
			100.0
Na_2O	4.2		
MgO, K_2O and Ignition Loss	2.0		
	100.0		

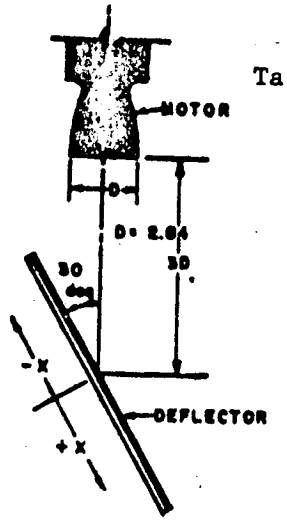

Table II-3 Flat Plate Erosion, 30-deg Deflector, Run 1

DEFLECTOR COATING Fondu Fyre WA-1

GRAIN DATA:

% Al = 18

$\dot{m}$ = 3.8 lbs/sec.

RUN DURATION (nom) 4 sec.

Chamber PRESSURE (nom) 650 psi

COMMENTS

1. POUNDS OF DEFLECTOR COATING ERODED = 2.00
2. MAXIMUM EROSION DEPTH 0.635 in
3. LOCATION OF MAXIMUM EROSION

$\frac{X}{D}$ = +0.35

$\frac{Y}{D}$ = -0.35

TOP OF DEFLECTOR

X/D	-2.11	-1.40	-0.70	-0.35	0	+0.35	+0.70	+1.40	+2.11
-2.46	-.005	+.002	000	-.002	-.002	+.005	000	000	-.002
-1.76	-.006	-.008	-.003	-.002	-.002	-.005	-.005	-.002	000
-1.40	-.005	-.003	+.005	000	+.017	-.017	+.015	000	000
-1.05	-.002	-.002	+.001	-.038	-.211	-.060	-.002	-.008	-.015
-0.70	-.007	-.001	-.028	-.296	-.452	-.350	-.035	-.006	-.019
-0.35	+.002	+.002	-.140	-.428	-.550	-.473	-.183	-.018	-.019
— ℄ of motor — 0	-.020	-.053	-.180	-.540	-.593	-.598	-.322	-.002	-.010
+0.35	+.080	+.050	-.260	-.635	-.587	-.622	-.420	-.010	-.004
+0.70	+.056	+.052	-.182	-.500	-.189	-.368	-.215	000	-.010
+1.05	+.060	+.070	-.055	-.178	-.289	-.208	-.130	+.082	-.013
+1.40	+.010	+.058	+.002	-.108	-.080	-.099	-.040	+.040	-.025
+1.76	+.028	000	+.125	+.033	-.034	-.038	+.063	+.028	-.040
+2.46	+.019	-.031	+.055	+.055	+.078	+.023	+.042	-.045	-.030
+3.16	+.015	-.023	+.042	+.070	+.070	+.047	+.005	-.045	-.040
+3.87	+.128	-.020	-.032	-.028	+.050	+.066	+.002	-.055	-.055

Y/D

℄ of motor

MEASUREMENTS ON DEFLECTOR SURFACE
(- VALUE, EROSION; + VALUE, BUILDUP)

NOTE:
DATA BOX NOT TO SCALE

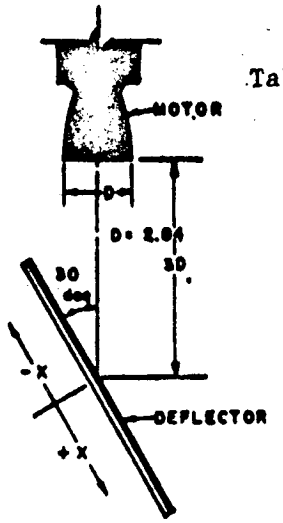

Table II-4 Flat Plate Erosion, 30-deg Deflector, Run 2

DEFLECTOR COATING Fondu Fyre XB-1

GRAIN DATA:

% al. = 18.

ṁ = 3.3 lbs/sec.

RUN DURATION (nom) 4 sec.

Chamber PRESSURE (nom) 650 psi

COMMENTS

1. POUNDS OF DEFLECTOR COATING ERODED = 1.25
2. MAXIMUM EROSION DEPTH 0.478 in
3. LOCATION OF MAXIMUM EROSION

$\frac{X}{D}$ = 0.35

$\frac{Y}{D}$ = 0

TOP OF DEFLECTOR

X/D									
-2.46	-.025	-.020	-.031	-.010	-.015	-.011	-.007	-.003	-.006
-1.76	-.015	-.024	-.023	-.015	-.018	-.035	-.005	-.003	+.002
-1.40	-.017	-.034	-.022	-.020	-.050	-.012	-.002	-.001	-.005
-1.06	-.018	-.017	-.032	-.095	-.241	-.025	-.011	-.002	+.002
-0.70	+.003	-.008	+.028	-.435	-.476	-.348	-.003	-.002	000
-0.35	-.005	-.018	-.022	-.388	-.478	-.400	-.022	-.024	-.006
℄ of motor 0	-.017	-.016	+.005	-.465	-.472	-.430	-.320	-.028	-.010
+0.35	-.025	-.021	-.002	-.451	-.310	-.443	-.363	-.013	-.022
+0.70	-.010	-.013	-.010	-.322	-.033	-.314	-.305	+.010	-.030
+1.06	-.017	-.003	-.159	-.219	-.015	-.019	-.045	+.018	-.029
+1.40	-.002	-.010	-.062	-.295	+.024	+.092	+.023	-.012	-.014
+1.76	-.010	+.024	+.023	+.015	+.004	+.016	-.021	-.031	+.028
+2.46	+.031	+.015	+.036	-.010	+.013	+.005	-.004	-.140	-.041
+3.16	+.052	+.022	+.022	+.038	-.004	-.001	+.026	-.152	-.132
+3.87	+.030	000	+.015	+.023	+.028	-.066	+.022	+.003	-.005
Y/D	-2.11	-1.40	-0.70	-0.35	0 (℄ of motor)	+0.35	+0.70	+1.40	+2.11

MEASUREMENTS ON DEFLECTOR SURFACE
(- VALUE, EROSION; + VALUE, BUILDUP)

NOTE:
DATA DON NOT TO SCALE

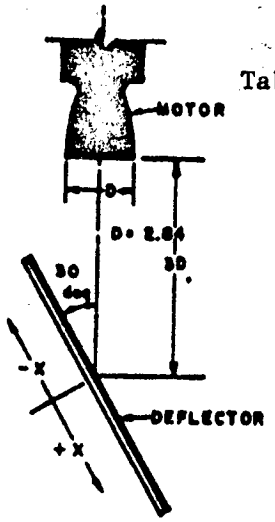

Table II-5 Flat Plate Erosion, 30-deg Deflector, Run 3

DEFLECTOR COATING Fondu Fyre #A-1

GRAIN DATA:

% Al = 18

$\dot{m}$ = 3.7 lbs/sec.

RUN DURATION (nom) 4 sec.

PRESSURE (nom) 650 psi

COMMENTS

1. POUNDS OF DEFLECTOR COATING ERODED = 2.25
2. MAXIMUM EROSION DEPTH 0.615 in
3. LOCATION OF MAXIMUM EROSION

   $\frac{X}{D}$ = +0.70

   $\frac{Y}{D}$ = +0.35
4. An artificial crack was built into the plate at x/D = +1.13

TOP OF DEFLECTOR

X/D									
-2.46	-.002	-.002	+.005	+.015	-.005	-.005	+.030	+.015	+.012
-1.76	-.005	+.010	+.005	+.015	+.003	+.005	+.020	000	000
-1.40	+.005	-.002	+.008	+.020	+.015	+.003	+.020	+.002	+.010
-1.05	+.010	+.008	+.020	+.005	+.030	+.045	000	+.015	+.030
-0.70	+.010	-.010	+.105	-.117	-.202	+.065	+.020	+.005	+.005
-0.35	+.013	+.055	-.090	-.303	-.433	-.170	-.025	+.115	+.020
— ℄ of motor — 0	+.005	+.105	-.107	-.388	-.500	-.425	-.120	+.120	+.015
+0.35	+.095	+.050	-.130	-.501	-.450	-.560	-.145	+.120	+.075
+0.70	+.055	+.060	-.260	-.333	-.173	-.615	-.200	+.075	+.040
+1.05					CRACK				
+1.40	+.032	+.088	-.010	-.068	-.038	-.119	+.005	+.098	+.095
+1.76	+.045	+.090	+.080	-.035	+.020	-.030	+.123	+.100	+.015
+2.46	+.005	-.002	+.093	+.107	+.132	-.117	+.082	+.010	+.005
+3.16	+.008	-.010	+.125	+.095	+.095	-.095	+.080	000	+.002
+3.87	-.005	-.013	+.040	+.065	+.115	+.075	+.035	-.005	+.015
Y/D	-2.11	-1.40	-0.70	-0.35	0 (℄ of motor)	+0.35	+0.70	+1.40	+2.11

MEASUREMENTS ON DEFLECTOR SURFACE
(- VALUE, EROSION; + VALUE, BUILDUP)

NOTE:
DATA BOX NOT TO SCALE

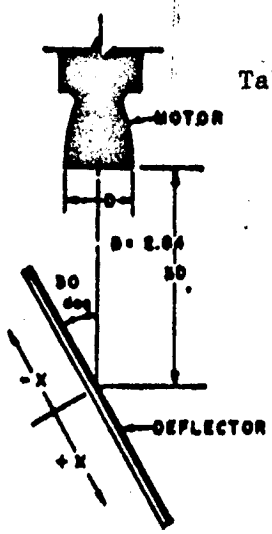

Table II-6 Flat Plate Erosion, 30-deg Deflector, Run 5

DEFLECTOR COATING Portland Cement Mix

GRAIN DATA:

% Al = 18

$\dot{m}$ = 3.3 lbs/sec.

RUN DURATION (nom) 4 sec.

Chamber PRESSURE (nom) 650 psi

COMMENTS

1. POUNDS OF DEFLECTOR COATING ERODED = 1.50
2. MAXIMUM EROSION DEPTH 0.972 in
3. LOCATION OF MAXIMUM EROSION

$\frac{X}{D}$ = 0

$\frac{Y}{D}$ = 0

TOP OF DEFLECTOR

X/D									
-2.46	+.018	+.008	+.015	-.008	+.020	+.003	+.005	+.002	-.003
-1.76	+.002	000	-.005	+.002	+.003	+.013	+.012	+.003	+.005
-1.40	-.022	-.001	+.040	+.011	+.029	+.017	+.001	-.004	-.009
-1.06	+.002	+.006	-.025	-.128	-.285	-.157	-.010	+.001	-.002
-0.70	+.112	-.010	-.060	-.334	-.525	-.339	-.062	-.010	+.017
-0.35	+.008	-.013	-.135	-.548	-.825	-.600	-.140	-.035	-.008
— ℄ of motor — 0	+.006	-.050	-.208	-.775	-.972	-.885	-.339	-.047	-.004
+0.35	-.033	-.044	-.290	-.818	-.955	-.912	-.410	-.055	-.043
+0.70	-.057	-.090	-.525	-.898	-.780	-.937	-.583	-.055	-.050
+1.06	-.060	-.042	-.514	-.653	-.234	-.545	-.612	-.057	-.050
+1.40	-.072	-.040	-.093	-.095	-.128	-.190	-.084	-.067	-.063
+1.76	-.057	-.135	-.048	-.063	-.064	000	-.043	-.048	-.068
+2.46	+.007	-.020	-.020	-.028	-.038	-.011	-.010	-.057	-.040
+3.16	+.013	-.006	-.057	-.051	-.005	-.017	-.030	000	-.013
+3.87	-.005	-.045	-.007	+.070	-.020	-.012	-.047	-.002	-.075
Y/D	-2.11	-1.40	-0.70	-0.35	0 (℄ of motor)	+0.35	+0.70	+1.40	+2.11

MEASUREMENTS ON DEFLECTOR SURFACE
(- VALUE, EROSION; + VALUE, BUILDUP)

NOTE:
DATA BOX NOT TO SCALE

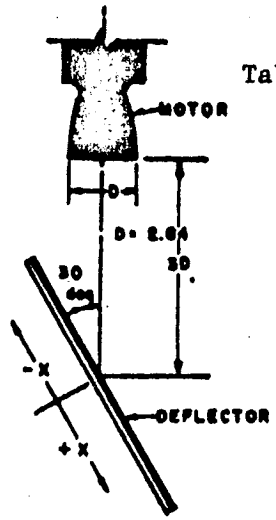

Table II-7 Flat Plate Erosion, 30-deg Deflector, Run 6

DEFLECTOR COATING Fondu Pyro WA-1

GRAIN DATA:

% ot = 18

ṁ = 3.3 lbs/sec.

RUN DURATION (nom) 4 sec.

Chamber PRESSURE (nom) 650 psi

COMMENTS

1. POUNDS OF DEFLECTOR COATING ERODED = 1.25
2. MAXIMUM EROSION DEPTH 0.679 in
3. LOCATION OF MAXIMUM EROSION

   $\frac{X}{D}$ = +0.35

   $\frac{Y}{D}$ = -0.35

4. Deflector used during Run 1 refurbished for this run.

TOP OF DEFLECTOR

X/D	-2.11	-1.40	-0.70	-0.35	0	+0.35	+0.70	+1.40	+2.11
-2.46	-.003	+.005	-.010	-.002	-.015	+.005	-.007	-.005	+.010
-1.76	+.013	+.007	-.003	+.003	+.003	-.015	-.007	-.005	-.070
-1.40	-.007	-.005	-.018	-.013	-.015	-.008	+.018	-.003	-.008
-1.05	+.010	000	-.030	-.090	-.240	-.150	000	-.003	-.010
-0.70	+.005	+.015	-.030	-.398	-.514	-.352	-.013	+.006	-.004
-0.35	+.005	-.013	-.122	-.528	-.630	-.508	-.105	+.009	-.015
— ℄ of motor — 0	-.002	-.008	-.223	-.608	-.490	-.617	-.160	+.005	+.003
+0.35	-.003	+.053	-.262	-.679	-.188	-.660	-.207	+.025	+.010
+0.70	+.005	-.020	-.295	-.522	-.131	-.432	-.220	+.027	+.035
+1.05	-.015	-.008	-.165	-.273	-.123	-.267	-.110	-.020	+.010
+1.40	-.010	-.023	-.050	-.185	-.100	-.105	-.010	+.040	-.019
+1.76	-.035	+.080	+.013	+.085	+.030	-.080	+.050	+.005	-.024
+2.46	-.032	-.025	+.068	+.110	+.100	+.085	+.085	-.030	-.025
+3.16	-.040	-.047	+.005	+.080	+.080	+.045	+.090	-.062	-.027
+3.87	-.035	-.050	-.047	-.065	-.024	+.010	+.090	-.065	-.030

Y/D

℄ of motor

MEASUREMENTS ON DEFLECTOR SURFACE
(- VALUE, EROSION; + VALUE, BUILDUP)

NOTE:
DATA BOX NOT TO SCALE

III. TEST FACILITY

The SPREE test facility was designed with the basic objective of duplicating as nearly as possible the actual environment that is expected to occur during a typical solid propellant vehicle liftoff. The effects of environment were measured and observed on typical deflector shapes and materials as well as on candidate facility protective coatings. The test environment was produced by firing solid rocket motors on test articles mounted on a mobile cart, which was allowed to move away from the solid rocket motors at a programed rate.

A. TEST FIXTURE

The SPREE test fixture is composed of two basic operational components:

1) Acceleration control mechanism;

2) Gravity drive mechanism.

The acceleration control mechanism provides an electromechanical means for programing the separation rate between the solid rocket motor and the test article as shown in Fig. III-1. This mechanism is operated by a constant speed 40-hp electric motor that drives two gear reduction boxes that are interconnected by drive chains to a large swing arm. The swing arm pays out cable to the test cart at a rate consistent with the programed acceleration. Varying rates of acceleration are accomplished by interchanging gears in combination with varying the swing arm radius. A simulated hold down is achieved by positioning the swing arm slightly past dead center so as to delay initial cart movement by approximately 0.20 sec. The solid motor ignition switch is tripped by the swing arm as it travels through its operational cycle. The acceleration control mechanism has a range capability of uniform accelerated cart movements of between 15 nozzle exit diameters (D_e) to 130 nozzle exit diameters in 10 sec. In actual full-scale applications these accelerations correspond to thrust/weight ratios of approximately 1.1 to 2.0.

Figure III-2 presents two typical simulated liftoff rates showing the comparison of the desired rate of separation and the expected rate of separation. Expected separation rates are regulated by the design of the acceleration control mechanism and are held close to the desired separation rate for the first 6 to 7 sec of a run. Deviations during the latter portion of the run are considered to be within an acceptable tolerance and to have a negligible effect on the test results. Figure III-3 compares expected and actual cart travel time histories.

The gravity drive mechanism is provided to insure a continuous pull on the test cart so that positive nonlagging movements are insured during the full range of test accelerations. Essentially the gravity drive mechanism operates by the action of a 500-lb falling weight that is connected to the cart through a pulley and a cable system (Fig. III-1).

B. TEST SETUPS

The SPREE program specified a series of test evaluations defined by the run schedule shown in Table I-1. Basically, these runs set forth the requirements for testing both J- and W-type deflectors as well as for measuring the exhaust plume characteristics during solid rocket motor firings. Material sample evaluations were integrated and run simultaneously with the J deflector test runs. Two of the J deflector runs were conducted with the solid rocket motor oriented at a 6-deg angle with respect to the deflector centerline in order to simulate actual exhaust impingement alignment during liftoff.

Scale effects are accounted for by expressing all separation distances in terms of nozzle exit diameters (D_e) from the nozzle exit plane or from the center of the exhaust plume, rather than in absolute scalar distances. In this way model geometry may be correlated with full-scale geometry by simply substituting the full-scale nozzle dimensions to get a comparable full-scale separation distance. All deflector tests were conducted at initial nozzle-to-deflector separation distances of either 2.5 or 3.0 D_e, and material sample tests were made at lateral separation distances of 1.25 and 1.50 D_e. Exhaust plume measurements were made beginning at 8 and 12 D_e for the single and double motor firings, respectively.

C. INSTRUMENTATION

SPREE instrumentation was designed to measure critical temperatures, pressures, heat fluxes, accelerations, and loads necessary to evaluate test performance. Figure III-4 shows the instrumentation that was monitored for the deflector and material tests. All instrumented data were transferred via cables directly from the test setup to the blockhouse for recording on automatic CEC oscillographs.

Deflector and material sample test instrumentation consisted of the following:

1) Six thermocouples to measure backside time-temperature characteristics of the material samples and deflector materials;

2) Five pressure transducers to measure the pressure level in the motor thrust chamber, on the material samples, and on the ground plane;

3) A single calorimeter for measuring heating environment in the area of the material samples;

4) Two test cart acceleration measurement devices:

   Pencil lead electrical signals actuated by cart movement,

   Photoelectric cell signals actuated by cable pulley movement;

5) A load cell integrated with the cable linkage to measure the time history of the load in the acceleration control mechanism.

Measurement of the critical plume characteristics of solid rocket motors in single and dual configurations was accomplished by using temperature and pressure-instrumented rakes.

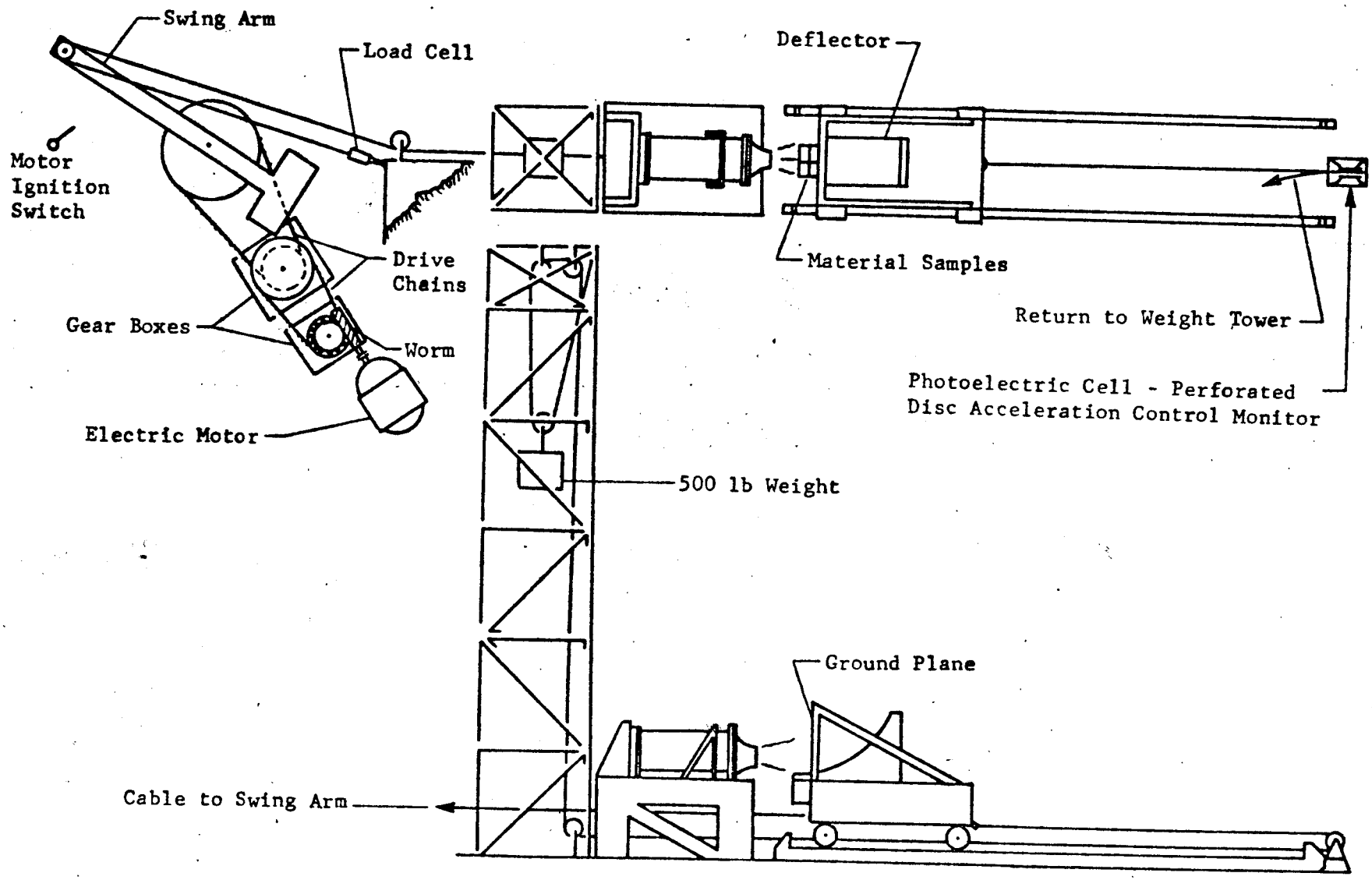

Fig. III-1 SPREE Acceleration Control Test Fixture

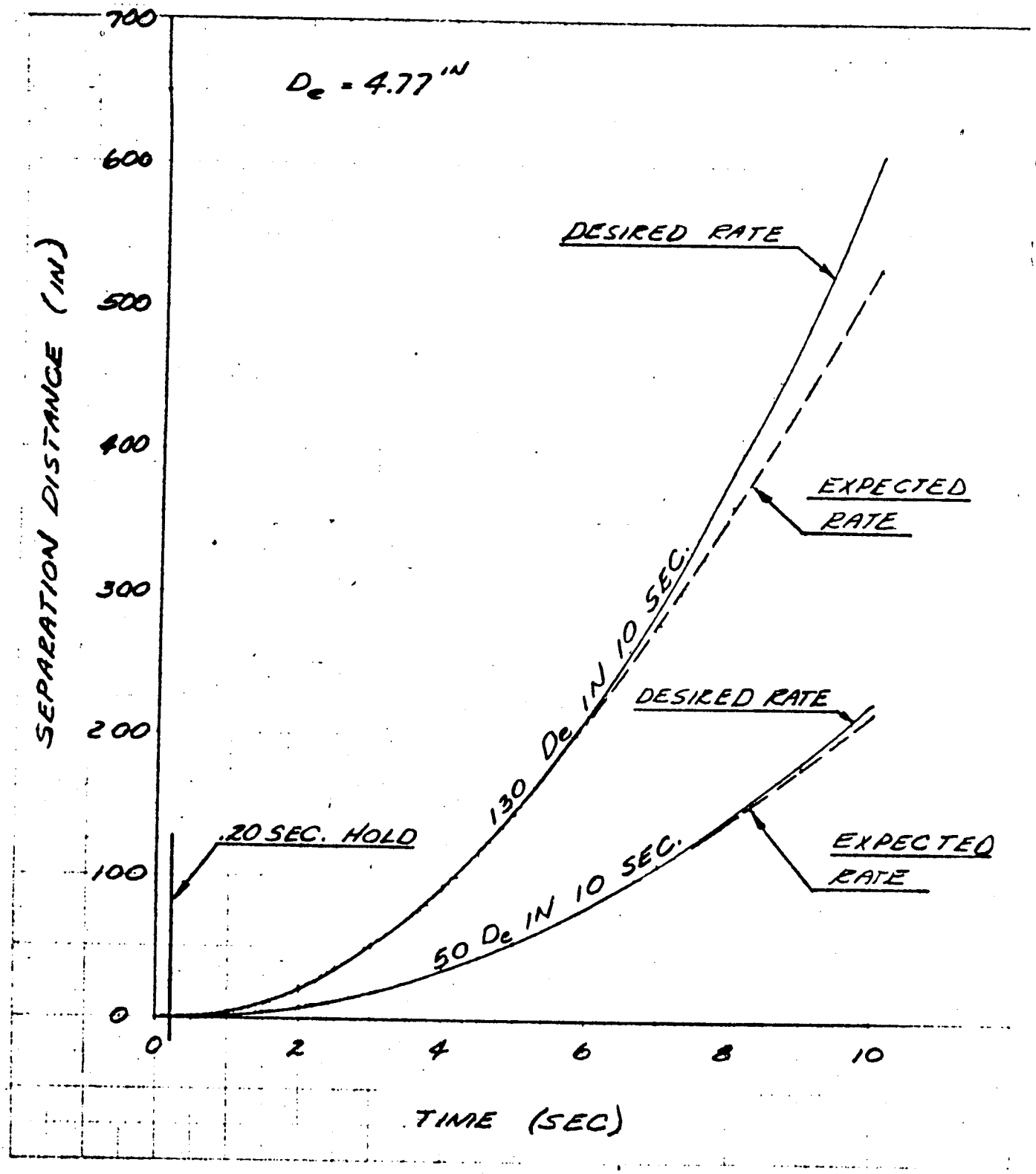

Fig. III-2 Comparison of Typical Desired and Expected Liftoff Rates

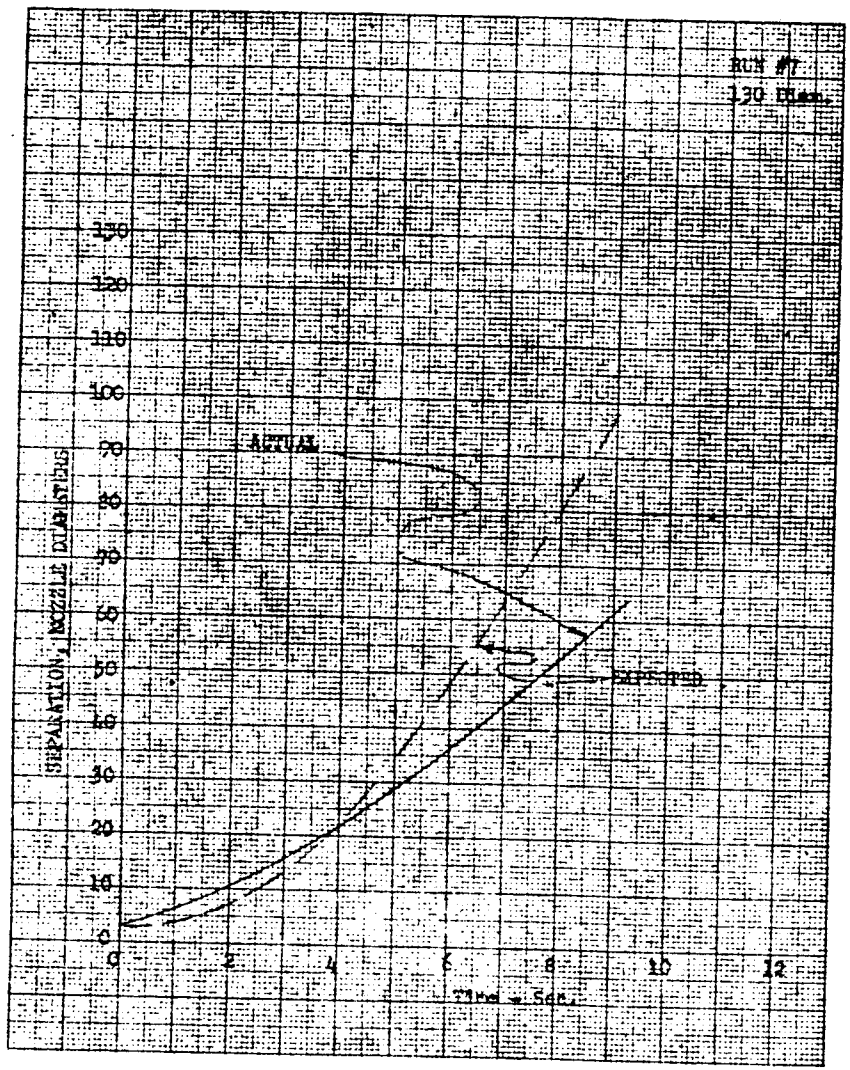

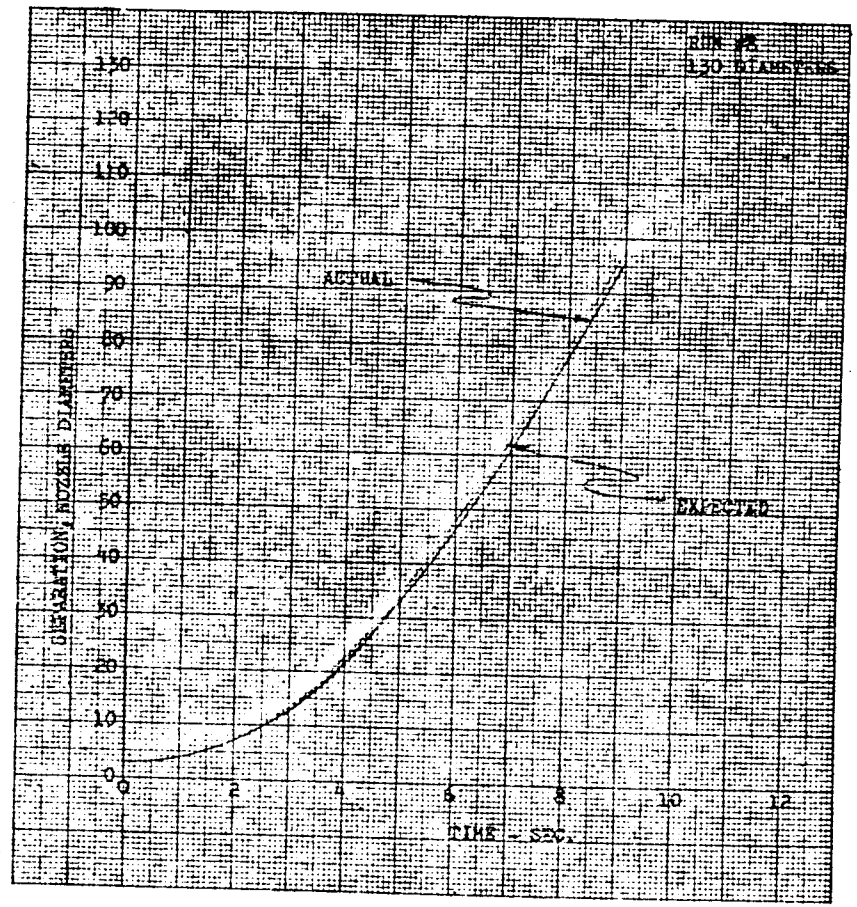

Fig. III-3 Cart Travel Time Histories, Runs 7 thru 27

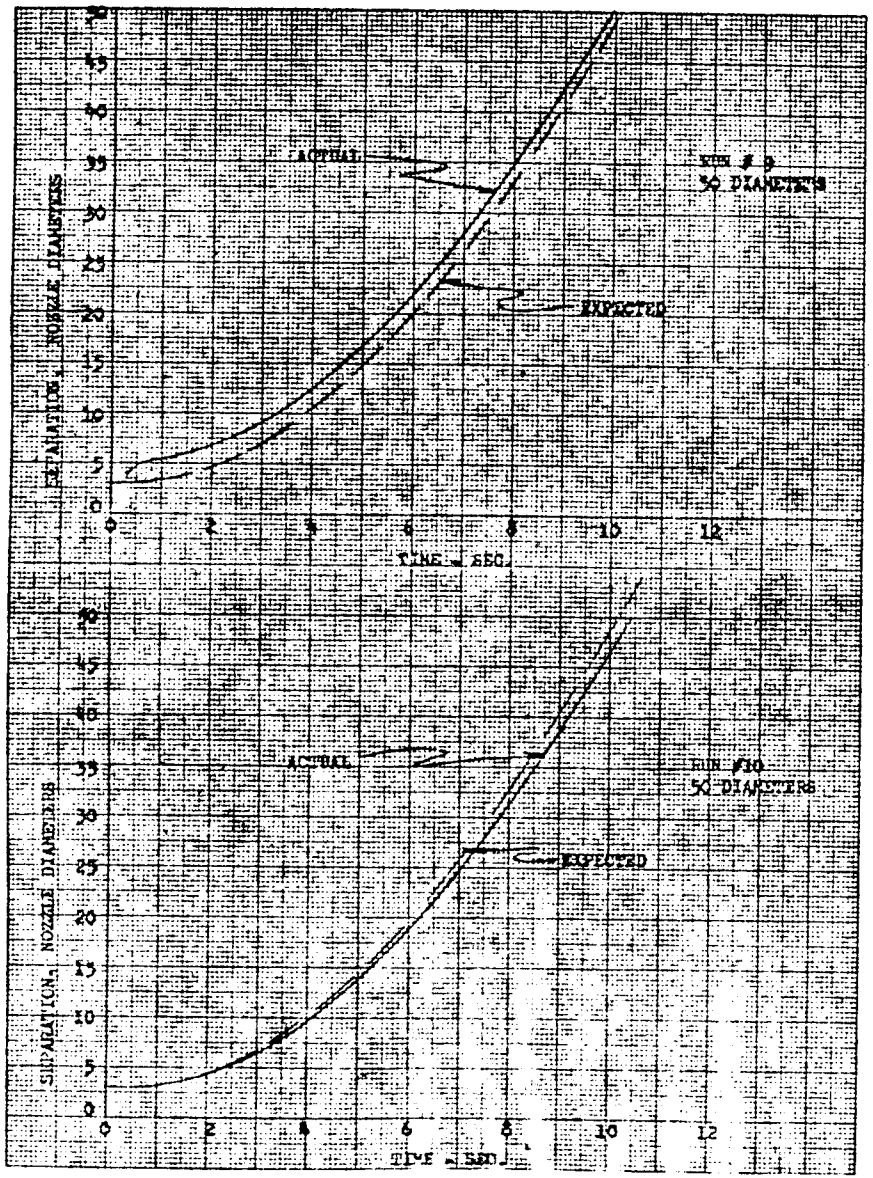

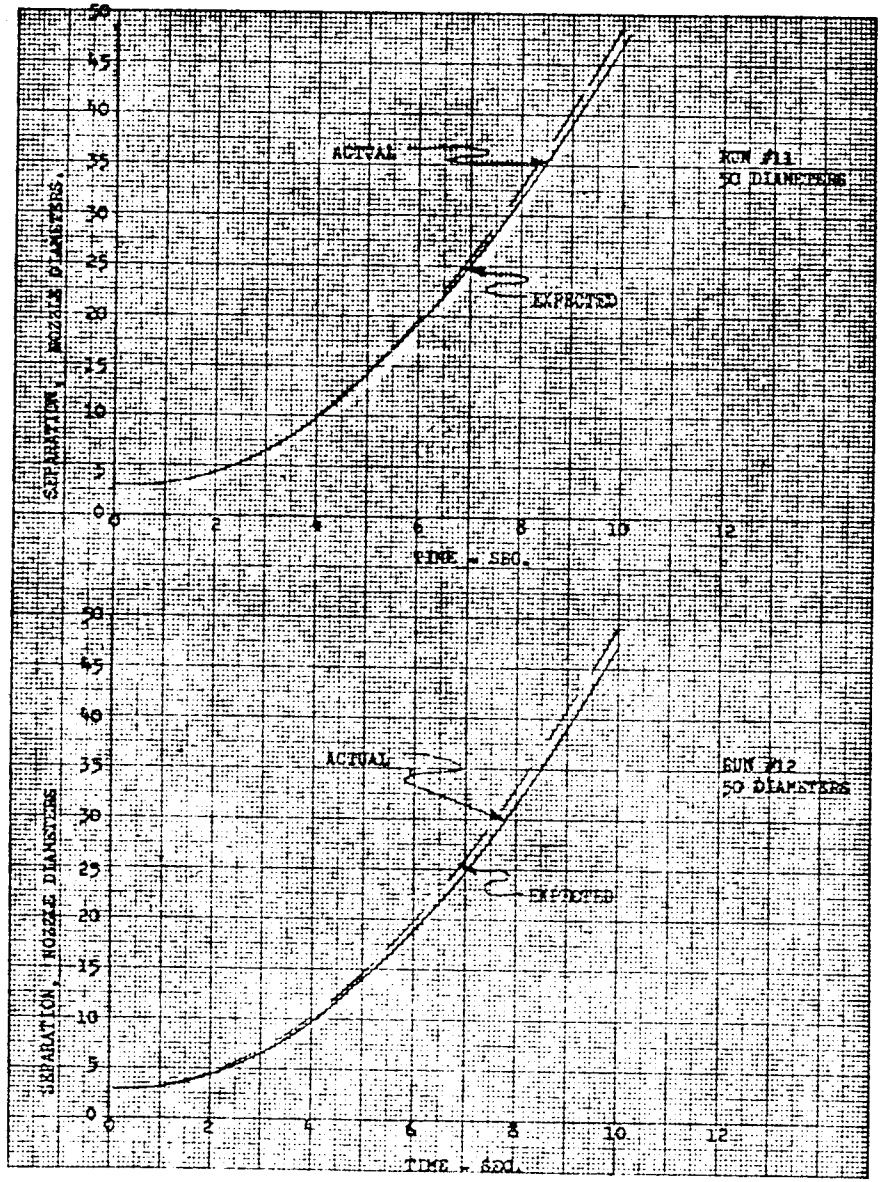

Fig. III-3 (cont)

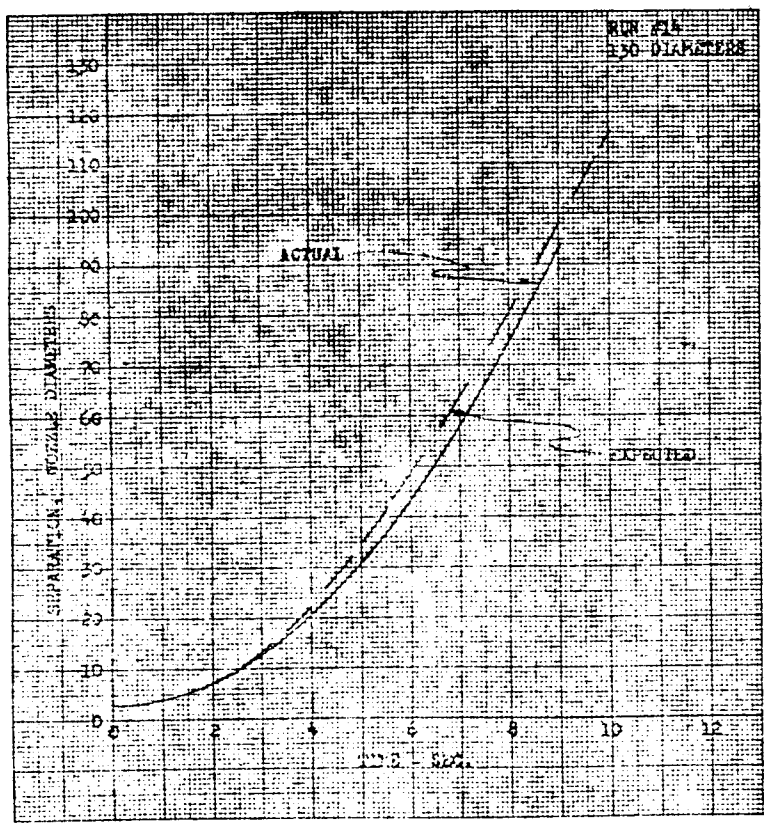

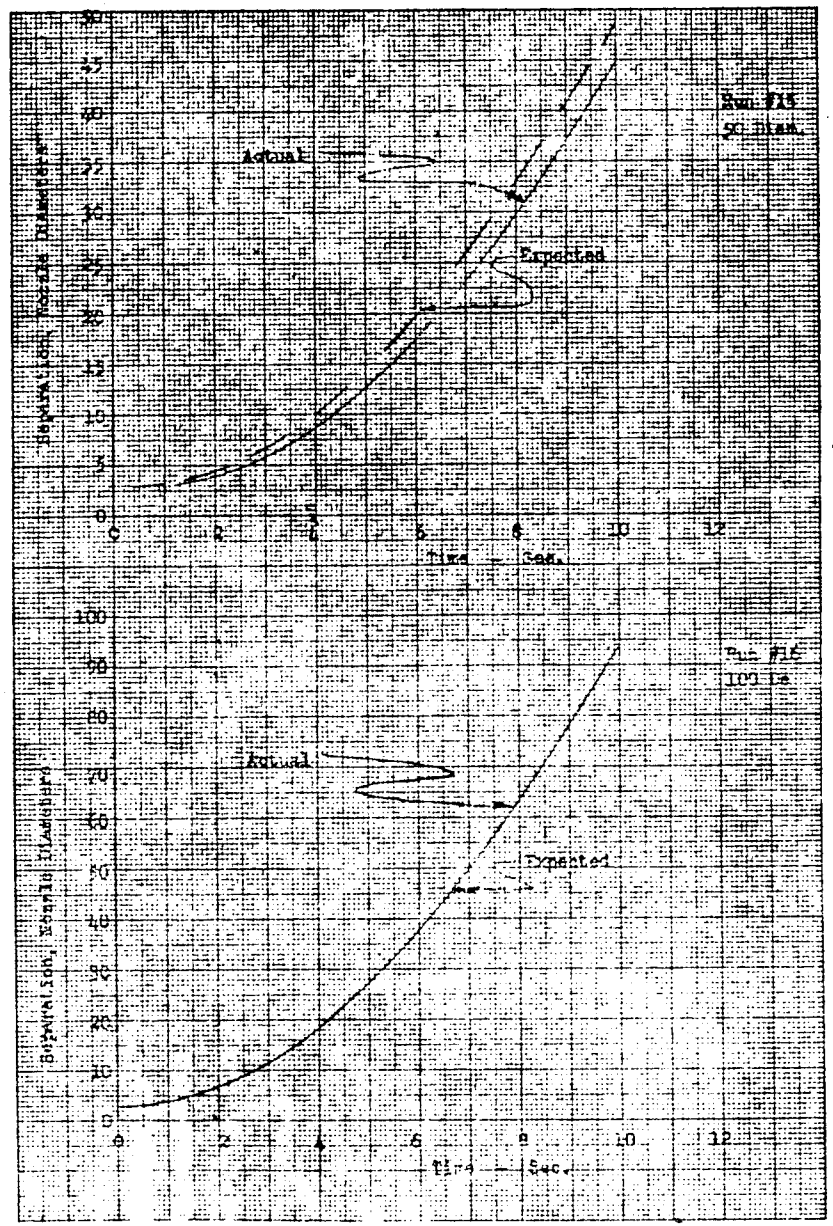

Fig. III-3 (cont)

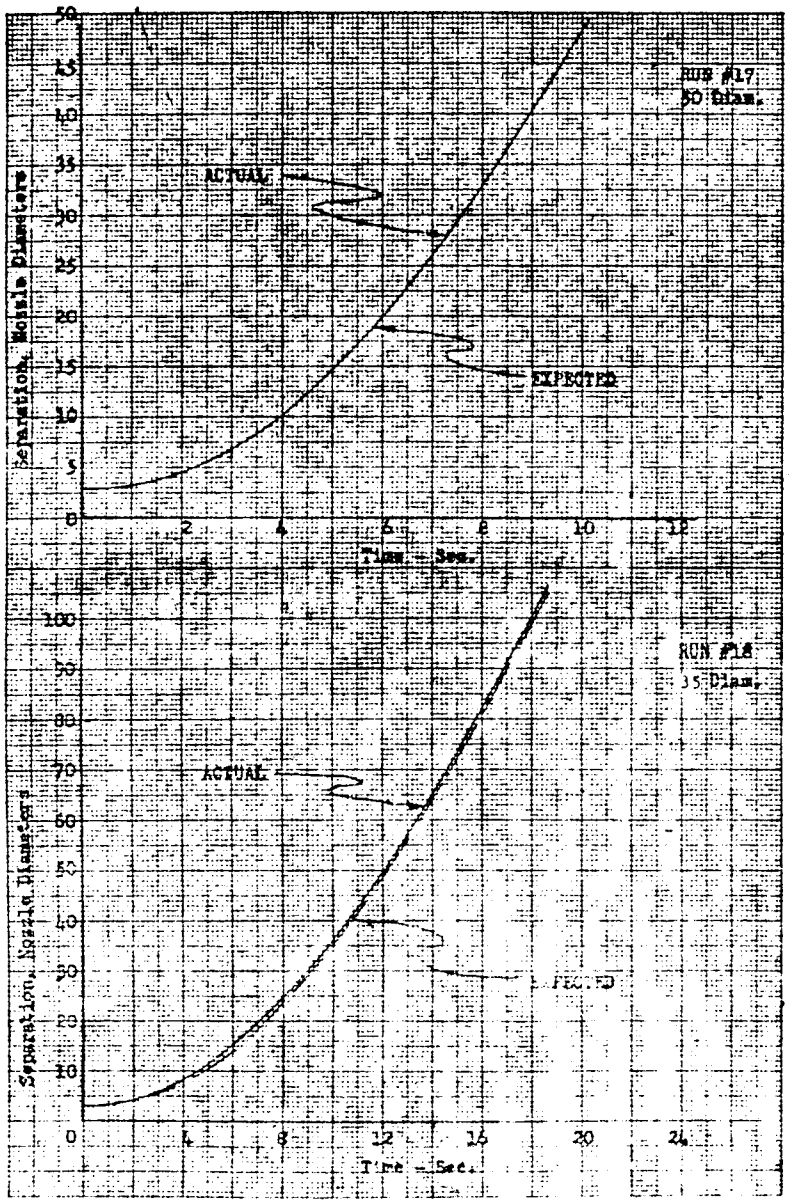

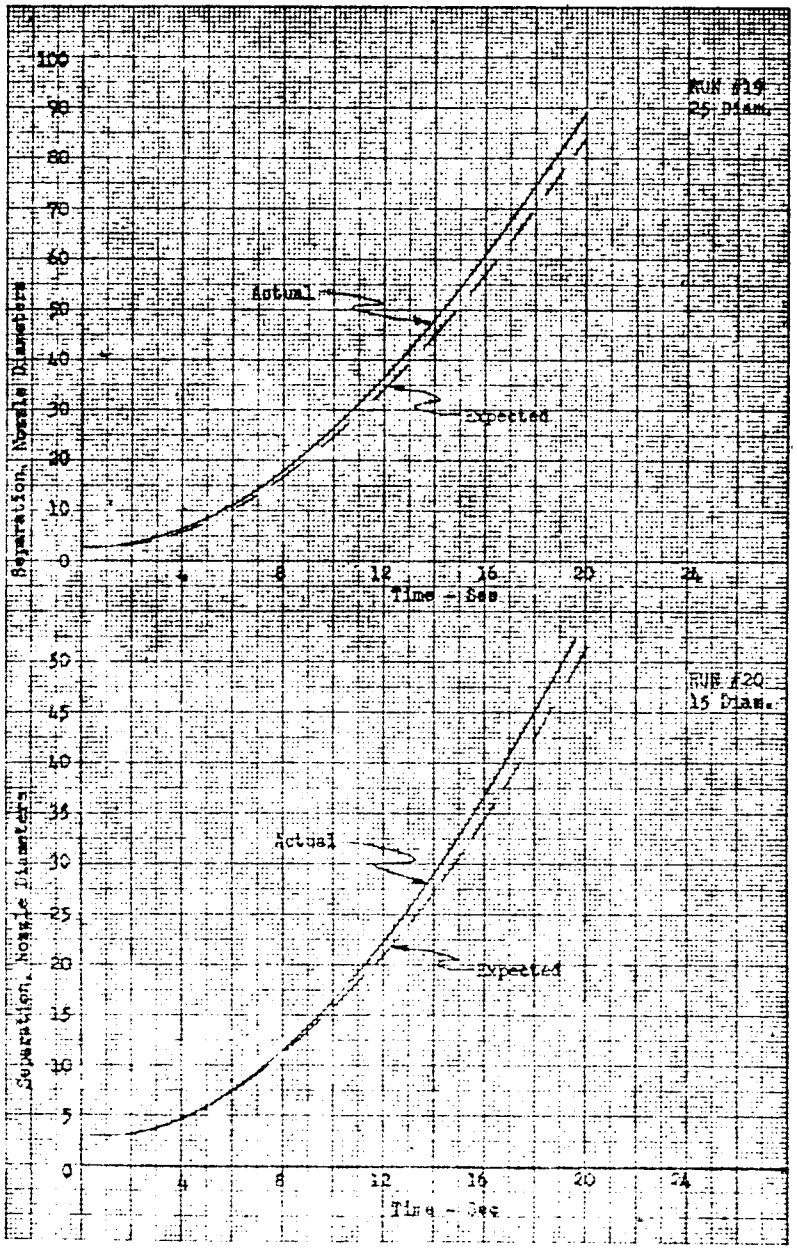

Fig. III-3 (cont)

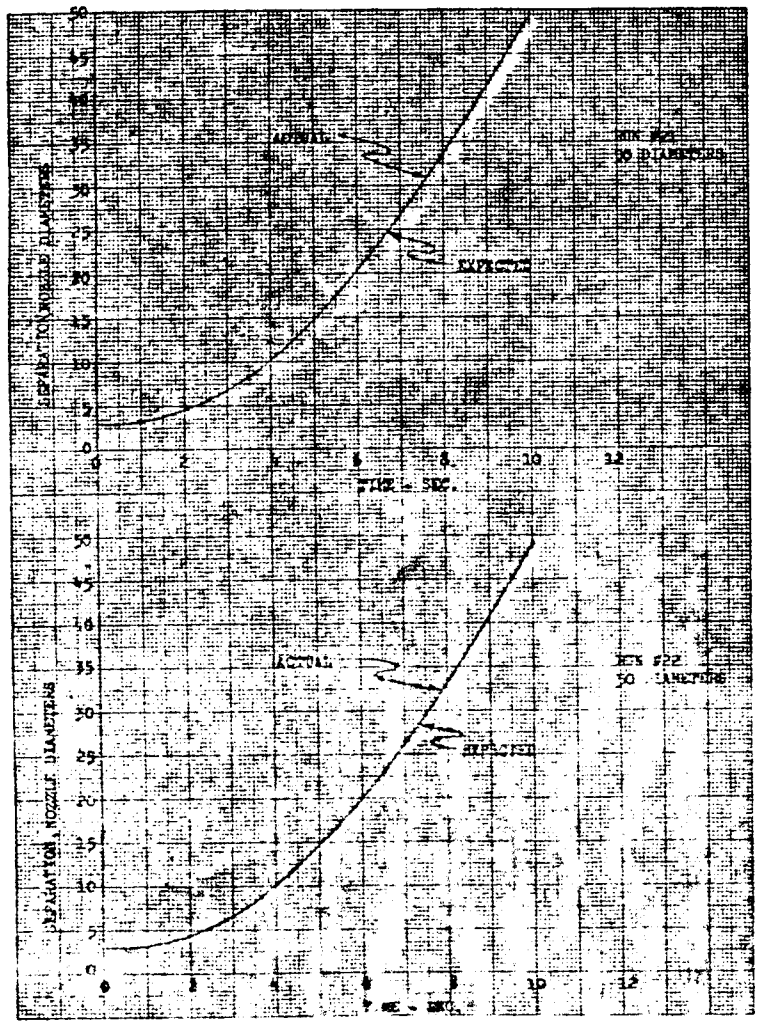

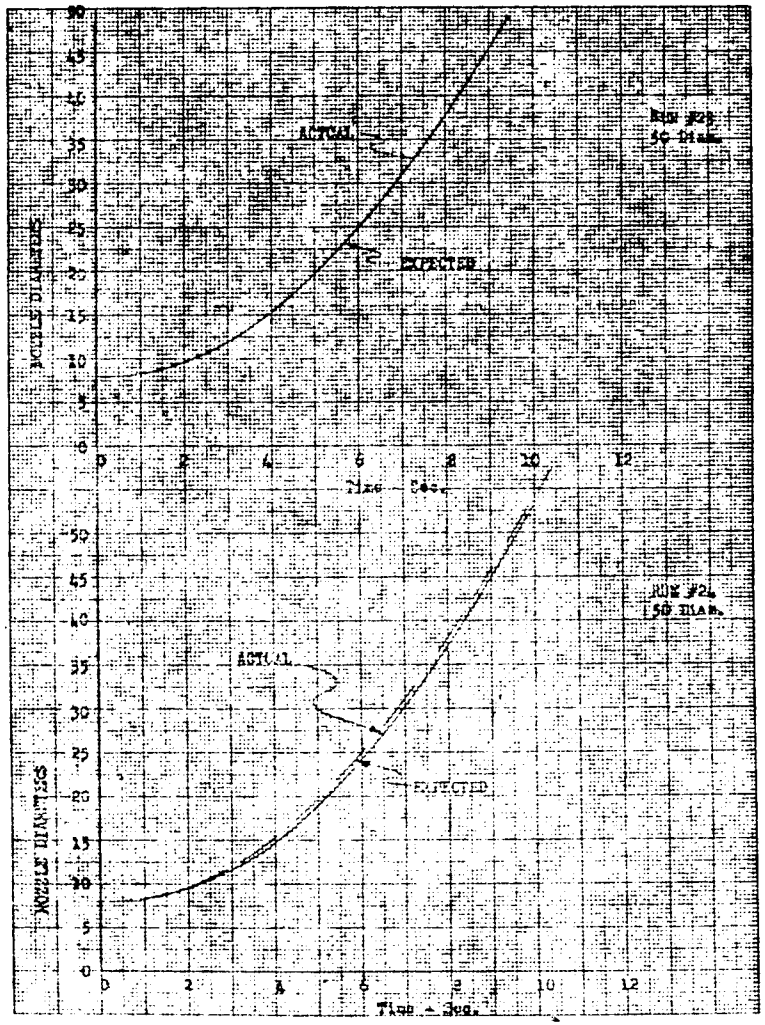

Fig. III-3 (cont)

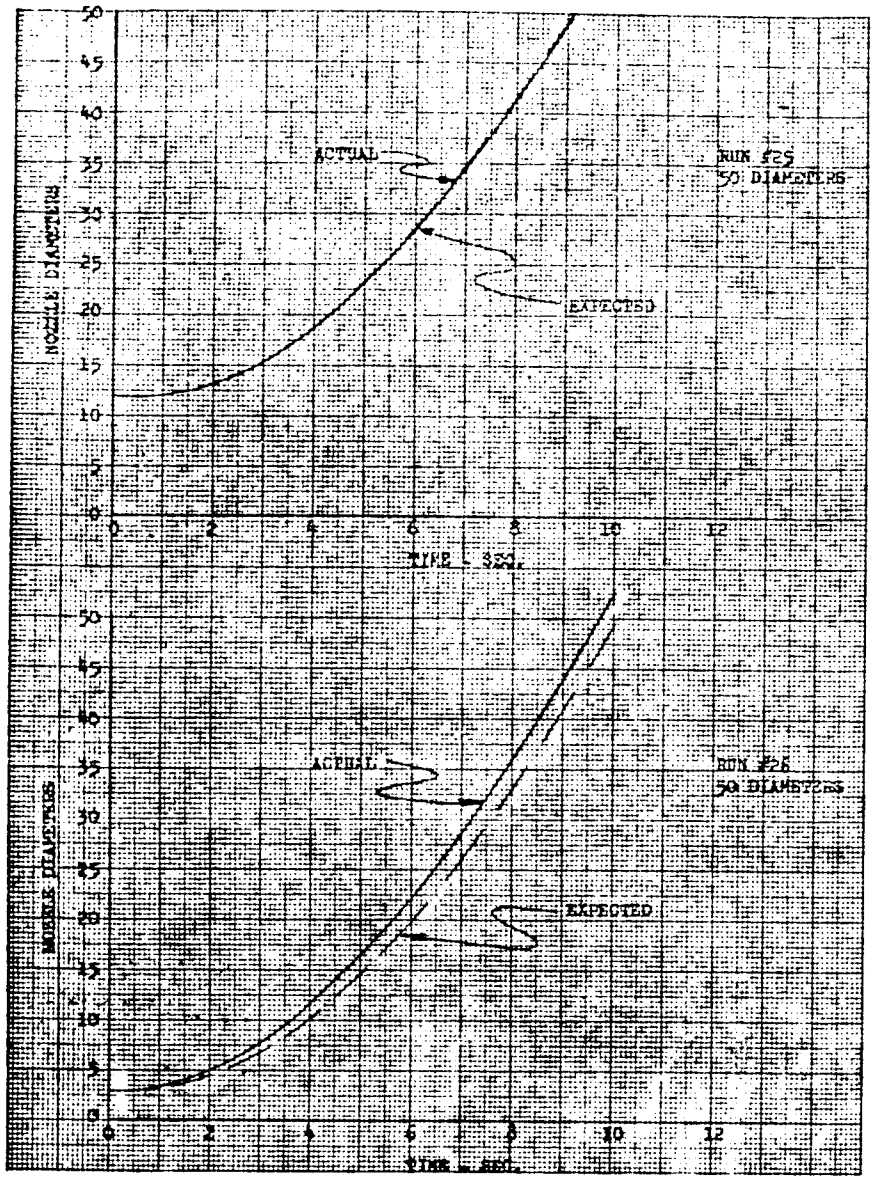

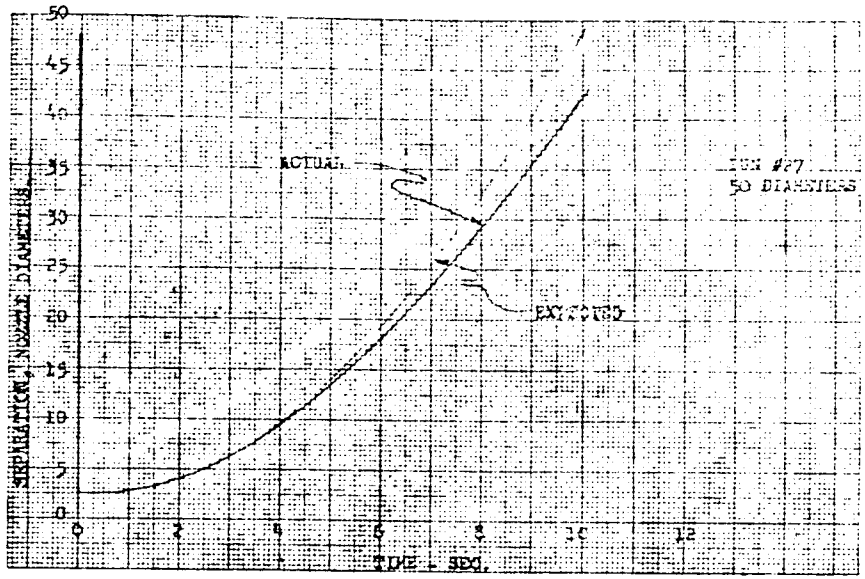

Fig. III-3 (concl)

IV. SOLID ROCKET MOTOR DESIGN

A. DESIGN CONSIDERATIONS

During the SPREE Phase II, Part I program it was shown that propellant aluminum content has no clearly discernible effect on erosion over the aluminum content range evaluated (14 to 22%). An objective of the SPREE Phase II, Part II program was to confirm this finding and determine whether a propellant formulated with considerably less aluminum powder would be significantly less erosive. It was decided to evaluate the effects of motors having 7, 14, 18, and 22% aluminum.

Grains that have different percentages of aluminum burn at different temperatures. The erosion of commonly used deflector coating materials is due in a large part to thermal effects. Therefore, the effects of aluminum should be as significant from the thermal erosion standpoint as from the mechanical erosion standpoint.

There is an optimum amount of aluminum that can be combined with a given set of ingredients in a grain formulation. A greater or lesser amount results in poorer motor performance. The propellant ingredients used for this program are given in Table IV-1. The optimum amount of aluminum is between 14 and 18%. A true evaluation of the effect of aluminum content on erosion would make use of formulations having optimum amounts of aluminum. These formulations would use different oxidizers and binders for the different aluminum percentages just as would be done by full-scale rocket motor manufacturers. Unfortunately, the SPREE program budget was too limited for this kind of rocket motor development. Thus, the same ingredients were used in each of the grain formulations.

Table IV-1 Propellant Formulations

Ingredients	Aluminum Content (%)			
	7	14	18	22
Polybutadiene Acrylic Acid	19.8	17.3	16.5	15.7
Ammonium Perchlorate	69.0	65.0	62.0	59.0
Aluminum	7.0	14.0	18.0	22.0
ERL-2795 Epoxy Resin	4.2	3.7	3.5	3.3

Ideally, motors for evaluating the aluminum content effects should have identical chamber pressures, mass flow rates, nozzle expansion ratios, and nozzle exit angles. All of these parameters could not be held constant for SPREE testing. This was because of the different densities and burn rates of the varying-aluminum-content propellant formulations. With identical nozzle geometries, motor case and grain size would have to be varied to arrive at the relationship between burning surface and nozzle throat area required for a chamber pressure and mass flow match. This would, of course, cause motor and grain costs to skyrocket. If the nozzle scale were changed to arrive at the proper ratio of throat-to-burning surface area, deflector size and cart motion would have to be altered since these are dependent on nozzle exit diameter. This would necessitate the design and manufacture of additional molds for the J deflectors and the purchase of more gears for the acceleration control test fixture. These alternatives were discarded and the nozzle throat size was allowed to vary while keeping the exit angle and exit diameter constant. The resulting nozzle throat diameters and expansion ratios are as follows:

Aluminum (%)	Throat Diameter	Nozzle Expansion Ratio, $\frac{A_e}{A_t}$
7	1.543	9.56
14	1.694	7.93
18	1.643	8.43
22	1.595	8.94

B. MOTOR DESCRIPTION

Two types of rocket motors were designed and fabricated. One type was required to burn for at least 10 sec, and the second type for at least 20 sec. The longer burn-time motor was for applications where low liftoff thrust-to-weight ratios were to be simulated (Runs 18, 19, and 20). Both motor types were designed to produce approximately 2200 lb of thrust at similar chamber pressures and mass flow rates. The case assembly inside diameter of the shorter burning motor was 10 in. while the other motor had a case assembly inside diameter of approximately 16 in.

The need for repeated motor test firings dictated that reusable components for the chamber, nozzle hull, and igniter adapter be provided. To minimize design and hardware costs, commercially available parts requiring minimum machining and off-the-shelf components were used. The motor case cylindrical section was fabricated from schedule 60 steel pipe and the end mating flanges were commercial weld-neck flanges welded to the steel pipe. The head-end flange was made from a blind flange and the head-end insulator from 1/2-in. thick Buena N rubber. The burst disc assembly consisted of 2-in. pipe, union-type stainless steel safety head fittings, and commercially available 1200 psi rupture discs. The nozzle hull was machined from a billet of 4130 steel, and a matching flange was welded to it. The nozzle insert was machined from a billet of Graph-I-Tite G high-density graphite specially selected to minimize throat erosion. It was held in place by a sheet steel retainer ring. The entrance ring located forward of the graphite insert was made from a 0.75-in. thick laminated plastic sheet with an asbestos fabric base known as Panelyte. Figures IV-1 and IV-2 are schematics of the short and long burn time motors, respectively. Figures IV-3 and IV-4 are motor photographs.

C. GRAINS AND IGNITERS

The basic grain configuration was cylindrical with a center perforation and open ends; one end was slotted. The burning surface was on the inside diameter. The grains were cast in a paper phenolic case by the standard mandrel casting cure process. The short burning grains weighed approximately 100 lb and the longer burning grains weighed about 200 lb. Composition data have already been given in Table IV-1. The size of the aluminum particles ranged from 20 to 45 microns. Figure IV-5 shows the grain assemblies.

The basket-type head end igniter consisted of a reusable adapter, an ignition primer, ignition granules, pellets with styra-foam spacers, the basket, and O-ring seals. The grains and igniters were supplied by Rocket Power, Inc, of Mesa, Arizona. One 22% aluminum Atlantic Research Corp grain and igniter left over from the last SPREE test series was also provided.

D. MOTOR PERFORMANCE

1. Predicted Performance

The motor design criteria for operating pressure, gas mass flow, duration, and size were established to be representative of current solid motor configurations and propellant formulations. The normal operating parameters were to be as follows:

Chamber pressure, 700 psia,

Mass flow, 10 lb/sec,

Duration, 10 and 20 sec (two motor types),

Propellant aluminum, 7, 14, 18, and 22%.

Performance design calculations were based on the scaling of data from Rohm and Hass 5-lb motor firings. The resulting predicted performance characteristics are given in Table IV-2.

2. Actual Performance

Table IV-3 shows data relative to the performance of each motor fired during Runs 7 thru 27. Included are firing duration data, average chamber pressure and mass flow data, before-firing nozzle throat dimensions, and after-firing nozzle throat dimensions. Figure IV-6 gives chamber pressure time histories for each of the firings. A rocket motor malfunction occurred during Run 13. It was probably due to an igniter boss plug gas leak attributable to a poor seat at the interface between the plug and chamber.

Postfire visual inspection of nozzles used with grains containing 18 and 22% aluminum revealed considerable $A\ell_2O_3$ and aluminum deposition on the nozzle entrance ring, throat section, and exit cone (Fig. IV-7). This accounts for the smaller postfiring nozzle throat dimensions. Because of the aluminum deposition, the actual quantity of aluminum in the exhaust was somewhat less than the specified values.

Each motor fell short of the predicted chamber pressure and mass flow. Higher chamber pressures and mass flows would have been desirable because they better simulate contemporary full-scale solid rocket motors. The deviation of mass flow and pressures from design values can be attributed to the assumption of linearity between 5-lb subscale test firings and the actual design.

Motor performance was excellent in regard to the neutrality and reproducibility of chamber pressure. Figure IV-8 shows a chamber pressure overlay for motors with each percentage of aluminum.

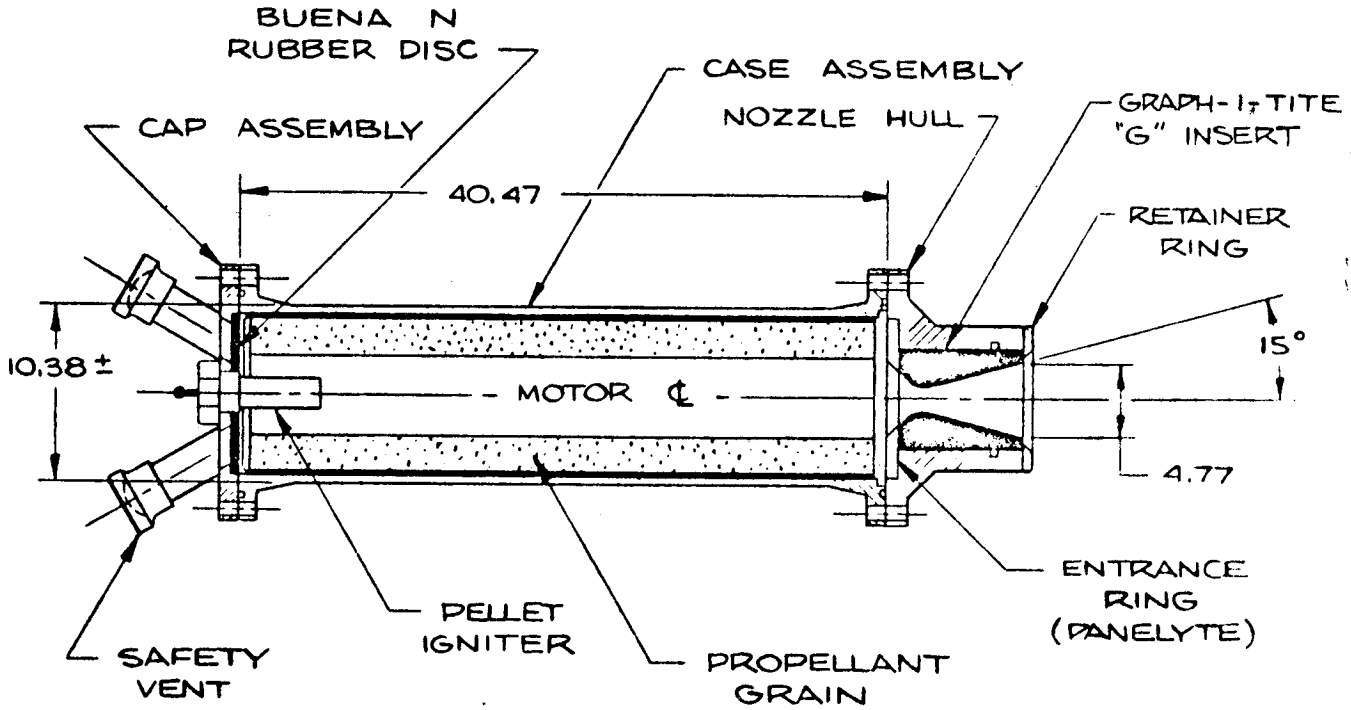

Fig. IV-1 13-sec Rocket Motor Schematic

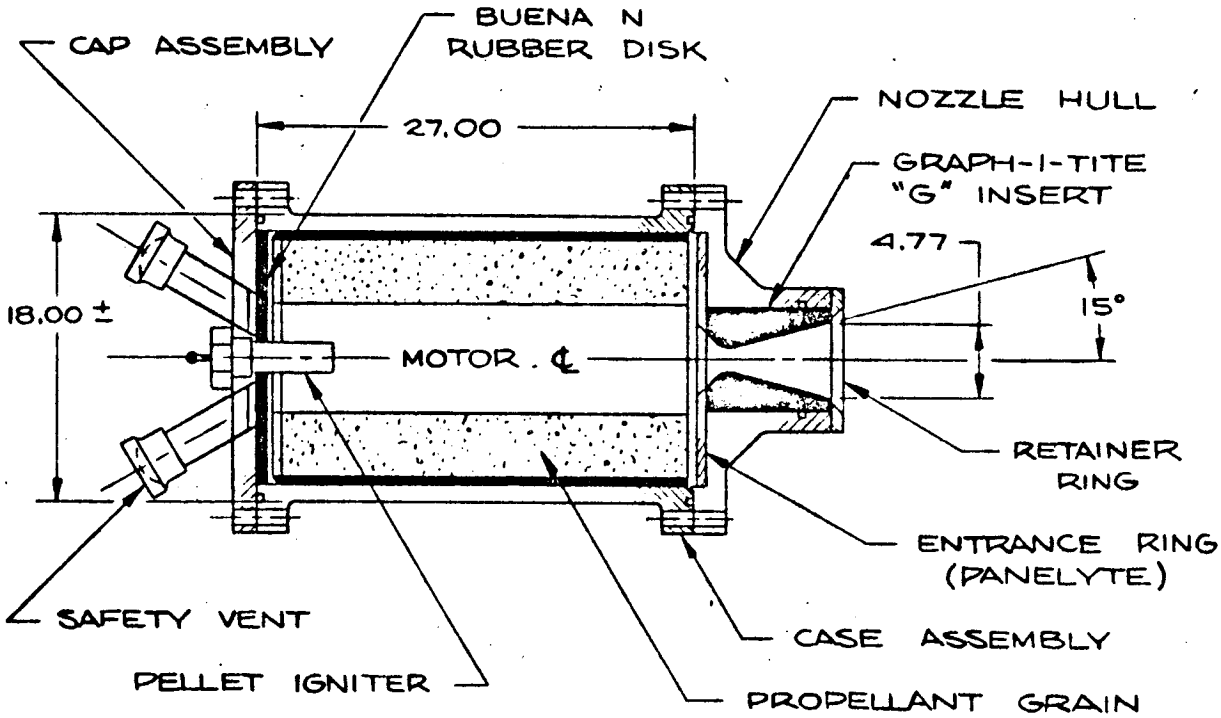

Fig. IV-2 24-sec Rocket Motor Schematic

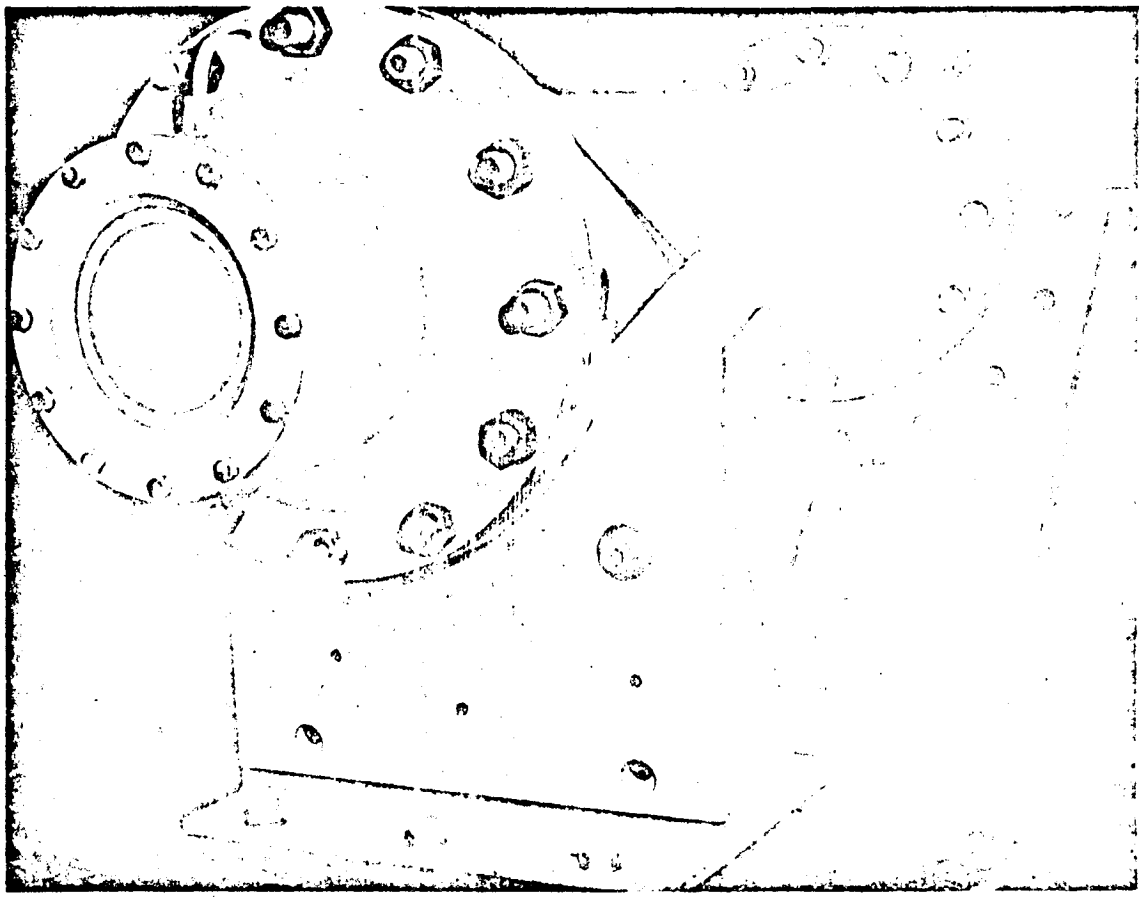

Fig. IV-3 13-sec Burntime Motor

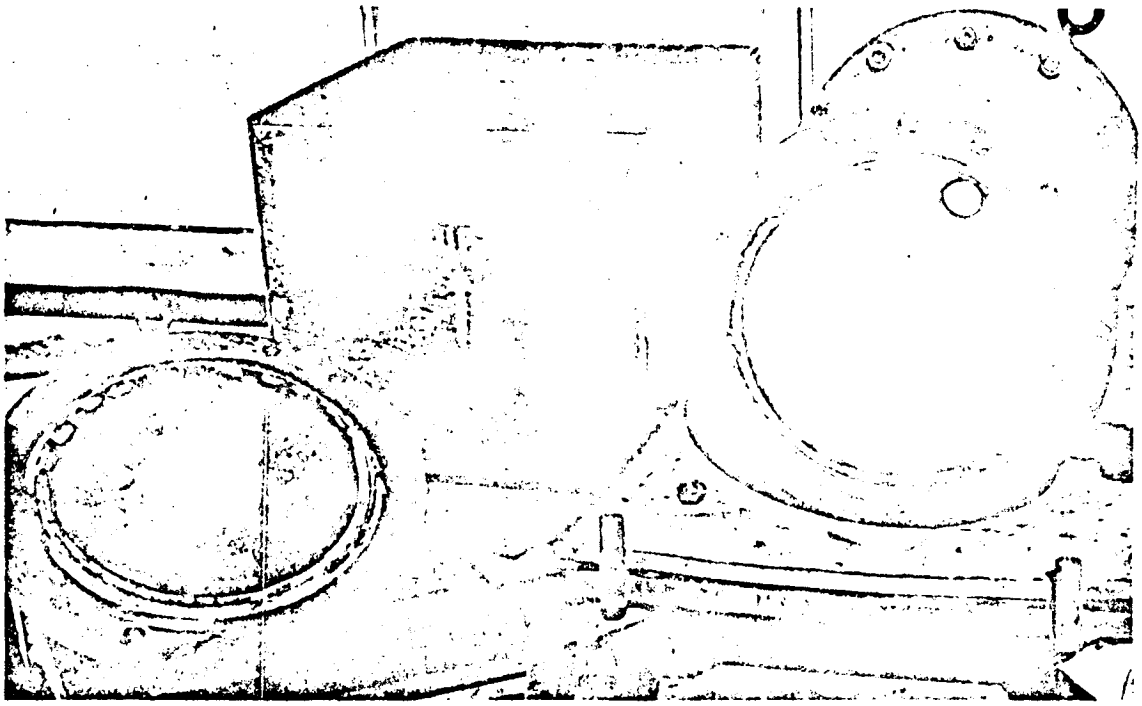

Fig. IV-4 24-sec Burntime Motor

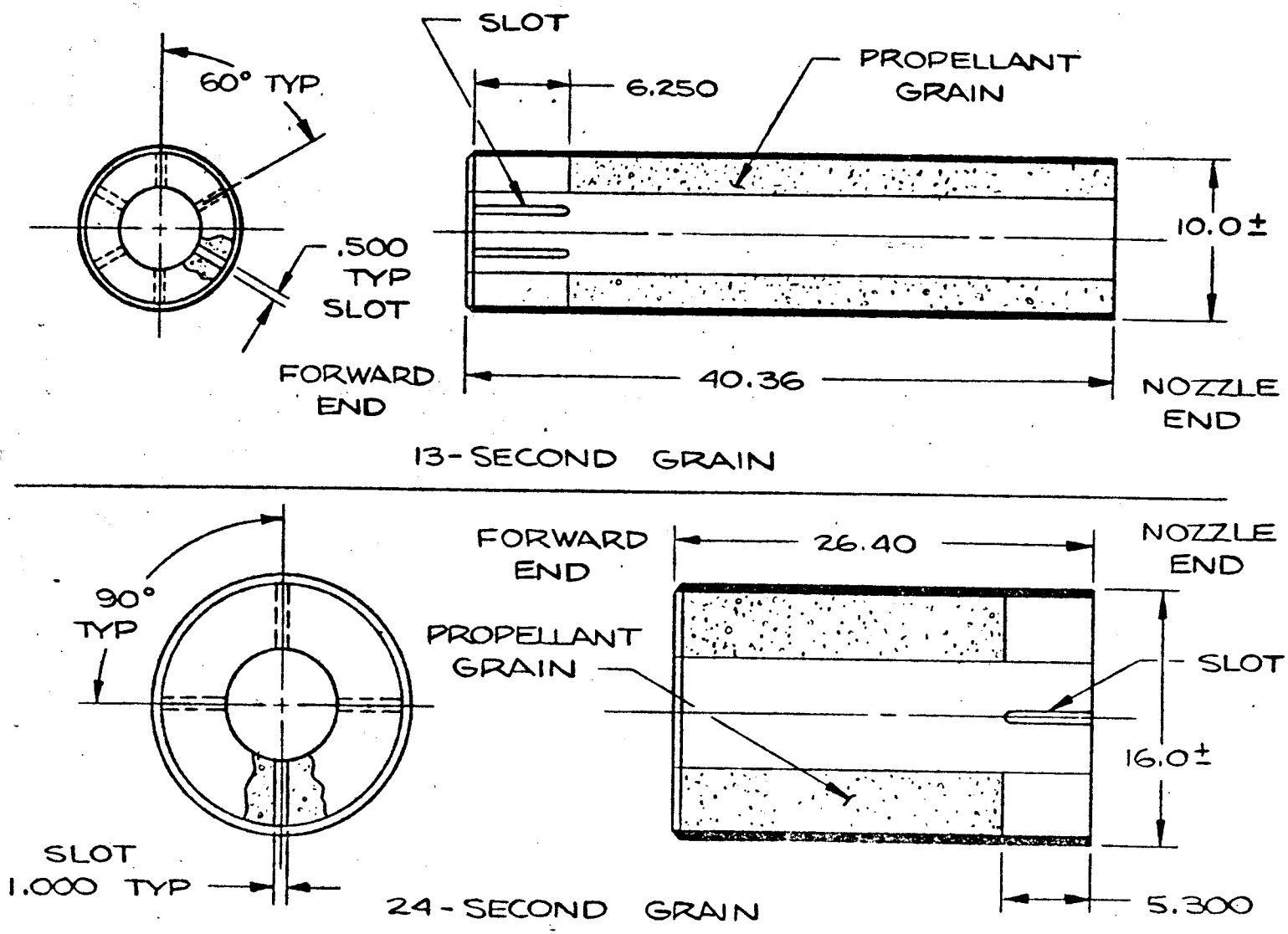

Fig. IV-5 Grain Assemblies

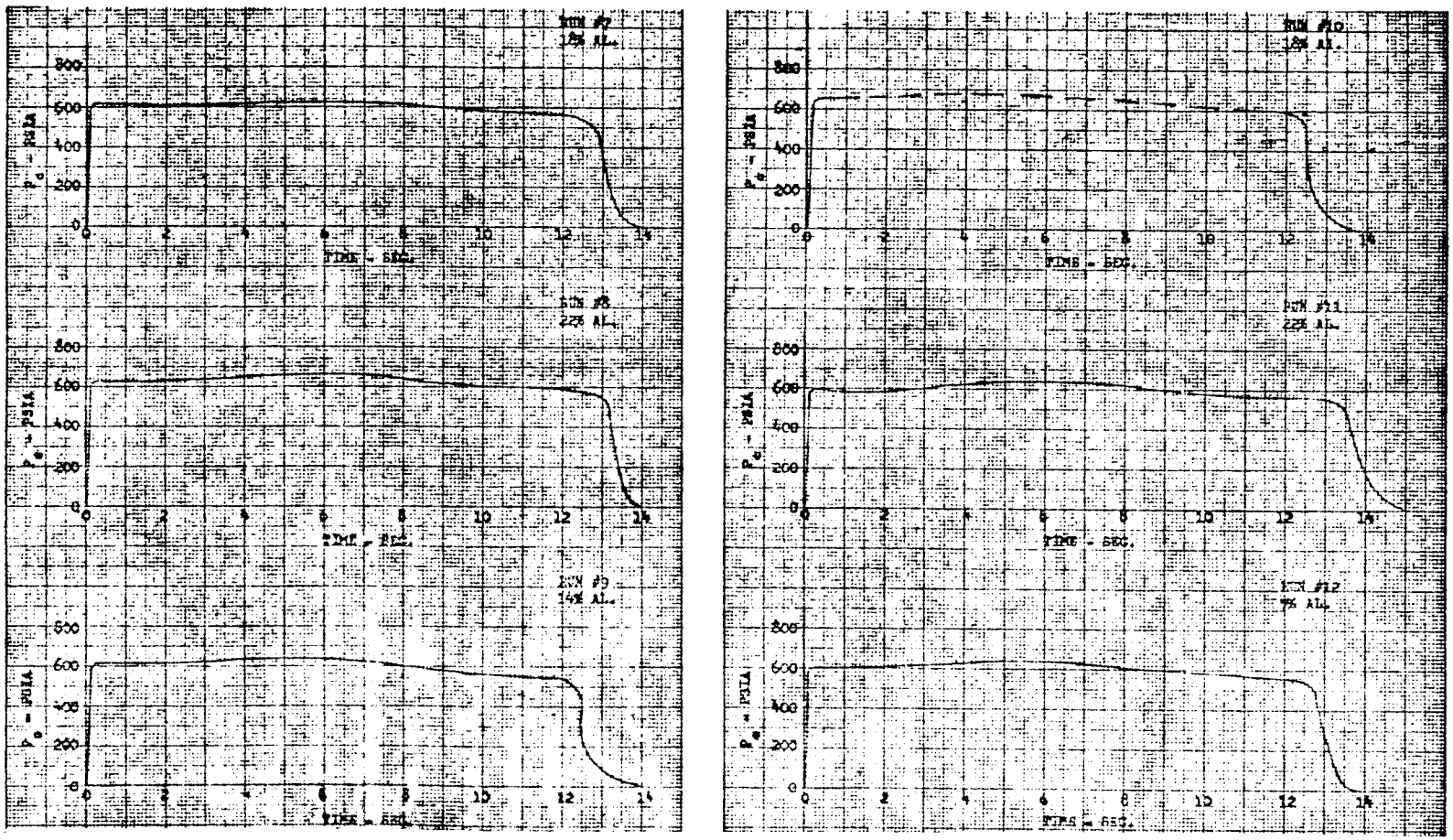

Fig. IV-6 Chamber Pressure Time Histories, Runs 7 thru 27

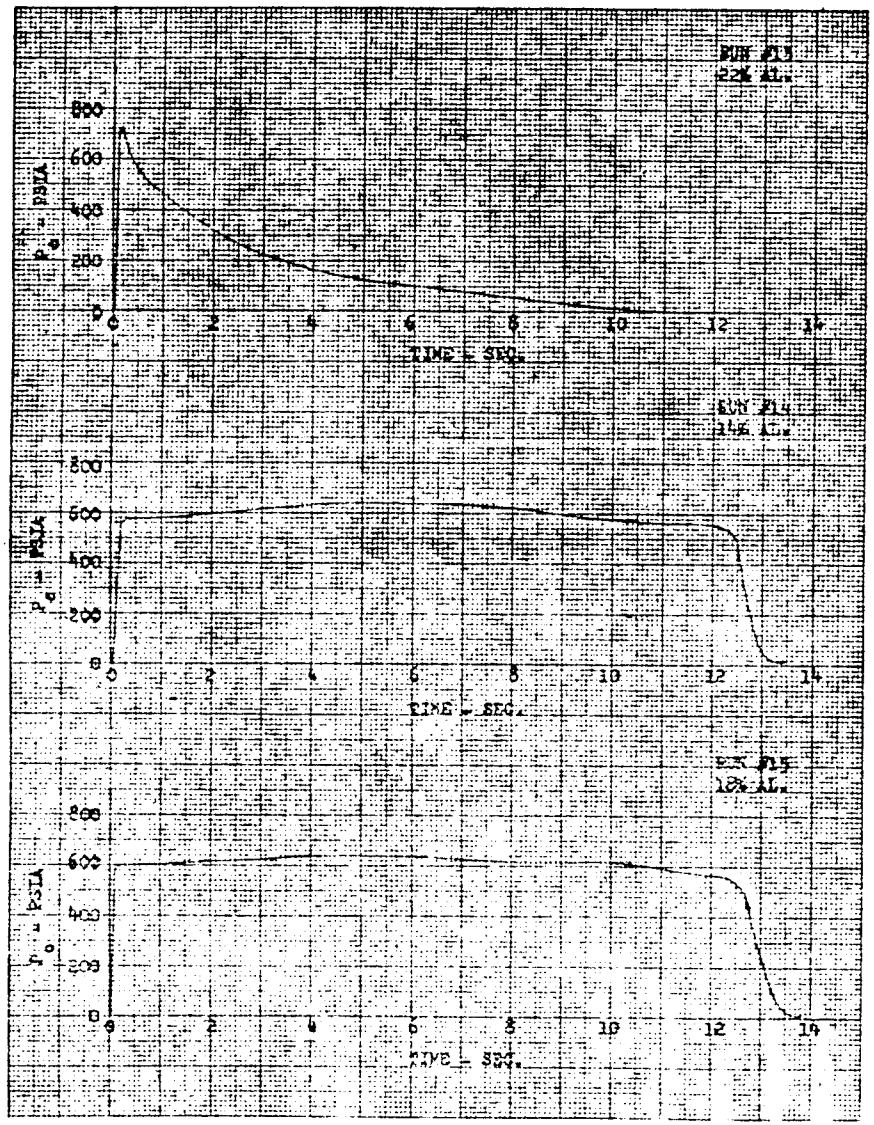
RUN #13
22% AL.
RUN #14
14% AL.
RUN #15
10% AL.
P_o - PSIA
TIME - SEC.

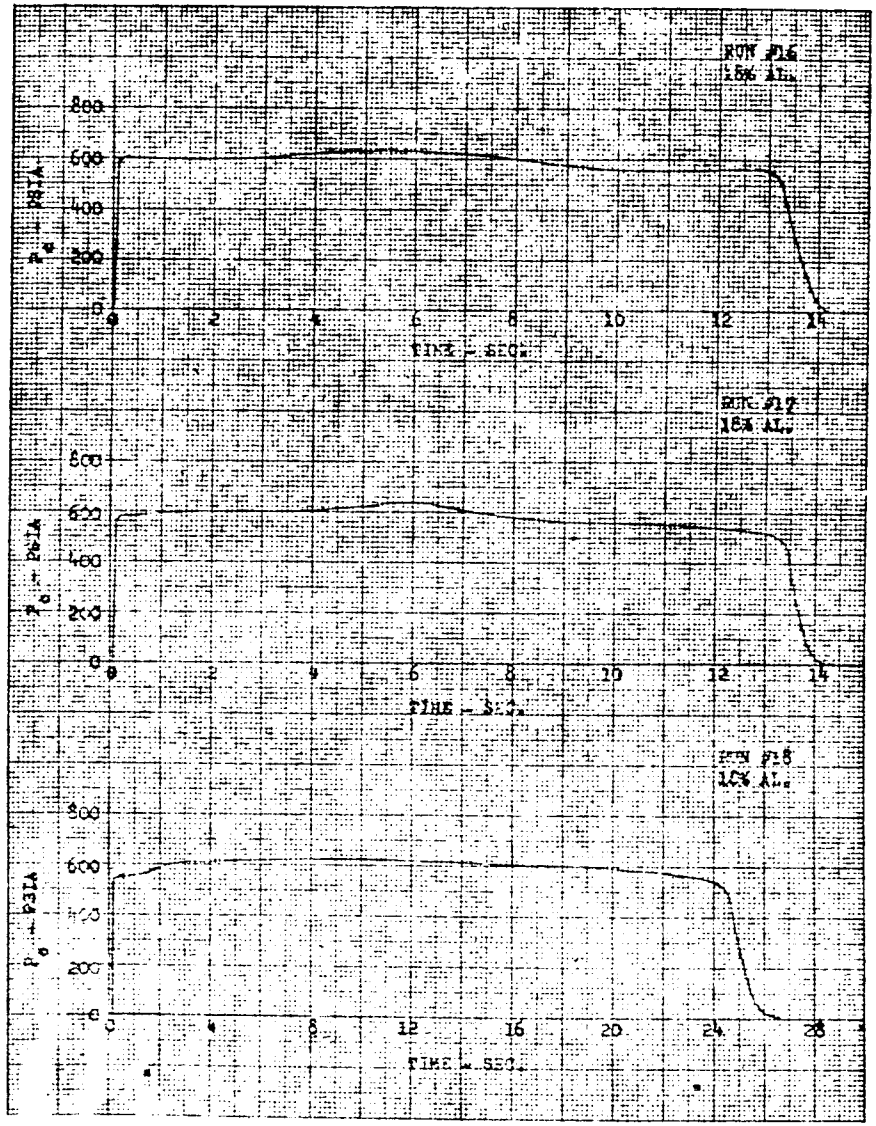
RUN #16
18% AL.
RUN #17
16% AL.
RUN #18
10% AL.
P_o - PSIA
TIME - SEC.

Fig. IV-6 (cont)

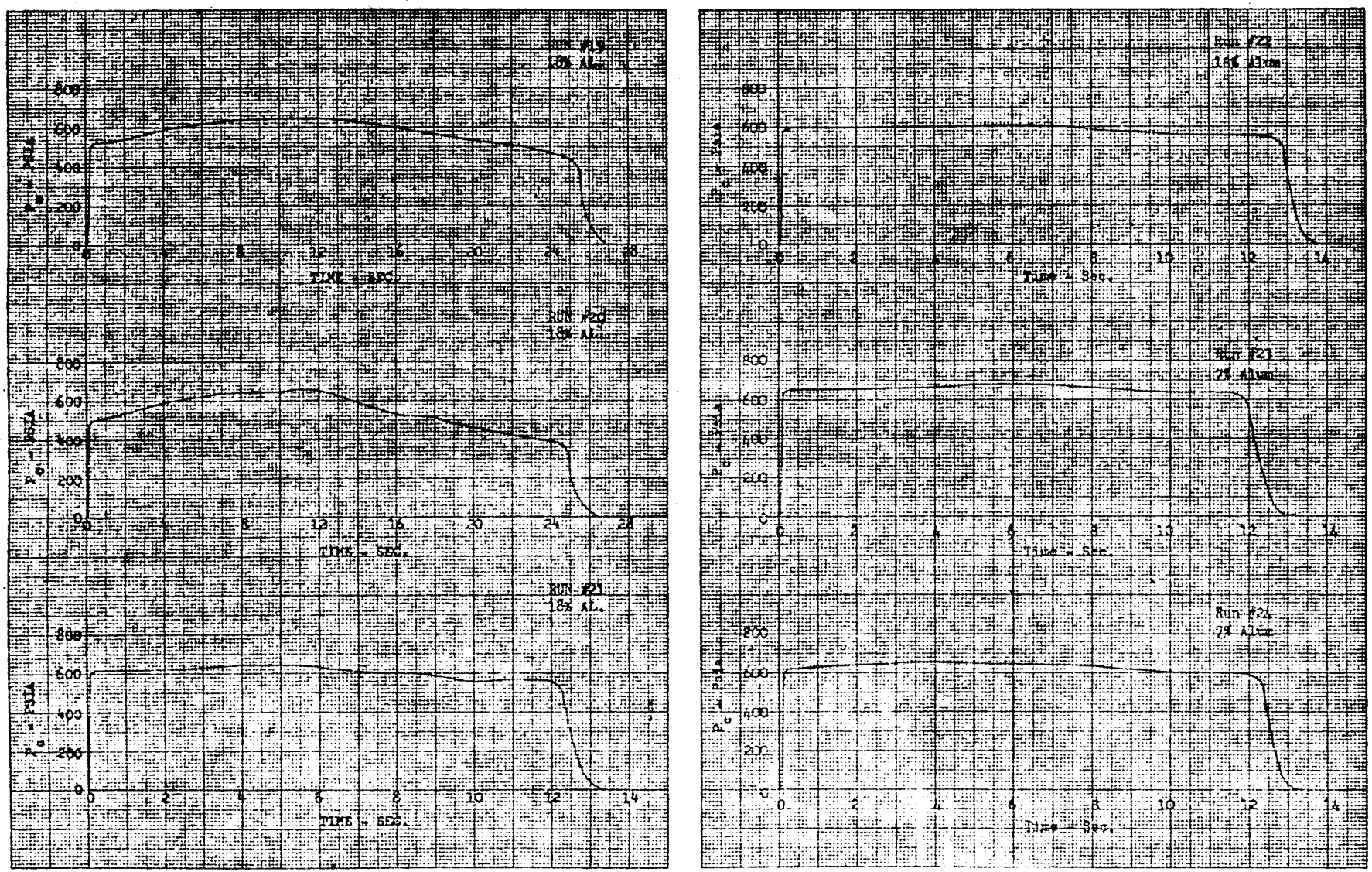
RUN #19
18% Al.
RUN #20
18% Al.
RUN #21
18% Al.
TIME - SEC.
Run #22
16% Alum
Run #23
7% Alum
Run #24
7% Alum
Time - Sec.

Fig. IV-6 (cont)

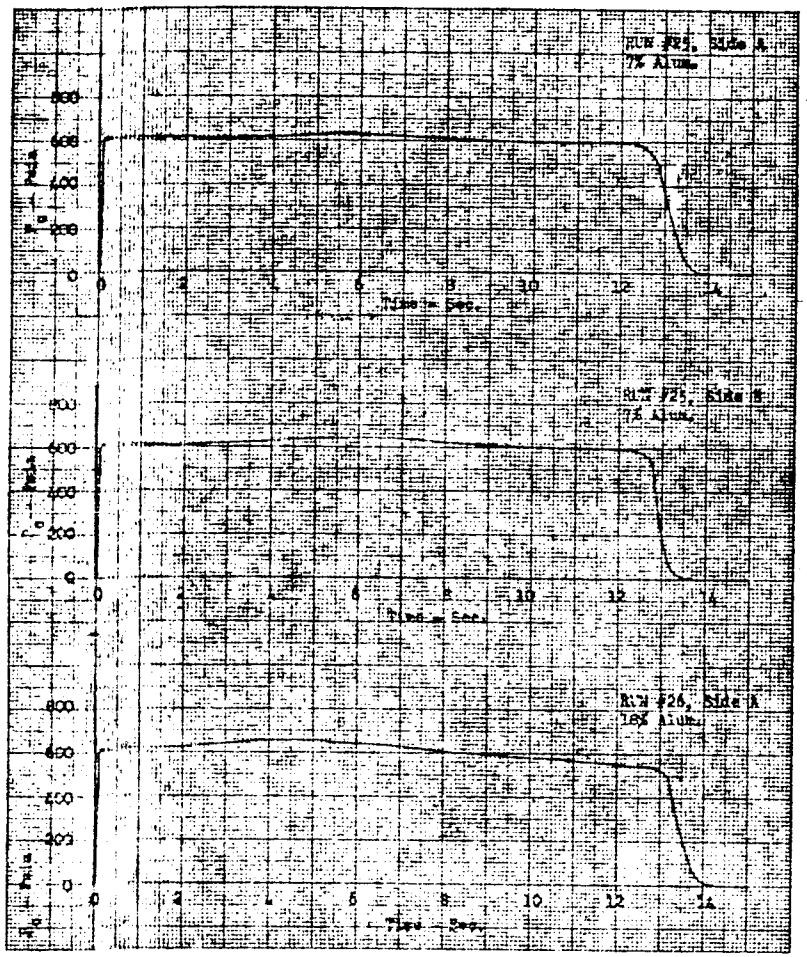

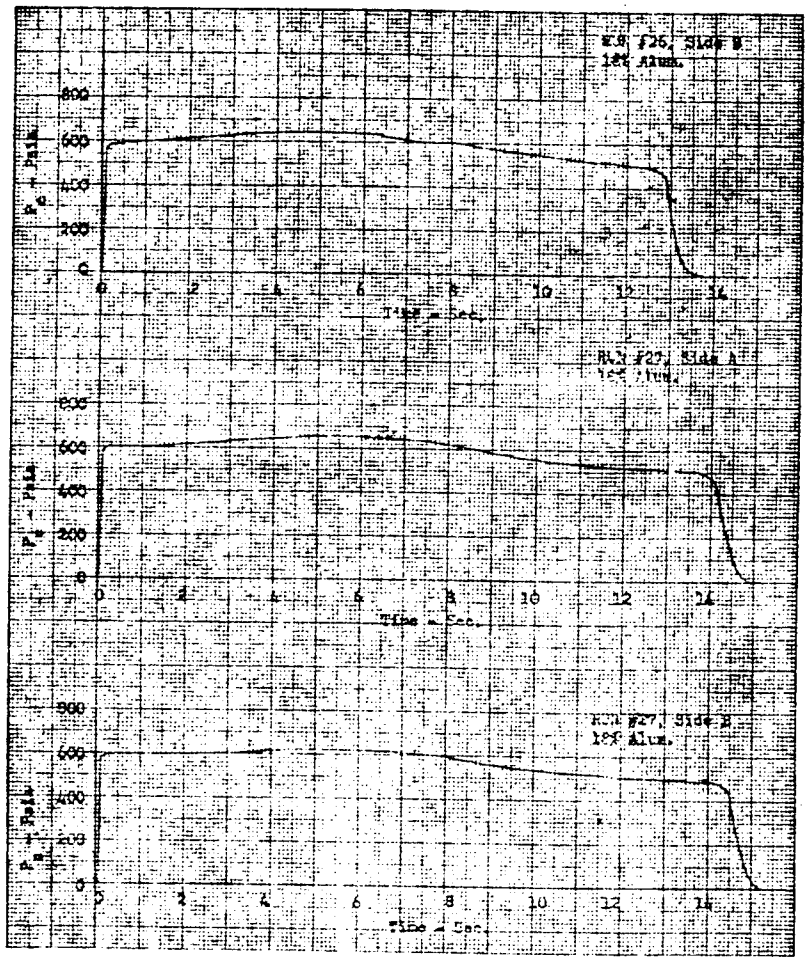

Fig. IV-6 (cont'd)

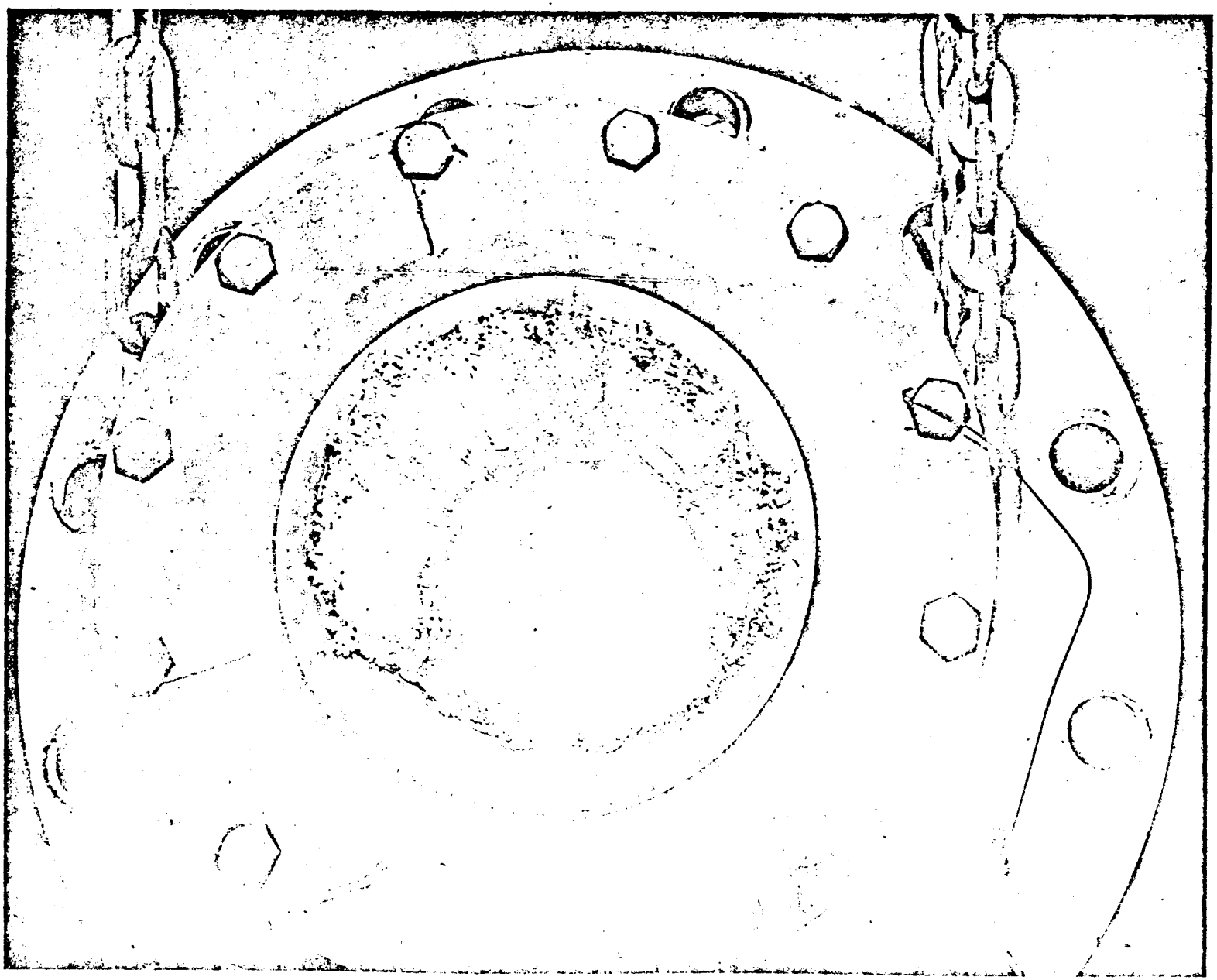

Fig. IV-7 Characteristic Alumina Deposit in Nozzle of 22% Aluminum SRM

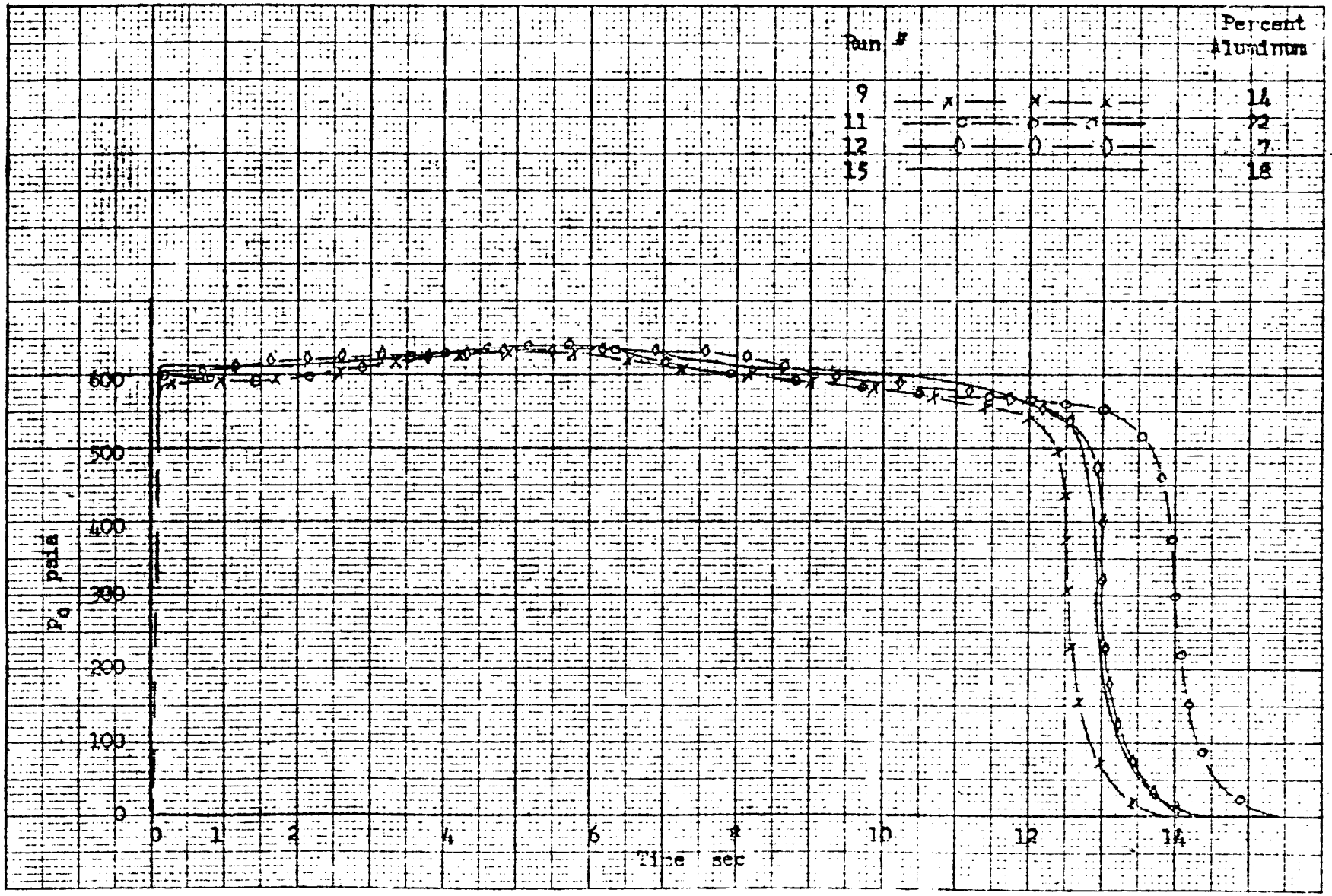

Fig. IV-8 Chamber Pressure Overlay for Motors with Varying Percents of Aluminum

Table IV-2 Predicted Motor Performance*

Aluminum (%)	7	14	18	22
Burning Rate at 700 psig (in./sec)	0.185	0.185	0.180	0.172
Chamber Pressure (psia)	700	700	700	700
Burn Rate Slope	0.27	0.25	0.18	0.16
Temperature Sensitivity (%/°F)	0.13	0.13	0.13	0.13
Propellant Density $(lb/in.^3)$	0.0570	0.0592	0.0610	0.0618
Erosive Burning	none	none	none	none
Characteristic Exhaust Velocity (ft/sec)	4548	5275	4948	4820
Specific Heat Ratio	1.251 to 1.288	1.233 to 1.245	1.217 to 1.229	1.215 to 1.213
Web Thickness (in.)	2.0	2.0	2.0	2.0
Nozzle Half Angle (deg)	15	15	15	15
Combustion Efficiency (%)	96	96	96	96
Ignition Delay (ms)	40.0	40.0	40.0	40.0
Burning Rate Constant	0.032	0.036	0.055	0.060
Throat Area $(in.^2)$	1.869	2.25	2.12	1.99
Throat Diameter (in.)	1.543	1.694	1.643	1.595
K_n at 700 psig $\left(\frac{\text{Propellant burning surface area}}{\text{throat area}}\right)$	470	390	415	440
Chamber Temperature (°F)**	3800	4510	4700	4670

*Computer (1620 Martin).
**These theoretical temperatures are expected to be somewhat lower than actual.

Table IV-3 Actual Motor Performance

Run No.	Aluminum (%)	Duration (sec)	Average P_c (psia)	Average $\dot{w}$ (lb/sec)	Average Nozzle Throat Diameter before Firing (in.)	Average Nozzle Throat Diameter after Firing (in.)
7	18	12.7	570	8.50	1.638	1.625
8	22	12.7	595	8.60	1.595	1.595
9	14	12.1	554	8.50	1.698	1.685
10	18	12.2	-	-	1.642	1.632
11	22	13.3	580	8.1	1.595	1.595
12	7	12.5	594	7.9	1.541	1.543
13	22	Motor Malfunctioned			1.693	1.642
14	14	12.5	582	8.20	1.693	1.647
15	18	12.2	591	8.80	1.642	1.634
16	18	13.3	583	8.0	1.641	1.628
17	18	13.3	570	7.9	1.642	1.631
18	18	24.0	590	8.3	1.641	1.638
19	18	25.4	532	7.87	1.640	1.599
20	18	24.7	537	8.05	1.642	1.613
21	18	12.1	573	8.75	1.644	1.623
22	18	12.5	612	8.50	1.644	1.627
23	7	11.8	619	8.40	1.540	1.543
24	7	12.1	614	8.20	1.540	1.539
25A	7	12.3	588	8.09	1.540	1.543
25B	7	12.3	588	8.05	1.540	1.540
26A	18	13.2	593	8.02	1.642	1.627
26B	18	12.7	585	8.43	1.642	1.628
27A	18	13.9	580	7.64	1.641	1.617
27B	18	14.3	560	7.42	1.643	1.605

V. ALUMINUM CONTENT AND SCALE EFFECTS (GROUP II)

A. GROUP II TECHNICAL OBJECTIVES

The primary objectives of the Group II tests were:

1) To determine the effect of solid rocket motor aluminum content on deflector erosion;

2) To evaluate scale effects via erosion measurements on full-scale and model Titan IIIC flame deflectors.

The secondary objectives were to evaluate a Harbison-Walker refractory castable, Harcast ES, especially developed for use in extreme abrasion applications and to screen the candidate umbilical mast, tower, and launcher coating materials.

The effect of solid rocket motor aluminum content on deflector erosion was investigated via the use of propellant grains having 7, 14, 18, and 22% aluminum by weight. In each case motors were fired on Fondu Fyre WA-1 deflectors poured and cured to be as nearly identical as possible.

Scale effects were investigated using deflectors coated with a Portland cement mix proportioned according to specifications set forth for Titan IIIC deflectors at Cape Kennedy (Pads 40 and 41). The model deflectors could not be coated by the gunite process like the full-scale deflectors, and it was recognized at the outset that these coatings would be less dense and more susceptible to erosion than the full-scale coatings. Nevertheless, the investigation of scale effects was important enough to merit tests

The secondary objective of evaluating the erosion resistance of the deflector coated with the Harbison-Walker Harcast ES was thwarted by a rocket motor malfunction. The results of tests of candidate umbilical mast, tower, and launcher coatings are discussed in Chapter X of this report.

B. TEST ARTICLES

Test articles for the Group II tests consisted of deflectors, a simulated umbilical mast, and coated test panels for mounting on the mast. A description of the deflectors and coated test panels is given in the following paragraphs.

1. Deflector

A total of eight deflectors were prepared for Group II testing. Three of these were coated with the Portland cement mix discussed under the Group I tests, four with Fondu Fyre WA-1, and one with Harbison-Walker Harcast ES. The three coated with Portland cement mix were configured somewhat differently from the other five. The difference involved a straight section at the top of the deflector. This section was added to make the geometry similar to the Titan IIIC flame deflector. Figure V-1 gives dimensional data appropriate to both deflector configurations.

Each deflector had a 3/16-in. steel base plate rolled to the proper contour. A 2-in. wire mesh was affixed ½-in. from the plate surface for reinforcement purposes (Fig. V-2). The base plate fit in a form into which coating material was poured. The deflectors and side plates were molded in one piece. Thickness of the deflector coating was approximately 2-in.

To ensure uniformity, coatings were mixed under carefully controlled conditions with special attention given to the amount of water added. At the time each deflector was poured, a 4-in. test cylinder was also poured. It was cured alongside the deflector and tested for compressive strength on or about the same day the deflector was fired upon. Compressive strength data, an indicator of the quality of the pour, is given in erosion data tables for each deflector. Figure V-3 shows two test cylinders, one before and one after crushing.

All deflectors coated with the Portland cement mix were allowed to cure for at least 28 days. The initial moist cure was for approximately 7 days, at least three of which were at near 100% humidity as established in an environmental chamber. The Fondu Fyre and Harbison-Walker deflectors were cured for two or more weeks, the first three days of which were in the environmental chamber at humidities near 100% and temperatures from 95 to 100°F.

2. Coated Test Panels

Forty-two test panels coated with 17 candidate materials for umbilical mast, umbilical tower, and launcher thermal protection were evaluated during Group II tests. Each panel consisted of a $2\frac{1}{2}x3\frac{3}{4}x\frac{3}{16}$-in. mild steel base plate to which a coating approximately ¼-in. thick was applied. The coatings overlapped the edges of the panels so that the overall dimensions were about 3x4¼ in. Figure V-4 is a sketch of a panel.

Some of the panels were instrumented to measure coating backside temperature, panel surface pressure, and/or heating rate. The heating rate was measured using a Hy-Cal asymptotic calorimeter.

The panels were mounted on a simulated umbilical mast so that the face of each was 1.5 nozzle exit diameters $(1.5\ D_e)$ from the rocket motor longitudinal centerline. During Runs 13 and 14 the panels were mounted 1.25 D_e from the rocket motor centerline. Figure V-5 shows some of the panels mounted in place before a test.

C. PROCEDURE

Before pouring each flame deflector, the steel base plate and wire mesh were weighed. After pouring and curing, each deflector was again weighed and a grid was marked on it. A reference point termed the target was also marked on the deflector. The target or origin of grid lines was located 0.06 D_e up along the deflector centerline from the point of tangency of curved and straight sections. Deflector thickness was measured at the grid intersection points and recorded on a form.

The test panels were weighed before coating and before thermocouple installation. After coating and curing, they were again weighed and thermocouples were installed in some of the plates.

The deflectors were mounted on the cart and aligned so that the rocket motor centerline passed through the target and made a 30-deg angle with the deflector centerline. A stop for the cart was welded across the track so that the nozzle exit-to-deflector separation distance was three nozzle diameters with the cart against the stop.

The test panels were installed, all instrumentation was hooked up, and the continuity was checked. The rocket motor charges were then removed from the 70-deg conditioning facility, weighed, and installed in the motor case. On cold days the motor case was preheated to minimize grain cooling. Nozzle throat dimensions were measured and recorded. The cart was moved to its position against the stop and the swing arm was set in the zero position (initial position for cable payout). The payout cable was then pretensioned to 2200 lb (approximate thrust load on the cart at motor ignition). The rocket motor ignition switch was positioned to allow simulation of a 200 millisecond holddown, and the swing arm was moved counterclockwise several degrees so that it would be up to speed by the time it tripped the motor ignition switch. The wheel for measuring cart travel was aligned with the light sensor, and the test area was cleared for ignitor installation. After ignitor installation the calorimeter cooling water was turned on.

A test consisted of a short countdown during which data recorders and cameras were turned on. Power was switched to the swing arm electric motor drive starting the arm in motion. The swing arm tripped the motor ignition switch and payed out cable to the cart at the desired rate.

Postfiring deflector and test sample photos were taken. The deflector and samples were removed from the cart and taken to the laboratory for weighing. A grid was reestablished on each deflector, and thickness measurements were made at grid intersection points. Nozzle throat dimensions were again measured and charge residue was weighed.

D. TEST RESULTS

Test results were considered satisfactory when the following items were successfully accomplished:

1) Simulated holddown was within ± 200 millisec of the desired value;

2) The rocket motor fired satisfactorily and the chamber pressure matched time histories of related firings within 5%;

3) Actual cart travel matched expected travel;

4) All key instrumentation operated satisfactorily;

5) There were no other anomalies.

Anomalies that did occur are listed in the remarks column of the basic erosion data sheets. The more significant anomalies such as occurred during Runs 7 and 13 are called out in the run schedule (Table I-1).

1. Aluminum Content Effects

The effect of propellant aluminum content on erosion is shown in Fig. V-6 and Tables V-3 thru V-6. An examination of these data reveals that there is little difference between deflector centerline erosion profiles resulting from firings made with the 14, 18, and 22% aluminum grains. This finding verifies a conclusion reached during the SPREE Phase II, Part I program. It is interesting to note that there was significantly less deflector erosion from the firing of the 7% aluminum grain. It is also interesting to note that the predicted chamber temperature of the 7% aluminum motor was approximately 800°F lower than the predicted chamber temperatures of the motors containing 14, 18, and 22% aluminum. Chamber temperatures of the latter motors were within 200°F of each other. This suggests that the effect of propellant aluminum content on mechanical erosion is minimal; the primary effect being on thermal erosion and related to aluminum content only insofar as aluminum content affects chamber temperature.

An unsuccessful attempt was made to correlate deflector erosion with the total heat incident on each deflector. Total heat was calculated by adjusting the plume data obtained during Runs 23 and 24 for chamber temperature. Theoretical chamber temperature data in Table IV-2 were used. Run 9 was selected as reference for the correlation.

Run	Aluminum (%)	Total Heat Ratio	Weight Loss Ratio	Erosion Depth Ratio
12	7	0.93	0.66	0.47
9	14	1.00	1.00	1.00
10	18	1.06	1.21	1.14
11	22	1.06	1.00	0.88

It is evident from the preceding tabulation that the erosion difference between 7% grain data and data obtained with the other grains cannot be attributed entirely to thermal effects, at least with the limited data available. The erosion differences applicable to the 18 and 22% grains cannot be explained on the basis of either thermal or mechanical effects. A more accurate correlation could have been made if accurate plume data were available for the four grain types.

Cart travel for Run 9 was somewhat erratic and this hampered correlation attempts. No method was found to incorporate deflector compressive strength into the study.

2. Scale Effects

Runs 7, 8, and 14 were made to investigate scale effects and propellant aluminum content effects. A cart travel malfunction during Run 7 nullified the attempt to determine aluminum content effects.

The deflectors used were coated with a Portland cement mix that was formulated to be as much like the full-scale Titan IIIC flame deflector coating as possible within program constraints. The aggregate was crushed and screened per specifications for Complex 40 and 41 deflectors, and cement-aggregate proportions were duplicated. The following differences in the mix must be kept in mind when interpreting the data:

1) Type III Portland cement was used in lieu of the Types I or II called out in the specification. This was done to expedite model deflector curing;

2) Aggregate was obtained locally and no doubt differed from that used at Cape Kennedy;

3) The model deflectors were cast, whereas, the full-scale deflectors were coated by the gunite process. Coatings applied by high pressure guning are generally more dense and stronger than cast coatings.

The differences between the model and full-scale deflector coatings were predominately in the direction of decreasing the erosion resistance of the model deflectors relative to full-scale.

During Run 14 the rocket motor was canted to simulate the 6-deg nozzle cant of the UTC 120-in. solid. The motor was oriented so that the nozzle centerline passed through the deflector target at the initial 3 D_e nozzle-to-deflector separation distance. The plume would then sweep across the deflector as lift-off was simulated. Because of the importance of nozzle cant as evidenced by a comparison of erosion data from Runs 8 and 14 (Fig. V-7), only Run 14 is considered satisfactory for the drawing of conclusions relative to scale effects. Any conclusions drawn must keep in mind the differences in model- and full-scale chamber pressure and aluminum content (Fig. IV-6 and V-8).

Full-Scale Data - Erosion measurements were obtained on the ETR Complex 40 flame deflector in conjunction with the launch of Titan IIIC SSLV-7, the first Titan IIIC launched, and the first launch from Complex 40. The work was done under Air Force contract and is presented in Martin Report SSLV-05-7 FER-1.

A total of 80 deflector erosion depth measurements were obtained. Eight measurements were taken at each of 10 stations spaced at 3-ft intervals along the deflector surface in the flow direction (Fig. V-8). Measurement accuracy was 1/16 in. The following technique was used to make the measurements:

1) A plumbline was dropped from the core centerline. The point of intersection of the plumbline and deflector surface was called Station 0. Stations up the deflector from Station 0 were negative and those down the deflector were positive;

2) Anchors were inserted in holes drilled in the deflector surface at the deflector edge and center at Stations -12 (ft), -9, -6, -3, 0, 3, 6, 9, 15, and 21;

3) A tool was inserted in the anchors and piano wire strung and tensioned across the deflector at each station. The distance from the piano wire to the deflector surface was measured at each of the 80 designated points. The piano wire and tools were then withdrawn from the anchors and the anchors were covered with Martyte for thermal protection during launch;

4) After launch, the Martyte was chipped away to expose the anchors. The tools and piano wire were again inserted in the anchors, and the distance from the piano wire to the deflector surface was measured. The difference between the after-launch and before-launch measurements was the erosion. Measured erosion data are given in Fig. V-8.

Maximum deflector erosion occurred at Stations 6B and 9D. Erosion depth was 0.50 in. at these points. The location of the area of maximum erosion was on the curved surface of the deflector near the exhaust plume periphery down the deflector from the projection of the nozzle centerline. This is the expected area of maximum erosion for deflectors configured like the LC 40 deflector when initial nozzle-to-deflector separation distance is three nozzle exit diameters.

The deflector erosion appeared to result from surface spalling rather than surface melting. Spalling also occurred on the side walls of the flame duct. The spalling was due to the breaking down of water in the crystalline structure of the concrete. This characteristic is inherent in Portland cement concretes when exposed to a high temperature environment.

Model Data - Erosion data for Runs 7, 8, and 14 are given in Tables V-1, V-2, and V-8. The data from Runs 7 and 8 do not contribute to the scale effects investigation for the reasons just discussed. It is interesting to note that the maximum deflector erosion occurring during Run 8 was 0.990 in. This is more than twice the maximum erosion observed on the Fondu Fyre coated deflector tested at a 100 D_e separation rate during Run 16. Maximum erosion on the deflector evaluated during Run 14 was 0.607 in. This is only slightly more than the 0.50-in. maximum full-scale erosion (greater model erosion was expected). Figure V-9 compares model- and full-scale centerline erosion data. Considering the accuracy with which full-scale erosion measurements can be made, and the various differences between model and full-scale motors and deflector coatings, the agreement is excellent. Thus, Run 14 would seem to validate full-scale applications of SPREE erosion data.

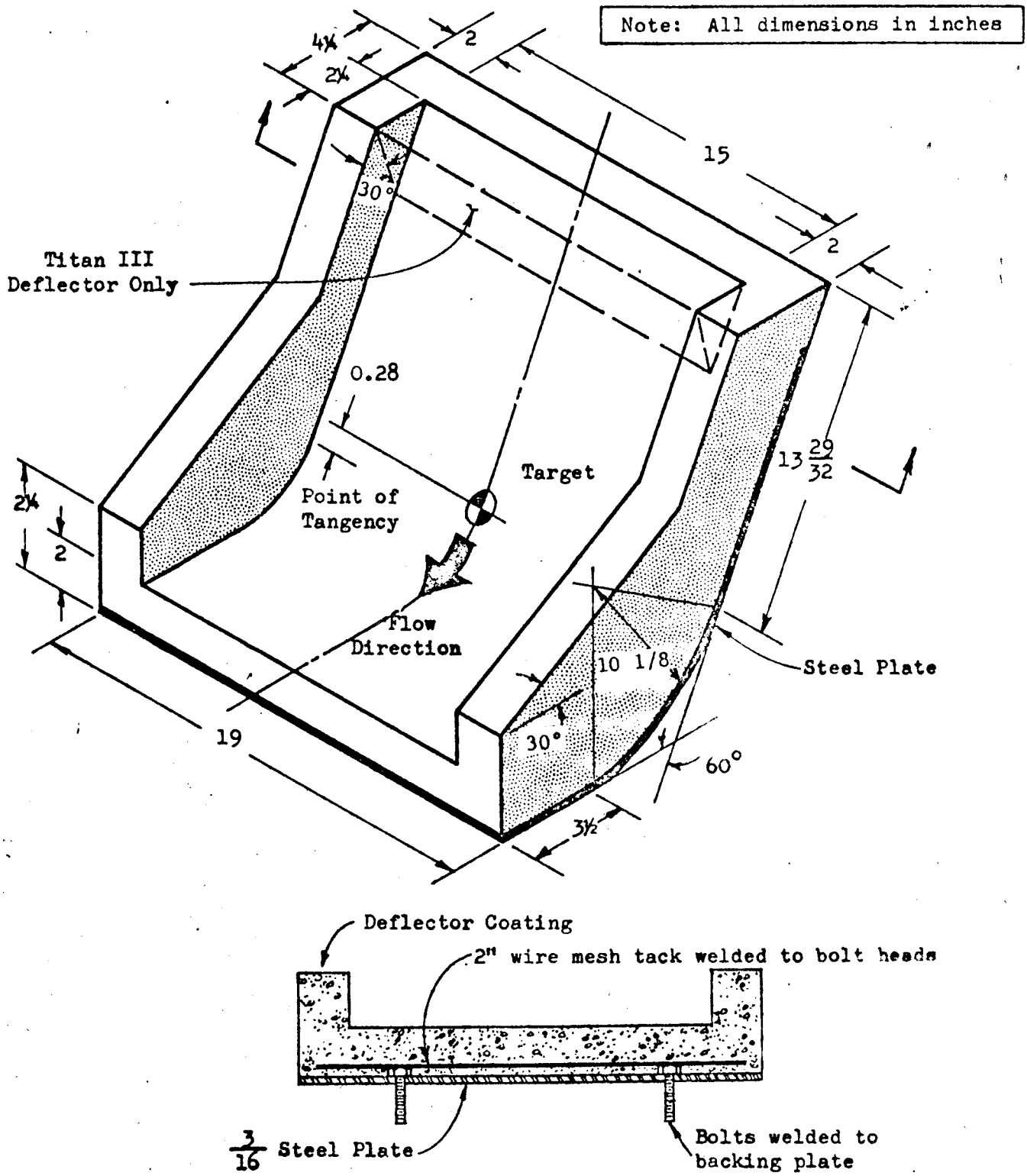

Fig. V-1 J Deflector

Fig. V-2 J Deflector Base Plate

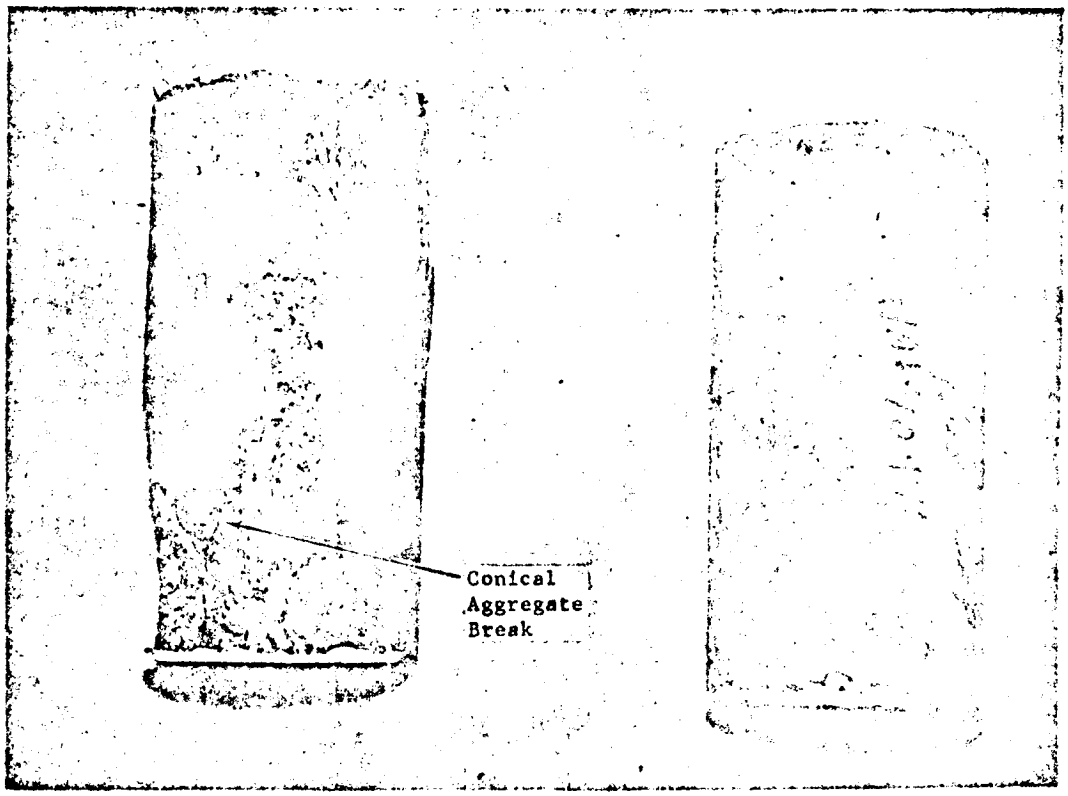

Fig. V-3 Fondu Fyre WA-1 Compression Test Cylinders before and after Crushing

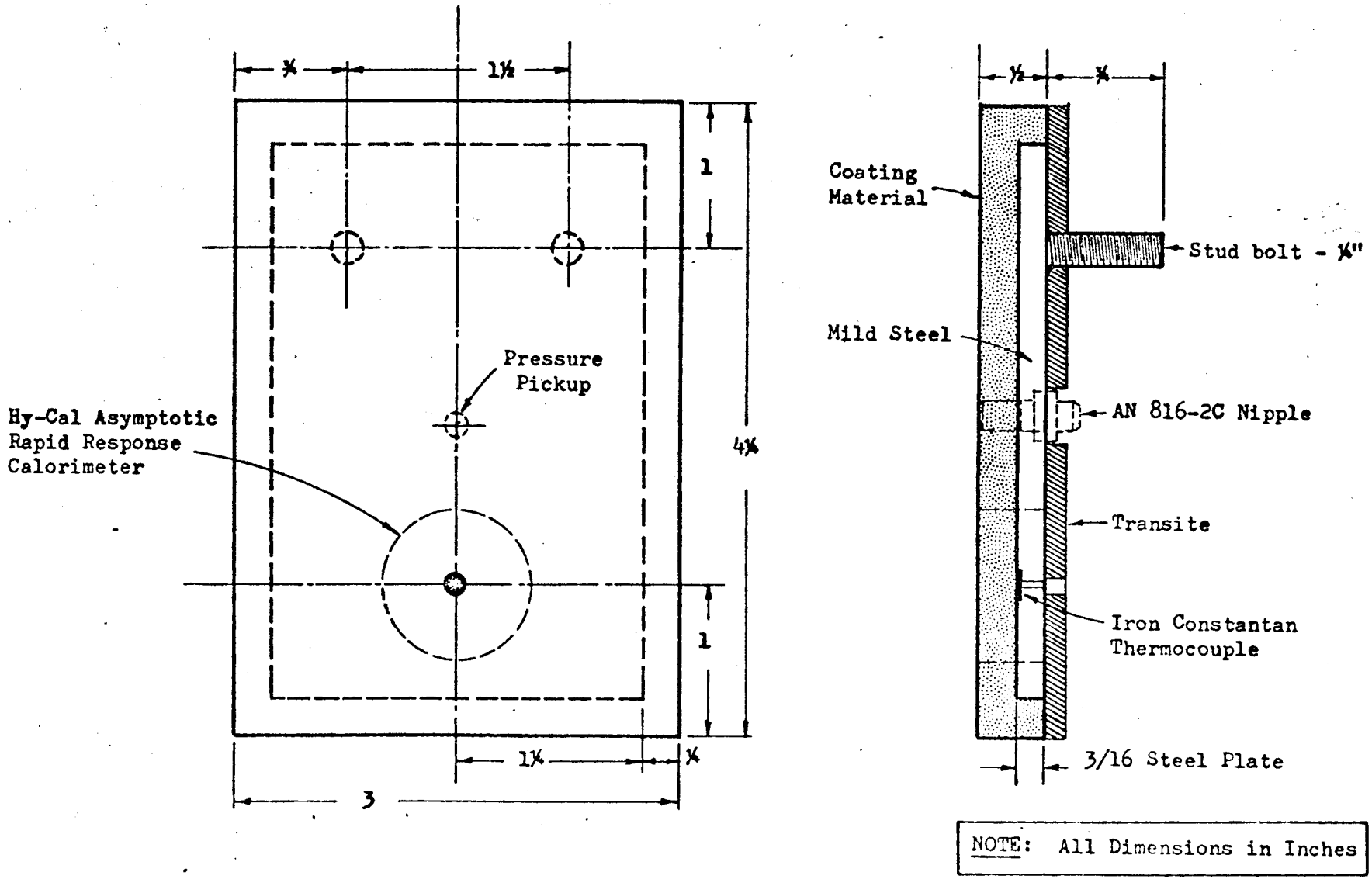

Fig. V-4 Coated Test Panel Sketch

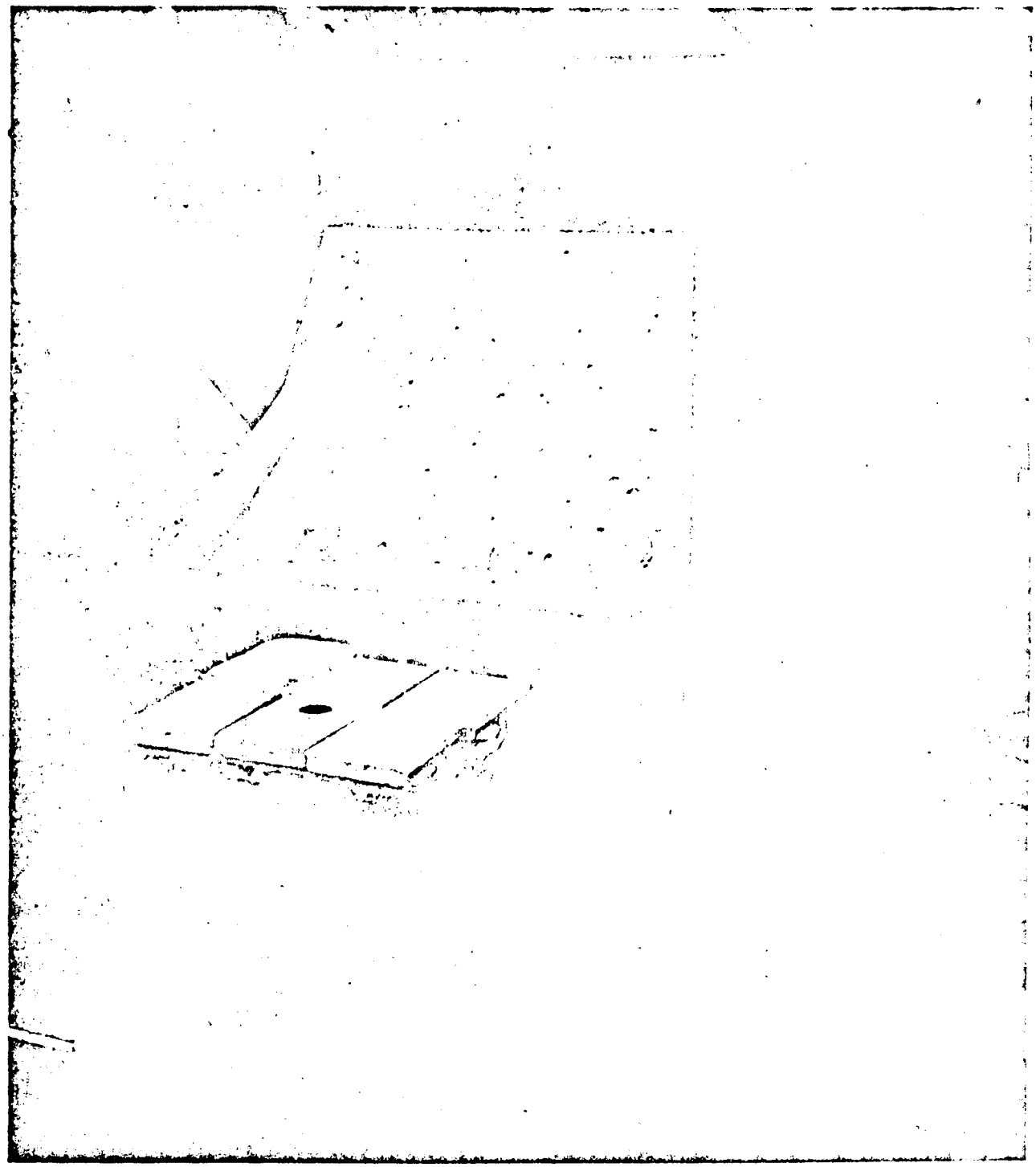

Fig. V-5 Coated Panels Mounted in Place before Firing 7

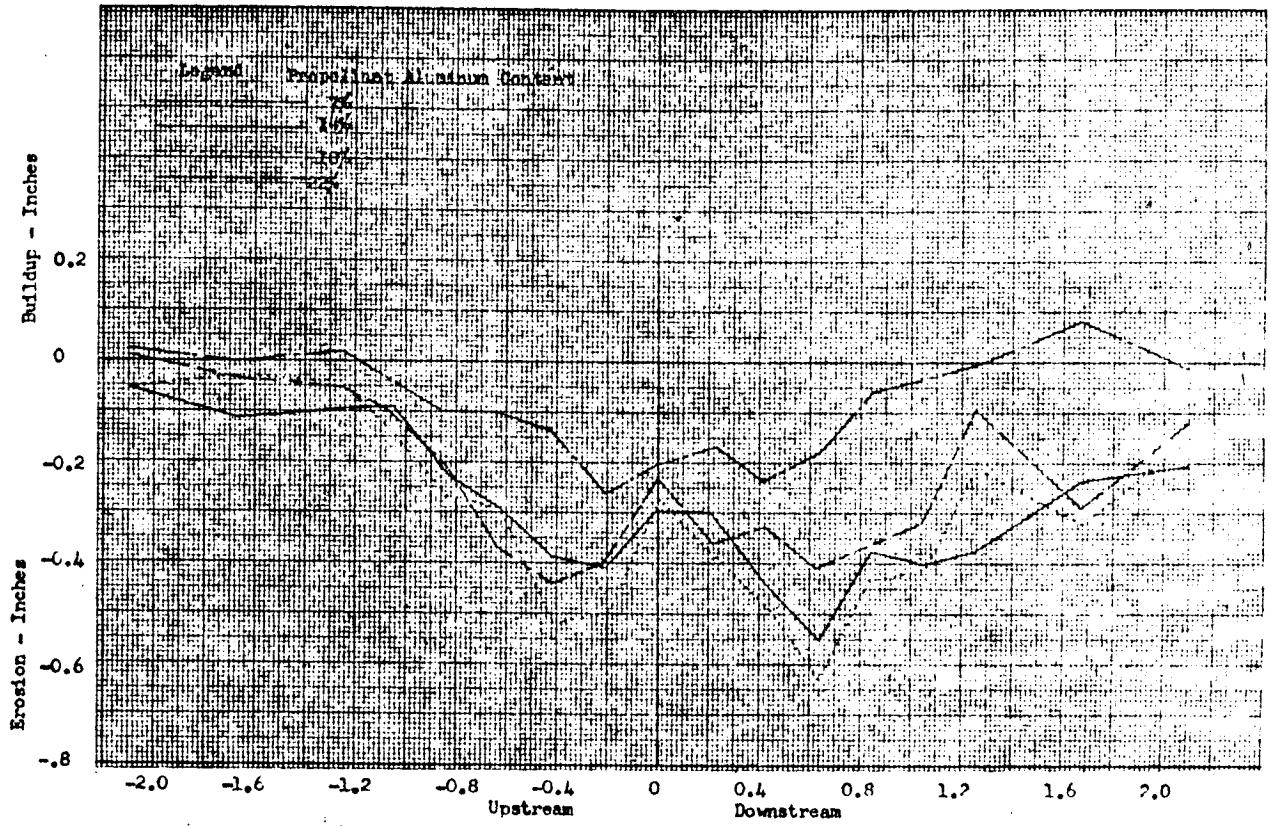

Fig. V-6 Effect of Propellant Aluminum Content on Deflector Centerline Erosion

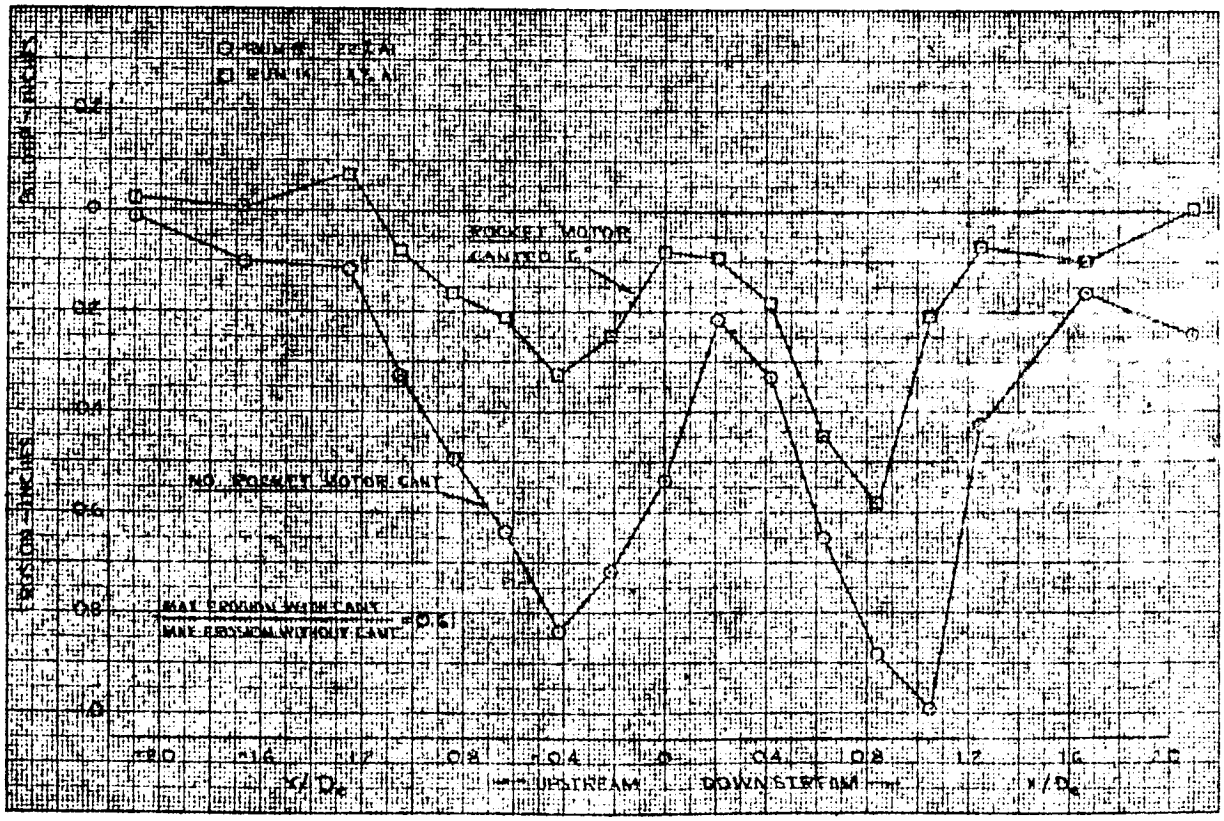

Fig. V-7 Effect of Rocket Motor Cant on Deflector Centerline Erosion

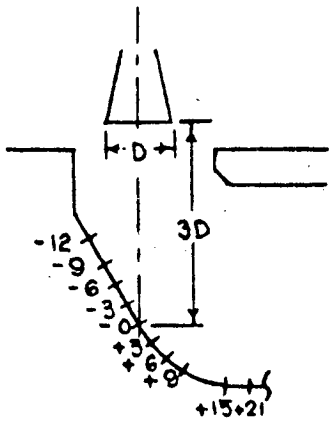

NOTES:

1. LAUNCH T/W = 1.69
2. MOTOR DATA:
   - % Al = 16.5
   - D = 8.886 FT
   - P_c = 720 PSIA (NOMINAL AFT END AT LAUNCH)
   - ϵ = 8

CORE ℄

	A	B	C	D	E	F	G	H
-12	0	.06	.06	.13	.13	.06	.06	.06
-9	.06	.13	.13	.13	.19	.19	.06	.19
-6	.25	.25	.38	.25	.31	.25	.13	.13
-3	.06	.06	.19	.25	.25	.25	.13	.19
0	.19	.25	.19	.31	.06	.13	.13	.06
3	.19	.19	.19	.25	.19	.19	.06	.13
6	.44	.50	.19	.44	.31	.13	.06	.06
9	.19	.31	.38	.50	.13	.06	.06	.06
15	.06	.13	.31	0	.25	.13	.13	.25
21	.06	.13	0	.13	.06	.13	.13	.13

3' 0" (TYP)

6' 0" (TYP)

3' 0" (TYP)

ig. V-8 Launch Complex 40 Deflector Erosion after First Titan IIIC Firing

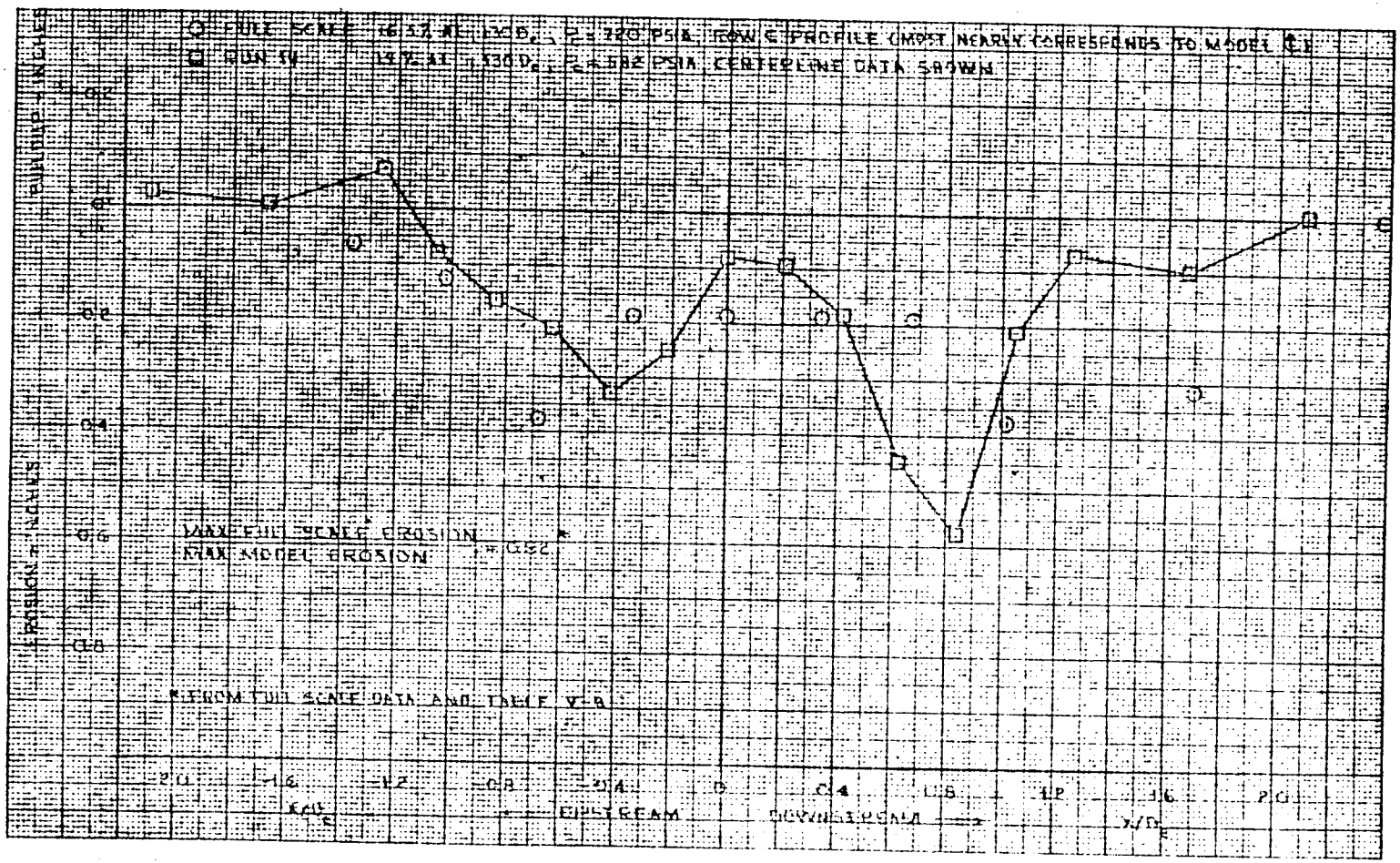

Fig V-9 Comparison of Titan IIIC Full-Scale and Model Deflector Erosion

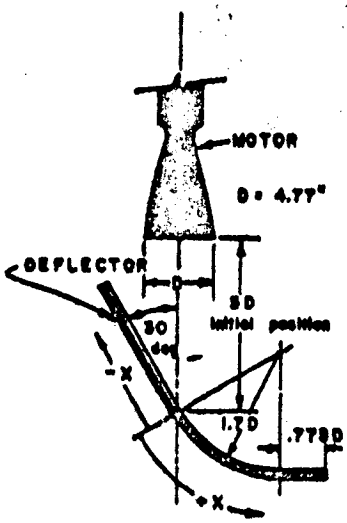

Table V-1 J Deflector Erosion, Run 7

DEFLECTOR COATING: Portland Cement Mix
LIFT-OFF RATE: 130 De in 10 sec.
GRAIN DATA:
% AL 18 , $\dot{m}$ 8.5 lb/sec
P_c (nom) 570 psi

COMMENTS

1. POUNDS OF DEFLECTOR COATING MATERIAL ERODED = 13.50 lb
2. MAXIMUM EROSION DEPTH = 0.892 in.
3. LOCATION OF MAXIMUM EROSION $\frac{X}{D}$ = +0.84
   $\frac{Y}{D}$ = -0.21
4. COMPRESSIVE STRENGTH OF DEFLECTOR COATING = 4050 psi
5. Cart Travel malfunction

TOP OF DEFLECTOR

X/D	-1.47	-1.05	-0.63	-0.42	-0.21	0	+0.21	+0.42	+0.63	+1.05	+1
-2.10	000 +	-.070 +	-.070 +	-.039 +	-.075 +	-.013 +	-.040 +	-.030 +	-.039 +	-.020 +	
-1.67	+.005 +	-.040 +	-.068 +	-.058 +	-.060 +	-.038 +	-.051 +	-.053 +	-.035 +	-.063 +	
-1.25	-.020 +	-.058 +	-.063 +	-.075 +	-.125 +	-.112 +	-.114 +	-.098 +	-.116 +	[illegible] +	
-1.05	-.007 +	-.023 +	-.075 +	-.090 +	-.171 +	-.160 +	-.124 +	-.103 +	-.085 +	[illegible] +	
-0.84	-.008 +	-.016 +	-.082 +	-.122 +	-.180 +	-.217 +	-.205 +	-.150 +	[illegible] +	[illegible] +	
-0.63	-.010 +	-.023 +	-.110 +	-.125 +	-.211 +	-.216 +	-.268 +	[illegible] +	[illegible] +	-.038 +	
-0.42	-.005 +	-.037 +	-.054 +	-.270 +	-.294 +	-.350 +	-.337 +	-.235 +	-.120 +	[illegible] +	
-0.21	-.003 +	-.007 +	-.128 +	-.226 +	-.285 +	-.297 +	-.370 +	-.230 +	-.122 +	+.006 +	
℄-0 of motor	-.007 +	-.012 +	-.105 +	-.218 +	-.225 +	-.202 +	-.229 +	-.238 +	-.129 +	-.014 +	
+0.21	-.040 +	-.058 +	-.113 +	-.250 +	-.222 +	-.194 +	-.205 +	-.232 +	-.125 +	[illegible] +	
+0.42	-.072 +	-.100 +	-.272 +	-.388 +	-.300 +	-.319 +	-.310 +	-.317 +	-.264 +	-.088 +	
+0.63	-.250 +	-.280 +	-.612 +	-.677 +	-.635 +	-.593 +	-.605 +	-.643 +	-.570 +	-.178 +	
+0.84	-.193 +	-.242 +	-.619 +	-.824 +	-.892 +	-.875 +	-.859 +	-.805 +	-.513 +	-.185 +	
+1.05	-.175 +	-.188 +	-.207 +	-.327 +	-.504 +	-.487 +	-.593 +	-.316 +	-.277 +	-.148 +	
+1.25	-.113 +	-.161 +	-.203 +	-.235 +	-.388 +	-.350 +	-.277 +	-.203 +	-.135 +	-.135 +	
+1.67	-.130 +	-.115 +	-.150 +	-.235 +	-.238 +	-.108 +	-.210 +	-.194 +	-.207 +	-.115 +	
+2.10	-.137 +	-.118 +	-.163 +	-.137 +	-.206 +	-.199 +	-.173 +	-.165 +	-.101 +	-.088 +	

℄ of motor

MEASUREMENTS ON DEFLECTOR SURFACE
(- VALUE, EROSION, + VALUE, BUILDUP)

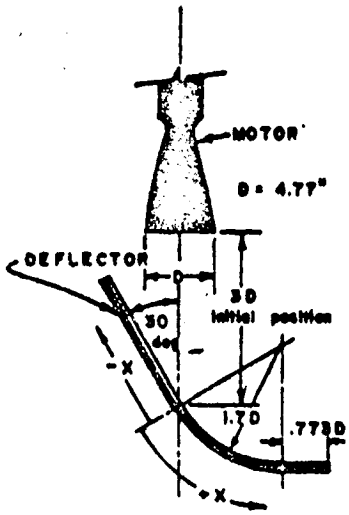

Table V-2 J Deflector Erosion, Run 8

DEFLECTOR COATING: Portland Cement Mix
LIFT-OFF RATE: 130 De in 10 sec.
GRAIN DATA:
% AL 22 , $\dot{m}$ 8.6 lb/sec
P_c (nom) 595 psi

COMMENTS

1. POUNDS OF DEFLECTOR COATING MATERIAL ERODED = 8.00 lb.
2. MAXIMUM EROSION DEPTH = 0.990 in.
3. LOCATION OF MAXIMUM EROSION $\frac{X}{D}$ = +1.05 $\frac{Y}{D}$ = 0
4. COMPRESSIVE STRENGTH OF DEFLECTOR COATING = not avbl. psi
5. Hold-down excessive (0.60 sec.)

TOP OF DEFLECTOR

X/D	-1.47	-1.05	-0.63	-0.42	-0.21	0	+0.21	+0.42	+0.63	+1.05	+1.47
-2.10	-.003 +	-.021 +	-.032 +	-.015 +	000 +	-.013 +	-.039 +	-.050 +	-.030 +	-.013 +	+.020 +
-1.67	-.035 +	-.025 +	-.049 +	-.050 +	-.075 +	-.100 +	-.065 +	-.042 +	-.103 +	-.005 +	+.015 +
-1.25	-.023 +	-.020 +	-.130 +	-.100 +	-.170 +	-.113 +	-.137 +	-.062 +	-.148 +	-.050 +	+.025 +
-1.05	+.050 +	-.005 +	-.035 +	-.150 +	-.330 +	-.325 +	-.370 +	-.250 +	-.185 +	-.130 +	-.120 +
-0.84	-.050 +	-.037 +	-.080 +	-.187 +	-.395 +	-.495 +	-.408 +	-.275 +	-.210 +	-.027 +	-.020 +
-0.63	-.043 +	-.025 +	-.060 +	-.285 +	-.578 +	-.638 +	-.523 +	-.325 +	-.170 +	+.011 +	+.018 +
-0.42	+.080 +	+.025 +	-.075 +	-.455 +	-.765 +	-.835 +	-.668 +	-.500 +	-.225 +	-.115 +	-.100 +
-0.21	+.028 +	+.031 +	-.063 +	-.465 +	-.738 +	-.715 +	-.713 +	-.565 +	-.165 +	-.115 +	-.115 +
℄ of motor 0	+.050 +	-.005 +	-.035 +	-.470 +	-.495 +	-.538 +	-.355 +	-.515 +	-.155 +	+.030 +	+.003 +
+0.21	-.023 +	+.060 +	-.238 +	-.370 +	-.265 +	-.215 +	-.290 +	-.390 +	-.345 +	-.033 +	-.085 +
+0.42	-.055 +	-.060 +	-.445 +	-.460 +	-.380 +	-.330 +	-.420 +	-.435 +	-.375 +	-.060 +	+.020 +
+0.63	-.065 +	-.150 +	-.730 +	-.710 +	-.628 +	-.648 +	-.640 +	-.620 +	-.700 +	-.145 +	-.030 +
+0.84	-.185 +	-.242 +	-.770 +	-.935 +	-.895 +	-.883 +	-.890 +	-.900 +	-.773 +	-.300 +	-.145 +
+1.05	-.170 +	-.130 +	-.158 +	-.522 +	-.622 +	-.990 +	-.968 +	-.640 +	-.305 +	-.105 +	-.095 +
+1.25	-.120 +	-.153 +	-.185 +	-.323 +	-.320 +	-.425 +	-.255 +	-.250 +	-.175 +	-.115 +	-.135 +
+1.67	-.060 +	-.110 +	-.148 +	-.188 +	-.180 +	-.157 +	-.175 +	-.195 +	-.175 +	-.095 +	-.150 +
+2.10	-.060 +	-.105 +	-.205 +	-.145 +	-.205 +	-.245 +	-.235 +	-.177 +	-.140 +	-.070 +	-.100 +

Y/D

℄ of motor

MEASUREMENTS ON DEFLECTOR SURFACE
(- VALUE, EROSION; + VALUE, BUILDUP)

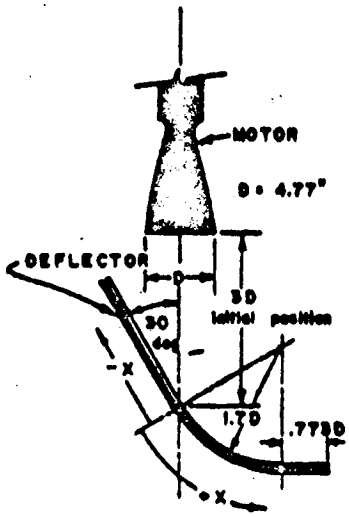

Table V-3 J Deflector Erosion, Run 9

DEFLECTOR COATING: Fondu Fyre WA-1
LIFT-OFF RATE: 50 De in 10 sec.
GRAIN DATA:
% AL 14 , $\dot{m}$ 8.5 lb/sec
P_c (nom) 554 psi

COMMENTS

1. POUNDS OF DEFLECTOR COATING MATERIAL ERODED = 4.75 lb.
2. MAXIMUM EROSION DEPTH = 0.550 in.
3. LOCATION OF MAXIMUM EROSION $\frac{X}{D}$ = +0.63
   $\frac{Y}{D}$ = 0
4. COMPRESSIVE STRENGTH OF DEFLECTOR COATING = 2980 psi
5. Cart Travel erratic due to insufficient system pretensioning.

TOP OF DEFLECTOR

X/D											
		-.065	-.045	-.008	-.035	-.055	-.027	-.015	-.005	+.013	
-2.10	+	+	+	+	+	+	+	+	+	+	+
		-.015	+.010	-.047	-.085	-.110	-.080	+.005	+.003	+.065	
-1.67	+	+	+	+	+	+	+	+	+	+	+
		+.085	-.050	-.035	-.070	-.090	-.095	+.010	-.015	000	
-1.25	+	+	+	+	+	+	+	+	+	+	+
		+.120	-.015	-.018	-.160	-.090	-.115	-.085	-.010	-.035	
-1.05	+	+	+	+	+	+	+	+	+	+	+
		+.182	-.022	-.065	-.235	-.225	-.200	-.110	000	+.065	
-0.84	+	+	+	+	+	+	+	+	+	+	+
		+.182	-.025	-.195	-.260	-.290	-.280	-.113	-.050	+.015	
-0.63	+	+	+	+	+	+	+	+	+	+	+
		+.055	-.048	-.225	-.310	-.390	-.295	-.260	-.025	+.070	
-0.42	+	+	+	+	+	+	+	+	+	+	+
		+.195	-.095	-.300	-.345	-.405	-.362	-.305	-.133	+.005	
-0.21	+	+	+	+	+	+	+	+	+	+	+
		+.175	-.035	-.255	-.270	-.290	-.242	-.195	-.050	+.480	
℄-0 of meter	+	+	+	+	+	+	+	+	+	+	+
		+.125	-.200	-.280	-.355	-.300	-.278	-.258	-.125	+.325	
+0.21	+	+	+	+	+	+	+	+	+	+	+
		-.160	-.315	-.480	-.415	-.440	-.430	-.459	-.283	-.068	
+0.42	+	+	+	+	+	+	+	+	+	+	+
		-.190	-.335	-.530	-.530	-.550	-.525	-.528	-.295	-.080	
+0.63	+	+	+	+	+	+	+	+	+	+	+
		-.138	-.137	-.238	-.318	-.375	-.395	-.283	-.155	-.015	
+0.84	+	+	+	+	+	+	+	+	+	+	+
		-.165	-.213	-.310	-.340	-.400	-.410	-.310	-.502	-.118	
+1.05	+	+	+	+	+	+	+	+	+	+	+
		-.090	-.213	-.255	-.275	-.373	-.415	-.238	-.215	-.185	
+1.25	+	+	+	+	+	+	+	+	+	+	+
		-.117	-.215	-.265	-.230	-.235	-.305	-.228	-.195	-.132	
+1.67	+	+	+	+	+	+	+	+	+	+	+
		-.095	-.140	-.140	-.157	-.202	-.205	-.245	-.255	-.205	
+2.10	+	+	+	+	+	+	+	+	+	+	+
Y/D	-1.47	-1.05	-0.63	-0.42	-0.21	0	+0.21	+0.42	+0.63	+1.05	+1.47

℄ of meter

MEASUREMENTS ON DEFLECTOR SURFACE
(- VALUE, EROSION; + VALUE, BUILDUP)

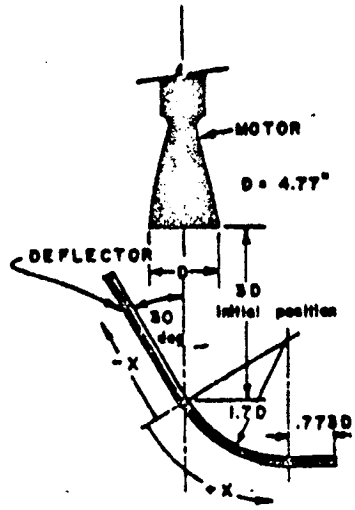

Table V-4 J Deflector Erosion, Run 10

DEFLECTOR COATING: Fondu Fyre - WA-1
LIFT-OFF RATE: 50 De in 10 sec.
GRAIN DATA:
% AL 18, $\dot{m}$ - lb/sec(5)
P_c (nom) - psi(5)

COMMENTS

1. POUNDS OF DEFLECTOR COATING MATERIAL ERODED = 5.75 lb
2. MAXIMUM EROSION DEPTH = 0.630 in.
3. LOCATION OF MAXIMUM EROSION $\frac{X}{D}$ = + 0.63
   $\frac{Y}{D}$ = 0
4. COMPRESSIVE STRENGTH OF DEFLECTOR COATING = 6040 psi
5. Chamber Pressure data lost in Processing

TOP OF DEFLECTOR

X/D	-1.47	-1.05	-0.63	-0.42	-0.21	0	+0.21	+0.42	+0.63	+1.05	+1.47
- 2.10	-.010 +	000 +	+.065 +	-.010 +	-.045 +	-.063 +	+.008 +	+.005 +	-.010 +	+.015 +	+.010 +
- 1.67	+.040 +	+.070 +	-.012 +	+.035 +	-.018 +	-.025 +	-.023 +	-.020 +	-.0[illegible] +	+.057 +	+.0[illegible] +
- 1.25	+.030 +	+.045 +	-.050 +	-.055 +	-.070 +	-.035 +	-.292 +	-.065 +	-.082 +	-.070 +	+.052 +
- 1.05	+.097 +	+.030 +	-.070 +	-.112 +	-.120 +	-.145 +	-.130 +	-.105 +	-.002 +	-.035 +	+.010 +
- 0.84	+.105 +	+.104 +	-.042 +	-.135 +	-.265 +	-.265 +	-.260 +	-.197 +	-.047 +	-.008 +	-.028 +
- 0.63	+.122 +	+.084 +	-.135 +	-.172 +	-.395 +	-.298 +	-.425 +	-.277 +	-.080 +	-.025 +	+.010 +
- 0.42	+.062 +	+.085 +	-.070 +	-.338 +	-.480 +	-.515 +	-.510 +	-.355 +	-.165 +	-.0[illegible] +	[illegible] +
- 0.21	+.005 +	+.005 +	-.130 +	-.408 +	-.495 +	-.500 +	-.542 +	-.340 +	-.160 +	+.070 +	+.032 +
— ℄ — 0 of meter	+.170 +	+.160 +	-.060 +	-.320 +	-.330 +	-.265 +	-.265 +	-.315 +	-.125 +	+.095 +	+.065 +
+ 0.21	+.135 +	+.095 +	-.240 +	-.463 +	-.400 +	-.350 +	-.400 +	-.395 +	-.268 +	+.072 +	+.100 +
+ 0.42	-.045 +	-.100 +	-.280 +	-.590 +	-.542 +	-.485 +	-.475 +	-.460 +	-.370 +	+.110 +	+.170 +
+ 0.63	+.005 +	-.110 +	-.185 +	-.315 +	-.420 +	-.630 +	-.614 +	-.575 +	-.180 +	+.120 +	+.235 +
+ 0.84	-.058 +	-.085 +	-.195 +	-.230 +	-.405 +	-.430 +	-.357 +	-.268 +	-.100 +	-.020 +	+.142 +
+ 1.05	-.027 +	-.100 +	-.190 +	-.215 +	-.375 +	-.410 +	-.375 +	-.225 +	-.090 +	-.035 +	+.060 +
+ 1.25	-.060 +	-.155 +	-.170 +	-.250 +	-.140 +	-.210 +	-.140 +	-.115 +	-.130 +	+.010 +	+.035 +
+ 1.67	-.075 +	-.155 +	-.277 +	-.315 +	-.305 +	-.320 +	-.300 +	-.285 +	-.202 +	-.108 +	-.115 +
+ 2.10	-.123 +	-.155 +	-.117 +	-.145 +	-.085 +	-.155 +	-.180 +	-.140 +	-.120 +	-.105 +	-.095 +

℄ of meter

MEASUREMENTS ON DEFLECTOR SURFACE
(- VALUE, EROSION; + VALUE, BUILDUP)

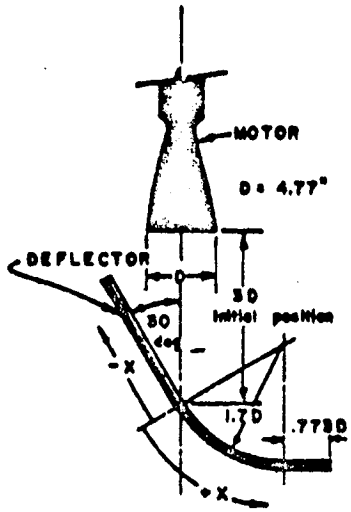

Table V-5 J Deflector Erosion, Run 11

DEFLECTOR COATING: Fondu-Fyre - WA-1
LIFT-OFF RATE: 50 Do in 10 sec
GRAIN DATA:
% AL 22, $\dot{m}$ 8.1 lb/sec
P_c (nom) 580 psi

COMMENTS

1. POUNDS OF DEFLECTOR COATING MATERIAL ERODED = 4.75 lb
2. MAXIMUM EROSION DEPTH = 0.485 in.
3. LOCATION OF MAXIMUM EROSION $\frac{X}{D}$ = +0.63
   $\frac{Y}{D}$ = +0.21
4. COMPRESSIVE STRENGTH OF DEFLECTOR COATING = 7950 psi

TOP OF DEFLECTOR

X/D	-1.47	-1.05	-0.63	-0.42	-0.21	0	+0.21	+0.42	+0.63	+1.05	+1.47
-2.10	-.012 +	-.030 +	-.040 +	-.025 +	-.025 +	+.010 +	+.020 +	+.015 +	-.010 +	+.080 +	+.125 +
-1.67	+.030 +	+.030 +	000 +	-.005 +	-.015 +	-.035 +	-.025 +	+.045 +	000 +	+.0[illegible] +	[illegible] +
-1.26	+.035 +	+.030 +	+.050 +	-.025 +	-.007 +	-.040 +	-.015 +	+.027 +	+.055 +	[illegible] +	+
-1.05	+.108 +	+.070 +	+.025 +	-.020 +	-.005 +	-.097 +	-.095 +	-.040 +	+.030 +	[illegible]	+
-0.84	+.130 +	+.090 +	-.015 +	-.030 +	-.105 +	-.210 +	-.235 +	-.120 +	+.005 +	+.135 +	+.145 +
-0.63	+.118 +	-.010 +	-.010 +	-.080 +	-.210 +	-.370 +	-.355 +	-.240 +	-.030 +	+.085 +	+.135 +
-0.42	+.095 +	000 +	-.055 +	-.165 +	-.345 +	-.435 +	-.430 +	-.355 +	-.135 +	+.055 +	+.105 +
-0.21	+.082 +	-.010 +	-.045 +	-.180 +	-.420 +	-.405 +	-.460 +	-.355 +	-.220 +	+.050 +	+.145 +
℄-0 of motor	+.160 +	+.235 +	-.060 +	-.115 +	-.243 +	-.230 +	-.217 +	-.150 +	-.175 +	+.190 +	+.250 +
+0.21	+.070 +	+.165 +	+.038 +	-.275 +	-.330 +	-.365 +	-.320 +	-.417 +	-.473 +	+.170 +	+.220 +
+0.42	+.105 +	+.135 +	-.040 +	-.435 +	-.330 +	-.330 +	-.225 +	-.278 +	-.320 +	+.235 +	+.310 +
+0.63	+.230 +	+.150 +	000 +	-.325 +	-.440 +	-.405 +	-.485 +	-.440 +	-.220 +	+.225 +	+.250 +
+0.84	+.180 +	+.170 +	+.015 +	-.130 +	-.360 +	-.365 +	-.360 +	-.350 +	-.070 +	+.140 +	+.175 +
+1.05	+.120 +	+.130 +	+.040 +	+.015 +	-.180 +	-.320 +	-.335 +	-.225 +	-.075 +	+.110 +	+.115 +
+1.26	+.055 +	+.080 +	000 +	+.005 +	-.120 +	-.095 +	-.115 +	-.040 +	-.020 +	000 +	+.020 +
+1.67	-.025 +	-.160 +	-.225 +	-.280 +	-.250 +	-.290 +	-.260 +	-.230 +	-.185 +	-.115 +	-.085 +
+2.10	+.050 +	-.045 +	-.025 +	-.040 +	-.050 +	-.120 +	-.090 +	-.110 +	-.070 +	-.110 +	-.105 +

Y/D

℄ of motor

MEASUREMENTS ON DEFLECTOR SURFACE
(- VALUE, EROSION; + VALUE, BUILDUP)

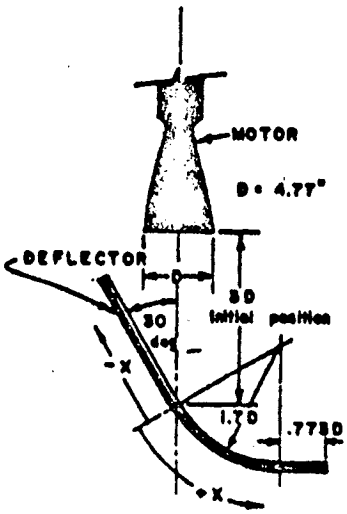

Table V-6 J Deflector Erosion, Run 12

DEFLECTOR COATING: Fondu Fyre - WA-1
LIFT-OFF RATE: 50 De in 10 sec
GRAIN DATA:
% AL 7, $\dot{m}$ 7.9 lb/sec
P_c (nom) 594 psi

COMMENTS

1. POUNDS OF DEFLECTOR COATING MATERIAL ERODED = 3.13 lb
2. MAXIMUM EROSION DEPTH = 0.260 in.
3. LOCATION OF MAXIMUM EROSION $\frac{X}{D}$ = -0.21, $\frac{Y}{D}$ = 0
4. COMPRESSIVE STRENGTH OF DEFLECTOR COATING = 8240 psi
5. Hold-down excessive. (0.55 sec)

TOP OF DEFLECTOR

X/D	-1.47	-1.05	-0.63	-0.42	-0.21	0	+0.21	+0.42	+0.63	+1.05	+1.47
-2.10	+.015 +	-.005 +	+.020 +	+.015 +	-.035 +	+.020 +	+.020 +	+.005 +	+.015 +	-.005 +	-.020 +
-1.67	-.005 +	+.010 +	+.020 +	+.015 +	+.005 +	-.005 +	+.010 +	000 +	-.010 +	[illegible] +	[illegible] +
-1.25	000 +	+.015 +	+.020 +	+.010 +	-.020 +	+.020 +	000 +	-.010 +	+.010 +	000 +	[illegible] +
-1.05	-.023 +	-.020 +	+.020 +	000 +	+.025 +	-.040 +	-.025 +	-.025 +	-.025 +	+.005 +	[illegible] +
-0.84	-.005 +	000 +	-.025 +	-.020 +	-.040 +	-.100 +	-.055 +	-.025 +	+.085 +	+.030 +	-.030 +
-0.63	000 +	-.010 +	+.080 +	+.110 +	-.080 +	-.100 +	-.105 +	-.055 +	+.075 +	-.015 +	-.040 +
-0.42	+.155 +	+.005 +	-.005 +	-.010 +	-.125 +	-.135 +	-.160 +	-.125 +	+.085 +	+.090 +	-.010 +
-0.21	+.090 +	+.005 +	-.045 +	-.030 +	-.160 +	-.260 +	-.240 +	-.168 +	-.045 +	+.005 +	+.005 +
℄-0 of motor	+.075 +	+.085 +	+.075 +	+.080 +	-.080 +	-.200 +	-.170 +	-.065 +	-.005 +	+.115 +	+.155 +
+0.21	+.230 +	+.030 +	+.035 +	+.010 +	-.175 +	-.165 +	-.185 +	-.085 +	+.005 +	+.080 +	[illegible] +
+0.42	+.300 +	+.015 +	-.075 +	-.047 +	-.225 +	-.235 +	-.225 +	-.220 +	+.005 +	-.010 +	[illegible] +
+0.63	+.240 +	-.005 +	+.040 +	-.075 +	-.160 +	-.180 +	-.185 +	-.175 +	-.125 +	+.055 +	+.280 +
+0.84	+.150 +	-.015 +	+.010 +	-.095 +	-.135 +	-.060 +	-.205 +	-.143 +	-.015 +	+.070 +	[illegible] +
+1.05	+.085 +	.005 +	-.020 +	-.050 +	-.090 +	-.050 +	-.102 +	-.065 +	-.025 +	-.005 +	[illegible] +
+1.25	+.190 +	-.040 +	+.025 +	-.025 +	-.035 +	-.005 +	-.045 +	-.025 +	-.020 +	+.010 +	+.140 +
+1.67	-.030 +	-.060 +	+.005 +	-.045 +	-.035 +	+.085 +	-.045 +	-.035 +	+.002 +	-.010 +	-.030 +
+2.10	-.050 +	-.080 +	-.065 +	-.005 +	-.050 +	-.015 +	-.015 +	+.010 +	-.027 +	-.020 +	-.020 +

Y/D

℄ of motor

MEASUREMENTS ON DEFLECTOR SURFACE
(- VALUE, EROSION; + VALUE, BUILDUP)

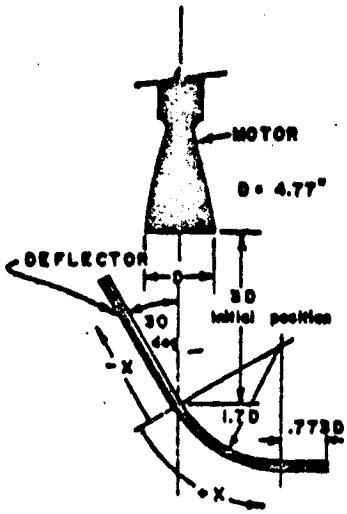

Table V-7 J Deflector Erosion, Run 13

DEFLECTOR COATING: Harbison - Walker Harcoat E.S.
LIFT-OFF RATE: 50 Do in 10 sec
GRAIN DATA:
% AL 22 ; $\dot{m}$ — lb/sec
P_c (nom) — psi

COMMENTS

1. POUNDS OF DEFLECTOR COATING MATERIAL ERODED = 1.88 lb
2. MAXIMUM EROSION DEPTH = 0.495 in.
3. LOCATION OF MAXIMUM EROSION $\frac{X}{D}$ = +0.63
   $\frac{Y}{D}$ = 0
4. COMPRESSIVE STRENGTH OF DEFLECTOR COATING = 6450 psi
5. Rocket Motor Malfunctioned

TOP OF DEFLECTOR

X/D	-1.47	-1.05	-0.63	-0.42	-0.21	0	+0.21	+0.42	+0.63	+1.05	+1.47
-2.10	+.055	+.007	+.040	+.035	+.020	+.040	+.015	+.030	+.035	-.005	-.050
-1.67	+.060	+.030	-.015	+.020	-.015	+.030	+.050	+.075	+.035	000	-.045
-1.25	+.012	+.005	-.035	-.030	-.030	+.015	+.090	+.070	+.015	-.015	-.045
-1.05	+.010	+.010	000	-.005	000	+.010	+.070	+.085	+.030	-.020	-.015
-0.84	+.010	+.010	+.010	-.005	-.010	+.005	+.010	+.065	+.045	+.025	-.020
-0.63	+.015	+.015	+.020	-.055	-.055	-.100	-.065	-.005	+.035	+.040	-.005
-0.42	-.005	+.020	-.005	-.025	-.145	-.215	-.155	-.045	+.025	+.065	+.035
-0.21	+.005	-.005	+.025	-.075	-.235	-.275	-.215	-.110	+.020	+.050	+.080
℄-0 of motor	+.075	+.075	+.070	-.040	-.120	-.160	-.115	-.065	+.100	+.150	+.200
+0.21	+.150	+.080	+.020	-.175	-.170	-.185	-.130	-.150	-.025	+.115	+.125
+0.42	+.055	-.010	-.110	-.300	-.340	-.310	-.300	-.305	-.225	+.090	+.155
+0.63	-.010	-.045	-.170	-.350	-.485	-.495	-.487	-.485	-.085	+.080	+.100
+0.84	-.010	-.020	-.065	-.140	-.270	-.220	-.230	-.135	-.115	+.085	+.085
+1.05	-.025	+.020	-.060	-.180	-.245	-.255	-.265	-.230	-.100	+.055	+.085
+1.25	-.030	-.040	-.115	-.155	-.325	-.305	-.360	-.245	-.190	-.030	+.035
+1.67	-.035	-.105	-.190	-.110	-.140	-.215	-.175	-.130	-.150	-.045	-.015
+2.10	+.040	-.040	-.050	+.010	-.075	-.120	-.105	-.100	-.040	-.010	+.040

℄ of motor

MEASUREMENTS ON DEFLECTOR SURFACE
(- VALUE, EROSION; + VALUE, BUILDUP)

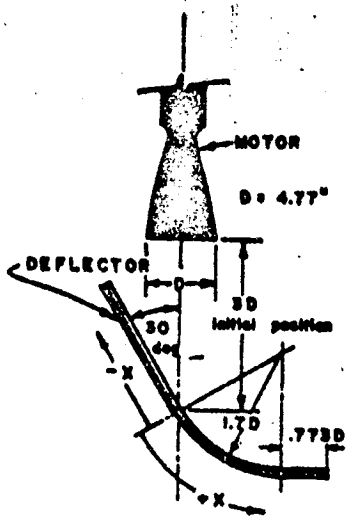

Table V-8 J Deflector Erosion, Run 14

DEFLECTOR COATING: Portland Cement Mix
LIFT-OFF RATE: 130 D in 10 sec
GRAIN DATA:
% AL 14 , $\dot{m}$ 8.2 lb/sec
P_c (nom) 582 psi

COMMENTS

1. POUNDS OF DEFLECTOR COATING MATERIAL ERODED = 3.25
2. MAXIMUM EROSION DEPTH = 0.607 in.
3. LOCATION OF MAXIMUM EROSION $\frac{X}{D}$ = +0.84
   $\frac{Y}{D}$ = +0.42
4. COMPRESSIVE STRENGTH OF DEFLECTOR COATING = 4060 psi
5. Rocket Motor Canted 6 Degrees in the +Y Direction.

TOP OF DEFLECTOR

X/D	-1.47	-1.05	-0.63	-0.42	-0.21	0	+0.21	+0.42	+0.63	+1.05	+1.47
-2.10	-.020 +	+.033 +	+.023 +	+.003 +	-.017 +	+.028 +	+.040 +	+.058 +	+.078 +	+.025 +	+.048 +
-1.67	+.013 +	+.033 +	+.028 +	+.020 +	+.008 +	+.008 +	+.048 +	+.023 +	+.071 +	+.032 +	+.028 +
-1.25	+.071 +	+.053 +	+.073 +	+.053 +	+.098 +	+.073 +	+.008 +	-.012 +	+.008 +	-.094 +	[illegible] +
-1.05	+.038 +	+.058 +	+.023 +	+.093 +	+.003 +	-.077 +	-.082 +	-.092 +	-.047 +	-.112 +	-.072 +
-0.84	+.043 +	+.068 +	+.043 +	+.080 +	+.008 +	-.162 +	-.192 +	-.077 +	-.142 +	-.147 +	-.097 +
-0.63	+.063 +	+.053 +	+.068 +	+.063 +	-.062 +	-.212 +	-.322 +	-.212 +	-.145 +	-.122 +	-.112 +
-0.42	+.88 +	+.061 +	+.063 +	+.042 +	-.152 +	-.327 +	-.377 +	-.294 +	-.252 +	-.135 +	-.107 +
-0.21	+.068 +	+.073 +	+.073 +	-.087 +	-.137 +	-.247 +	-.382 +	-.377 +	-.312 +	-.172 +	-.082 +
℄-0 of motor	+.113 +	+.058 +	+.138 +	-.002 +	-.075 +	-.080 +	-.322 +	-.239 +	-.207 +	-.099 +	+.013 +
+0.21	+.058 +	+.058 +	+.033 +	-.067 +	-.107 +	-.092 +	-.232 +	-.277 +	-.302 +	-.217 +	-.132 +
+0.42	+.068 +	+.053 +	-.142 +	-.255 +	-.172 +	-.182 +	-.162 +	-.267 +	-.277 +	-.275 +	+.098 +
+0.63	+.013 +	-.007 +	-.217 +	-.397 +	-.482 +	-.447 +	-.405 +	-.452 +	-.557 +	-.397 +	-.137 +
+0.84	-.007 +	+.033 +	-.047 +	-.302 +	-.477 +	-.579 +	-.582 +	-.607 +	-.590 +	-.442 +	-.322 +
+1.05	+.033 +	+.053 +	+.068 +	+.045 +	-.132 +	-.207 +	-.312 +	-.162 +	-.172 +	-.187 +	-.152 +
+1.25	-.002 +	+.033 +	-.028 +	-.017 +	-.022 +	-.069 +	-.137 +	-.132 +	-.182 +	-.252 +	-.217 +
+1.67	-.052 +	-.037 +	-.017 +	-.065 +	-.079 +	-.097 +	-.125 +	-.135 +	-.222 +	-.190 +	-.122 +
+2.10	-.072 +	-.062 +	-.027 +	+.008 +	+.043 +	+.003 +	-.032 +	-.022 +	-.007 +	-.074 +	-.087 +

Y/D

℄ of motor

MEASUREMENTS ON DEFLECTOR SURFACE
(- VALUE, EROSION; + VALUE, BUILDUP)

VI. LIFTOFF ACCELERATION EFFECTS (GROUP III)

A. GROUP III TECHNICAL OBJECTIVES

During the previous SPREE test program it became evident that liftoff acceleration has a profound effect on deflector erosion, but the effect was not evaluated. Objective of the Group III tests was to evaluate liftoff acceleration effects, quantitatively. Accelerations corresponding to 15, 25, 35, and 100 D_e in 10 sec were investigated using motors having 18% aluminum and Fondu Fyre WA-1 deflectors. Run 10 (a Group II test) was made at a 50 D_e in 10 sec liftoff rate and compliments the four Group III runs.

B. MEANING OF ACCELERATION RATE TERMINOLOGY

All Group III tests were made with an initial nozzle-to-deflector separation distance of 3 D_e and a simulated 200 millisec holddown. After the holddown, the cart was accelerated at a constant value so that 10 sec after motor ignition the nozzle-to-deflector separation distance was one of the values specified in the run schedule (Table I-1). Accelerations were calculated on the basis of the cart moving 12,22, 32, 47, and 97 D_e in 9.8 sec.

Acceleration is not constant during missile liftoff (it increases as propellant is burned); however, it is nearly constant. Curves accounting for propellant consumption were derived and are termed desired acceleration curves in this document. Cart motion has been programed to provide a best match to these time-distance curves considering swing arm limitations and the desirability of matching the curve at close-in distances. Curves considered a best match are termed expected curves. Desired and expected curves are compared in Fig. III-2 while expected and actual curves are compared in Fig. III-3.

There has been much confusion relative to the meaning of an acceleration corresponding to a given number of nozzle diameters separation in 10 sec. Figure VI-1 was prepared to eliminate this confusion and provide a tie-in between the terminology and liftoff thrust-to-weight ratio. Thrust-to-weight ratio, of course, corresponds to what an accelerometer measuring missile longitudinal acceleration would read during vertical ascent. Figure VI-1 shows that the simulated Group III liftoff rates encompass the rates that would be expected to give full-scale deflector erosion problems.

C. TEST ARTICLES

The test articles used for Group III tests were similar to those used during Group II tests. Included were four Fondu Fyre WA-1 deflectors and 15 instrumented test panels. Six of the panels were evaluated on Run 16 and three panels each on Runs 18, 19, and 20. Identical test panel coating materials (three materials) were used on each run to allow evaluation of acceleration effects.

Because of the low acceleration rates evaluated during three of the four runs, it was necessary to use long burning rocket motors. Three motors with 24-sec burn times were used for Runs 18, 19, and 20 to ensure that no motor would burn out while erosion was taking place on the deflectors and test panels.

D. TEST PROCEDURE

The procedure used for Group III tests was similar to that used during Group II tests. Because cart acceleration was varied during each run, prefiring calibrations were made to ensure that cart travel corresponded to the expected time-distance curves. Some difficulty was experienced with the calibrations because of lack of thrust loads on the deflectors. Actual time-distance curves during the firings were in excellent agreement with the expected curves.

One additional bit of information was obtained on the coated panels during this test series. This was panel thickness loss as determined from before- and after-firing panel thickness measurements. The measurements were made by drilling a hole in the coating material and measuring coating thickness with a wire.

E. RESULTS

1. Liftoff Acceleration Effects on Deflector Erosion

Firings 10, 16, 18, 19, and 20 were made to evaluate missile liftoff acceleration effects on erosion. Test results portraying the important acceleration influence are presented in Fig. VI-2 and VI-3 and Tables VI-1 thru VI-4. Data from the firings were also used to determine whether erosion information from one firing could be used to predict the information obtained from the other firings. If this could be done, an insight into the major cause of erosion would be gained; i.e., whether it is caused primarily by thermal or mechanical effects.

Previous SPREE work (Ref 1) has indicated that approximately 90% of deflector erosion is due to thermal effects. Therefore, for this study, only thermal effects were considered in seeking the data correlations. This decision simplified computations; if thermal effects were predominant, the correlations would be satisfactory. Since thermal effects are proportional to dwell time in the plume environment, it was necessary to define the environment with sufficient accuracy to allow computation of heat transfer rates at various distances downstream from the nozzle exit plane. Work at Martin (Ref 2) has indicated that heat transfer coefficient is proportional to $(P_t\ U/\ T_t)^{0.8}$, where P_t = total pressure, U = axial velocity, and T_t = total temperature of the exhaust plume gases. The plume profile used to determine the heat transfer coefficients was assembled from pressure and temperature data from SPREE rake probes (Firings 23 thru 25) together with velocity data from a United Technology Corporation 120-in. solid motor plume profile. The reference heat transfer coefficient was taken as 0.110 Btu/ft^2-sec-°R as determined during SPREE Phase II, Part I work (Ref 1). The heat transfer coefficient was assumed constant at 0.110 from the nozzle exit plane to a point five nozzle exit diameters downstream from the exit plane. Heat transfer coefficients aft of this point were then computed from plume profile and reference heat transfer coefficient data. The coefficients obtained are presented in Fig. VI-4.

Plume centerline heat transfer rates were then computed for various positions downstream from the nozzle exit plane assuming a 1000°F impingement surface temperature.

$$\dot{q}_x/D_e = h_x/D_e \left(T_x/D_e - T_w\right); \text{ where, } T_w = 1000°F.$$

Total heat incident on a deflector unit area was obtained by graphically integrating $\dot{q}$ dt for the appropriate acceleration history. The data were then correlated using firing 10 data as reference. The liftoff acceleration for this firing was 50 nozzle diameters in 10 sec. No erosion was considered to occur at separation distances in excess of 50 nozzle diameters.

Since it was assumed that all erosion would be considered as being due to thermal effects, the deflector weight loss and maximum erosion depth should be proportional to the total integrated heat load. Figure VI-5 presents a comparison of total heat load ratio vs deflector weight loss ratio. Notice that there is almost a direct relationship between the two parameters.

Maximum erosion depth also appears to be approximately directly proportional to the total heat incident on the deflectors. Correlation of maximum erosion depth ratios with total heat ratios is presented in Fig. VI-6. The correlation is good except for firing 18, where the liftoff rate was 35 nozzle diameters in 10 sec. Examination of the erosion data (Table VI-2) shows that the 0.93-in. maximum erosion for this firing was considerably more than shown in surrounding areas. The possibility exists that there was localized erosion not representative of the true condition. Using erosion data at the corresponding position across the deflector centerline improves the correlation.

From the data presented in Fig. VI-5 and VI-6, it is felt that if test or prototype deflector erosion data are available for one vehicle liftoff rate, the data can be extrapolated to other liftoff rates, if the exhaust plume profiles are known and if a reference heat transfer coefficient is used.

2. Liftoff Acceleration Effects on Coated Panels

The thickness of protective coating required on an umbilical mast is a function of the coating properties, the distance of the mast from the rocket motor, the slope of the mast surface, the geometry and characteristics of the rocket motor, missile liftoff thrust-to-weight ratio, missile drift, and thrust vectoring during ascent. The task of defining the incremental effects attributable to each of these factors for a large number of candidate coatings was beyond the scope of the SPREE investigation. Gross effects involving several of the more important factors, including liftoff acceleration, were evaluated for two promising coatings. The coatings were Martyte and Dynatherm E-300.

Martyte is a light weight refractory ceramic that combines the properties of plastics and ceramics. It is mixed at the sight where it is applied like plaster to verifical surfaces. It can be pressure-sprayed. Martyte is manufactured and sold by Presstite Division of Interchemical Corporation under license from Martin Company, Orlando Division. Dynatherm E-300 is manufactured by the Dynatherm Chemical Corporation and is similar to Martyte in terms of consistency, applicability, hardness, density, adhesion characteristics, thermal conductivity, etc.

Figure VI-7 was compiled from data obtained during Runs 16, 18, 19, 20, 21, and 22 and shows the reduction in thickness of umbilical mast coating material (Martyte WN-3 and Dynatherm E-300) that can be expected during launch for a typically situated umbilical mast. The Martyte WN-3 coating is a modified version of the Martyte used on the Titan IIIC transporter-launcher. The modification, made to improve applicability, traded off some of the protective qualities of Martyte to attain this. For results of tests involving other Martyte formulations and protective coatings, refer to Chapter X.

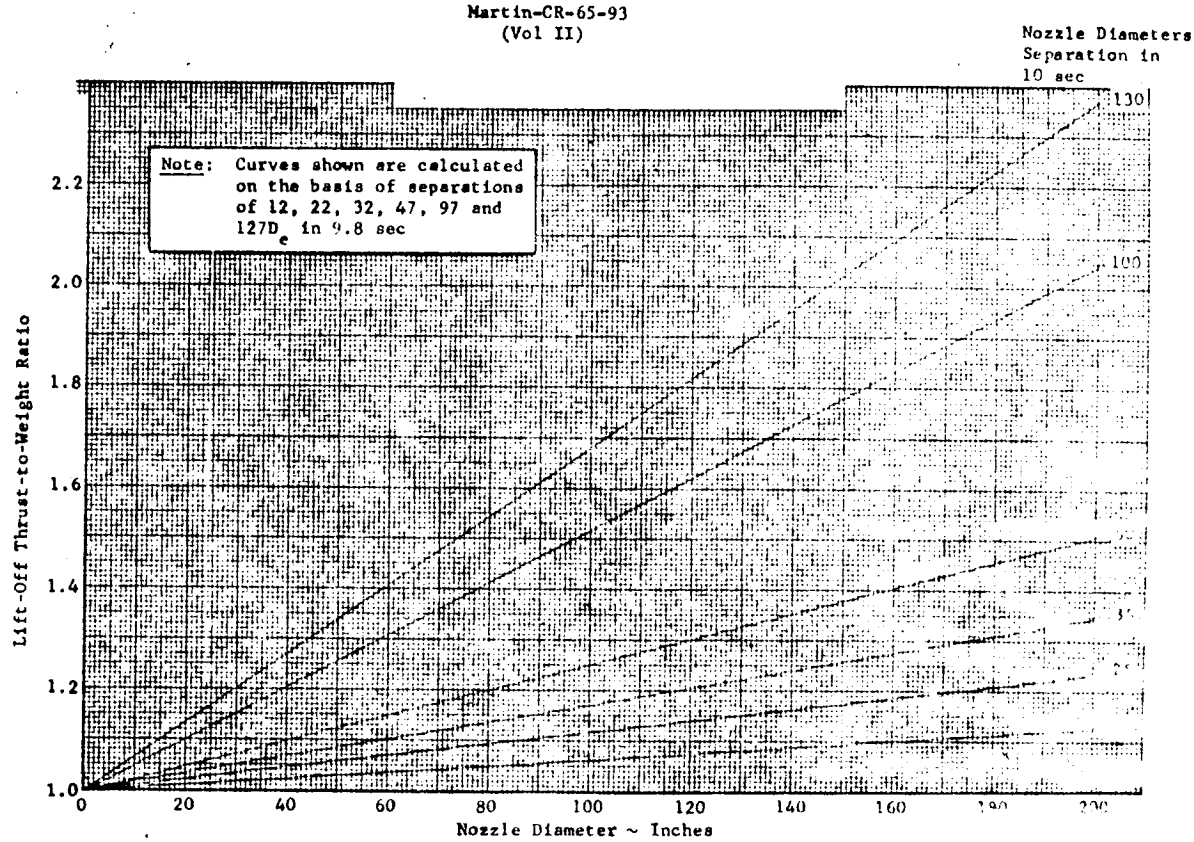

Fig. VI-1 Relationship between Liftoff Thrust-to-Weight Ratio and Nozzle Diameters Separation in 10 sec

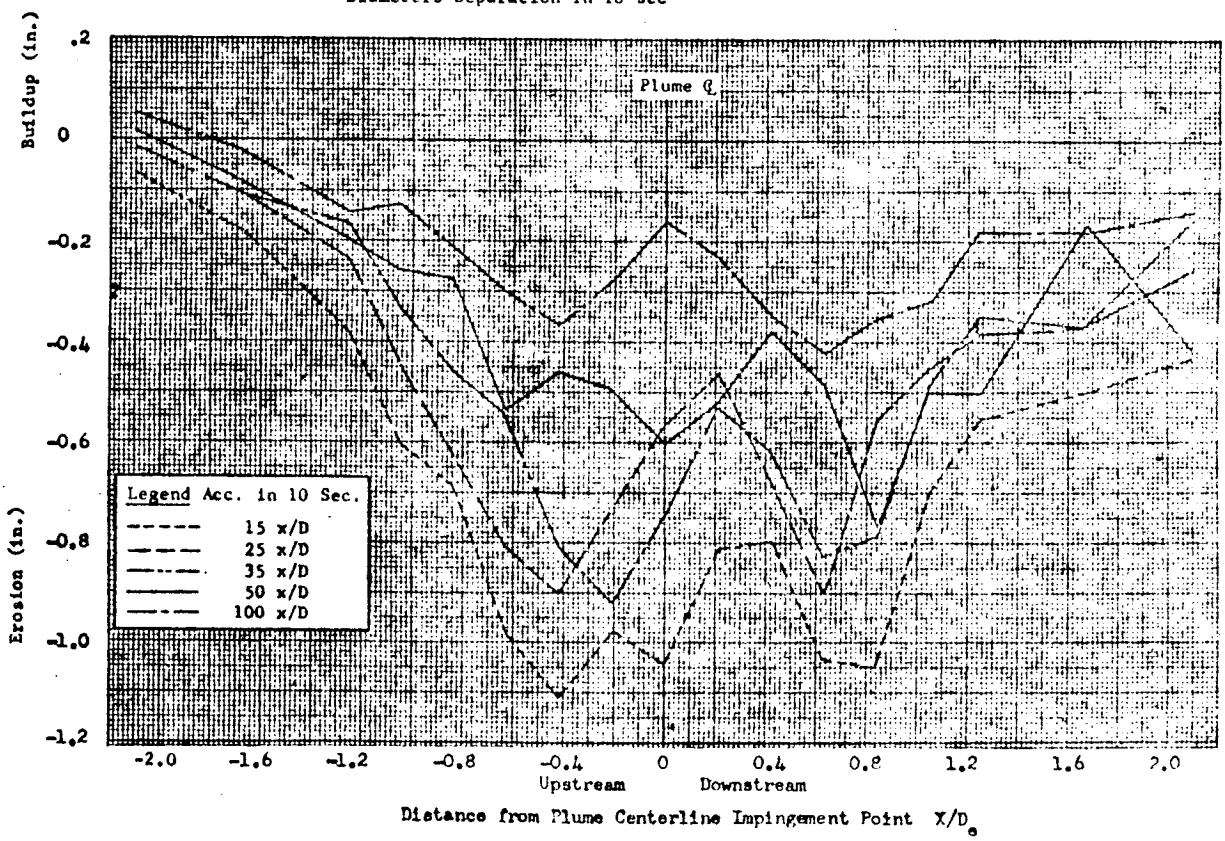

Fig. VI-2 Effect of Liftoff Acceleration on Deflector Centerline Erosion

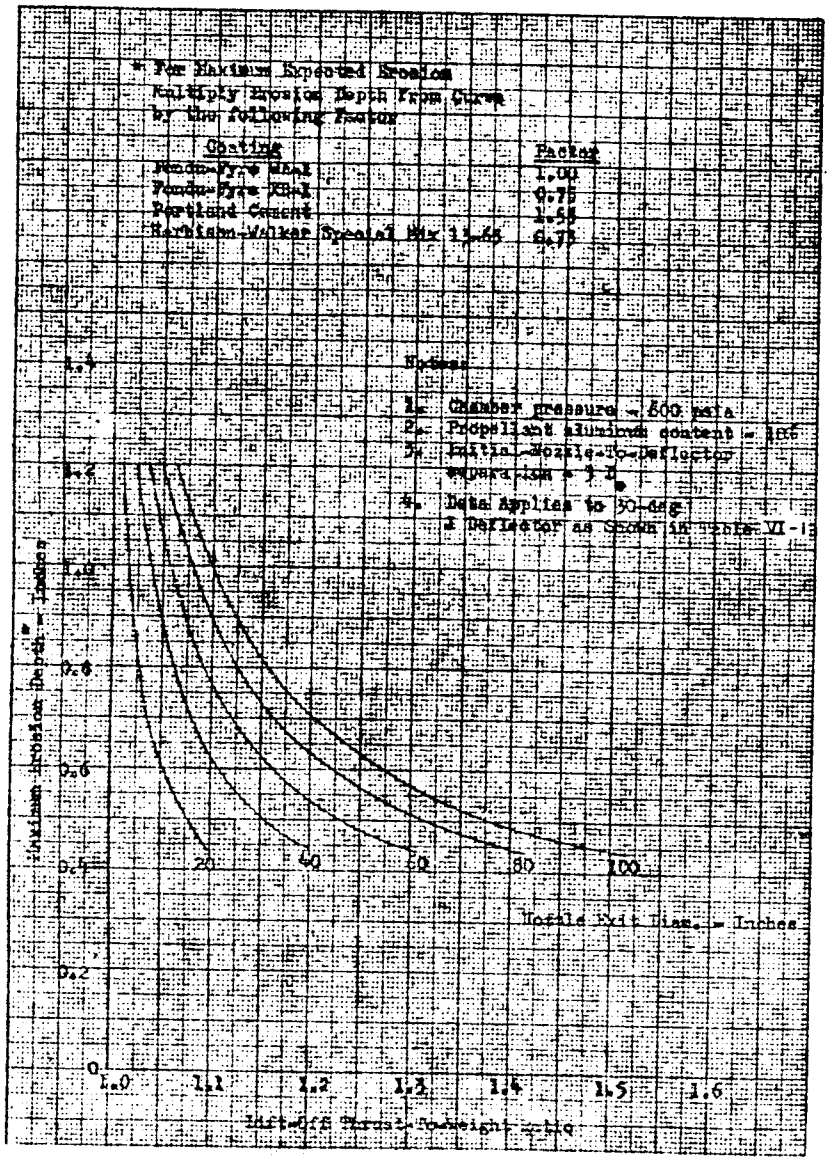

Fig. VI-3 Effect of Liftoff Thrust-to Weight Ratio on Erosion of Several Deflector Coating Materials

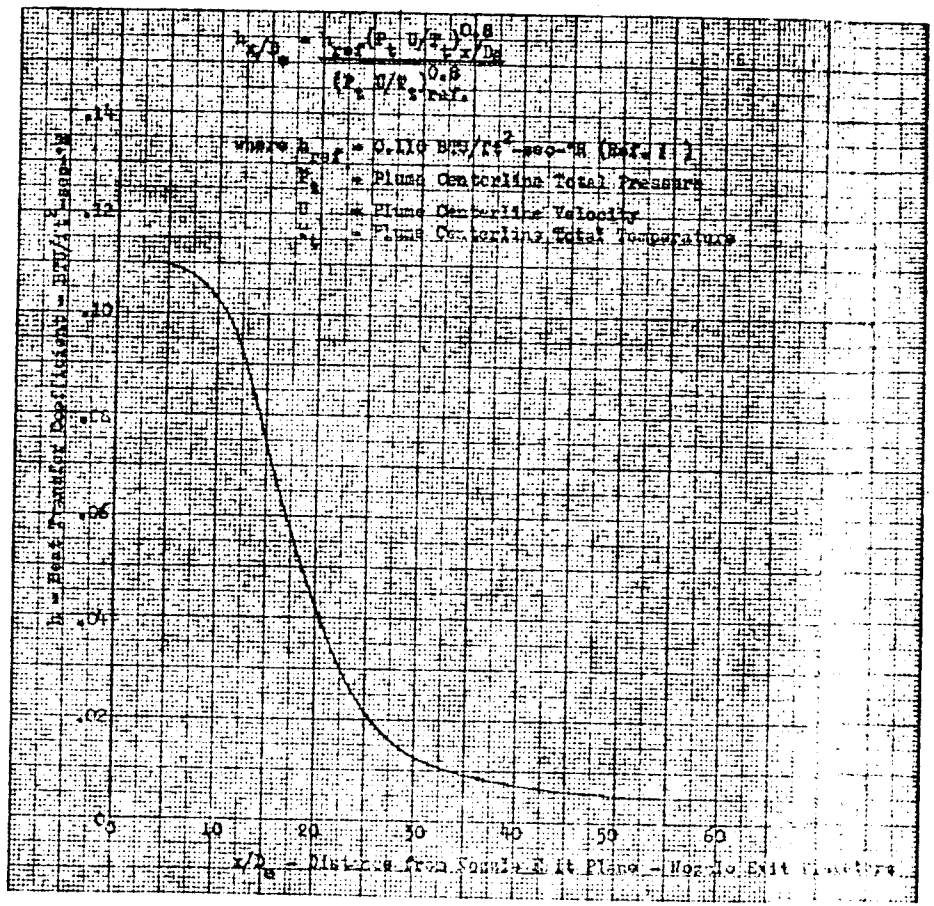

Fig. VI-4 Variation of Exhaust Plume Centerline Heat Transfer Coefficient with Distance from Nozzle Exit

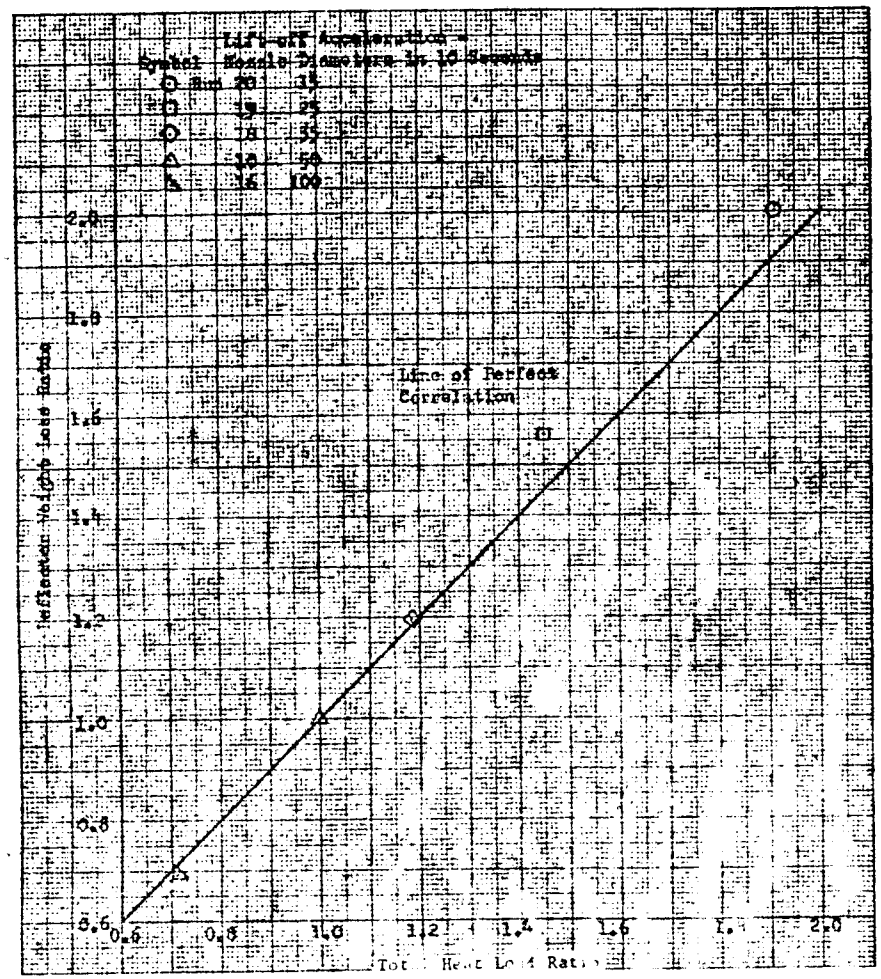

Fig. VI-5 Correlation of Heat and Weight Loss Ratios

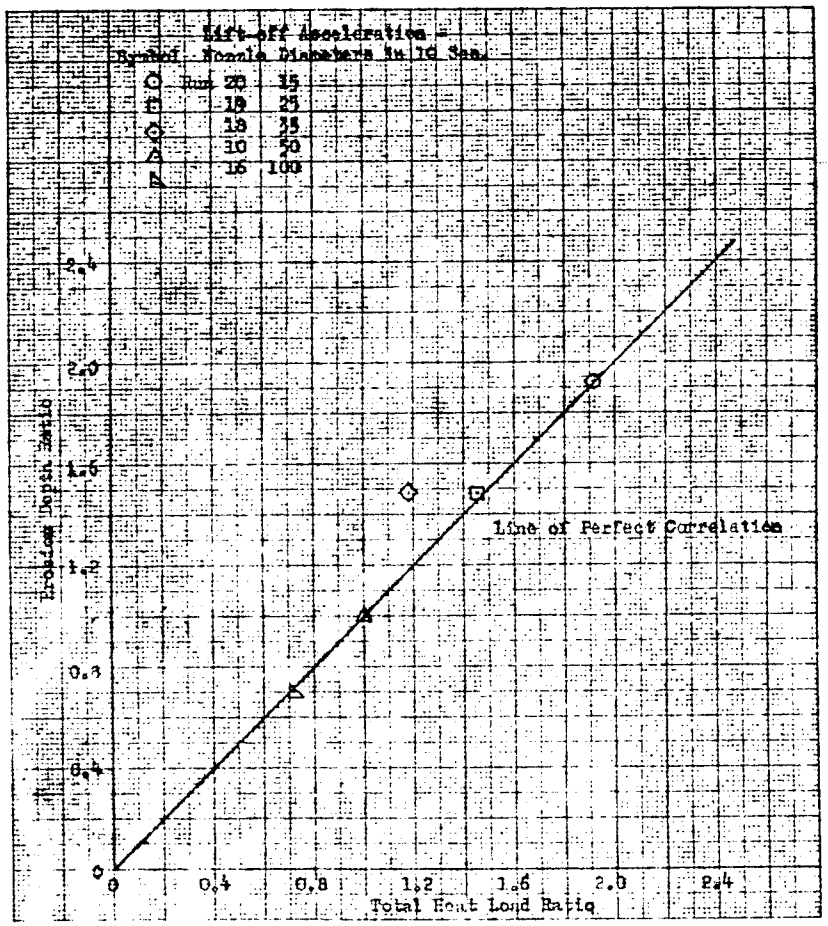

Fig. VI-6 Correlation of Maximum Erosion Depth and Total Heat Ratios

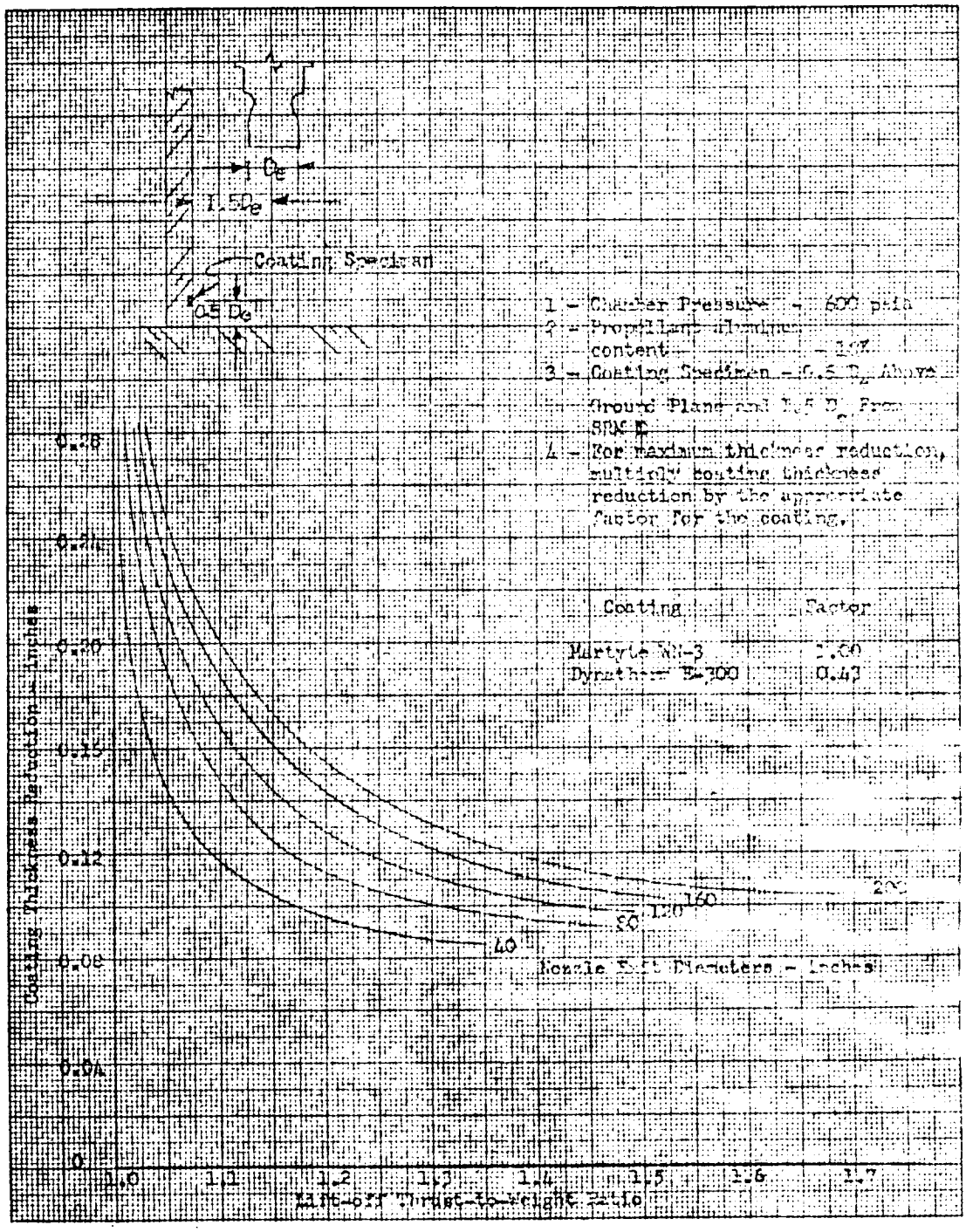

Fig. VI-7 Thickness Reduction of Two Umbilical Mast Protective Coatings during Simulated Liftoff

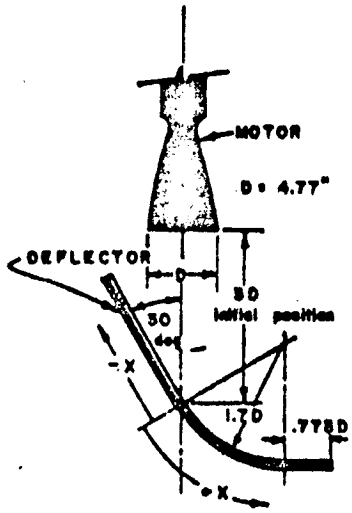

Table VI-1 J Deflector Erosion, Run 16

DEFLECTOR COATING: Fondu Fyre WA-1
LIFT-OFF RATE: 100 lb in 10 sec
GRAIN DATA:
% AL 18 ; $\dot{m}$ 8.0 lb/sec
P_c (nom) 583 psi

COMMENTS

1. POUNDS OF DEFLECTOR COATING MATERIAL ERODED = 4.00
2. MAXIMUM EROSION DEPTH = 0.440 in.
3. LOCATION OF MAXIMUM EROSION $\frac{X}{D}$ = +0.63
   $\frac{Y}{D}$ = -0.21
4. COMPRESSIVE STRENGTH OF DEFLECTOR COATING = 3420 psi

TOP OF DEFLECTOR

X/D	-1.47	-1.05	-0.63	-0.42	-0.21	0	+0.21	+0.42	+0.63	+1.05	+1.47
-2.10	+.015	+.045	+.060	+.045	+.015	+.057	+.035	+.035	+.015	-.010	000
-1.67	+.010	+.030	-.005	-.015	-.035	-.020	-.040	-.015	+.035	+.025	[illegible]
-1.25	+.050	+.075	-.025	-.080	-.065	-.143	-.090	-.075	-.060	+.075	+.015
-1.05	+.070	+.070	-.025	-.010	-.090	-.125	-.105	-.040	-.040	+.080	+.025
-0.84	+.095	+.070	-.005	-.080	-.226	-.215	-.195	-.095	-.053	+.070	+.030
-0.63	+.100	+.060	-.035	-.220	-.295	-.305	-.270	-.155	-.050	+.080	+.100
-0.42	+.100	+.050	-.060	-.235	-.340	-.365	-.330	-.275	-.135	+.090	+.105
-0.21	+.105	+.060	-.085	-.210	-.300	-.275	-.295	-.260	-.140	+.055	+.115
℄-0 of motor	+.155	+.150	+.035	-.155	-.150	-.160	-.115	-.185	-.030	+.160	[illegible]
+0.21	+.909	+.180	-.155	-.260	-.270	-.235	-.230	-.280	-.180	[illegible]	[illegible]
+0.42	+.040	+.015	-.300	-.415	-.410	-.345	-.400	-.390	-.320	-.045	+.095
+0.63	-.035	-.060	-.150	-.330	-.440	-.420	-.405	-.360	-.165	-.070	+.035
+0.84	+.015	-.065	-.130	-.215	-.365	-.355	-.375	-.300	-.160	-.070	+.020
+1.05	.000	-.075	-.150	-.202	-.305	-.315	-.300	-.245	-.160	-.105	+.025
+1.25	-.025	-.080	-.150	-.160	-.185	-.175	-.155	-.155	-.160	-.090	+.010
+1.67	-.030	-.085	-.130	-.185	-.220	-.180	-.170	-.150	-.150	-.085	-.050
+2.10	-.015	-.090	-.100	-.095	-.120	-.140	-.130	-.135	-.150	-.140	-.085

℄ of motor

MEASUREMENTS ON DEFLECTOR SURFACE
(- VALUE, EROSION; + VALUE, BUILDUP)

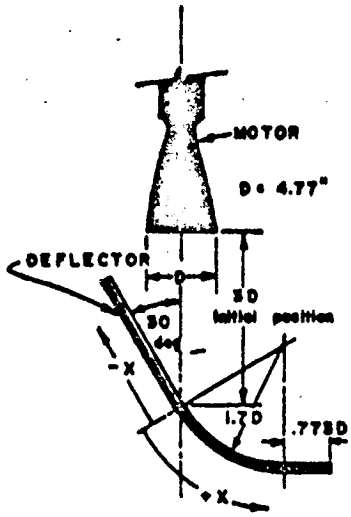

Table VI-2 J Deflector Erosion, Run 18

DEFLECTOR COATING: Fondu-Fyre WA-1
LIFT-OFF RATE: 35 Da in 10 sec
GRAIN DATA:
% AL 18, $\dot{m}$ 8.3 lb/sec
P_c (nom) 590 psi

COMMENTS

1. POUNDS OF DEFLECTOR COATING MATERIAL ERODED = 6.88
2. MAXIMUM EROSION DEPTH = 0.930 in.
3. LOCATION OF MAXIMUM EROSION $\frac{X}{D}$ = +0.63, $\frac{Y}{D}$ = +0.42
4. COMPRESSIVE STRENGTH OF DEFLECTOR COATING = 5600 psi

TOP OF DEFLECTOR

X/D	-1.47	-1.05	-0.63	-0.42	-0.21	0	+0.21	+0.42	+0.63	+1.05	+1.47
-2.10	+.070	-.020	-.045	-.050	-.065	-.015	+.035	+.040	+.055	+.060	+.055
-1.67	+.065	-.045	-.100	-.145	-.135	-.105	+.040	+.035	+.060	+.025	-.005
-1.25	+.135	-.030	-.125	-.200	-.195	-.165	-.070	-.015	+.030	+.035	+.025
-1.05	+.150	+.115	-.120	-.150	-.315	-.335	-.175	-.075	-.010	-.030	+.070
-0.84	+.150	+.080	-.130	-.195	-.380	-.457	-.390	-.185	-.035	000	+.080
-0.63	+.160	+.030	-.105	-.290	-.488	-.545	-.525	-.275	-.100	-.025	+.135
-0.42	+.175	+.110	-.095	-.350	-.670	-.810	-.785	-.550	-.195	-.010	+.010
-0.21	+.155	+.100	-.125	-.485	-.845	-.920	-.915	-.600	-.290	000	+.165
℄-0 of motor	+.225	+.105	-.135	-.585	-.745	-.740	-.565	-.600	-.255	+.000	+.095
+0.21	+.005	+.085	-.270	-.580	-.650	-.513	-.585	-.675	-.440	+.025	+.015
+0.42	-.065	-.140	-.410	-.720	-.740	-.630	-.685	-.780	-.605	-.050	+.100
+0.63	-.145	-.200	-.510	-.865	-.895	-.825	-.865	-.930	-.585	-.075	+.010
+0.84	-.120	-.235	-.355	-.570	-.780	-.785	-.780	-.550	-.290	-.060	000
+1.05	-.110	-.260	-.290	-.330	-.400	-.480	-.525	-.235	-.220	-.090	+.015
+1.25	-.100	-.250	-.250	-.310	-.320	-.345	-.375	-.380	-.245	-.075	+.010
+1.67	-.205	-.260	-.320	-.385	-.435	-.370	-.385	-.360	-.355	-.105	-.075
+2.10	-.235	-.330	-.275	-.285	-.275	-.255	-.275	-.290	-.245	-.205	-.115

℄ of motor

MEASUREMENTS ON DEFLECTOR SURFACE
(- VALUE, EROSION; + VALUE, BUILDUP)

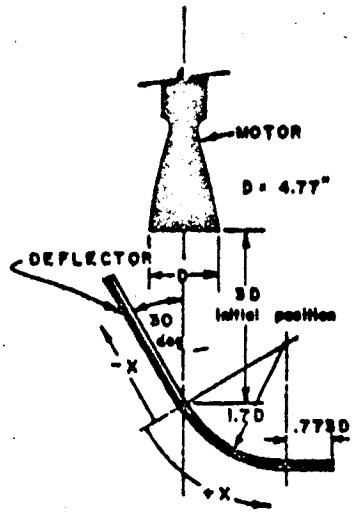

Table VI-3 J Deflector Erosion, Run 19

DEFLECTOR COATING: Fondu-Fyre WA-1
LIFT-OFF RATE: 25 De in 10 sec
GRAIN DATA:
% AL 18 ; $\dot{m}$ 7.87 lb/sec
P_c (nom) 532 psi

TOP OF DEFLECTOR

X/D	-1.47	-1.05	-0.63	-0.42	-0.21	0	+0.21	+0.42	+0.63	+1.05	+1.47
-2.10	-.025 +	+.005 +	-.005 +	-.040 +	-.030 +	-.005 +	-.022 +	+.005 +	-.005 +	-.015 +	+.015 +
-1.67	+.035 +	-.035 +	-.035 +	-.067 +	-.095 +	-.105 +	-.125 +	-.075 +	-.030 +	+.007 +	+.030 +
-1.25	-.010 +	+.040 +	-.075 +	-.190 +	-.235 +	-.225 +	-.290 +	-.205 +	-.093 +	+.005 +	-.057 +
-1.05	+.005 +	-.030 +	-.100 +	-.230 +	-.380 +	-.440 +	-.370 +	-.193 +	-.130 +	-.007 +	-.025 +
-0.84	+.010 +	-.040 +	-.170 +	-.270 +	-.555 +	-.617 +	-.615 +	-.215 +	-.130 +	-.035 +	-.020 +
-0.63	-.005 +	-.025 +	-.125 +	-.420 +	-.700 +	-.810 +	-.755 +	-.410 +	-.175 +	-.015 +	-.035 +
-0.42	+.010 +	-.060 +	-.195 +	-.490 +	-.785 +	-.900 +	-.850 +	-.495 +	-.275 +	-.020 +	-.005 +
-0.21	.000 +	-.050 +	-.125 +	-.510 +	-.845 +	-.735 +	-.810 +	-.570 +	-.185 +	+.110 +	-.015 +
℄ of meter 0	+.015 +	+.020 +	-.200 +	-.710 +	-.640 +	-.555 +	-.600 +	-.645 +	-.290 +	+.085 +	-.045 +
+0.21	+.015 +	-.075 +	-.305 +	-.710 +	-.660 +	-.455 +	-.600 +	-.725 +	-.415 +	-.035 +	-.015 +
+0.42	+.005 +	-.130 +	-.520 +	-.920 +	-.790 +	-.685 +	-.755 +	-.895 +	-.510 +	-.095 +	-.045 +
+0.63	-.100 +	-.180 +	-.315 +	-.665 +	-.930 +	-.900 +	-.925 +	-.665 +	-.340 +	-.110 +	+.045 +
+0.84	-.050 +	-.175 +	-.185 +	-.280 +	-.320 +	-.550 +	-.505 +	-.290 +	-.190 +	-.130 +	-.030 +
+1.05	-.060 +	-.195 +	-.215 +	-.275 +	-.220 +	-.445 +	-.375 +	-.310 +	-.240 +	-.185 +	-.030 +
+1.25	-.060 +	-.205 +	-.230 +	-.285 +	-.290 +	-.380 +	-.392 +	-.300 +	-.270 +	-.215 +	-.100 +
+1.67	-.120 +	-.120 +	-.260 +	-.270 +	-.340 +	-.365 +	-.280 +	-.355 +	-.330 +	-.210 +	-.155 +
+2.10	-.085 +	-.128 +	-.135 +	-.115 +	-.130 +	-.150 +	-.165 +	-.195 +	-.150 +	-.195 +	-.210 +

℄ of meter

MEASUREMENTS ON DEFLECTOR SURFACE:
(- VALUE, EROSION; + VALUE, BUILDUP)

COMMENTS

1. POUNDS OF DEFLECTOR COATING MATERIAL ERODED = 9.00
2. MAXIMUM EROSION DEPTH = .930 in.
3. LOCATION OF MAXIMUM EROSION $\frac{X}{D}$ = +0.63
   $\frac{Y}{D}$ = -0.21
4. COMPRESSIVE STRENGTH OF DEFLECTOR COATING = 7050 psi
5. Hold-down excessive (0.69 sec)
6. Deflector was wet before this firing.

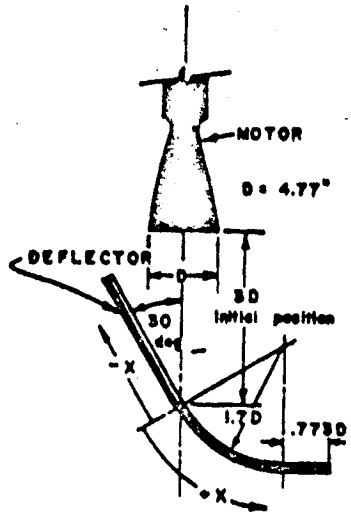

Table VI-4 J Deflector Erosion, Run 20

DEFLECTOR COATING: Fondu-Fyre WA-1
LIFT-OFF RATE: 15 D in 10 sec
GRAIN DATA:
% AL 18, $\dot{m}$ 8.05 lb/sec
P_c (nom) 537 psi

TOP OF DEFLECTOR

X/D											
-2.10	-.014 +	-.025 +	-.129 +	-.065 +	-.063 +	-.065 +	-.075 +	-.075 +	-.062 +	-.006 +	-.011 +
-1.67	+.051 +	-.084 +	-.153 +	-.102 +	-.150 +	-.183 +	-.165 +	-.218 +	-.112 +	-.090 +	-.008 +
-1.25	+.040 +	-.037 +	-.150 +	-.244 +	-.344 +	-.384 +	-.339 +	-.206 +	-.170 +	-.087 +	+.026 +
-1.05	+.048 +	+.085 +	-.173 +	-.312 +	-.546 +	-.605 +	-.504 +	-.351 +	-.237 +	-.055 +	+.118 +
-0.84	+.065 +	-.050 +	-.201 +	-.390 +	-.660 +	-.687 +	-.644 +	-.390 +	-.273 +	-.047 +	+.070 +
-0.63	+.115 +	-.090 +	-.170 +	-.460 +	-.820 +	-.988 +	-.860 +	-.560 +	-.223 +	-.059 +	-.198 +
-0.42	+.090 +	+.075 +	-.270 +	-.540 +	-.955 +	-1.111 +	-.950 +	-.690 +	-.350 +	-.050 +	+.215 +
-0.21	+.165 +	+.245 +	-.235 +	-.695 +	-1.110 +	-.975 +	-1.110 +	-.755 +	-.320 +	+.065 +	+.0[illegible] +
℄-0 of meter	-.120 +	-.055 +	-.365 +	-.920 +	-1.025 +	-1.040 +	-1.035 +	-.890 +	-.300 +	+.055 +	+.[illegible] +
+0.21	+.155 +	-.075 +	-.535 +	-.970 +	-.880 +	-.810 +	-.840 +	-1.005 +	-.545 +	-.100 +	+.[illegible] +
+0.42	+.205 +	-.050 +	-.595 +	-1.065 +	-.950 +	-.795 +	-.895 +	-1.065 +	-.615 +	-.100 +	-.095 +
+0.63	+.075 +	-.140 +	-.695 +	-1.205 +	-1.095 +	-1.035 +	-1.100 +	-1.205 +	-.735 +	-.155 +	-.030 +
+0.84	-.105 +	-.205 +	-.450 +	-.700 +	-.985 +	-1.050 +	-1.010 +	-.845 +	-.500 +	-.245 +	-.115 +
+1.05	-.180 +	-.290 +	-.310 +	-.445 +	-.655 +	-.695 +	-.715 +	-.585 +	-.395 +	-.240 +	-.090 +
+1.25	-.180 +	-.360 +	-.365 +	-.450 +	-.490 +	-.550 +	-.560 +	-.560 +	-.455 +	-.345 +	-.165 +
+1.67	-.280 +	-.335 +	-.445 +	-.535 +	-.495 +	-.500 +	-.560 +	-.575 +	-.480 +	-.285 +	-.275 +
+2.10	-.290 +	-.300 +	-.390 +	-.415 +	-.430 +	-.460 +	-.475 +	-.345 +	-.345 +	-.360 +	-.360 +
Y/D	-1.47	-1.05	-0.63	-0.42	-0.21	0	+0.21	+0.42	+0.63	+1.05	+1.47

℄ of motor

MEASUREMENTS ON DEFLECTOR SURFACE
(- VALUE, EROSION, + VALUE, BUILDUP)

COMMENTS

1. POUNDS OF DEFLECTOR COATING MATERIAL ERODED = 11.50
2. MAXIMUM EROSION DEPTH = 1.205 in.
3. LOCATION OF MAXIMUM EROSION $\frac{X}{D}$ = +0.63
   $\frac{Y}{D}$ = +0.42
4. COMPRESSIVE STRENGTH OF DEFLECTOR COATING = 9560 psi
5. Hold-down excessive (0.60 sec)

VII. SPECIAL EVALUATIONS (GROUP IV)

A. GROUP IV TECHNICAL OBJECTIVES

The Group IV tests were conceived to provide data to supplement information obtained during the other groups of firings and make the test program findings more meaningful. Each run had its own unique objectives as follows.

Run 15 - Solid rocket motors are widely used in the strap-on configuration. Strap-ons usually have canted nozzles that point the motor thrust vector toward the missile center of gravity at booster burnout to minimize stability problems associated with unsymmetrical thrust decays. During liftoff the flame from a canted nozzle sweeps across a flame deflector rather than dwelling on a single area. A considerable erosion difference due to cant would be expected unless erosion occurs predominately during the very early stages of liftoff. Run 15 was made to evaluate the effect of cant on erosion and to provide a factor for converting maximum erosion data obtained with straight nozzles to the canted nozzle situation. A 6-deg cant was used and the nozzle centerline passed through the target on the deflector at the 3 D_e initial nozzle-to-deflector separation distance.

Run 17 - An evaluation of Fondu Fyre WA-1 or any candidate deflector coating material would not be complete without first checking for the effects of multiple firings on a deflector. A Portland cement concrete, for instance, is seriously weakened after exposure to high temperature gases due to dehydration and a resulting cement bond deterioration. A second firing on this type coating would be expected to produce more erosion than the initial firing. The objective of Run 17 was to fire a second time on the Fondu Fyre WA-1 deflector used during Run 10. Both firings were made at a separation rate of 50 D_e in 10 sec using rocket motor grains containing 18% aluminum.

Run 21 - Harbison-Walker Refractories Company recently introduced a new refractory castable mix especially designed for launch pad applications. This mix is referred to as H-W Special Mix 13-65 Fused Silica Castable. The purpose of Run 21 was to evaluate this material and compare its performance with Fondu Fyre WA-1.

Run 22 - An important attribute of a deflector coating is the ease with which it can be refurbished. During Run 6 of the Group I tests a Fondu Fyre WA-1 deflector was simply refurbished by packing a wet mix into the area to be refurbished. The results were satisfactory. During Run 22, the suitability of another refurbishment technique (that recommended by the manufacturer of Fondu Fyre) was investigated. This technique involves the spreading of an epoxy over the area to be refurbished before packing in the wet Fondu Fyre mix.

B. TEST ARTICLES

Four deflectors and 15 test panels coated with six different materials were evaluated during Group IV tests. The deflector coated with Harbison-Walker Special Mix 13-65 was poured and cured in much the same way as Fondu Fyre WA-1 deflectors. The first 3 days of cure were in an environmental chamber at humidities near 100% and temperatures from 95 to 100°F. The deflector used during Runs 10 and 17, and refurbished for Run 22, was refurbished using an epoxy with constitutents in the following proportion:

75 cc of Epon 828 (Shell Chemical Co)

80 cc of Versamid 140 (General Mills)

15 cc of phenol glycidyl ether (PGE)(Shell Chemical Co)

400 gm Fondu Fyre WA-1.

Refurbishment involved:

1) Wire brushing the deflector to remove loose scale;

2) Spreading the epoxy over the area to be refurbished and allowing the epoxy to set up over night;

3) Filling in with Fondu Fyre WA-1 mixed with 16% water (by weight).

The refurbished deflector was covered with a felt pad that was wet down periodically for a week. The cure was at room temperature. After curing, the deflector was smoothed with a carborundum wheel.

C. TEST PROCEDURE

The procedure used for Group IV tests was similar to that used for Group II and Group III tests.

D. TEST RESULTS

1. Effect of Nozzle Cant

The effect of a 6-deg nozzle cant on erosion is shown in Fig. VII-1 and Tables V-4 and VII-1. Note that the ratio of the average centerline erosion with cant to that without cant is approximately 0.88 whereas the maximum erosion with cant is greater than that without cant. The comparison of Runs 8 and 14 (Fig. V-7) for effects of cant, shows that maximum erosion with cant is about 61% of the maximum erosion without cant (ignoring aluminum content effects). Holddown times for each of the firings is as follows:

$$\begin{cases} \text{Run 15 (with cant)} = 0.92 \text{ sec} \\ \text{Run 10 (without cant)} = 0.20 \text{ sec} \end{cases}$$

$$\begin{cases} \text{Run 14 (with cant)} = 0.40 \text{ sec} \\ \text{Run 8 (without cant)} = 0.60 \text{ sec.} \end{cases}$$

Note the excessive holddown for Run 15.

From Run 1 we see that a maximum of 0.635 in. of Fondu Fyre WA-1 is eroded during a 4.2-sec motor firing at a constant 3-nozzle exit diameter standoff distance. This represents approximately 0.151 in. of erosion per second. Correcting Run 15 data for the 0.72-sec holddown excess we get a maximum erosion of 0.690 - 0.151 x 0.72 or 0.581 in., which is 92% of the maximum erosion without cant. Making similar corrections for holddown excesses for the Portland cement deflectors we find that maximum erosion with cant is 63% of the maximum erosion without cant. Considering the lower rocket motor chamber pressure attained during Run 14 this figure can be raised to about 67%.

Disparities between the two sets of runs to evaluate the effect of cant cannot be explained. Thus, it can be concluded only that a 6-deg motor cant reduces maximum erosion by 8 to 33%.

2. Effect of Multiple Firings

Figure VII-2 compares the incremental erosion experienced during a second firing on a Fondu Fyre WA-1 deflector with first firing erosion. From these data, it is evident that more erosion occurs during a second firing than during the first firing. Deflector weight loss data indicate that equal amounts of deflector material (5.75 lb) were lost during Firings 10 and 17. By averaging all 187 erosion data points for each run it became apparent that the weight data are not accurate and that nearly 38% more erosion occurs during a second firing on Fondu Fyre WA-1 than during a first firing.

3. Comparison of Performance of Fondu Fyre WA-1 and Harbison-Walker (H-W) Special Mix 13-65

Figure VII-3 compares centerline erosion profiles for deflectors coated with Fondu Fyre WA-1 and H-W Special mix 13-65. The fused silica H-W mix performed better from an erosion standpoint than Fondu Fyre; however, the H-W mix spalled badly (Fig. VII-4). Figure VII-5 is a postfiring photograph of a Fondu Fyre WA-1 deflector showing no evidence of spalling. Similar quality control was exercised in the pouring and curing of both coatings. The H-W mix spalling tendency might have been reduced by exercising more care during pouring and curing. Coatings must be evaluated, however, not only on performance but on the ease by which a satisfactory pour and cure can be effected. The H-W mix apparently falls short in this regard. Because of the spall tendency and associated need for special procedures during pouring and curing, and the cost of the H-W mix ($15/cwt or approximately three times the cost of Fondu Fyre WA-1), Fondu Fyre is preferred for deflector coating applications.

4. Refurbishability Evaluation

Figure VII-6 compares centerline erosion data of the refurbished Fondu Fyre WA-1 deflector with initial firing data (also see Tables V-4 and VII-4). Note the excellent performance of the refurbished deflector. There was no tendency for refurbished material to disassociate from the deflector other than by the normal erosion process as shown by Fig. VII-7. Run 22 results indicate that an epoxy can be used successfully for preparing an area for refurbishment although the epoxy would hardly seem needed on the basis of Run 6 results.

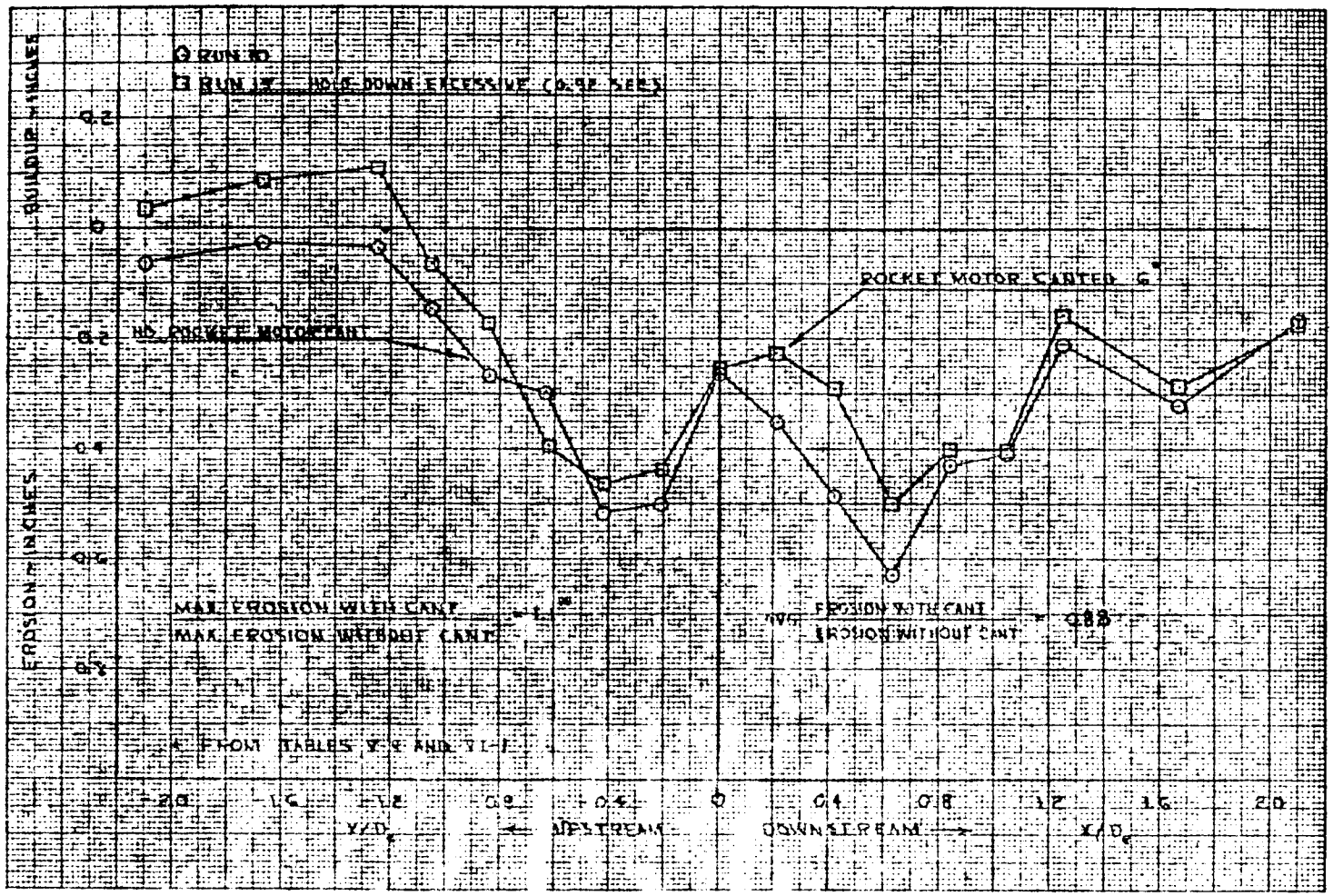

Fig. VII-1 Effect of Rocket Motor Cant on Deflector Centerline Erosion

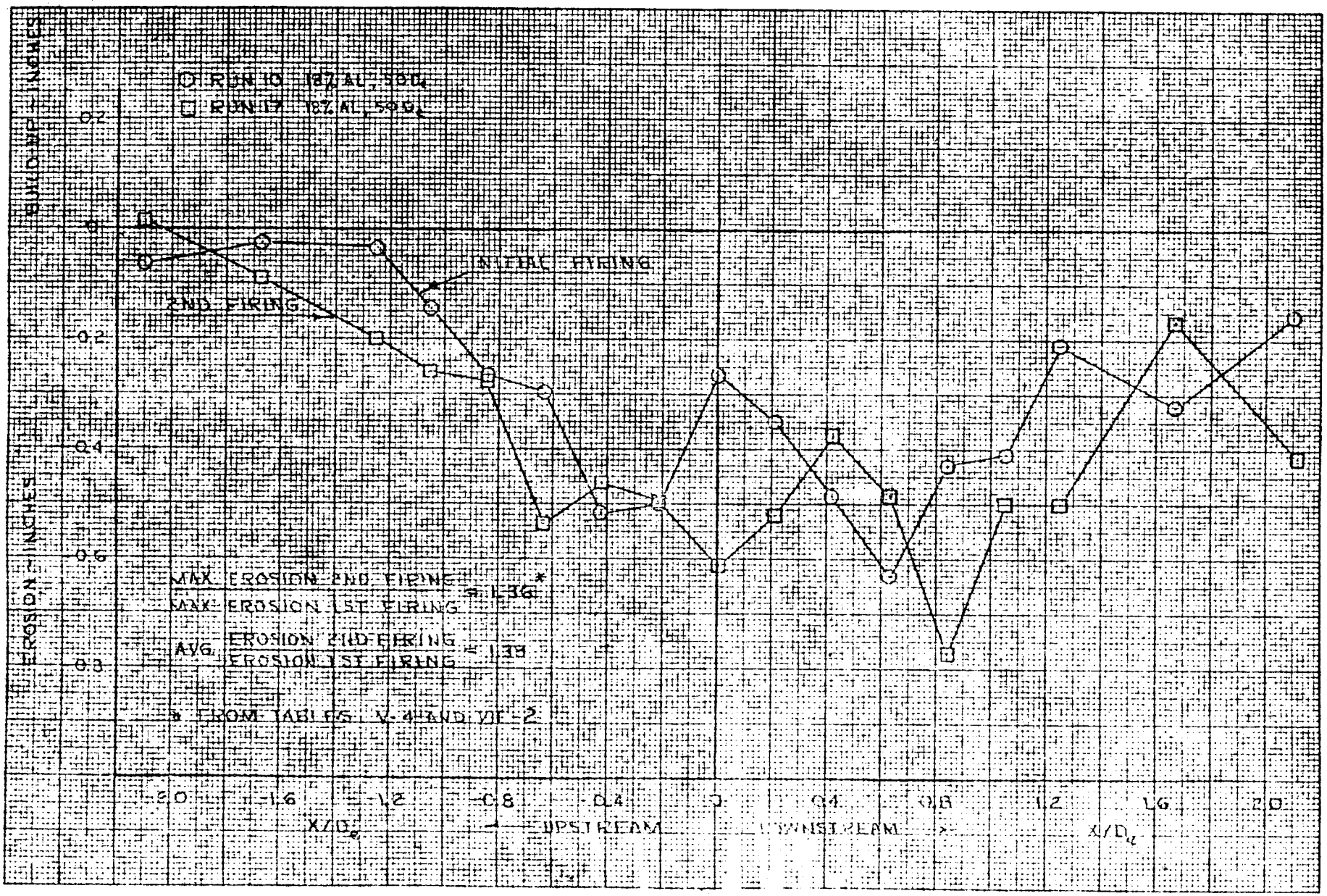

Fig. VII-2 Effect of Successive Firings on Deflector Centerline Erosion

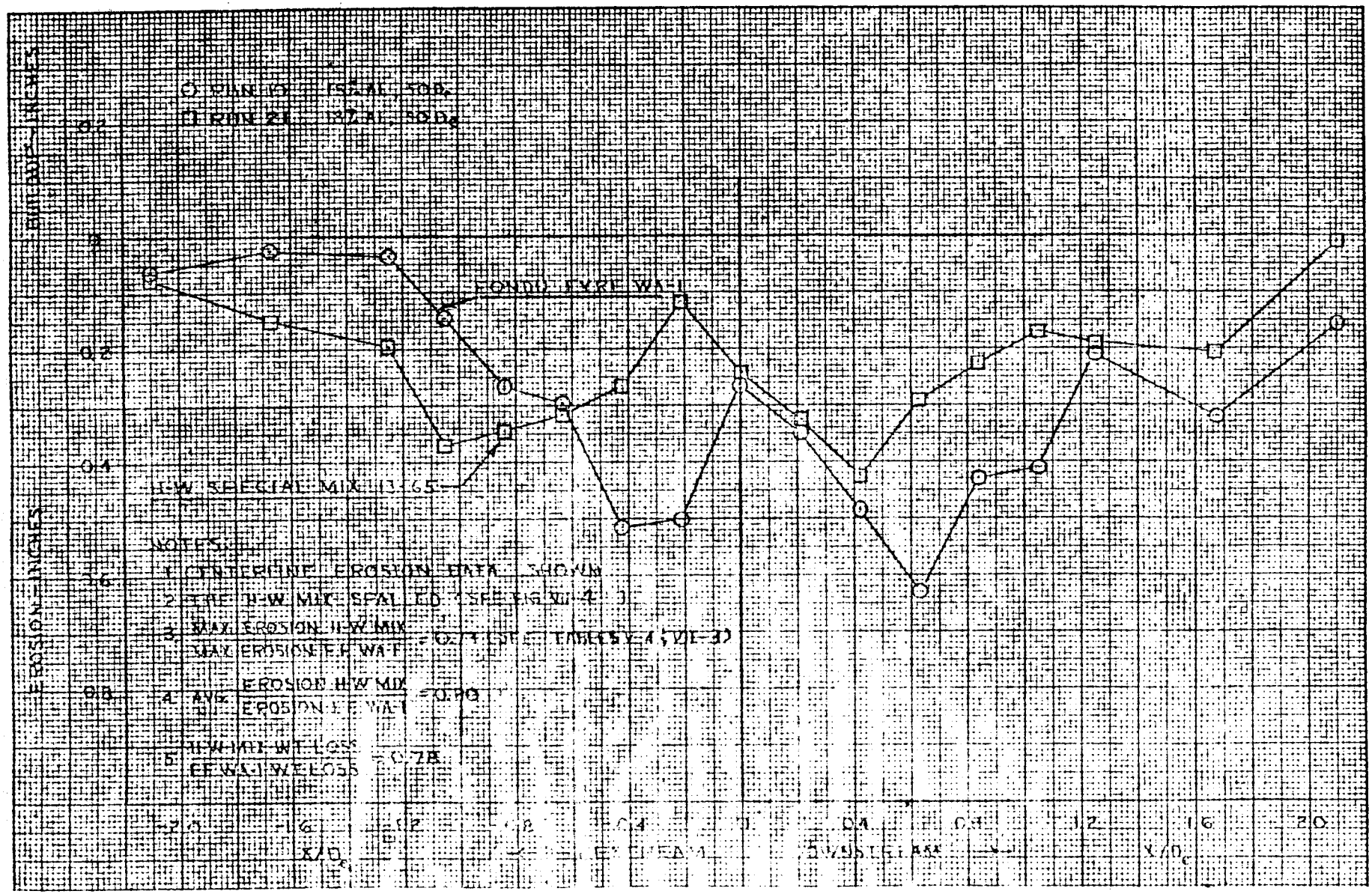

Fig. VII-3 Erosion Resistance of Deflectors Coated with H-W Special Mix 13-65 and Fondu Fyre WA-1

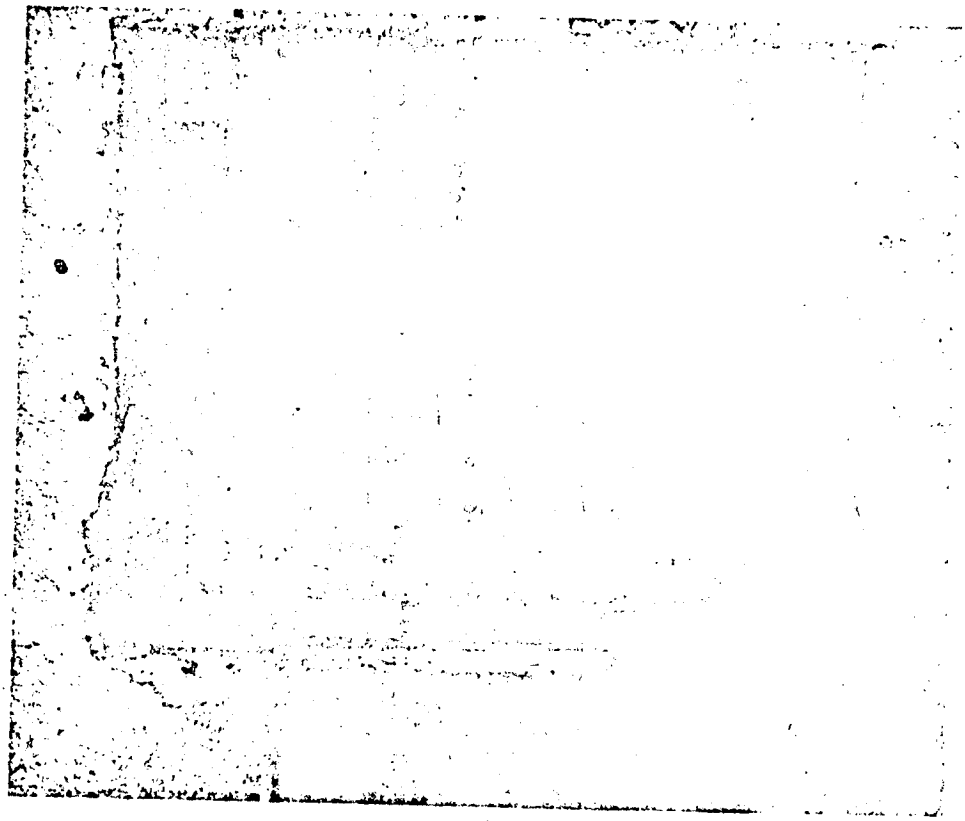

(a)

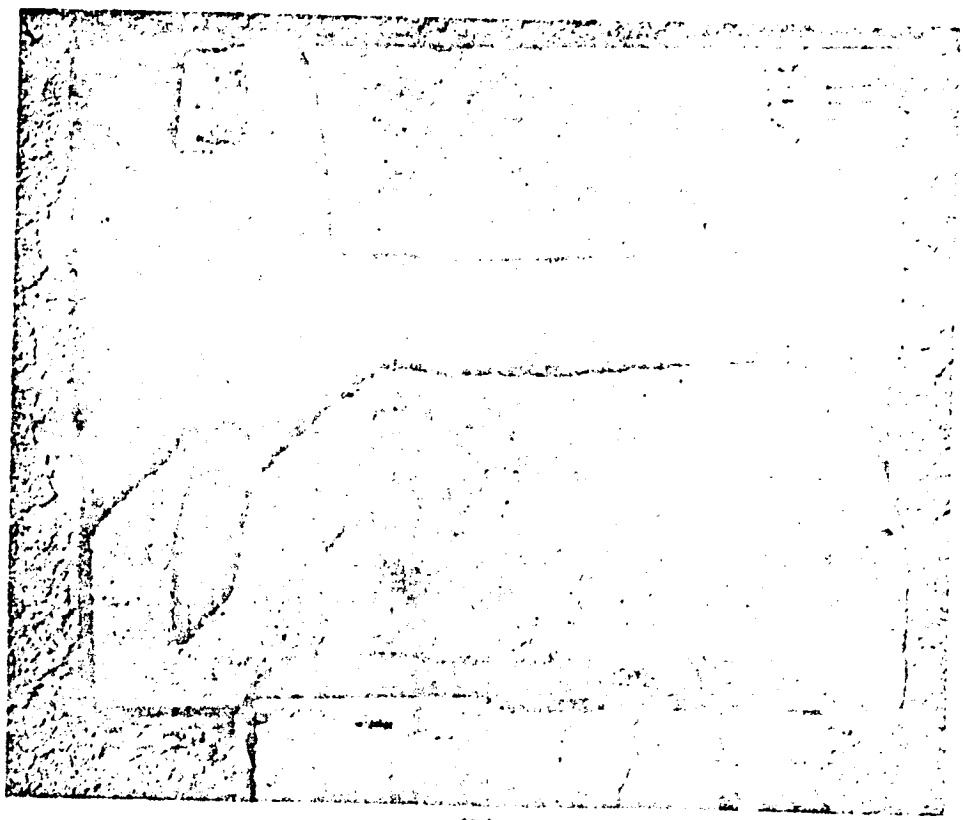

(b)

Fig. VII-4 Deflector Coated with H-W Special Mix 13-65, before and after Firing 21